

**Understanding posttranslational modifications and subcellular
localization of Siah proteins and their roles in *Helicobacter pylori*-
mediated gastric cancer**

By

SHRIKANT BABANRAO KOKATE

LIFE11201204003

**National Institute of Science Education and Research (NISER)
Bhubaneswar**

*A thesis submitted to the
Board of Studies in Life Sciences*

*In partial fulfilment of the requirements
for the Degree of*

DOCTOR OF PHILOSOPHY

of

HOMI BHABHA NATIONAL INSTITUTE



DECEMBER, 2018

Homi Bhabha National Institute

Recommendations of the Viva Voce Committee

As members of the Viva Voce Committee, we certify that we have read the dissertation prepared by Mr. Shrikant Babanrao Kokate entitled "Understanding posttranslational modifications and subcellular localization of Siah proteins and their roles in *Helicobacter pylori*- mediated gastric cancer" and recommend that it may be accepted as fulfilling the thesis requirement for the award of Degree of Doctor of Philosophy.

Chairman – Dr. Chandan Goswami

Date:


14/12/18

Guide / Convener – Dr. Asima Bhattacharyya

Date:

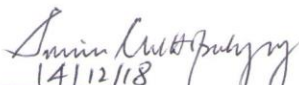

14.12.18

Co-guide - <Name> (if any)- NA

Date:

Member 1 – Dr. Subhasis Chattopadhyay

Date:


14/12/18

Member 2- Dr. Harapriya Mohapatra

Date:


14.12.18

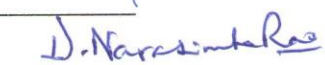
Member 3 – Prof. Jagneshwar Dandapat, Utkal Univ.

Date:


14/12.18

External – Prof. D. Narasimha Rao, IISc Bangalore

Date:


14 Dec 2018

Final approval and acceptance of this thesis is contingent upon the candidate's submission of the final copies of the thesis to HBNI.

I/We hereby certify that I/we have read this thesis prepared under my/our direction and recommend that it may be accepted as fulfilling the thesis requirement.

Date: 14.12.2018

Signature

Signature

Place: NISER Bhubaneswar

Co-guide (if applicable)

Guide

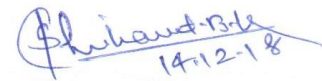
1 This page is to be included only for final submission after successful completion of viva voce.

STATEMENT BY AUTHOR

This dissertation has been submitted in partial fulfillment of requirements for an advanced degree at Homi Bhabha National Institute (HBNI) and is deposited in the Library to be made available to borrowers under rules of the HBNI.

Brief quotations from this dissertation are allowable without special permission, provided that accurate acknowledgement of source is made. Requests for permission for extended quotation from or reproduction of this manuscript in whole or in part may be granted by the Competent Authority of HBNI when in his or her judgment the proposed use of the material is in the interests of scholarship. In all other instances, however, permission must be obtained from the author.

Signature

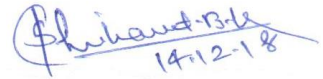


Shrikant Babanrao Kokate

DECLARATION

I hereby declare that the investigation presented in the thesis has been carried out by me. The work is original and has not been submitted earlier as a whole or in part for a degree / diploma at this or any other Institution / University.

Signature

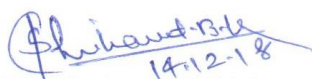


Shrikant Babanrao Kokate

CERTIFICATE

This is to certify that the thesis entitled “**Understanding posttranslational modification and subcellular localization of Siah proteins and their roles in *Helicobacter pylori*-mediated gastric cancer**”, which is being submitted by Mr. Shrikant Babanrao Kokate in partial fulfilment of the degree of Doctor of Philosophy (PhD) in Life Sciences of Homi Bhabha National Institute is a record of his own research work carried by him. He has carried out his investigations for the last six years on the subject matter of the thesis under my supervision at National Institute of Science Education and Research (NISER), Bhubaneswar. To the best of our knowledge, the matter embodied in this thesis has not been submitted for the award of any other degree.

Signature of the Candidate

Handwritten signature of Shrikant Babanrao Kokate in blue ink, with the date 14.12.18 written below it.

Shrikant Babanrao Kokate
National Institute of Science
Education and Research (NISER)
Bhubaneswar

Signature of the Supervisor

Handwritten signature of Asima Bhattacharyya in blue ink, with the date 14.12.18 written below it.

Dr. Asima Bhattacharyya
Associate Professor
National Institute of Science
Education and Research (NISER)
Bhubaneswar

List of Publications arising from the thesis

a. Published

1. *Testin and Filamin-C downregulation by acetylated Siah2 results in increased invasiveness of *Helicobacter pylori*-infected gastric cancer cells. **Shrikant Babanrao Kokate**, Pragyesh Dixit, Indrajit Poirah, Arjama Dhar Roy, Debashish Chakraborty, Niranjana Rout, Shivaram Prasad Singh, Hassan Ashktorab, Duane T Smoot, Asima Bhattacharyya. *The International Journal of Biochemistry & Cell Biology* 2018, 103: 14-24.
2. *Acetylation-mediated Siah2 stabilization enhances PHD3 degradation in *Helicobacter pylori*-infected gastric epithelial cancer cells. **Shrikant Babanrao Kokate**, Pragyesh Dixit, Lopamudra Das, Suvasmita Rath, Arjama Dhar Roy, Indrajit Poirah, Debashish Chakraborty, Niranjana Rout, Shivaram Prasad Singh, Asima Bhattacharyya. *The FASEB Journal* (2018): fj-201701344RRR.
3. **Helicobacter pylori* enhances membrane-bound β -Catenin degradation in the gastric epithelial cancer cell via ETS2-mediated Siah1 induction. Lopamudra Das#, **Shrikant Babanrao Kokate**#, Suvasmita Rath, Pragyesh Dixit, Niranjana Rout, Shivaram Prasad Singh, Asima Bhattacharyya. *Oncogenesis* 6, no. 5 (2017): e327.
4. ETS2 and Twist1 promote invasiveness of *Helicobacter pylori*-infected gastric cancer cells by inducing Siah2. Lopamudra Das, **Shrikant Babanrao Kokate**, Suvasmita Rath, Niranjana Rout, Shivaram Prasad Singh, Sheila Eileen Crowe, Asish K Mukhopadhyay, Asima Bhattacharyya. *Biochemical Journal* 473, no. 11 (2016): 1629-1640.
5. Inhibition of Histone/Lysine Acetyltransferase Activity by CTK7A Selectively Kills Hypoxic Gastric Cancer Cells. Suvasmita Rath, Lopamudra Das, **Shrikant Babanrao Kokate**, Niranjana Rout, Shivaram P Singh, Subhasis Chattopadhyay, Hassan Ashktorab, Duane T Smoot, Mahadeva M Swamy, Tapas K Kundu, Sheila E Crowe, Asima Bhattacharyya. *The international journal of biochemistry & cell biology* 82 (2017): 28-40.
6. Cobalt chloride-mediated protein kinase C α (PKC α) phosphorylation induces hypoxia-inducible factor 1 α (HIF1 α) in the nucleus of gastric cancer cell. Suvasmita Rath, Aditya Anand, Nilabh Ghosh, Lopamudra Das, **Shrikant Babanrao Kokate**, Pragyesh Dixit, Swetapadma Majhi, Niranjana Rout, Shivaram Prasad Singh, Asima Bhattacharyya. *Biochemical and biophysical research communications* 471, no. 1 (2016): 205-212.
7. Regulation of Noxa-mediated apoptosis in *Helicobacter pylori*-infected gastric epithelial cells. Suvasmita Rath, Lopamudra Das, **Shrikant Babanrao Kokate**, B M Pratheek, Subhasis Chattopadhyay, Chandan Goswami, Ranajoy Chattopadhyay, Sheila Eileen Crowe, Asima Bhattacharyya. *The FASEB Journal* 29, no. 3 (2014): 796-806.

b. Other Publications (Conference Proceedings):

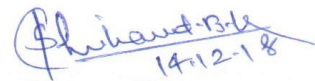
1. Role of Siah1 in *Helicobacter pylori*-infected gastric epithelial cancer cells. Lopamudra Das, **Shrikant Babanrao Kokate**, Suvasmita Rath, Shivaram Prasad Singh, Asima Bhattacharyya. *International Journal of Molecular Medicine* 01/2014; 34: S46- S46

*pertaining to this thesis; #equal contribution

Conference Presentations:

1. Siah2 Acetylation Regulates Invasiveness of *Helicobacter pylori*-Infected Human Gastric Epithelial Cells. **S. B. Kokate**, P. Dixit, L. Das, S. Rath, A. Dhar Roy, I. Poirah, D. Chakraborty, N. Rout, S. P. Singh, A. Bhattacharyya. *13th National Research Scholars Meet (13th NRSM- 2017, OP-01), ACTREC, Mumbai, MH, India.*
2. Regulation of Mitochondria-Mediated Apoptosis Induction in Hypoxic Gastric Epithelial Cancer Cells. S. Rath, **S. B. Kokate**, L. Das, T. K. Kundu, S. P. Singh, A. Bhattacharyya. *Cell Symposia: Multifaceted Mitochondria, P 1.088, 2015, Chicago, IL, USA.*
3. Regulation of Apoptosis induction in hypoxic gastric epithelial cancer cells with metastatic property. S. Rath, L. Das, **S. B. Kokate**, T. K. Kundu, S. P. Singh, A. Bhattacharyya. *2nd international conference on frontiers in Biological Sciences (InCoFIBS-2015), NIT Rourkela, WB, India.*
4. Selective killing of hypoxic gastric epithelial cancer cells showing metastatic properties. S. Rath, L. Das, **S. B. Kokate**, T.K. Kundu, S. P. Singh, A. Bhattacharyya. *2nd International meet on advanced studies on cell signaling network (CeSiN-2014, IL-20) IICB, Kolkata, WB, India.*
5. Regulation of *Helicobacter pylori* mediated gastric cancer: a prospective on Siah2. L. Das, **S. B. Kokate**, S. Rath, S. P. Singh, A. Bhattacharyya. *2nd International meet on advanced studies on cell signaling network (CeSiN-2014, OP-7), IICB, WB, Kolkata, India.*
6. Regulation and role of the E3 ubiquitin ligase SIAH1 in *Helicobacter pylori* mediated gastric cancer. L. Das, **S. B. Kokate**, S. Rath, S. P. Singh, A. Bhattacharyya. *2nd International meet on advanced studies on cell signaling network (CeSiN-2014, PP-1), IICB, Kolkata, WB, India.*

Signature



Shrikant Babanrao Kokate

Dedicated to my family...

ACKNOWLEDGEMENT

Firstly, I would like to express my sincere gratitude to my Ph.D. mentor Dr. Asima Bhattacharyya for her continuous valuable guidance, support and moral boosting throughout my Ph.D. tenure. Her attitude towards research, sincerity, sacrifice, dedication and determination to achieve the best have always inspired me to never back down by failures. She has not only helped in improving my research skills but also my writing and communication skills a lot. Her motivation always made me believe in myself and encouraged me to accomplish this work.

Besides my thesis supervisor, I would like to thank my thesis monitoring committee members: Dr. Chandan Goswami, Dr. Harapriya Mohapatra, Dr. Subhasis Chattopadhyay and Dr. Jagneshwar Dandapat for their continuous advice, suggestions and expertise from different fields of research which helped to learn various other techniques and address problems associated with my work. I would also like to thank Prof. Shivaram Prasad Singh, SCB Medical College, Cuttack and Prof. Niranjana Rout, AHRCC, Cuttack for providing us gastric biopsy tissue samples from gastric cancer patients and helping us in the pathophysiological examinations of gastric cancer stages. I would also thank Mrs. Niharika Mohanty, Assistant to Dr. S. P. Singh for helping us in sample collection and getting consents from gastric cancer patients.

My sincere thanks also go to NISER, SBS faculty members for providing us with various instrumentation facilities for confocal imaging, cell culturing, molecular biology and animal study-related works. I am grateful to Dr. Saurabh Chawla, NISER animal house in-charge, for teaching us animal handling techniques. His expertise during the examination of infectious work carried out in his presence and collecting vital organs post infectious work for our study is deeply appreciated. I also extend out thanks to Mr. Sarangi and Mr. Kuna, staff members of NISER animal house facility for taking care of animals. I thank Dr. Sarita Jena, Animal house in-charge, Institute of Life Sciences, Bhubaneswar for allowing us to perform our initial animal experiments in their central facility.

I am very grateful to my lab seniors Dr. Lopamudra Das and Dr. Suvasmita Rath for helping me with my experiments and teaching me various techniques related to my thesis work. I also thank my lab juniors Mr. Pragyesh Dixit, Mr. Indrajit Poirah, Mr. Arjama Dhar Roy, Mr. Debashish Chakraborty, Miss. Swathi Sivaram Suratkal, Mr. Satyaranjan Sahoo, Mr. Nilabhi Ghosh and Mr. Aditya Anand for all their timely help during my work. I would also thank Miss. Aditi Nayak, Ph.D. student of IIT Bhubaneswar, for her collegiality. I appreciate my batchmates Sony, Subhransu and Rakesh for their constant moral support. I especially thank Sony for being there by my side in all difficult times. My Ph.D. journey would have been very difficult without the company of Dr. Ashutosh, Dr. Sanjima, Dr. Tapas, Dr. Ankit, Dr. Manoj, Mitali, Subhransu, Sony and others none the less with whom I shared very special bonds. Their love, timely suggestions, critiques and our fun times together will always be cherished throughout my life.

Words fall short to express my gratitude and acknowledgment for my parents who were the greatest inspiration behind me in completing my work. I am also thankful to my late uncle who will always be remembered for his moral support and guidance. I specially thank my sister-in-law, brothers-in-law, cousins, aunt and all other family members for their love and belief in me.

I gratefully acknowledge HBNI, DAE for providing me financial support and Director, NISER for allowing me to carry out my research work in this esteemed institution.

Shrikant Babanrao Kokate

Shrikant B. K.
14-12-18

CONTENTS

List of Contents	Page No.
SYNOPSIS	i
Abstract	xii
List of Publications	xiii
Abbreviations	xiv
List of figures	xx
List of tables	xxiii
Chapter 1. INTRODUCTION	1
Section A. Gastric cancer (GC), its progression and dissemination	2
1.A.1. Etiology	2
1.A.1.1. Diet and food habits	3
1.A.1.2. Family history	4
1.A.1.3. Socioeconomic status	4
1.A.1.4. <i>H. pylori</i> infection	4
1.A.2. <i>H. pylori</i>: causative agent for GC	4
1.A.2.1. Pathogenesis by <i>H. pylori</i>	6
1.A.2.2. Virulence factors of <i>H. pylori</i>	7
1.A.2.2.1. The cytotoxin-associated gene pathogenicity island (cag PAI) and cagA	8
1.A.2.2.2. Vacuolating-cytotoxin protein (VacA)	9
1.A.2.2.3. Neutrophil-activating protein (NapA)	9
1.A.2.2.4. Urease	9
1.A.2.3. Epidemiology and routes of transmission	10

1.A.2.4 Role of <i>H. pylori</i> in Hif1 activation	10
1.A.3. Cancer metastasis	11
1.A.4. Factors regulating invasiveness in <i>H. pylori</i> infection	13
1.A.4.1. Epithelial to mesenchymal transition (EMT)	13
1.A.4.2. Cell adhesion molecules	15
1.A.4.3. Role of cadherins and β -catenin in cancer progression	17
1.A.4.4. Role of <i>H. pylori</i> in disruption of cell-adhesion molecules	20
1.A.4.5. Filamins and their roles in cancers	21
1.A.4.6. Testin and its roles in cancers	22
Section B. Ubiquitination-mediated proteasomal degradation pathways and GC	22
1.B.1. Proteasome machinery	23
1.B.2. E3 Ub ligases	24
1.B.3. RING type E3 Ub ligases and their involvement in cancer	25
1.B.3.1. Involvement of RING type E3 Ub ligases in human cancers	26
1.B.4. Siah proteins	27
1.B.4.1. Role of Siah proteins in cancer progression	28
Section C. Factors regulating PTM of Siah proteins	29
1.C.1. Role of acetylation in regulating structure and function of proteins	30
Chapter 2-6. RESULTS	32
Chapter 2. Induced expression of Siah proteins in mouse stomach infected with <i>H. felis</i> and in human gastric adenocarcinoma samples	33

2.1. <i>Helicobacter</i> -infected human and mouse gastric epithelia show induced expression of Siah proteins	33
2.3. Discussion	36
Chapter 3. Siah2, but not Siah1 is acetylated by <i>H. pylori</i> infection	38
3.1. Siah2 undergoes acetylation in <i>H. pylori</i> -infected human GCCs	39
3.2. Discussion	43
Chapter 4. Acetylation at K¹³⁹ increases Siah2 stability	45
4.1. <i>H. pylori</i> induces Siah2 acetylation in the infected GCCs	46
4.2 p300 interacts with Siah2 and induces its acetylation in <i>H. pylori</i> -infected GCCs	48
4.3 p300 HAT inhibitor CTK7A decreases the migration and invasiveness of <i>H. pylori</i> -infected GCCs	51
4.4 Acetylation of Siah2 K139 protects Siah2 from ubiquitination-mediated proteasomal degradation	53
4.5. Discussion	54
Chapter 5. ac-K¹³⁹ Siah2 induces Hif1-mediated invasiveness of <i>H. pylori</i>-infected GCCs	57
5.1. <i>H. pylori</i> causes ac-Siah2-mediated PHD3 degradation and Hif1 α accumulation in infected GCCs	58
5.2. Hif1 α silencing decreases cell migration and invasiveness of <i>H. pylori</i> -infected GCCs	60
5.3. Siah2 K ¹³⁹ acetylation enhances invasiveness of GCCs	63
5.4. <i>Helicobacter</i> -infected mouse and human gastric epithelia have remarkably low PHD3 but high ac-K ¹³⁹ Siah2, Siah2 and Hif1 α protein level	67

5.5. Discussion	70
Chapter 6. TES and FLN-C degradation is promoted by ac-K¹³⁹	73
Siah2 in <i>H. pylori</i>-infected GCCs	
6.1. <i>H. pylori</i> infection downregulates TES and FLN-C expression in GCCs	74
6.2. p300 causes downregulation of TES and FLN-C in <i>H. pylori</i> -infected GCCs	76
6.3. Siah2 K ¹³⁹ acetylation enhances TES and FLN-C degradation	78
6.4. TES and FLN-C silencing leads to enhanced invasion and migration of GECs	81
6.5. TES and FLN-C are stabilized in K139R acetylation-null Siah2-expressed GCCs	84
6.6. TES and FLN-C expression is decreased in infected mouse and human gastric epithelia after <i>Helicobacter</i> infection	86
6.7. Discussion	88
Chapter 7. SUMMARY AND CONCLUSION	91
7.1. Regulation of p300-mediated Siah2 acetylation enhances PHD3 degradation and Hif1 α accumulation in <i>H. pylori</i> -infected GCCs	92
7.2. Acetylated Siah2 elevates GC invasiveness by degrading TES and FLN-C	93
Chapter 8. MATERIALS AND METHODS	95
8.1 MATERIALS USED	96
8.1.1. Cell lines	96
8.1.2. <i>Helicobacter</i> strains	96
8.1.3. DH5 α and XL10 competent cells	96

8.1.4. Biopsy samples	96
8.1.5. Antibodies, siRNAs and plasmid constructs	97
8.2. METHODOLOGY	97
8.2.1. Cloning, site-directed mutagenesis and expression	97
8.2.1.1. Cloning of human <i>siah2</i> acetylation-null lysine to arginine (K-R) mutants	97
8.2.1.1.1. Primer designing	97
8.2.1.1.2. Generation of mutants of <i>Siah2</i> by site-directed mutagenesis	98
8.2.1.1.3. Agarose gel electrophoresis (AGE) and gel extraction of the PCR product	99
8.2.1.1.4. PCR product purification	99
8.2.1.1.5. Restriction digestion of PCR product	99
8.2.1.1.6. DNA ligation	99
8.2.1.1.7. Transformation	99
8.2.1.1.8. Selection of positive clones	100
8.2.1.1.9. Plasmid isolation	101
8.2.1.1.10. Clone confirmation by double digestion and AGE	101
8.2.1.1.11. Glycerol stock preparation	103
8.2.2. Culture of MKN45, AGS, Kato III and HFE145	103
8.2.3. Freezing and revival of cell lines	104
8.2.4. Transient transfection of cell lines	105
8.2.5. Generation of stable cell lines overexpressing empty vector, <i>siah2</i> WT and <i>siah2</i> ac-lys mutants	106
8.2.6. Maintenance of <i>Helicobacter</i> strains and cell infections	107
8.2.7. Maintenance of C57BL/6 mice and <i>H. felis</i> infections	107

8.2.8. Infection of GECs with <i>H. pylori</i>	108
8.2.9. Treatment of cells with proteasomal inhibitor MG132 and a p300 HAT inhibitor (CTK7A)	108
8.2.10. Whole cell lysate preparation	109
8.2.11. Sodium dodecyl sulfate polyacrylamide gel electrophoresis (SDS-PAGE)	109
8.2.12. Immunoblotting	112
8.2.13. Immunoprecipitation (IP) assay	116
8.2.14. Identification of proteins by mass spectrometry	118
8.2.15. Soft-agar colony formation assay or anchorage-independent growth assay	119
8.2.16. Wound-healing assay or scratch assay	121
8.2.17. Transwell migration and invasion assay	122
8.2.18. Clonogenicity or cell proliferation assay	123
8.2.19. Tetrazolium dye 3-[4, 5- dimethylthiazol-2-yl]-2, 5-diphenyl tetrazolium bromide (MTT) assay	124
8.2.20. Peptide synthesis and custom antibody generation	125
8.2.21. C57BL/6 mouse experiments	126
8.2.22. Embedding and sectioning of gastric biopsy samples	126
8.2.23. Hematoxylin and eosin (H&E) staining	127
8.2.24. Immunofluorescence microscopy	127
8.2.25. Confocal microscopy	128
8.2.26. Densitometric and statistical analysis	128
BIBLIOGRAPHY	130
APPENDIX	146



Homi Bhabha National Institute

SYNOPSIS OF Ph. D. THESIS

- | | |
|--|--|
| 1. Name of the Student: | Shrikant Babanrao Kokate |
| 2. Name of the Constituent Institution: | National Institute of Science Education and Research |
| 3. Enrolment No.: | LIFE11201204003 |
| 4. Title of the Thesis: | Understanding posttranslational modifications and subcellular localization of Siah proteins and their roles in <i>Helicobacter pylori</i> -mediated gastric cancer |
| 5. Board of Studies: | Life Sciences |

SYNOPSIS

(Limited to 10 pages in double spacing)

Siah proteins have been recently shown to have metastasis-inducing effects in *Helicobacter pylori*-mediated gastric cancer (1, 2). The primary objective of this thesis work is to understand the molecular mechanism involved in the posttranslational modification of Siah proteins and their roles in *H. pylori*-mediated gastric cancer. In addition, as acetylation of Siah proteins has never been studied, I aimed to identify the effects of *H. pylori* on acetylating Siah proteins and thereby, in regulating their functions.

Gastric cancer is one of the most common cancers and leads to the most frequent cancer-related deaths (3). Approximately, 0.7 million deaths occur every year due to gastric cancer. Infection with *H. pylori*, a gastric bacterial pathogen, is recognized as the highest risk of gastric cancer (4). *H. pylori* is a microaerophilic, Gram-negative, slow-growing, spiral bacterium mainly colonizing the antrum and the pylorus part of the human stomach

(5). Although, 80% of the global gastric cancer burden is attributable to *H. pylori*-induced inflammation and injury (6), the precise mechanisms regulating cancer development in response to this pathogen is not properly understood. *H. pylori* induces the expression of several inflammatory, stress-inducible and oncogenic factors. Studies by Das *et al.* show that Siah1 and Siah2 proteins have metastasis-inducing effects on *H. pylori*-infected gastric epithelial cancer cells (GCCs) (1, 2) Siah proteins are the evolutionarily conserved E3 ubiquitin ligases. E3 ubiquitin ligases ubiquitinate and are the rate-limiting factors regulating proteasome-dependent degradation of various target proteins. Posttranslational modifications (PTMs) are crucial regulators of E3 ubiquitin ligases (7-9). Effects of phosphorylation on Siah proteins are known to some extent (7, 10). However, as acetylation of Siah proteins has never been reported, my study focuses to understand the effect of *H. pylori* on acetylation and stability of Siah proteins. As the prolyl hydroxylase PHD3 is one of the major stress-related proteins expressed in *H. pylori* infection (11) and PHD3 is a target of Siah2 in hypoxia (12, 13), its regulation in *H. pylori*-infected GCCs becomes a part of this study. Since gastric cancer invasiveness is induced by Siah2 (2), search for novel Siah2 binding partners involved in cell adhesion is an important part of this study. Understanding the interaction of two adhesion-related proteins testin (TES) and filamin-C (FLN-C) with Siah proteins in infected GCCs is another component of this work. This thesis has been organized in eight chapters and the contents of each chapter are presented below.

Chapter 1- Introduction: This section presents detailed discussions of human and mouse gastric pathogens *H. pylori* and *H. felis*, gastric cancer progression as well as events influencing the epithelial mesenchymal transition (EMT), an essential event in cancer metastasis. The really interesting new gene (RING) family E3 ubiquitin ligases, especially Siah proteins, and their effects in various cancers including gastric cancer have been discussed. Role of cell adhesion proteins in the regulation of cancer invasiveness is

elaborated here. Moreover, this chapter describes the involvement of hypoxia-inducible factor 1(Hif1) in gastric cancer and in regulating Hif1 stability by PHD proteins. This section also narrates the involvement of RING family E3 ubiquitin ligases in regulating Hif1 and in *H. pylori*-mediated gastric cancer. The known effects of PTMs on Siah proteins (mainly phosphorylation) in various cancers and their effects on the disease outcome have also been discussed.

Chapter 2- Siah1 and Siah2 protein level increases in mouse stomach infected with *H. felis* and in human gastric adenocarcinoma samples: Effect of Siah proteins on cancer progression and metastasis is often dependent on their interaction with target proteins as they belong to E3 ubiquitin ligase family and are involved in proteasome-mediated degradation of various target proteins. Animal studies support oncogenic roles of Siah1 and 2 in various cancers while tumor-promoting roles of Siah2 and apoptosis-inducing role of Siah1 are mostly reported from cell-based assays (14). This chapter describes animal experiments using C57BL/6 mice. C57BL/6 mice infected with *H. felis* represent the classical cascade of *H. pylori*-driven carcinogenic changes observed in humans (15). Enhanced expression of Siah1, Siah2 proteins is noticed in *H. felis*-infected mouse gastric tissue samples as compared to the uninfected tissues (1). Human gastric adenocarcinoma biopsy samples also show marked induction of Siah proteins compared to non-cancer tissues.

Chapter 3- Siah2, but not Siah1 is acetylated by *H. pylori* infection: This chapter shows that only Siah2 and not Siah1, undergoes acetylation in *H. pylori*-infected GCCs. By using the GPS-PAIL tool, probable Siah2-acetylations at several lysine (K) residues are predicted. Various acetylation-null mutants (K to R mutants, R=arginine) are generated accordingly and validated. Out of all mutations, K129R and K139R result in complete reduction in acetylated Siah2 (ac-Siah2) protein level post infection (p.i.) but only K139R is found to

decrease total Siah2 protein. K129R mutation on Siah2 shows only a slight decrease in total Siah2 level indicating that K139 is the major residue acetylated in *H. pylori*-infected GCCs. Acetylation set enrichment based (ASEB) computer program predicts that HAT/KAT acetyltransferase activity of p300 is responsible for Siah2 acetylation and indicates very high probability of acetylation at the K139 residue.

Chapter 4- Acetylation at K139 increases Siah2 stability: Acetylation leads to ubiquitin-mediated proteasomal degradation of acetylated proteins (16) or as a complete contradiction, may compete with ubiquitination to suppress proteasomal degradation of acetylated proteins (17). We find that Siah2 is acetylated in various gastric cancer cell lines including MKN45, Kato III and AGS. This chapter further shows that the HAT function of p300 acetylates Siah2 mainly at the K139 residue in *H. pylori*-infected GCCs enhancing its stability. This chapter also demonstrates that the proteasome inhibitor MG132 rescues Siah2 K139R protein from being degraded indicating that Siah2 acetylation at K139 protects Siah2 from ubiquitination-mediated proteasomal degradation. Effects of Siah2 acetylation on Siah2 targets are studied next.

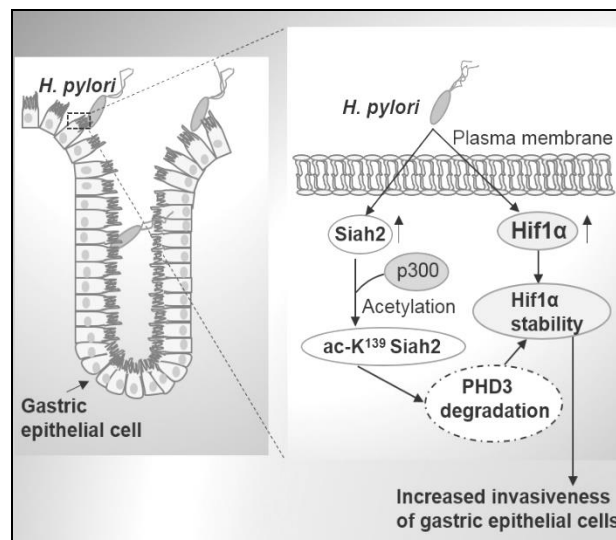
Chapter 5- ac-K139 Siah2 induces Hif1-mediated invasiveness of *H. pylori*-infected GCCs: This chapter describes the effect of acetylation on Siah2 function. *H. pylori* infection is known to induce oxidative stress in GCCs through ROS generation (18), which in turn affects many cellular functions. ROS generation enhances the expression of Hif1 (19). Hif1 is a dimeric protein consisting of α and β subunits. The α subunit is proteasomally degraded in normoxia and PHD proteins and/or von-Hippel-Lindau (VHL)- ubiquitin ligase complexes are involved in the normoxic degradation of Hif1 α . The stability of Hif1 α is enhanced by Siah2 as the latter degrades prolyl hydroxylase 3 (PHD3) (10). My results determine that acetylation of Siah2 at the K139 residue is crucial to increase Hif1 α stability in the infected epithelium. Enhanced stability of ac-Siah2 results in significantly increased

stability of PHD3 in the infected GCCs. This phenomenon is *H. pylori* cytotoxin-associated gene pathogenicity island (*cag* PAI) independent. PHD3 degradation leads to the accumulation of oncogenic and metastasis-inducing Hif1 α in the infected gastric epithelium, promoting invasiveness of infected cells. As immunofluorescence microscopy performed on *H. pylori*-infected human metastatic gastric cancer biopsy samples and *H. felis*-infected C57BL/6 gastric tissue samples also show markedly increased ac-K139 Siah2 and Hif1 α expression, this study establishes the importance of ac-Siah2-Hif1 α axis in *H. pylori*-mediated gastric cancer invasiveness.

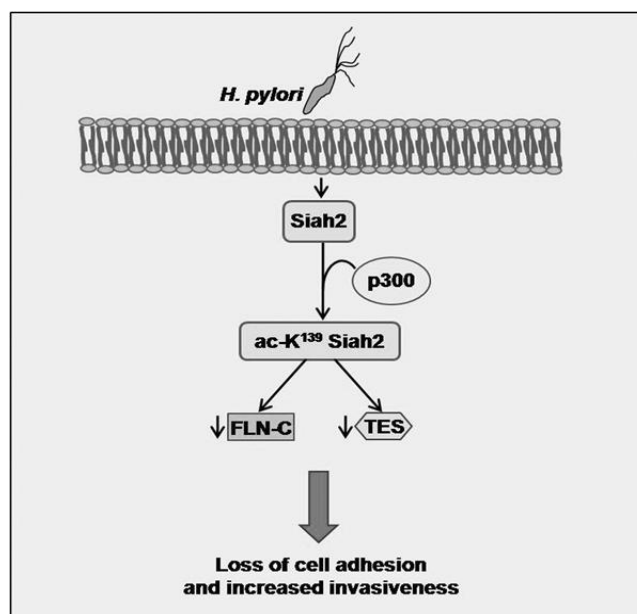
Chapter 6- TES and FLN-C degradation is promoted by ac-K139 Siah2 in *H. pylori*-infected GCCs: Cell adhesion and metastasis are tightly dependent on cytoskeletal proteins. This chapter identifies the interaction of Siah2 with the cytoskeleton. Mass spectrometry identifies two novel Siah2-binding cell adhesion proteins, TES and FLN-C. Tumor suppressor role of TES and FLN-C in various cancers including gastric cancer is well established (20, 21). TES is a scaffolding protein and FLN-C is a member of actin-filament cross linking family proteins that plays a role in cell adhesion, cell spreading (22, 23), and may act as a tumor suppressor (24). My study identifies that TES and FLN-C protein levels decrease in *H. pylori*-infected GCCs in a *cag* PAI-independent manner. Siah2 silencing upregulates TES and FLN-C whereas overexpression leads to their downregulation. Downregulation of TES and FLN-C disrupts actin filament arrangement, decreases filopodia formation and promotes invasiveness of infected GCCs. Biopsy samples collected from *H. pylori*-positive gastric cancer patients also show high expression of ac-K139 Siah2 but low TES and FLN-C as compared to the uninfected non-cancerous samples. The expression of TES and FLN-C is also found to be decreased while ac-K139 remains markedly induced in *H. felis*-infected C57BL/6 gastric tissues as compared to uninfected samples. Thus, this

study establishes the role of ac-K139 Siah2 in regulating TES and FLN-C degradation in infected GCCs.

Chapter 7- Summary and conclusion: This section presents the concluding remarks on my findings which demonstrate the crucial effect of Siah2 acetylation in regulating invasion and migration of *H. pylori*-infected GCCs. These studies indicate the crucial role of p300 HAT in acetylating Siah2 primarily at the K139 residue and protecting Siah2 from undergoing proteasome-mediated degradation in the infected GCCs. ac-K139 Siah2-mediated enhanced degradation of PHD3, TES and FLN-C promotes invasiveness of *H. pylori*-infected gastric epithelial cancer cells.



Summary figure 1: Regulation of p300-mediated Siah2 acetylation enhances PHD3 degradation and Hif1 α accumulation in *H. pylori*-infected GCCs. p300 HAT function promotes acetylation of Siah2 at K139 residue in *H. pylori*-infected GCCs. ac-K139 Siah2 is more stable than non-acetylated Siah2 and therefore, it enhances PHD3 degradation, Hif1 α accumulation and increases gastric cancer invasiveness.



Summary figure 2: Acetylated Siah2 elevates gastric cancer invasiveness by degrading TES and FLN-C. *H. pylori* induced Siah2 acetylation enhances TES and FLN-C degradation in the infected GCCs. TES and FLN-C downregulation disrupts actin filaments and filopodia formation resulting in enhanced invasiveness of *H. pylori*-infected GCCs.

Chapter 8- Materials and methods: This chapter provides details of the used strains of *Helicobacter*, GCCs, human and mouse gastric tissue samples. In addition, this chapter elaborates on the procedures used for the culturing and maintenance of various GCCs as well as protocols for infecting GCCs and C57BL/6 mice. Various cell and molecular biology techniques, microscopy and histopathological sample preparation methods have been discussed. Cloning and site-directed mutagenesis to generate various human *siah2* constructs have been elaborated in this chapter. Detailed methodologies of immunoblotting and immunofluorescence and confocal microscopy are elucidated. Transient transfections and procedures for the generation of stable cell lines are explained. Methods for MTT (3-(4, 5-dimethylthiazol-2-yl)-2, 5-diphenyltetrazolium bromide) assay, colony formation assay, cell invasion and migration assays (soft agar assay, transwell migration-matrigel assay and wound healing assay) have been explained in this section.

References:

1. Das L, Kokate S, Dixit P, Rath S, Rout N, Singh S, et al. Membrane-bound β -catenin degradation is enhanced by ETS2-mediated Siah1 induction in *Helicobacter pylori*-infected gastric cancer cells. *Oncogenesis*. 2017;6(5):e327.
2. Das L, Kokate SB, Rath S, Rout N, Singh SP, Crowe SE, et al. ETS2 and Twist1 promote invasiveness of *Helicobacter pylori*-infected gastric cancer cells by inducing Siah2. *Biochemical Journal*. 2016;473(11):1629-40.
3. Catalano V, Labianca R, Beretta GD, Gatta G, De Braud F, Van Cutsem E. Gastric cancer. *Critical reviews in oncology/hematology*. 2009;71(2):127-64.
4. Harbower DM, Peek RM, Wilson KT. At the Bench: *Helicobacter pylori*, dysregulated host responses, DNA damage, and gastric cancer. *Journal of leukocyte biology*. 2014;96(2):201-12.
5. Goodwin C, Armstrong J. Microbiological aspects of *Helicobacter pylori* (*Campylobacter pylori*). *European Journal of Clinical Microbiology and Infectious Diseases*. 1990;9(1):1-13.
6. Parkin DM, Bray F, Ferlay J, Pisani P. Global cancer statistics, 2002. *CA: a cancer journal for clinicians*. 2005;55(2):74-108.
7. Calzado MA, De La Vega L, Möller A, Bowtell DD, Schmitz ML. An inducible autoregulatory loop between HIPK2 and Siah2 at the apex of the hypoxic response. *Nature cell biology*. 2009;11(1):85.
8. Carbia-Nagashima A, Gerez J, Perez-Castro C, Paez-Pereda M, Silberstein S, Stalla GK, et al. RSUME, a small RWD-containing protein, enhances SUMO conjugation and stabilizes HIF-1 α during hypoxia. *Cell*. 2007;131(2):309-23.
9. Richard DE, Berra E, Gothié E, Roux D, Pouyssegur J. p42/p44 mitogen-activated protein kinases phosphorylate hypoxia-inducible factor 1 α (HIF-1 α) and enhance the transcriptional activity of HIF-1. *Journal of Biological Chemistry*. 1999;274(46):32631-7.
10. Khurana A, Nakayama K, Williams S, Davis RJ, Mustelin T, Ronai Ze. Regulation of the ring finger E3 ligase Siah2 by p38 MAPK. *Journal of Biological Chemistry*. 2006;281(46):35316-26.
11. Nakayama K, Frew IJ, Hagensen M, Skals M, Habelhah H, Bhoumik A, et al. Siah2 regulates stability of prolyl-hydroxylases, controls HIF1 α abundance, and modulates physiological responses to hypoxia. *Cell*. 2004;117(7):941-52.
12. Nakayama K, Qi J, Ronai Ze. The ubiquitin ligase Siah2 and the hypoxia response. *Molecular Cancer Research*. 2009;7(4):443-51.
13. Qi J, Nakayama K, Gaitonde S, Goydos JS, Krajewski S, Eroshkin A, et al. The ubiquitin ligase Siah2 regulates tumorigenesis and metastasis by HIF-dependent and-independent pathways. *Proceedings of the National Academy of Sciences*. 2008;105(43):16713-8.
14. Wong CS, Möller A. Siah-a promising anti-cancer target. *Cancer research*. 2013;canres. 4348.2012.
15. Cai X, Carlson J, Stoicov C, Li H, Wang TC, Houghton J. *Helicobacter felis* eradication restores normal architecture and inhibits gastric cancer progression in C57BL/6 mice. *Gastroenterology*. 2005;128(7):1937-52.
16. Winter M, Sombroek D, Dauth I, Moehlenbrink J, Scheuermann K, Crone J, et al. Control of HIPK2 stability by ubiquitin ligase Siah-1 and checkpoint kinases ATM and ATR. *Nature cell biology*. 2008;10(7):812.
17. Malz M, Aulmann A, Samarín J, Bissinger M, Longerich T, Schmitt S, et al. Nuclear accumulation of seven in absentia homologue-2 supports motility and proliferation of liver cancer cells. *International journal of cancer*. 2012;131(9):2016-26.

18. Du Z, Song J, Wang Y, Zhao Y, Guda K, Yang S, et al. DNMT1 stability is regulated by proteins coordinating deubiquitination and acetylation-driven ubiquitination. *Sci Signal*. 2010;3(146):ra80-ra.
19. Li M, Luo J, Brooks CL, Gu W. Acetylation of p53 inhibits its ubiquitination by Mdm2. *Journal of Biological Chemistry*. 2002;277(52):50607-11.
20. Ding S-Z, O'Hara AM, Denning TL, Dirden-Kramer B, Mifflin RC, Reyes VE, et al. *Helicobacter pylori* and H₂O₂ increase AP endonuclease-1/redox factor-1 expression in human gastric epithelial cells. *Gastroenterology*. 2004;127(3):845-58.
21. O'Hara AM, Bhattacharyya A, Mifflin RC, Smith MF, Ryan KA, Scott KG-E, et al. Interleukin-8 induction by *Helicobacter pylori* in gastric epithelial cells is dependent on apurinic/apyrimidinic endonuclease-1/redox factor-1. *The Journal of Immunology*. 2006;177(11):7990-9.
22. Ding S-Z, Minohara Y, Fan XJ, Wang J, Reyes VE, Patel J, et al. *Helicobacter pylori* infection induces oxidative stress and programmed cell death in human gastric epithelial cells. *Infection and immunity*. 2007;75(8):4030-9.
23. Park J-H, Kim T-Y, Jong H-S, Kim TY, Chun Y-S, Park J-W, et al. Gastric epithelial reactive oxygen species prevent normoxic degradation of hypoxia-inducible factor-1 α in gastric cancer cells. *Clinical Cancer Research*. 2003;9(1):433-40.
24. Qiao J, Cui S-J, Xu L-L, Chen S-J, Yao J, Jiang Y-H, et al. Filamin C, a dysregulated protein in cancer revealed by label-free quantitative proteomic analyses of human gastric cancer cells. *Oncotarget*. 2015;6(2):1171.
25. Drusco A, Zanesi N, Roldo C, Trapasso F, Farber JL, Fong LY, et al. Knockout mice reveal a tumor suppressor function for Testin. *Proceedings of the National Academy of Sciences of the United States of America*. 2005;102(31):10947-51.
26. Coutts AS, MacKenzie E, Griffith E, Black DM. TES is a novel focal adhesion protein with a role in cell spreading. *Journal of cell science*. 2003;116(5):897-906.
27. Griffith E, Coutts AS, Black DM. Characterisation of chicken TES and its role in cell spreading and motility. *Cytoskeleton*. 2004;57(3):133-42.
28. Tobias E, Hurlstone A, MacKenzie E, McFarlane R, Black D. The TES gene at 7q31.1 is methylated in tumours and encodes a novel growth-suppressing LIM domain protein. *Oncogene*. 2001;20(22):2844.

Publications in Refereed Journals:

a. Published

1. *Acetylation-mediated Siah2 stabilization enhances PHD3 degradation in *Helicobacter pylori*-infected gastric epithelial cancer cells. **Shrikant Babanrao Kokate**, Pragyesh Dixit, Lopamudra Das, Suvasmita Rath, Arjama Dhar Roy, Indrajit Poirah, Debashish Chakraborty, Niranjana Rout, Shivaram Prasad Singh, Asima Bhattacharyya. (Accepted, *FASEB J* April 2018)
2. **Helicobacter pylori* enhances membrane-bound β -Catenin degradation in the gastric epithelial cancer cell via ETS2-mediated Siah1 induction. Lopamudra Das#, **Shrikant Babanrao Kokate**#, Suvasmita Rath, Pragyesh Dixit, Niranjana Rout, Shivaram Prasad Singh, Asima Bhattacharyya. *Oncogenesis* (2017) 6, e327; doi:10.1038/oncsis.2017.26
3. ETS2 and Twist1 promote invasiveness of *Helicobacter pylori*-infected gastric cancer cells by inducing Siah2. Lopamudra Das, **Shrikant Babanrao Kokate**, Suvasmita Rath, Niranjana Rout, Shivaram Prasad Singh, Sheila Eileen Crowe, Asish K Mukhopadhyay, Asima Bhattacharyya. *Biochemical Journal* (2016) DOI: 10.1042/BCJ20160187
4. Inhibition of Histone/Lysine Acetyltransferase Activity by CTK7A Selectively Kills Hypoxic Gastric Cancer Cells. Suvasmita Rath, Lopamudra Das, **Shrikant Babanrao Kokate**, Niranjana Rout, Shivaram P Singh, Subhasis Chattopadhyay, Hassan Ashktorab, Duane T Smoot, Mahadeva M Swamy, Tapas K Kundu, Sheila E Crowe, Asima Bhattacharyya. *International Journal of Biochemistry and Cell Biology* <http://dx.doi.org/10.1016/j.biocel.2016.11.014>
5. Cobalt chloride-mediated protein kinase $C\alpha$ (PKC α) phosphorylation induces hypoxia-inducible factor 1 α (HIF1 α) in the nucleus of gastric cancer cell. Suvasmita Rath, Aditya Anand, Nilabh Ghosh, Lopamudra Das, **Shrikant Babanrao Kokate**, Pragyesh Dixit, Swetapadma Majhi, Niranjana Rout, Shivaram Prasad Singh, Asima Bhattacharyya. *Biochem Biophys Res Commun.* 2016 Feb 26; 471(1): 205-12
6. Regulation of Noxa-mediated apoptosis in *Helicobacter pylori*-infected gastric epithelial cells. Suvasmita Rath, Lopamudra Das, **Shrikant Babanrao Kokate**, B M Pratheek, Subhasis Chattopadhyay, Chandan Goswami, Ranajoy Chattopadhyay, Sheila Eileen Crowe, Asima Bhattacharyya. *FASEB J.* 2015 Mar; 29(3): 796-8

b. Under review:

Testin and Filamin-C downregulation by acetylated Siah2 results in increased invasiveness of *Helicobacter pylori*-infected gastric cancer cells. **Shrikant Babanrao Kokate**, Pragyesh Dixit, Indrajit Poirah, Arjama Dhar Roy, Debashish Chakraborty, Niranjana Rout, Shivaram Prasad Singh, Hassan Ashktorab, Duane T Smoot, Asima Bhattacharyya

c. Other Publications (Conference Proceedings):

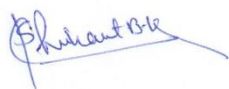
1. Role of Siah1 in *Helicobacter pylori*-infected gastric epithelial cancer cells. Lopamudra Das, **Shrikant Babanrao Kokate**, Suvasmita Rath, Shivaram Prasad Singh, Asima Bhattacharyya. *International Journal of Molecular Medicine* 01/2014; 34: S46- S46
*pertaining to this thesis; #equal contribution

Conference Presentations:

1. Siah2 Acetylation Regulates Invasiveness of *Helicobacter pylori*-Infected Human Gastric Epithelial Cells. **S. B. Kokate**, P. Dixit, L. Das, S. Rath, A. Dhar Roy, I. Poirah, D. Chakraborty, N. Rout, S. P. Singh, A. Bhattacharyya. *13th National Research Scholars Meet (13th NRSM- 2017, OP-01), ACTREC, Mumbai, MH, India.*

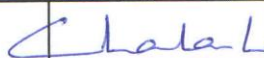
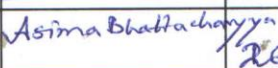
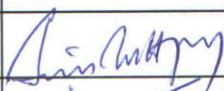
2. Regulation of Mitochondria-Mediated Apoptosis Induction in Hypoxic Gastric Epithelial Cancer Cells. S. Rath, **S. B. Kokate**, L. Das, T. K. Kundu, S. P. Singh, A. Bhattacharyya. *Cell Symposia: Multifaceted Mitochondria, P 1.088, 2015, Chicago, IL, USA.*
3. Regulation of Apoptosis induction in hypoxic gastric epithelial cancer cells with metastatic property. S. Rath, L. Das, **S. B. Kokate**, T. K. Kundu, S. P. Singh, A. Bhattacharyya. *2nd international conference on frontiers in Biological Sciences (InCoFIBS-2015), NIT Rourkela, WB, India.*
4. Selective elective killing of hypoxic gastric epithelial cancer cells showing metastatic properties. S. Rath, L. Das, **S. B. Kokate**, T.K. Kundu, S. P. Singh, A. Bhattacharyya. *2nd International meet on advanced studies on cell signaling network (CeSiN-2014, IL-20) IICB, Kolkata, WB, India.*
5. Regulation of *Helicobacter pylori* mediated gastric cancer: a prospective on Siah2. L. Das, **S. B. Kokate**, S. Rath, S. P. Singh, A. Bhattacharyya. *2nd International meet on advanced studies on cell signaling network (CeSiN-2014, OP-7), IICB, WB, Kolkata, India.*
6. Regulation and role of the E3 ubiquitin ligase SIAH1 in *Helicobacter pylori* mediated gastric cancer. L. Das, **S. B. Kokate**, S. Rath, S. P. Singh, A. Bhattacharyya. *2nd International meet on advanced studies on cell signaling network (CeSiN-2014, PP-1), IICB, Kolkata, WB, India.*

Signature of the Student:



Date: 26.04.2018

Doctoral Committee:

S. No.	Name	Designation	Signature	Date
1.	Dr. Chandan Goswami	Chairman		26/4/18
2.	Dr. Asima Bhattacharyya	Guide & Convener		26.4.18
3.		Co-guide (if any) Member		
4.	Dr. Subhasis Chattopadhyay	Member		
5.	Dr. Harapriya Mohapatra	Member		26.4.18
6.	Prof. Jagneshwar Dandapat	Member		26.4.18
7.		Technology Adviser		

ABSTRACT: *Helicobacter pylori* is the most potent risk factor for gastric carcinogenesis. It regulates many stress-inducible and oncogenic events. Siah proteins, belonging to the RING family of E3 Ub ligases, are among the several proteins upregulated during *H. pylori* infection. Phosphorylation is known to enhance Siah functions. Since acetylation of Siah proteins was completely unexplored, my work focused to understand the effect of acetylation of Siah proteins in *H. pylori*-infected GCCs.

This study confirmed that Siah2 and not Siah1, was acetylated in the nuclear-cytoplasmic compartments after *H. pylori* infection. Since our group identified that gastric cancer (GC) invasiveness is induced by Siah2, the search for novel Siah2-binding partners related to cell was an important part of this study. The prolyl-hydroxylase PHD3 is a stress-response protein and a Siah2 target under hypoxia. I studied its regulation in *H. pylori*-infected GCCs. Two adhesion-related proteins, testin (TES) and filamin-C (FLN-C), were studied for their interaction with Siah proteins. Histone acetyltransferase (HAT) activity of p300 led to the acetylation of Siah2 at lysine (K) 139 residue. This acetylation stabilized Siah2, thereby increasing its efficiency to degrade PHD3 protein leading to the accumulation of hypoxia-inducible factor 1 α (Hif1 α). Siah2 acetylation-mediated stabilization also enhanced the degradation of TES and FLN-C. HAT inhibition by a curcumin-derived chemical CTK7A and an acetylation-null mutation of Siah2 (K139R) abrogated Siah2 acetylation and rescued PHD3, TES and FLN-C from degradation. In addition, disruption of Siah2 acetylation decreased Hif1 α accumulation. As Hif1 α is a major oncogenic transcription factor whereas TES and FLN-C are tumor-suppressors, I wanted to verify the tumor-promoting effects of ac-Siah2. My study revealed that *siah2* K139R mutant-expressing cells had much less invasiveness as compared to the WT *siah2*-expressing cells. High ac-Siah2 in infected human and murine gastric tissues further confirmed the role of Siah2 acetylation in promoting GC invasiveness.

Publications in Refereed Journals:

a. Published

1. *Acetylation-mediated Siah2 stabilization enhances PHD3 degradation in *Helicobacter pylori*-infected gastric epithelial cancer cells. **Shrikant Babanrao Kokate**, Pragyesh Dixit, Lopamudra Das, Suvasmita Rath, Arjama Dhar Roy, Indrajit Poirah, Debashish Chakraborty, Niranjana Rout, Shivaram Prasad Singh, Asima Bhattacharyya. (Accepted, *FASEB J* April 2018)
2. **Helicobacter pylori* enhances membrane-bound β -Catenin degradation in the gastric epithelial cancer cell via ETS2-mediated Siah1 induction. Lopamudra Das#, **Shrikant Babanrao Kokate**#, Suvasmita Rath, Pragyesh Dixit, Niranjana Rout, Shivaram Prasad Singh, Asima Bhattacharyya. *Oncogenesis* (2017) 6, e327; doi:10.1038/oncsis.2017.26
3. ETS2 and Twist1 promote invasiveness of *Helicobacter pylori*-infected gastric cancer cells by inducing Siah2. Lopamudra Das, **Shrikant Babanrao Kokate**, Suvasmita Rath, Niranjana Rout, Shivaram Prasad Singh, Sheila Eileen Crowe, Asish K Mukhopadhyay, Asima Bhattacharyya. *Biochemical Journal* (2016) DOI: 10.1042/BCJ20160187
4. Inhibition of Histone/Lysine Acetyltransferase Activity by CTK7A Selectively Kills Hypoxic Gastric Cancer Cells. Suvasmita Rath, Lopamudra Das, **Shrikant Babanrao Kokate**, Niranjana Rout, Shivaram P Singh, Subhasis Chattopadhyay, Hassan Ashktorab, Duane T Smoot, Mahadeva M Swamy, Tapas K Kundu, Sheila E Crowe, Asima Bhattacharyya. *International Journal of Biochemistry and Cell Biology* <http://dx.doi.org/10.1016/j.biocel.2016.11.014>
5. Cobalt chloride-mediated protein kinase C α (PKC α) phosphorylation induces hypoxia-inducible factor 1 α (HIF1 α) in the nucleus of gastric cancer cell. Suvasmita Rath, Aditya Anand, Nilabh Ghosh, Lopamudra Das, **Shrikant Babanrao Kokate**, Pragyesh Dixit, Swetapadma Majhi, Niranjana Rout, Shivaram Prasad Singh, Asima Bhattacharyya. *Biochem Biophys Res Commun.* 2016 Feb 26; 471(1): 205-12
6. Regulation of Noxa-mediated apoptosis in *Helicobacter pylori*-infected gastric epithelial cells. Suvasmita Rath, Lopamudra Das, **Shrikant Babanrao Kokate**, B M Pratheek, Subhasis Chattopadhyay, Chandan Goswami, Ranajoy Chattopadhyay, Sheila Eileen Crowe, Asima Bhattacharyya. *FASEB J.* 2015 Mar; 29(3): 796-8

b. Under review:

*Testin and Filamin-C downregulation by acetylated Siah2 results in increased invasiveness of *Helicobacter pylori*-infected gastric cancer cells. **Shrikant Babanrao Kokate**, Pragyesh Dixit, Indrajit Poirah, Arjama Dhar Roy, Debashish Chakraborty, Niranjana Rout, Shivaram Prasad Singh, Hassan Ashktorab, Duane T Smoot, Asima Bhattacharyya

c. Other Publications (Conference Proceedings):

1. Role of Siah1 in *Helicobacter pylori*-infected gastric epithelial cancer cells. Lopamudra Das, **Shrikant Babanrao Kokate**, Suvasmita Rath, Shivaram Prasad Singh, Asima Bhattacharyya. *International Journal of Molecular Medicine* 01/2014; 34: S46- S46.

*pertaining to this thesis; #equal contribution

ABBREVIATIONS

ac-Siah2	Acetylated Siah2
ac-K139Siah2	Acetylated K139 Siah2
AGE	Agarose gel electrophoresis
AJ	Adherence junction
APS	Ammonium per sulfate
ASEB	Acetylation-specific enrichment-based program
BabA/B	Blood group antigen binding adhesins A/B
bcl-XL	B-cell lymphoma- XL
β -ME	β -mercapto ethanol
BMI1	B cell-specific Moloney murine leukemia virus integration site 1
BRCA1	Breast and Ovarian cancer 1
BSA	Bovine serum albumin
CagA	Cytotoxin associated gene A
<i>cag</i> PAI	Cytotoxin associated gene Pathogenicity associated island
CBB	Coomassie brilliant blue
Cbl	Casitas B-lineage lymphoma
ccRCC	Clear cell renal cell carcinoma
CD	Cluster of differentiation
CDC42	Cell division cycle 42
C/EBP δ	CCAAT/ enhancer-binding protein delta
CFU	Colony forming unit
CP	Core particle
CPCSEA	Committee for the purpose of control and supervision of experiments
<i>C. pyloridis</i>	<i>Campylobacter pyloridis</i>

CRL	cullin-RING Ub-protein ligase
CSC	Cancer stem cell
CTC	Circulating tumor cell
CTK7A	sodium-4-(3,5-bis(4-hydroxy-3-methoxystyryl)-1H-pyrazol-1-yl) benzoate
DAPI	4', 6-Diamidino-2-phenylindolehydrochloride
Degron	Degradation on
DMSO	Dimethyl sulfoxide
DUB	Deubiquitinating
E2A-TBX1	Eukaryotic transcription factor 2A-T-box factor 1
ECM	Extra cellular matrix
EDTA	Ethidium diamine tetra acetic acid
EGFR	Extracellular growth factor receptor
ELISA	Enzyme-linked immune sorbent assay
EMT	Epithelial to mesenchymal transition
ERK	Extra-cellular signal-regulated kinase
FAK	Focal adhesion kinase
FBS	Fetal bovine serum
FITC	Fluorescein isothiocyanate
FlaA/B	Flagellins A/B
FLNs	Filamins
GAPDH	Glyceraldehyde-3-phosphate dehydrogenase
GC	Gastric cancer
GCCs	Gastric cancer cells
GECs	Gastric epithelial cells
GI	Gastrointestinal

GSK-3 β	Glycogen synthase kinase-3 β
H&E	Hematoxylin and eosin
HAT/KAT	Histone acetyltransferase/ Lysine acetyltransferase
HECT	Homology to E6-associated protein (E6AP) carboxyl terminus
<i>H. felis</i>	<i>Helicobacter felis</i>
Hif1 α	Hypoxia inducible factor 1 α
HIPK2	Hypoxia inducible protein kinase 2
<i>H. pylori</i>	<i>Helicobacter pylori</i>
HRE	Hypoxia responsive element
HRP	Horse-radish peroxidase
HSP60	Heat shock protein 60
HtrA	5-Hydroxytryptamine receptor A
IAEC	Institutional animal ethics committee
IARC	International agency for research on cancer
IF	Immunofluorescence
IP	Immunoprecipitation
JNK	c-Jun N-terminal kinase
Kb	Kilobases
KDa	Kilo Dalton
LB	Luria and Bertani
LC-MS/MS	Liquid chromatography-mass spectrometry/ mass spectrometry
LOH	Loss of heterozygosity
LSM	Laser scanning microscope
MAG	Multifocal atrophic gastritis
MALT	Mucosa-associated lymphoid tissue

MAPK	Mitogen-activated protein kinase
MDM2	Murine double mutant 2
MDR1	Multiple drug resistant 1
MET	Mesenchymal to epithelial transformation
MMP	Matrix Metalloproteinase
MOI	Multiplicity of infection
mRNA	micro Ribonucleic acid
MTT	Tetrazolium dye 3-[4, 5-dimethylthiazol-2-yl]-2, 5-diphenyl tetrazolium bromide
NAG	Non-atrophic gastritis
NapA	Neutrophil activating protein A
NFDM	Nonfat dried milk
NF- κ B	Nuclear factor- κ B
NLS	Nuclear localization signal/ sequence
NO	Nitrous oxide
NPCC	Non-polyposis colon cancer
OCT	Optimum cutting temperature
OMP	Outer membrane protein
O/N	Overnight
ORF	Open reading frame
PAGE	Polyacrylamide gel electrophoresis
PAIL	Prediction of acetylation on internal lysines
PBS/T	Phosphate buffer saline/ tween 20
PHD3	Prolyl hydroxylase 3
p.i.	Post infection

PML	Polymorphonuclear leucocytes
PTMs	Posttranslational modifications
PVDF	Polyvinyl difluoride
RAG1	Recombination activating gene 1
Rbx1	Ring-box protein 1
RING	Really interesting new gene
ROS	Reactive oxygen species
RP	Regulatory protein
RPM	Rotations per minute
RT	Room temperature
RT-PCR	Reverse transcriptase-polymerase chain reaction
RUNX3	Runt-related transcription factor-3
SabA	Sialic acid binding adhesin A
SBD	Substrate binding domain
SDS	Sodium dodecyl sulphate
Ser	Serine
SFM	Serum free medium
Siah	The Seven in absentia homologue
Sina	The seven in absentia
SIP	Siah-interacting protein
shRNA	Short hairpin Ribonucleic acid
siRNA	Small interfering Ribonucleic acid
SUMO	Small upstream modifier
T4SS	Type-IV secretion system
TAE	Tris acetate-EDTA

TBS/T	Tris buffer saline/ tween-20
TE	Tris EDTA
TEMED	N, N, N', N'-Tetra methyl ethylene diamine
TERT	Telomerase reverse transcriptase
TES	Testin
TGF- β	Transforming growth factor- β
TGS	Tris-glycine-SDS
TIP60	Tat-interacting protein of 60 kDa
TJ	Tight junction
TNF	Tumor necrosis factor
TRAF	TNF receptor-associated factor
TRIM	Tripartite motif
TSA	Trypticase soya agar
UHRF1	Ubiquitin-like with PHD and RING-finger domain 1
VacA	Vacuolating cytotoxin A
VHL	Von Hippel-Lindau
WB	Western blotting
WT	wild type
ZEB1/2	Zinc finger box-binding 1/2
ZNF	Zinc finger protein 139 transcription factor

LIST OF FIGURES

Description	Page No.
CHAPTER 1	
Figure 1.A.1: Factors responsible for GC	3
Figure 1.A.2: Predispositions to <i>H. pylori</i> infection	5
Figure 1.A.2.1: Disease pathogenesis by <i>H. pylori</i>	7
Figure 1.A.2.2: Virulence factors of <i>H. pylori</i>	8
Figure 1.A.3: The invasion-metastasis cascade	13
Figure 1.A.4.1: EMT and MET markers	14
Figure 1.A.4.2.1: Intercellular junctions of epithelial cell	15
Figure 1.A.4.2.2: Association of E-cadherin with various cellular components	16
Figure 1.A.4.3.1: Regulation of E-cadherin in cancer	18
Figure 1.A.4.3.2: β -catenin-Wnt signaling events in cancer	19
Figure 1.A.4.4: Epithelial barrier disruption by <i>H. pylori</i>	21
Figure 1.B.1.1: The Ub-proteasome pathway	25
Figure 1.B.3: Types of E3 Ub ligases	26
Figure 1.B.4: The RING domain structure of Siah proteins	28
CHAPTER 2	
Figure 2.1: Induced expression of Siah1 is noticed in <i>Helicobacter</i> -infected human and mouse gastric epithelia	34
Figure 2.2: Induced expression of Siah2 in <i>Helicobacter</i> -infected human and mouse gastric epithelia	35
CHAPTER 3	
Figure 3.1: Siah2 undergoes acetylation in <i>H. pylori</i> -infected GCCs	40

Figure 3.2: Siah2 undergoes acetylation at several residues in <i>H. pylori</i> -infected GCCs	41
Figure 3.3: p300 is predicted to acetylate Siah2 in <i>H. pylori</i> -infected GCCs	42
CHAPTER 4	
4.1 <i>H. pylori</i> induces Siah2 acetylation in the infected GCCs	47
4.2 p300 interacts with Siah2 and induces its acetylation in <i>H. pylori</i> -infected GCCs	50
4.3 p300 HAT inhibitor CTK7A decreases the migration and invasiveness of <i>H. pylori</i> -infected GCCs	52
4.4 Acetylation of Siah2 K139 protects Siah2 from ubiquitination-mediated proteasomal degradation	54
CHAPTER 5	
Figure 5.1: <i>H. pylori</i> -mediated Siah2 acetylation at K ¹³⁹ causes PHD3 degradation and Hif1 α accumulation in infected GCCs	59
Figure 5.2: Hif1 α silencing decreases cell migration and invasiveness of <i>H. pylori</i> -infected GCCs	61
Figure 5.3: Siah2 K ¹³⁹ acetylation leads to invasion and migration of GCCs	64
Figure 5.4: Siah2 K ¹³⁹ acetylation enhances invasiveness of GCCs	66
Figure 5.5: <i>Helicobacter</i> -infected mouse show splenomegaly and advanced stages of gastric carcinoma	68
Figure 5.6: <i>Helicobacter</i> -infected mouse and human gastric epithelia have remarkably low PHD3 but high ac-K139 Siah2, Siah2 and Hif1 α protein level	69

CHAPTER 6

- Figure 6.1: *H. pylori* infection downregulates TES and FLN-C expression in GCCs **75**
- Figure 6.2: p300 causes downregulation of TES and FLN-C in *H. pylori*-infected GCCs **77**
- Figure 6.3: Siah2 K¹³⁹ acetylation enhances TES and FLN-C degradation **79**
- Figure 6.4: TES and FLN-C silencing leads to enhanced invasion and migration of GCCs **82**
- Figure 6.5: TES and FLN-C silencing increases invasiveness of GCCs **83**
- Figure 6.6: TES and FLN-C are stabilized in K139R acetylation-null Siah2-expressed GCCs **85**
- Figure 6.7: TES and FLN-C expression is decreased in infected mouse and human gastric epithelia following *Helicobacter* infection **87**

CHAPTER 7

- Figure 7.1: Regulation of p300-mediated Siah2 acetylation enhances PHD3 degradation and Hif1 α accumulation in *H. pylori*-infected GCCs **92**
- Figure 7.2: Acetylated Siah2 elevates GC invasiveness by degrading TES and FLN-C **93**

List of Tables	Page No.
Table 1. Components for site-directed mutagenesis	98
Table 2. Components for restriction digestion	102
Table 3. Parameters for transient transfection	105
Table 4. Components for resolving gel	110
Table 5. Components for stacking gel	111
Table 6. Components for 10X TBS solution	113
Table 7. Components for 10X PBS solution	113
Table 8. Components of TEN + Triton X-100 buffer	117
Table 9. Components of TEN – Triton X-100 buffer	117
Table 10. Composition for CBB-R250 destaining solution	119
Table 11. Components for soft-agar assay (For single well)	121

INTRODUCTION

Chapter 1

Section A: Gastric cancer (GC), its progression and dissemination

GC is the fifth frequent cancer in the world (1). It ranks second in cancer-related mortalities with more than 0.7 million deaths occurring every year on a global scale. The incidence for stomach cancer is higher in males than in females but the mortality rate is completely opposite. GC prevails highest in eastern Asia, central and eastern Europe and South America. Low incidences are observed in the developed nations like North America or western Europe (2). In India, it is the second most fatal cancer in males and fourth amongst females (1). GC is broadly classified into two types, diffuse and intestinal types (3). Gastric carcinogenesis is a multistep and multifactorial process which occurs through successive changes in the gastric epithelium starting with normal gastric mucosa, non-atrophic gastritis (NAG) or superficial gastritis, chronic inflammation, multi focal atrophic gastritis (MAG), metaplasia of small, colonic intestine and spasmodic polypeptide expressing metaplasia (4), non-invasive neoplasia which ends with invasive adenocarcinoma (5-7). The normal gastric mucosa may show initial symptoms of inflammation with infiltration of leucocytes and neutrophils, also called as gastritis. Gastric pathogen *H. pylori* is the most common cause of gastritis. Atrophic gastritis is differentiated by marked morphological loss in glandular tissues which indicates the initial phase precancerous process. When the epithelial cells change their phenotype to intestinal cells is known as intestinal metaplasia. Neoplasia is characterized by hyperchromatic, bigger, densely populated nuclei with loss in architecture of stomach linings. However, the cells are noninvasive at this stage and bound to their basal membranes. In invasive adenocarcinoma stage of GC cells by virtue of mutations attain property to degrade the matrix to enter into surrounding stroma and metastasize further (5).

1.A.1. Etiology

GC development is a multifactorial process. However, more than 80% cases are attributed to

Helicobacter pylori infections (8). Apart from *H. pylori*, diet, socio-economic habits, environmental factors and host genetic factors also contribute to the development of this disease (**Figure 1.A.1**) (9). In 1994 population-based studies led International Agency for Research on Cancer (IARC) to classify *H. pylori* as a “class I carcinogen” (10). GC is the interplay of these factors which influence GC progression making it complex and difficult for early diagnosis.

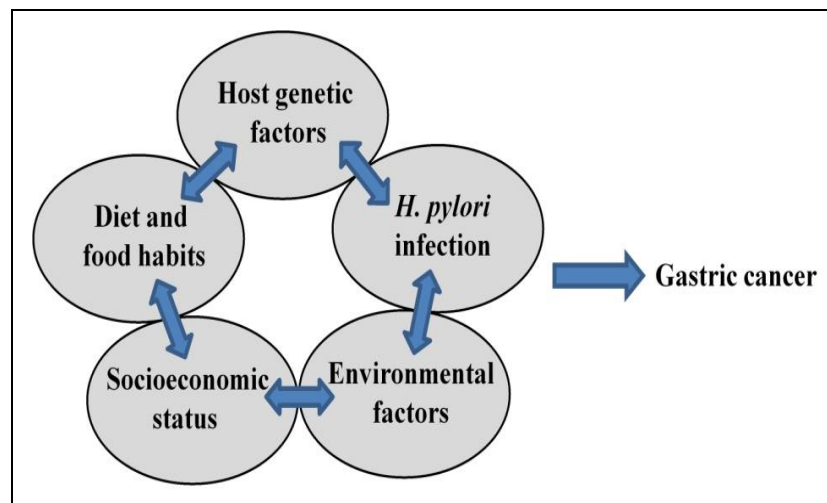


Figure 1.A.1: Factors responsible for GC

1.A.1.1. Diet and food habits

Population consuming high amounts of starchy food poor in protein amount and minimal consumption of fruits and green, leafy vegetables have increased chances of having stomach cancer. Acid-catalyzed nitrosation, a result of starch-rich and low protein diets causes stomach inner lining destruction (11-13). Excessive intake of salts is also positively correlated to GC (14). Excess salt intake enhances *H. pylori* growth, increases loss of parietal cells by hyper-gastrinemia and endogenous mutations leading to promotion of GC (15, 16). Polycyclic aromatic hydrocarbons such as benzo[a]pyrene formed in overcooked and smoked food are also contributing factors (17).

1.A.1.2. Family history

Approximately, 10-15% of GCs occur due to hereditary cancers like nonpolyposis colon cancer (NPCC) or Von Hippel-Lindau (VHL) syndrome whereas, 85-90% are sporadic in nature (18). The risk of GC increases due to gene variations (19) and polymorphisms (20). The risk of GC also increases by two-to-three folds depending on the genetic relatedness with the patient diagnosed with cancer (21). These risk factors may interact with other genetic factors or act independently and increase the risk of cancer.

1.A.1.3. Socioeconomic status

From population studies, a positive correlation is drawn between poor socioeconomic status (which correlates with unhygienic living as well as occupation conditions, poor sanitation, increased habits of smoking, alcohol consumption) and stomach cancer risk (22). GC threat multiplies with the duration of smoking and smoking combined with alcohol consumption drastically accelerates the risk of GC (22, 23). Dusty and high-temperature environment or jobs in extreme heated surroundings also contribute to GC (24, 25).

1.A.1.4. *H. pylori* infection

H. pylori infection is the main contributor towards stomach cancer development (26). However, infection with *H. pylori* alone may not lead to GC as dissimilarities in the host vulnerability to infection and the bacterial virulence together bring in the resultant effects. Its high prevalence is observed in the developing countries where health and sanitation conditions are not optimal. Whereas, developed countries with minimal *H. pylori* infection rate show low GC occurrences (27, 28). *H. pylori* gastritis is the universal precursor state of gastric carcinogenesis.

1.A.2. *H. pylori*: causative agent for GC

H. pylori is a Gram-negative microaerophilic, non spore-forming, spiral-shaped pathogenic bacterium with a cluster of 5-7 polar sheathed flagella and inhabits mucosa of the stomach

(29, 30). At present, nearly half the human population are infected with *H. pylori* and these individuals have nearly two-times more probability of GC development (31). Other than GC, it causes various other diseases including gastric and duodenal ulceration and in rare cases may lead to lymphoma of surrounding lymphoid organs, also known as mucosa-associated lymphoid tissue (MALT) lymphoma (32, 33).

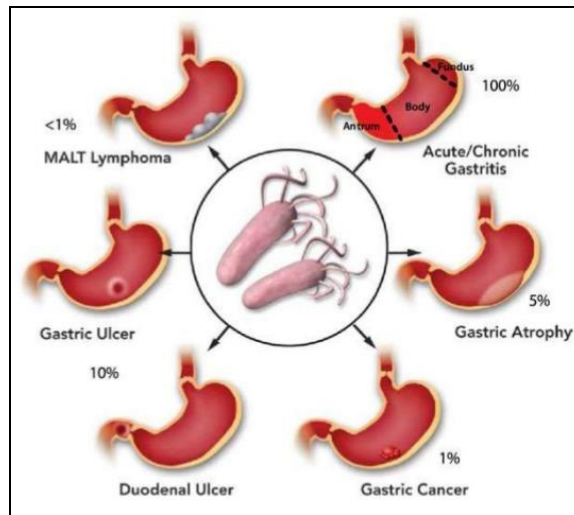


Figure 1.A.2: Predispositions to *H. pylori* infection. Courtesy: Ref. (34).

The identification of *H. pylori* as a major causative agent for GC has led to in-depth investigation on numerous mechanisms of *H. pylori*-induced carcinogenesis (35). Barry J. Marshall and J. Robin Warren first isolated and cultured this bacterium from human gastric biopsy specimens in 1984 (36). Goodwin *et al.*, in 1989, first classified *H. pylori* under the newly formed genus *Helicobacter* (35). They found the presence of *H. pylori* in almost all patients suffering from prolonged persistent duodenal and gastric inflammation leading to ulceration and so, classified it to be an important etiological factor for diseases affecting the upper GI tract. Marshall *et al.* initially named this organism as *Campylobacter pyloridis* based on their preliminary observation but subsequently renamed it to *Campylobacter pylori*. Comparative analysis between *Campylobacter* genus and *Wolinella* genus was done by Goodwin *et al.* in the year 1989 (35). The chemotaxonomic properties, DNA base

composition, cellular fatty acids and bacterial growth characteristics differ considerably between *H. pylori*, *Wolinella* genus and the neighbouring *Campylobacter* genus which provided very concrete evidences for naming it into a completely new genus *Helicobacter* and *Helicobacter pylori* as the name of the species. The ultrastructural studies of bacterial glycocalyx also provided vital structural features which helped them to determine the distinct nature of the bacterium (37).

1.A.2.1. Pathogenesis by *H. pylori*

Nearly 50% human population possesses *H. pylori* infection early in life but only 3% are predisposed to GC. Acute infection with the bacterium is rarely diagnosed. Both the spiral-shaped and coccoid forms of the bacteria (38, 39) have developed a unique mechanism to thrive in the harsh acidic stomach environment and are able to cause a severe inflammation in gastric mucosa (40). The bacterium drives a restrictive immune response to the infection, due to which the organism persists for decades in the infected host stomach. Variations in the associated factors may alter the epidemiology and outcomes. Recent studies have supported the possible role of precursor gastric stem cells in *H. pylori*-mediated tumor progression (41-43). *H. pylori* infection results in two equally exclusive conditions. In the first case, patients with low acid secretions suffer from corpus-predominant gastritis, which includes gastric inflammation resulting in the degradation of normal gastric glands and replacement with intestinal-type epithelium resulting in gastric atrophy succeeded by metaplasia of the intestine, hypochlorhydria, dysplasia, finally leading to in rare cases, gastric carcinoma. In the second case, patients suffering from high acid secretion usually have gastritis of the antral mucosa and are prone to duodenal ulcers. Mucosa-associated lymphoid tissue (MALT) lymphoma is a rare complication of *H. pylori* infection (44).

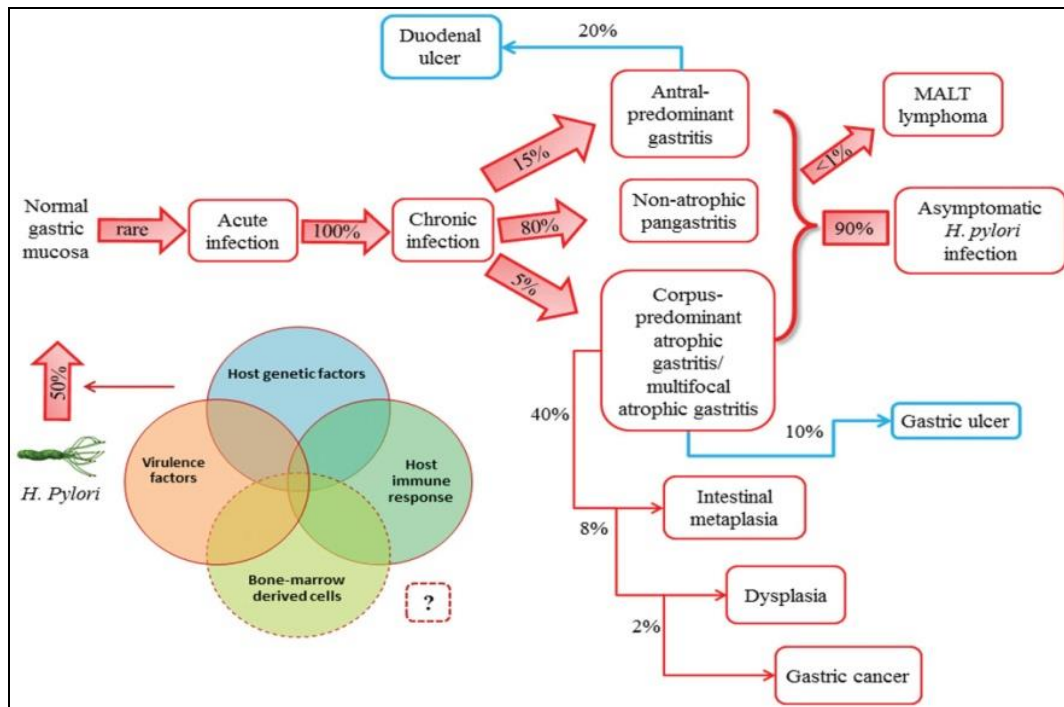


Figure 1.A.2.1: Disease pathogenesis by *H. pylori*. Courtesy: Ref. (45).

1.A.2.2. Virulence factors of *H. pylori*

Genomic and phenotypic attributes of a bacterium, together with the conditions of the gastric microenvironment, enable the expression of certain virulence factors which might facilitate the survivability of some strains and cause disease pathogenesis. Genes of several virulence factors of *H. pylori* such as cytotoxin-associated gene A (*cagA*), neutrophil activating protein (*napA*), vacuolating cytotoxin A (*vacA*), *Helicobacter*-specific outer membrane proteins (*omp*) and several other accessory genes like urease, phospholipase, peptidoglycan also play critical roles in disease pathogenesis.

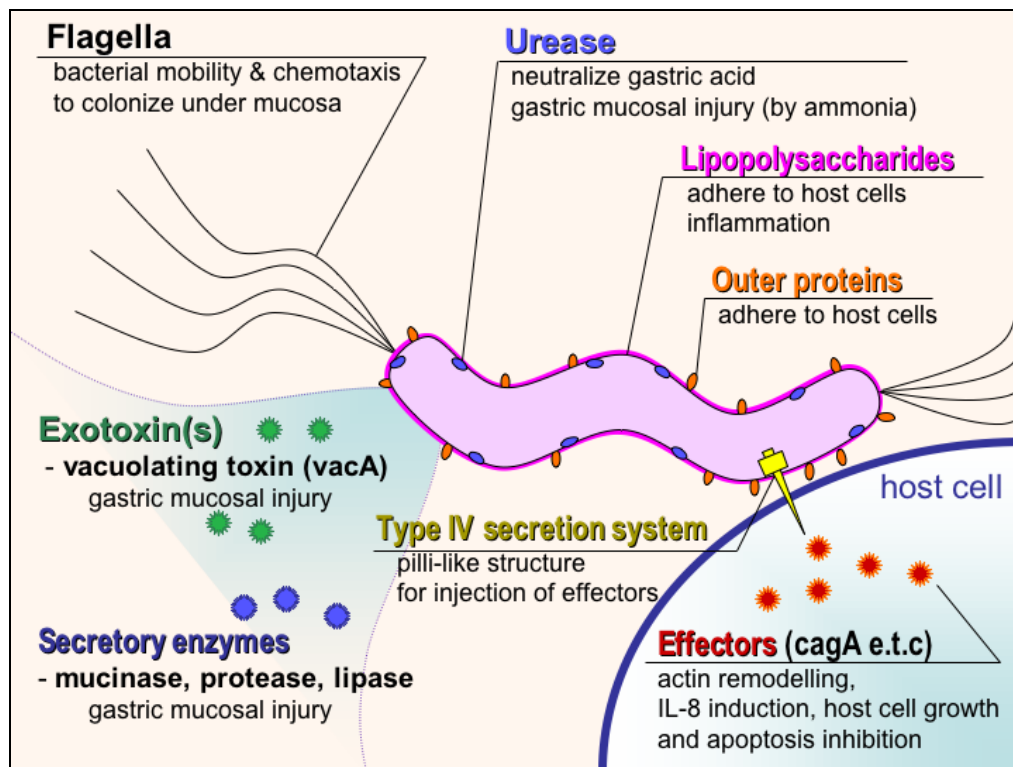


Figure 1.A.2.2: Virulence factors of *H. pylori*. Courtesy: Ref. (46).

1.A.2.2.1. The cytotoxin-associated gene pathogenicity island (*cag* PAI) and *cagA*

The *cag* PAI is a 40 Kb genomic region containing 32 genes encoding a type IV secretion system (T4SS) that includes the *cagA* gene (47). Bacterial virulent factors are transported into the eukaryotic cells by the formation of a syringe-like arrangement which penetrates into the host cell membrane. *H. pylori* strains are broadly classified into two families on the basis of occurrence of *cagA* i.e. *cagA*-positive and *cagA*-negative strains. CagA modulates cell signaling causing derangement of the cellular architecture (48). The *cagA*-negative strains are less virulent. CagA undergoes tyrosine phosphorylation in the host cells and these modifications are used to experimentally prove CagA protein release into the host (49). The extent of tyrosine phosphorylation is commonly associated with carcinogenesis (47). CagA triggers numerous signaling cascades inducing host cells elongation, adhesion and spreading due to actin polymerization, a typical morphological adaptation known as the “scattering

phenotype” or the “hummingbird phenotype”. Along with this cytoskeletal rearrangement, degradation of various cell adhesion and tight junction proteins occur which make the transformed cells more motile.

Other virulence-associated factors of *H. pylori* which also contribute to outcome of GC are discussed briefly in the following sections.

1.A.2.2.2. Vacuolating-cytotoxin protein (VacA)

VacA, another crucial virulence factor in the gastric pathogenesis, changes epithelial cell structure and function. This toxin can induce multiple cellular events including the modification of endo-lysosomal trafficking, immunomodulation and apoptosis (50-52). The prolonged outcome of infection with *vacA*-positive strains, thus, is the prevention of bacterial clearance by the host immune system.

1.A.2.2.3. Neutrophil-activating protein (NapA)

NapA is a 150 kDa, 10 identical subunits-containing protein, coded by the *napA* gene. Its binding to a specific receptor triggers a cascade of signaling events leading to superoxide anion generation, adhesion of neutrophils to endothelial cells and increased chemotaxis (53).

1.A.2.2.4. Urease

The *H. pylori* urease is a hexameric, 540 kDa nickel-containing molecule. It is a crucial component of *H. pylori* for colonizing the bacterium in the host mucosa of stomach. *H. pylori* urease degrades urea into ammonia (NH₃) and carbon dioxide (CO₂). NH₃ neutralizes acidity, thus helping in the survival of the bacterium (54). The urease enzyme assimilates organic nitrogen present in the microenvironment. The released ammonia increases the permeability of gastric epithelium by disrupting the tight junctions (54, 55). Other bacterial enzymes like mucinase and lipase degrade the mucus secreted by gastric epithelial cells increasing its adherence.

H. pylori genome also consists of 30 related hop genes encoding outer membrane proteins (OMP). These proteins help the bacterium in adhesion to the microvilli-containing regions of mucus-secreting gastric epithelial cells. Other than these cytotoxins, the following important virulence factors are also crucial - flagellins (FlaA/B), adhesins (Blood group antigen binding adhesins- BabA/B, Sialic acid binding adhesins SabA, heat shock protein 60 (HSP60) (56).

1.A.2.3. Epidemiology and routes of transmission

The prevalence of *H. pylori* is variable from country-to-country (57). For example, in Latin America and eastern parts of Asia, *H. pylori* infect usually in the childhood with 80% population showing infection by 20 years age. Whereas, in developed countries like North America, UK, western Europe and Australia, childhood infection is a rarity. However, the infection drastically increases to 40% by the age of 30-40 years. Socioeconomic status plays a very significant role in acquiring infection. Even, within a region, the prevalence of *H. pylori* may vary within various ethnic groups. Surprisingly, migrants from high to low risk areas, show a significant reduction in infection.

Direct or person-to-person transmissions may occur in institutionalized populations like mentally or physically challenged persons and criminal inmates staying together (58-60). Other causes like familial exposures (61), oral-oral route (62), faecal-oral route (63) have also been reported equally responsible for possible direct transmission. Indirect ways of transmissions are waterborne, zoonotic or vector-borne and nosocomial transmissions.

1.A.2.4. Role of *H. pylori* in Hif1 activation

Infection by *H. pylori* generates free radicles which are responsible for regulating inflammation and apoptosis of infected gastric epithelial cancer cells (GCCs) (64-67). The reactive oxygen species (ROS) generated alter the growth of GCCs and thus, induce apoptosis. *H. pylori* CagA modulates endo-lysosomal trafficking followed by cellular

vacuolation. Free radicals produced during this process enhances hypoxia-inducible factor 1 (Hif1) expression (68). Hif1 is a member of Hif family of proteins and is one of the crucial transcriptions and pro-survival factors which are expressed in hypoxia. Hif1 is involved in the regulation of the expression of various genes involved in cancer progression (69). Hif1 is a heterodimeric protein made-up of two subunits, an oxygen-dependent α subunit, and a constitutively-expressed β subunit. Role of Hif1 is significant in cancer progression as it is a regulator of several downstream effector expression that are pro-cancerous (70), epithelial to mesenchymal transition (EMT) and metastasis. Hif1 binding to the hypoxia-response element (HRE) of various target genes regulates their transcription (70).

p300 is a transcriptional cofactor of Hif1. It has histone acetyltransferase (HAT) activity and is recruited to Hif1 (71). p300 might regulate cancer progression act by activating several protooncogenic factors (72). Autoacetylation of p300 promotes its HAT activity. Enhanced HAT function in tumor cells may disrupt cell cycle, while suppressed activity leads to apoptosis (73, 74). Several studies have suggested crucial roles acetylation and deacetylation of histones in carcinogenesis and metastasis (75, 76).

1.A.3. Cancer metastasis

Metastasis is a complex phenomenon in which cancer cells dissociate from primary tumor sites, migrate to distant locations of the body and adapt to new physiological conditions (77). Genetic and epigenetic changes taking place in tumor cells during each of these steps help cancer cells to metastasize and adjust to the new environment (78). Tumors restricted at initial primary sites can be successfully removed surgically or by local irradiations but, if detected after metastasis, the therapeutic interventions mostly become unsuccessful. Metastases often show organ-specific spreading (79). Tumor cells become chemo-resistant by overexpressing multidrug-resistant gene product MDR1, which channelizes various chemotherapeutics outside tumor cells, thus helping in spreading of cancer cells (80).

Suppression of cell cycle and DNA-damage checkpoints create genomic instability which further contribute to evolution of tumors.

Metastatic process consists of several steps tumor (79). This includes local invasion, intravasation, survival of the invading cells in the circulation, extravasation and colonization in a destined organ. The metastatic cascade is initiated by angiogenesis of primary tumor for blood supply required for the metabolic needs (81). Local invasion involves entry of cancer cells from a primary tumor into the surrounding tumor-associated tissue. The locally invasive tumor cells enter into the lumina of the lymphatics or blood vessels by a process called intravasation, characterized by molecular changes that promote the carcinoma cell's ability to adhere and grow on the walls of micro vessels (82). After successful intravasation, circulating tumor cells reside in the venous and arterial circulation for a brief time period. The tumor cells surviving in the circulation are called circulating tumor cells (CTCs). The CTCs then get arrested within the capillary beds at a specific distant site probably due to the layout of the vasculature and size restrictions imposed by blood vessel diameters (78). Next step is the extravasation in which the CTCs form a miniature growth that further ruptures the walls of surrounding vessels. This penetration through the endothelial cells is known as trans-endothelial migration. These cells undergo mesenchymal to epithelial transition (MET) to form micrometastases. Micrometastasis is followed by metastatic colonization in which the migrated carcinoma cells succeed in persisting in the new microenvironment, eventually proliferating to form macroscopic metastasis at the new site. *Figure 1.A.3.* summarizes these events. The epithelial to mesenchymal transition (EMT) acts as a driving force and the initiator of metastatic progression which is discussed in the subsequent section.

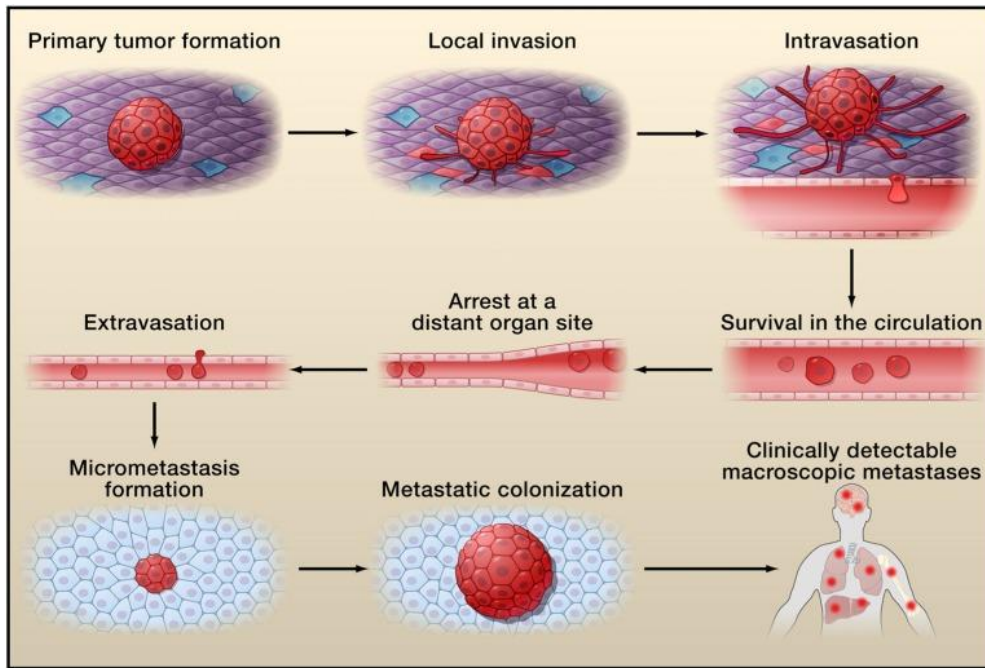


Figure 1.A.3: The invasion-metastasis cascade. Courtesy: Ref. (83).

1.A.4. Factors regulating invasiveness in *H. pylori* infection

1.A.4.1. Epithelial to mesenchymal transition (EMT)

It is a biological process comprising of numerous biochemical interactions that take place between cancer cells of epithelial origin and their surrounding extracellular matrix (ECM) which ultimately confer mesenchymal properties to the epithelial cells. Regulated EMT is necessary for the development of embryo (mesoderm and neural tube formation) and in adult life, during wound healing. But, if unregulated in adult life, it may transform epithelial tissues to invasive tumors. The opposite event of EMT is seen in the last stage of metastasis which is called MET where invasive nature of cancer cells is lost and epithelial markers are regained (84). **Figure 1.A.4.1.** depicts the factors involved in EMT and MET processes.

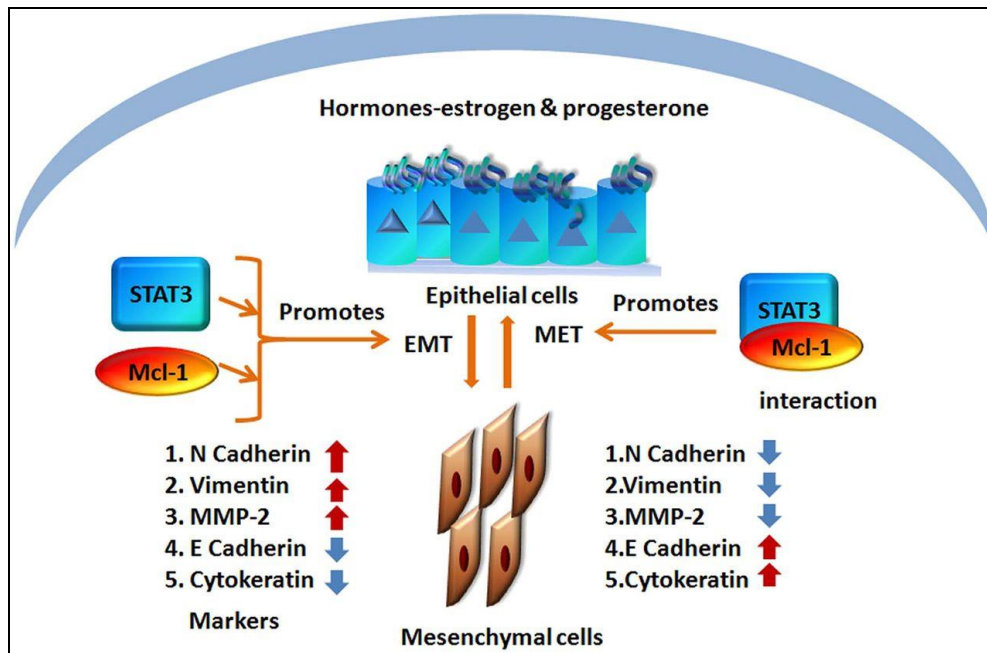


Figure 1.A.4.1: EMT and MET markers. Courtesy: Ref. (85).

H. pylori CagA downregulates epithelial cell surface marker E-cadherin (86). Expression of several EMT markers like N-cadherin, TGF- β 1, Twist, Snail, Slug, ZEB (zinc-finger E-box-binding) 1, ZEB2, twist1, N cadherin, vimentin and CD44, which are considered as hallmarks of EMT, are upregulated in *H. pylori*-positive stomach cancer (87). Among various genes that are either upregulated or downregulated in EMT are mostly regulated by transcription factors like Snail, ZEB, Twist and RING family transcription factor zinc finger protein 139 (ZNF-139) (88). miRNAs are also critical regulators of GC invasiveness. They target mRNAs of tumor suppressors (89) leading to activation of EMT and metastasis pathways (90). EMT causes the downregulation of various tumor suppressors like p53, runt-related transcription factor 3 (RUNX3) and transforming growth factor β (TGF β)-activated kinase 1 (TAK1), to name a few, which otherwise, are known to inhibit the EMT process (91-93). *H. pylori*-infected cells undergo EMT and might express cancer stem cell (CSC)-specific markers (86, 94).

1.A.4.2. Cell adhesion molecules

A number of intercellular junctions are present in vertebrates that are essential for the maintenance of cell polarity, structural integrity of the cell and cell-cell adhesions. The morphological properties of GCCs are manifested by the discrete arrangements of cell adhesion molecules. Various cell adhesion structures like tight junctions (TJs), cadherin-based adherens junction (AJs), gap junctions, desmosomes and cell-ECM junctions help in maintaining cell integrity and cytoskeletal dynamics (95). Cadherins are essential components of junctional complexes, are involved in signaling pathways of β -catenin-Wnt and regulate function of growth factors, cell polarity and tumorigenesis (96) as represented in *Figure 1.A.4.2.1*.

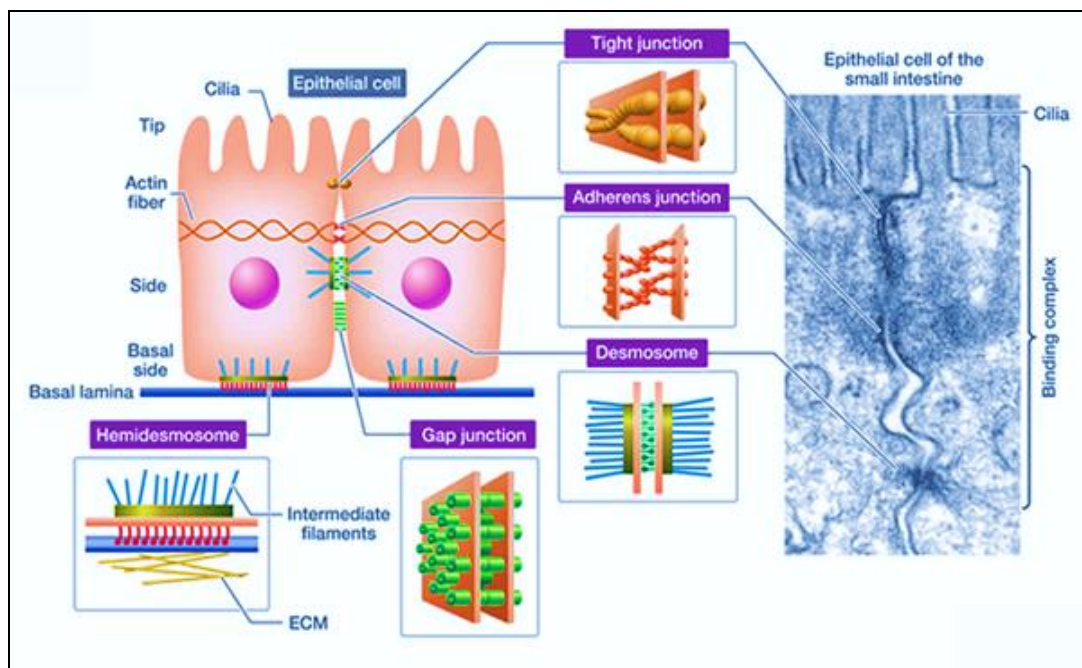


Figure 1.A.4.2.1: Intercellular junctions of epithelial cell. Courtesy: Ref. (97).

AJs are glycoproteins which bind epithelial sheets together and regulate molecular communications within cells. They not only direct cellular organization but also transmit information between cells. These are cadherin-dependent structures which are connected with intracellular cytoskeletal components. AJs belong to cadherin family of cell adhesion proteins

which include various cadherins, desmogleins-collins and other subclasses of cadherins and kinases. Cadherins are present from unicellular yeasts to multicellular organisms (98). They are crucial in the morphogenesis and patterning in higher eukaryotes (99). The extracellular domain of classical cadherins is made up of five ectodomains which bind with calcium ion forming a rod-like homophilic structure which helps its binding with epithelial cadherin (E-cadherin) on neighbouring cell membranes. Classical cadherins are evolutionarily highly conserved. Their cytoplasmic tail binds with β -catenin or γ -catenin, members of armadillo superfamily of repeat proteins. Twelve consecutive β -catenin bound with the cytoplasmic tail of cadherin recruit E-cadherin to the surface of the cells. α -catenin acts as a bridge for binding β -catenin to actin and several actin-associated proteins that help E-cadherin to modulate actin filament organization (97, 100, 101). This ordered structure promotes association between β -catenin and p120 with α -catenin. Intra or inter cellular communications for alterations in gene expressions are transduced to the nucleus through the cytoplasmic tails of E-cadherin as shown in **Figure 1.A.4.2.2**.

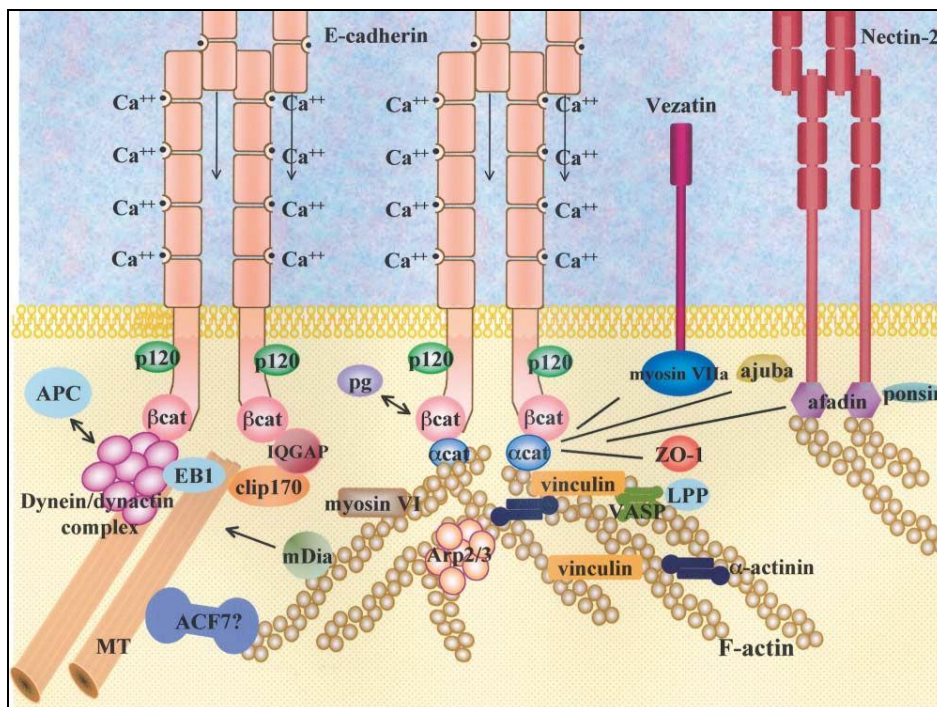


Figure 1.A.4.2.2: Association of E-cadherin with various cellular components.

Courtesy: Ref. (101).

Cell-cell adhesion molecules and E-cadherin are important components of cell polarity, cell differentiation and homeostasis. Most of the human carcinomas are derived from epithelial cells in which tumor suppressor E-cadherin undergo changes due to genetic, epigenetic silencing or degradation. These factors ultimately result in the complete or partial loss of E-cadherin leading to their malignancy. The role of cadherins in cancers are discussed in the next section.

1.A.4.3. Role of cadherins and β -catenin in cancer progression

Several studies have shown that loss of heterozygosity (LOH) containing the E-cadherin gene (*CDH1*) locus at 16q21-q22.1 lead to cancers of the GI tract, liver, prostate, as well as ductal breast carcinoma (102). Somatic mutations leading to in-frame deletions and truncations in *CDH1* gene also are established causes of diffusive GC (**Figure 1.A.4.3.1**). In-frame deletions produce truncated E-cadherin fragments that are non-functional. *CDH1* promoter hypermethylation also contribute to silencing of E-cadherin expression in breast, head and neck and nasopharyngeal cancers (103, 104). Extensive promoter hypermethylation at a distinct CpG island on the 5' promoter region of *CDH1* was shown to be responsible for E-cadherin downregulation. However, the heterogeneity of this phenomenon is dependent on tumor microenvironments. Increased expression of various tumor-promoters like Snail, Slug, Twist1/2, SIP1/ZEB2, delta EF1/ZEB1, HER1/neu, VHL, Hif1 family has been associated with the transcriptional repression of E-cadherin while up-regulating N-cadherin (*CDH2* gene-encoded) and cadherin-11 in multiple cancer types. There functional correlation with E-cadherin was established from animal models, RT-PCR analysis of tumors, overexpression studies, mutagenesis studies and histopathological analysis of these tumor-associated markers (105-107).

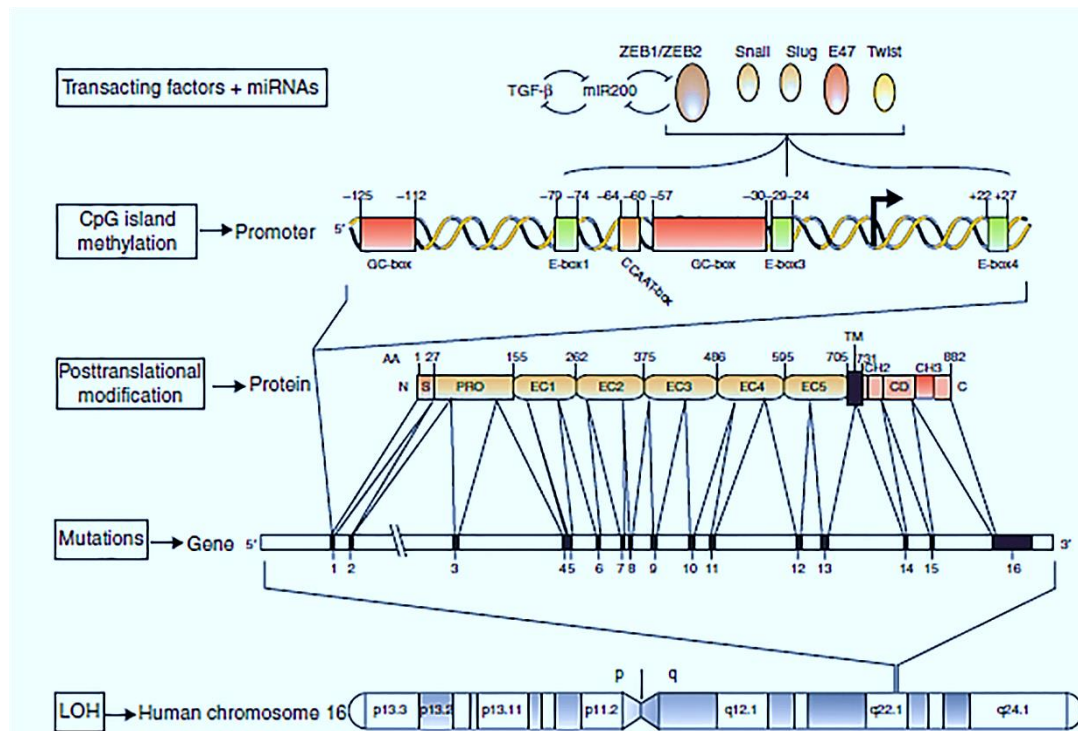


Figure 1.A.4.3.1: Regulation of E-cadherin in cancers. Courtesy: Ref. (102).

Members of miRNA 200 and 205 family repress the transcriptional activities of ZEB1/2, deltaEF1, SIP1, TGFβ2, Snail, Twist mRNAs by directly binding to these mRNAs and repressing their translation (108). Upregulation of various proto-oncogenes like c-Met, Src, EGFR and matrix metalloproteinases like MMP3, 7, 9, 14 leads to E-cadherin degradation and rapid internalization which causes destabilization of cadherin-catenin complex (109). Nieman *et al.* in 1999 showed that overexpression of N-cadherin in epithelial cells led to appearance of mesenchymal phenotype inducing migration, invasion and metastatic ability of cells which helped in survival in the vasculature and in secondary tumor sites (110). Other cadherins like VE-cadherin is known as anti-angiogenic marker and is used in antiangiogenic tumor therapy (111) whereas, less explored cadherin-13 (or T-cadherin, *CDH13* gene) and R-cadherin are considered as tumor suppressors (111).

β-catenin was originally recognized for its ability to bind with E-cadherin at the AJs. Now, it is known for its dual function in gene regulation and cell-cell adhesion (112). In

vertebrates, the membrane-bound pool and the cytoplasmic pool of β -catenin are present. β -catenin mainly binds with E-cadherin in AJs which is released into cytoplasm after being phosphorylated by GSK-3 β which triggers its degradation by 26s proteasome pathway. Wnt signaling leads to the inactivation of Axin/APC/GSK-3 β complex which promotes β -catenin translocation to the nuclear compartment where it transcriptionally upregulates pro-tumorigenic genes (111, 113). Deregulation of E-cadherin or Axin/APC/GSK-3 β genes may also lead to various malignancies (114). β -catenin is also reported as a coactivator of telomerase reverse transcriptase (TERT) which maintains long telomeres, a characteristic of stem cells (115). It also imparts chemoresistance to tumors by activating various MDR-specific genes (116). The importance of β -catenin in cadherin-catenin complex can be understood by the fact that cadherin mutants lacking the β -catenin-binding domain are often less adhesive whereas, mutations in β -catenin lead to non-functional E-cadherin with reduced cell-cell adhesion.

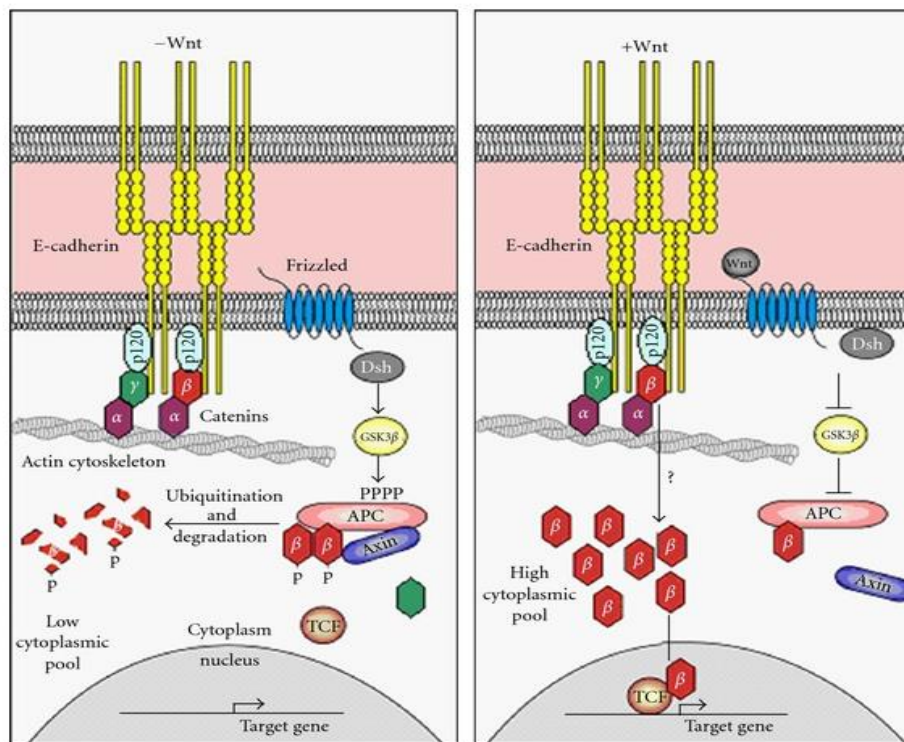


Figure 1.A.4.3.2: β -catenin-Wnt signaling events in cancer. Courtesy: Ref. (97).

Role of tight junctions has also been reported in cell proliferation and cancers (117). Cytoskeletal and actin-binding proteins like filamin family of proteins (FLNs) and Testin (TES) have been attributed for their role as tumor suppressors.

1.A.4.4. Role of *H. pylori* in the disruption of cell-adhesion molecules

The duration of *H. pylori* infection determines the disease outcome. Virulence factors of *H. pylori* disrupt the cell-cell junctions and cell-cytoskeletal matrix arrangement in the infected host (**Figure 1.A.4.4.**) (56). Actin cytoskeletal rearrangements are the bases of *H. pylori* pathogenicity (118). After binding onto the epithelial cells, *H. pylori* injects CagA and associated factors into the host cell via the T4SS. This leads to intracellular changes from signaling pathways to production of proinflammatory chemokines and cytokines. NF- κ B is the principal regulator of major signaling pathways activated by this bacterium. One of the target molecules, Bcl-XL helps in cell proliferation by repressing mitochondrial apoptosis pathway (119). CagA upon translocation into the cytoplasm of infected cells undergoes multiple tyrosine phosphorylation at EPIYA motifs by Src-family of kinases. Phosphorylated CagA activates MAPK/ERK pathway and inactivates tyrosine kinase called focal adhesion kinase (FAK) which is a crucial regulator of focal adhesion spots. Its inhibition leads to cell elongation also known as the “hummingbird” phenotype, a hallmark of *H. pylori* infection. FAK regulates Rho family of GTPases which control mDia/RhoA/Rac/Cdc42 axis, thereby modulating microtubule assembly-disassembly, stress fibres, lamellipodia and filopodia formations. These cytoskeletal components are essential for cell migration and proliferation (120). *H. pylori*-secreted protease, HtrA cleaves E-cadherin leading to the destabilization of AJs and increasing the cytoplasmic pool of β -catenin which further translocates to the nucleus upon Wnt activation to transcribe numerous oncogenes (121).

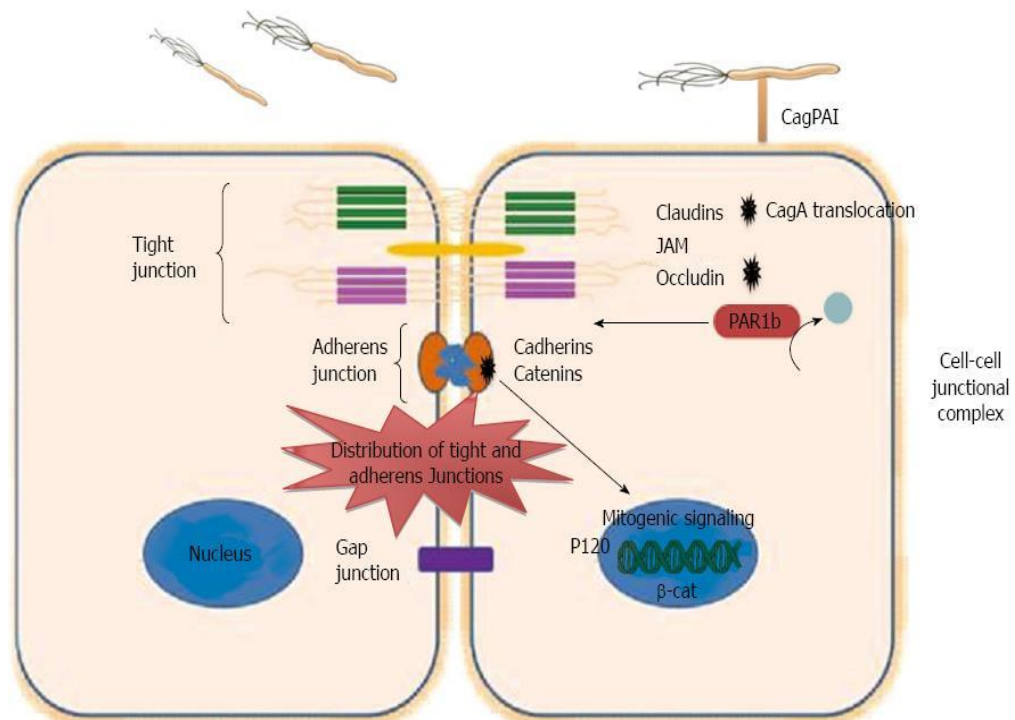


Figure 1.A.4.4.: Epithelial barrier disruption by *H. pylori*. Courtesy: Ref. (120).

1.A.4.5. FLNs and their roles in cancers

Components of epithelial cell junctions are attached to the cytoskeletal actin filaments which provide contractile forces and regulate cell turgor pressure, shape as well as motility (122). Actins are very abundant molecules in gastric epithelial cells. The family of cytoskeleton proteins, FLNs (FLN-A, B and C), are composed of two parallel 280 kDa subunits. They stabilize actin networks and connect the latter with the cell membrane (123). Each subunit contains N-terminus actin-binding region, with 23 repeating domains following it. Filamin and actin form either loose microfilament networks in the cell cortex or form stress fibres with tightly packed bundles.

Cell adhesion and metastasis are dependent on cytoskeletal proteins. Filamins hold transmembrane proteins and intracellular signaling molecules together. Filamins are also found in some focal adhesions. Deregulated FLN-C has been associated with various diseases including primary as well as secondary GCs (124). FLN-C expression decreases in

various cancers where it undergoes degradation by promoter hypermethylation (125). As FLN-C is a part of cell cytoskeletal network, it plays crucial functions in maintaining cell polarity and adhesion (126) and mostly associated with tumor suppression (127). However, Adachi-Hayama group has identified pro-cancerous roles of FLN-C in low-grade gliomas (128).

1.A.4.6. TES and its roles in cancers

TES is a LIM-domain-containing scaffolding protein and has functional significance in adhesion of cells, cell-spreading and actin cytoskeletal arrangement. It is also present at focal adhesion points helping in the cell-cell interactions. LIM domains are the evolutionarily conserved double zinc-finger motifs that are crucial in protein-protein interactions such as transcriptional activity, cytoskeletal binding and cell signaling. It is also associated with cell proliferation and motility (129). Mutational analysis and detection of methylation sites in TES have supported its tumor-suppressive roles (130). TES is also a known tumor suppressor in GC (130, 131) as well as in other cancers (132, 133). However, effects of FLN-C and TES in *H. pylori*-mediated GC remain completely unknown.

Section B. Ubiquitination-mediated proteasomal degradation pathways and GC

Cellular stress, even stress due to infection, is regulated most often, by ubiquitin (Ub)-mediated proteasomal degradation pathways. E1 enzymes (Ub activators), E2 enzymes (Ub conjugating enzymes) and E3 enzymes (Ub ligases) carry out targeted proteasomal degradation of misfolded or short-lived proteins or proteins that need to be cleared from the system. This important machinery is responsible for the maintenance of protein homeostasis, vesicular trafficking, cell cycle regulation as well as immunity, to name a few (134). It is not surprising that infectious agents most often evolve strategies to interfere with this system. Genetic and epigenetic alteration of the components in this machinery is accountable for various diseases including cancer. A recent report has shown that *H. pylori* exploits

ubiquitination of host proteins to adhere to host cell surface (134). Another study long back in the year 2003 by Eguchi *et al.* has shown that the cyclin-dependent kinase (cdk) inhibitor, p27 is downregulated by proteasomal degradation induced by *H. pylori* and increases the risk of GC (135). E3 Ub ligases are the rate-limiting enzymes regulating proteasomal degradation. Studies from our group have found that Siah family E3 Ub-ligases are upregulated in *H. pylori*-infected GCCs and increase invasiveness (136, 137). Posttranslational modifications (PTMs) are crucial regulators of E3 Ub ligase function (138-140). Effects of phosphorylation on Siah proteins are known to some extent (138, 141). However, as acetylation of Siah proteins has never been reported, my study focuses to understand the effect of *H. pylori* on acetylation and stability of Siah proteins. This section will elaborate on proteasome machinery, E3 Ub-ligases, Siah proteins and lastly the known effects of these proteins in cancer.

1.B.1. Proteasome machinery

The degradation of cellular proteins is a highly intricate, timely and tightly-regulated event which affects a broad array of basic cellular processes. It is accomplished by a complex cascade of enzymes which exhibit extreme specificity towards their numerous target molecules. Proteasomal targets can be regulators of cell growth, signal transduction pathway components, housekeeping and cell-specific metabolic pathways enzymes and damaged proteins. Degradation of a protein by the Ub pathway consists of two distinct and successive steps: i) Covalent attachment of multiple Ub molecules to the substrate and ii) Marked-substrate degradation by 26S proteasomal pathway. Ub is a highly conserved, 76 aa-containing small modifier protein found only in the eukaryotes. Whether an ubiquitinated protein will be targeted for degradation or regulation of intracellular processes is dependent on the size of the target molecule (142) and also on the extent of ubiquitination (143). Polyubiquitination leads to proteasomal degradation of target proteins (144).

26S proteasome is the proteolytic machinery of the Ub-mediated degradation pathway. It is complex and highly conserved in eukaryotes in terms of its structure and which includes more than 30 different subunits. The proteasome complex consists of a barrel-shaped 20S protease core particle (CP) in the middle part (145). The CP is made up of two identical inner β -rings and outer α units are stacked on one another in an axial heptameric pattern. Each end of CP is made up from 19S regulatory particle (RP) that regulates the functional core. The 19S RP is further divided in two components; base-lid sub-complexes (145). Ub attachment to the target protein is a reversible process catalyzed by specific Ub-ligases and proteases or deubiquitinating enzymes (DUBs) which help in maintaining Ub monomers in the cellular pool (146).

Ub conjugates to its substrate by a three-step process (147). First, the ubiquitin-activating enzyme, E1 activates Ub at its C-terminal in an ATP-dependent manner, followed by transferring it from E1 to E2 enzymes (Ub-carrier proteins or Ub-conjugating enzymes, UBCs) and finally to ubiquitin-ligase family enzyme E3 which causes covalent attachment of Ub to a Lys residue of the target substrate as shown in *Figure 1.B.1.1*. Subsequent additions of multiple Ub is followed. Specific substrate recognition adds to the significance of E3 ligase, which upon identification, undergoes mono or polyubiquitination.

1.B.2 E3 Ub ligases

E3s are divided into three classes based on recognition of substrate and their domain structures: N-terminal targeting proteins, homology to E6-associated protein (E6AP) carboxyl terminus (HECT) domain-containing proteins and the really interesting new gene (RING) finger domain-containing proteins, including its derivatives, the U-box and the plant homeo-domain (148).

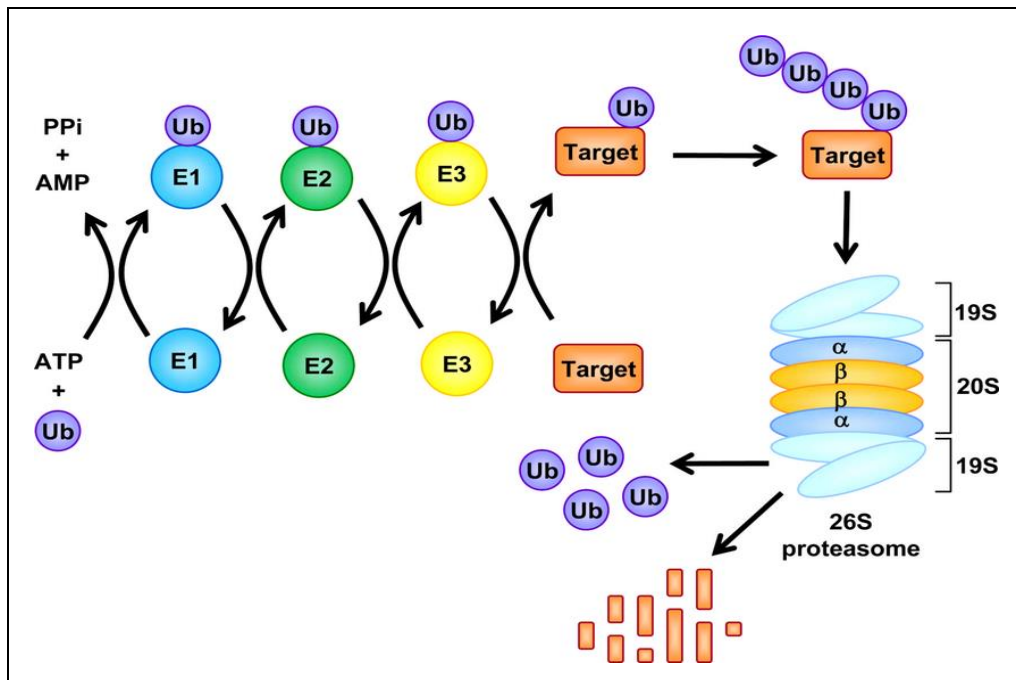


Figure 1.B.1.1: The Ub-proteasome pathway. Courtesy: Ref. (149).

1.B.3. RING type E3 Ub ligases and their involvement in cancer

The RING type and the HECT type are the two most commonly found E3s. In humans, nearly 95% of E3s belong to the RING family and only 28 enzymes belong to the HECT family. As represented in **Figure 1.B.3.1**, these two families show dissimilarity only in the way of substrate presentation. RING type E3s have a RING finger, a small zinc-binding domain that specifically binds to E2 Ub ligases, thereby promoting Ub targeting (150). The proteins with RING domain may act as E3 Ub ligases. It is the product of human gene *RING1* (*Really Interesting New Gene 1*) located near to the major histocompatibility region on chromosome 6. A RING finger contains two Zn^{2+} -coordinating domains which aid in E2-dependent ubiquitination of targeted substrate (151).

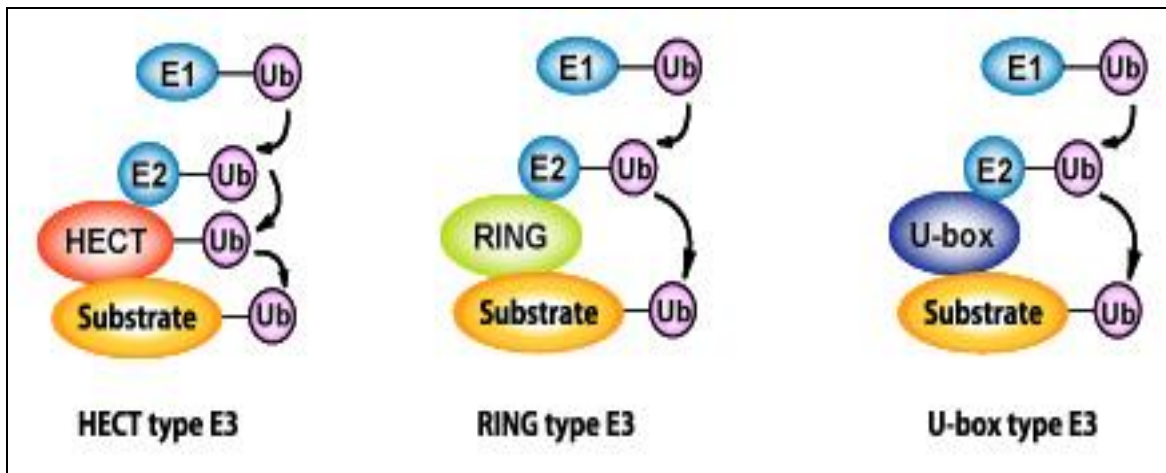


Figure 1.B.3: Types of E3 Ub ligases. Courtesy: Ref. (152).

1.B.3.1. Involvement of RING type E3 Ub ligases in human cancers

Members of the RING family E3 Ub ligases are crucial for DNA repair, cell cycle, apoptosis, receptor and transporter regulation, endoplasmic reticulum-associated degradation (ERAD) and angiogenesis (151). Several members of these subfamily are associated with various disease pathogenesis including cancer, acting as both oncogenes and tumor suppressors. Point mutation within E3 Ub ligase BRCA1, a gene product of breast cancer associated gene 1 (*BRCA1*) predisposes female carriers to breast and ovarian cancers (153). Mutations in components of FANCD1 (Fanconi) E3 ligase, also crucial in DNA repair process leads to the multisystemic Fanconi anemia, multiple developmental defects in children who survive but with heightened risk of acute myeloid leukemia (154). E3 ligases like casitas B-lineage lymphoma family members (Cbl), the tripartite motif (TRIM) superfamily, BMI-1, PML, RAG1, Rbx1 and MDM2 act as protooncogenes (155-159). Many members of the cullin-RING Ub-protein ligases (CRL) superfamily are reported in colorectal cancer, stomach cancer, breast cancer and skin cancer (160).

Metastasis is a fundamental process in cancer progression and is the principal reason for mortalities by cancer. Hypoxia or low oxygen stress formed in tumor microenvironment

is a critical factor in metastases (161). The RING finger E3 ubiquitin ligase protein Von Hippel-Lindau (pVHL), which has pro-apoptotic function, is found inactivated in clear-cell renal cell carcinoma (ccRCC) leading to stabilization of Hif1 α , a potent oncoprotein (162). Another class of RING finger E3 Ub ligases regulating Hif1 α stability are Siah proteins. The functional implications of Siah proteins in various cancers are discussed in the next section.

1.B.4. Siah proteins

The human homolog of *Drosophila* seven in absentia (*sina*) gene, a superfamily of RING finger E3 Ub ligases, is extremely conserved from lower vertebrates to mammals. Humans have three *siah* genes, *siah1*, *siah2* and *siah3*, whereas mice have three *siah* genes- *siah1a*, *siah1b* and *siah2*. *Siah3* has not yet been functionally characterized. They share 85.7% homology which sometimes makes them functionally redundant (163). Siah proteins are dimeric with two novel zinc-containing motifs. Siah proteins feature a less-conserved N-terminal region, a functionally-important RING domain which is extremely conserved and a substrate-binding domain (SBD) at the C-terminal as shown in **Figure 1.B.3.1**. The RING domain regions of human Siah1 (hSiah1) and hSiah2 are between 41-75 aa (164) and between 80-115 aa, respectively (4). This difference facilitates their interaction with distinct target molecules (165). Proteins containing Siah “degron” (degradation on) motif (PxAxVxP; x=any amino acid) bind with the SBD of Siah proteins to undergo ubiquitination (163, 166). The SBD of Siah proteins is fully characterized (167) and shows homology with tumor necrosis factor (TNF) receptor-associated factor (TRAF) proteins (9). There are more than 30 recognized substrates that interact with Siah proteins (168). Interaction is either direct with substrates or through proteins like Siah-interacting protein (SIP) that act as an adaptor molecule (169, 170). Like other E3 Ub-ligases, Siah proteins are also implicated in several cellular processes e.g. angiogenesis, inflammation, cell proliferation, migration, apoptosis and maintenance of cellular homeostasis (171-175).

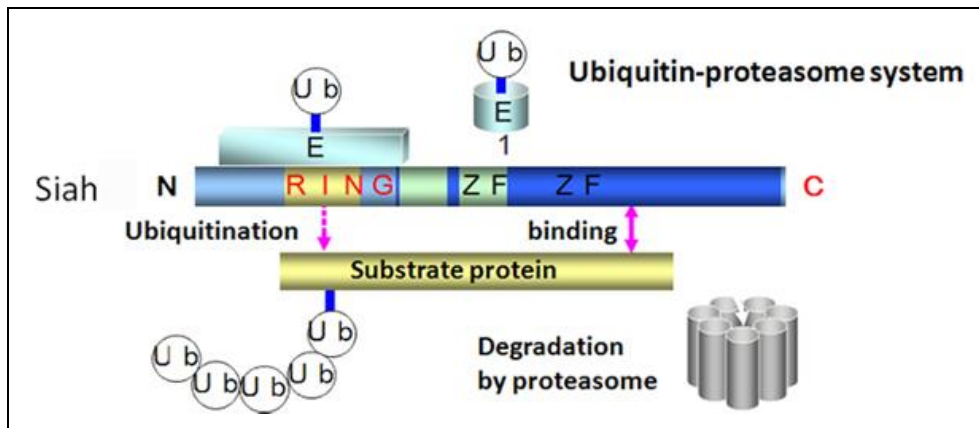


Figure 1.B.4: The RING domain structure of Siah proteins. Courtesy: Ref. (176).

1.B.4.1. Role of Siah proteins in cancer progression

Siah proteins target ubiquitination and degradation of several regulators such as TNF-associated factor (TRAF2), prolyl hydroxylases (PHDs), β -catenin, NUMB, Sprouty2, etc., (168). Das *et al.* established that Siah1 and Siah2 proteins have metastasis-inducing effects in GCCs infected with *H. pylori* (136, 137). Siah2 also regulates survival and growth of hypoxic tumor cells in hypoxic microenvironment (177). Siah1 and Siah2 have oncogenic functions in animal models, while *in vitro* cell-based assays suggest precancerous functions of Siah2 and anti-cancerous functions of Siah1 (178). Siah2 can act as a prosurvival factor in oral (179) and breast (180) cancers and are crucial in ROS metabolism (181). Some substrates are targeted by both Siah proteins while some are targeted by one and not by the other. This selectivity can be attributed to PTMs of these proteins or their subcellular localization (178). Substantive efforts have been made to understand their functions in cancer, but mechanisms of various posttranslational modifications (PTMs) regulating their functions are poorly understood. Factors regulating PTMs of Siah proteins and their implications in cancer progression are described in the next section.

Section C. Factors regulating PTMs of Siah proteins

Effect of PTMs on the stability and function of Siah proteins has been reported by various groups. Siah1 stabilization by c-Jun N-terminal kinase (JNK) leads to JNK pathway-mediated cell death of neuronal cells (182). Siah phosphorylation stabilizes tumor suppressor-protein HIPK2 in DNA damage-induced ATM/ATR pathway, resulting in increased apoptosis (138, 183). Under normoxia, HIPK2 binding with Siah2 is very less while hypoxia induces Siah2-HIPK2 interaction (138). As a result, Siah2 is phosphorylated in hypoxia, inhibits Siah2-HIPK2 interaction and leads to HIPK2 stabilization which exerts its apoptotic effects (138). Tumor-promoting functions of Siah2 in hypoxia have been linked with Ras/ERK or p38 MAPK pathways (141, 184). RAS-mediated pancreatic cancer cell growth is suppressed by inhibition of Siah2-dependent proteolysis (185). In hypoxia, p38 MAPK-mediated Siah2 phosphorylation induces interaction of Siah2 with PHD3, a factor responsible for Hif1 α degradation (141). A Ser/ Thr kinase DYRK2 also regulates Siah2 function by phosphorylation at five S and T residues which stabilizes Hif1 α protein (4). Upstream survival protein 13 (USP13) protects Siah2 from autoubiquitination and degradation by phosphorylation (186).

The effect of phosphorylation on subcellular localization Siah proteins is also reported. Phospho-Siah2 is excluded from the nucleus and compartmentalized in the perinuclear region (4). Phosphorylated Siah1 transports GAPDH to the nucleus which activates the cell death cascade signifying additional roles that Siah could play in cellular processes (172). Phosphorylation and SUMOylation also regulate Siah2 activity (139, 140). These reports clearly indicate that both Siah1 and 2 proteins have varied roles in regulating cancer depending on their posttranslational modification status, tissue types, and physiological conditions. Apart from phosphorylation and SUMOylation, Ub ligases are also known to be regulated by acetylation which is described in the next section.

1.C.1. Role of acetylation in regulating the structure and function of proteins

Protein acetylation is a common posttranslational event among eukaryotes. More than 85% of eukaryotic proteins undergo acetylation at the N α -terminus (187). A less common, but more critical, form of protein acetylation takes place at the ξ -amino group of lysine (K). There are only a few reports on the effect of acetylation on E3 Ub ligases altering their activity. Many non-histone proteins have been elucidated as acetylation targets and reversible K-acetylations in these proteins play significant function(s) in mRNA/protein stability regulation (188), protein subcellular localization and proteasome dependent and independent degradation (189), interactions in between DNA and proteins (190). The degradation of anti-tumorigenic protein p53 by E3 ligase Mdm2 is abrogated by p53 acetylation. There are also other reports which contradict this study. p53 degradation by TIP60 (Tat-interacting protein of 60KDa)-mediated acetylation is suppressed by UHRF1 (Ub- like protein with PHD and ring finger domains 1) protein by inhibiting their interaction (191). GCN5 also regulates the stability of oncoprotein E2A-PBX1 by acetylation resulting in cell transformation (192). Another E3 ligase pVHL causes Hif1 α degradation upon being acetylated in normoxia (193). The acetylation can even inhibit degradation of proteins by inhibiting ubiquitination (194) or can recruit E3 ligases for degradation of acetylated proteins (156). E3 ligase acetylation is not only linked with different cancers but also with many other physiological abnormalities like glucocorticoid-induced muscle atrophy in which E3 ligase (MuRF1) acetylation by p300 inhibits ubiquitination of factors regulating transcription in muscle atrophy like C/EBP- β and δ , FOXO1/3a, and p65 (195).

Compartment-specific accumulation of certain proteins are critical in cell proliferation, differentiation and cancers. Various reports have investigated acetylation induced compartmentalization of proteins thereby modulating their subcellular localization. c-Abl accumulates in the nucleus by translocation from the cytoplasm during DNA damage and

apoptosis. p300, CBP and PCAF HAT have been found to acetylate c-Abl at Lys 730 leading to its cytoplasmic retention which cause myogenic differentiation (196). What causes differential subcellular localization of E3 Ub ligases is not clearly known but recent data suggest that acetylation along with other PTMs can result in their different subcellular localization and function. Acetylation at the nuclear localization signal (NLS) of E3 Ub ligase Skp2 helps in its stability and translocation to cytoplasm (197). Besides regulating various functions of proteins, acetylation also regulates accessibility of proteins by affecting subcellular localization. One such example is acetylation-mediated nuclear localization of glyceraldehyde-3-phosphate dehydrogenase (GAPDH) (198). Siah1 has nuclear localization signal (NLS) and helps in the nuclear translocation of GAPDH. Upon nuclear translocation, GAPDH is acetylated at K¹⁶⁰ and thereafter, it leads to p53-mediated cell death (199).

Given the effect of acetylation on protein structure, stability, protein-protein interactions, translocations and protein function, especially, on various E3 Ub ligases, we sought to investigate the role of acetylation on Siah proteins and its role in *H. pylori*-mediated GC in this thesis work.

RESULTS

(Chapters 2-6)

**Induced expression of Siah proteins in mouse
stomach infected with *H. felis* and in human
gastric adenocarcinoma samples**

Chapter 2

Chapter 2: Induced expression of Siah proteins in mouse stomach infected with *H. felis* and in human gastric adenocarcinoma samples

2.1. *Helicobacter*-infected human and mouse gastric epithelia show increased level of Siah proteins

Siah proteins belong to the family of RING type E3 Ub ligases that degrade their substrates by proteasome-mediated pathway (163). Both Siah1 and 2 are reported as oncogenic proteins in various cancers whereas, few reports suggest Siah1 as tumor suppressor and Siah2 as pro-cancerous (168). But, the role of Siah proteins in GC progression is poorly understood. To determine the role of Siah proteins in GC, it was a prerequisite to assess their expression in human gastric carcinoma samples and in animal models. *Helicobacter*-infected human gastric adenocarcinoma and metastatic biopsy tissue samples were obtained from antral portion of stomach of consenting patients (stage III, rapid urease test-positive). *H. felis* infection in C57BL/6 mice progresses through metaplasia and dysplasia leading to carcinogenesis and this model system mimics the classical morphological cascade of events occurring in gastric carcinogenesis in humans (200). *H. felis*-infected C57BL/6 mice were used for animal studies. C57BL/6 mice were infected with 1×10^{10} CFU of O/N-grown *H. felis* and the infected mice were maintained for 8-12 months following which animals were sacrificed and their stomachs were isolated. Human and mouse gastric tissues were stained for Siah1 and Siah2 proteins and were assessed by immunofluorescence (IF) microscopy (Figure 2.1 and Figure 2.2). Haematoxylin and Eosin (H&E) and IF staining exhibited marked increase in Siah1 and Siah2 protein level in the infected, cancer tissue samples in comparison to their respective controls. *H. felis*-infected mice showed symptoms of gastritis and precancerous ulcerations representing distinct metaplasia of mucus glands, dysplasia with marked induction of Siah proteins compared to non-cancer tissues. Thickening of mucosa with extensive submucosal invasion was also observed (136).

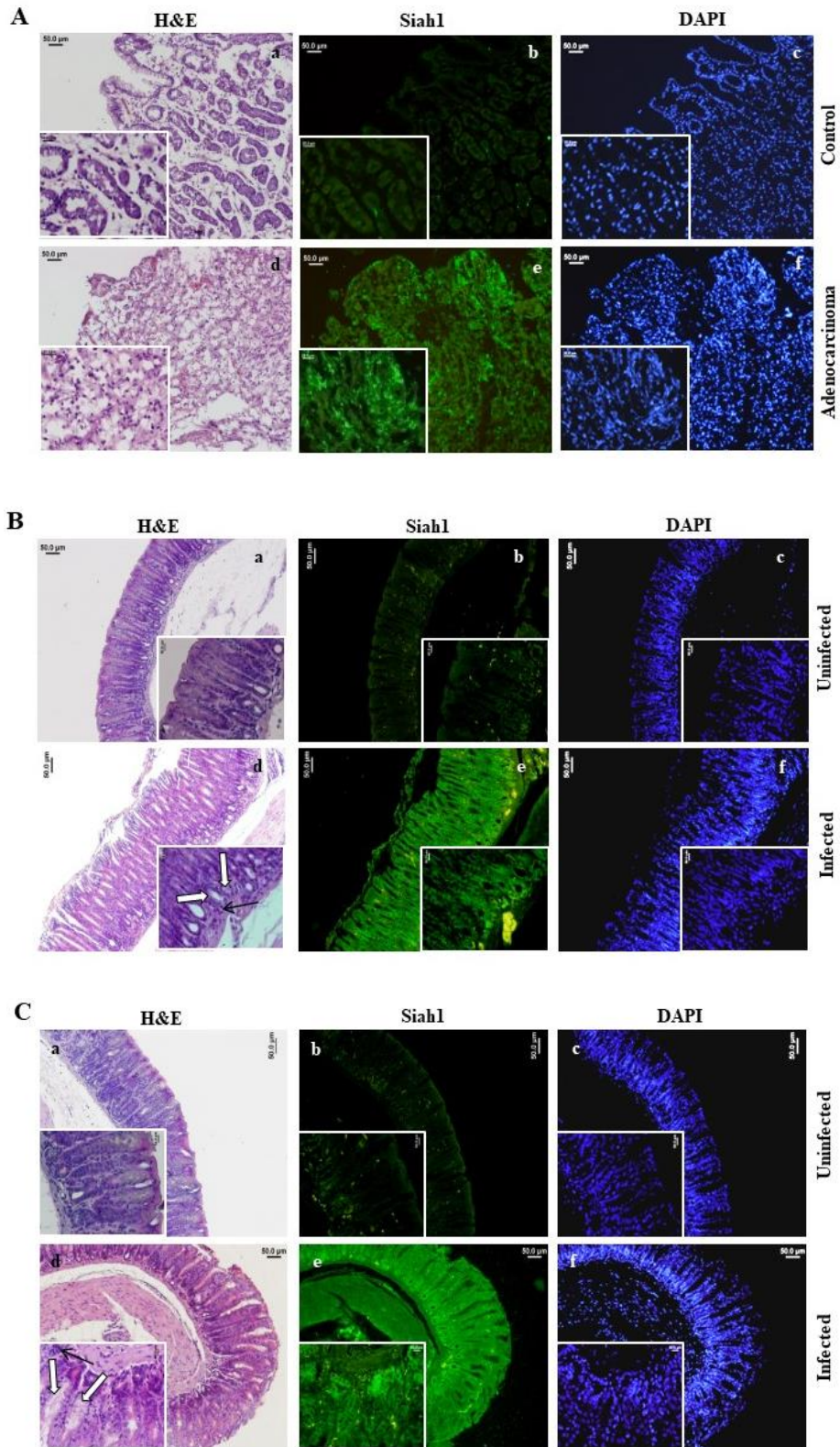


Figure 2.1: Induced expression of Siah1 is noticed in *Helicobacter*-infected human and mouse gastric epithelia. (A) H&E staining of human non-cancer (a) and adenocarcinoma (d) biopsy samples (n=10 for each group) and IF staining for Siah1 (b and e) and DAPI (c and

f). Original magnification 100X, inset 400X. Scales shown 50 μ m. Inset scale 20 μ m. (B) H&E staining of uninfected (n=16) and infected (n=16) antral gastric tissues from C57BL/6 mice (a and d) and their corresponding fluorescence microscopy images showing Siah1 (b and e) and DAPI (c and f) staining. Infected mice showing inflammation (thin arrow), mucus metaplasia (thick arrow) in the mucosa. (C) Data representing similar observations in another set of uninfected and infected mouse gastric tissues. Original magnification 100X, inset 400X. Scales shown in (B) and (C) 50 μ m. Inset scales 50 μ m.

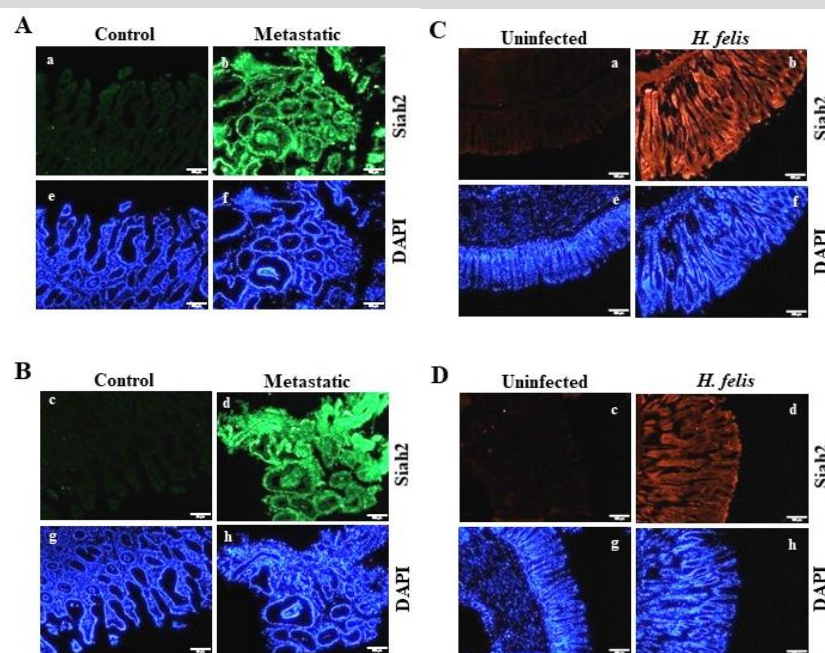


Figure 2.2: Induced expression of Siah2 in *Helicobacter*-infected human and mouse gastric epithelia. (A) and (B): IF staining images of human non-cancer and infected metastatic GC biopsy samples (n=14) showing expression of Siah2 (a, b, c and d) and DAPI (e, f, g and h). Original magnification 100X. Scales shown 100 μ m. (C) and (D): IF images of uninfected and infected (n=16) antral stomach tissues from C57BL/6 mice showing expression of Siah2 (a, b, c and d) and DAPI (e, f, g and h) staining. Original magnification 100X. Scales shown 100 μ m.

2.3. Discussion

Gastric adenocarcinoma, a major cause of cancer-related mortalities worldwide is the second and fourth most frequent cancer in males and females, respectively (10). Infection with *H. pylori* is reported as the most important risk factor for GC. As a result of colonization by *Helicobacter* responses to inflammations and neoplastic changes increase resulting in loss of the gastric epithelial cell polarity, membrane integrity and barrier function (145, 201). We found that *H. felis* infection in C57BL/6 mouse gastric mucosa enhanced Siah1 and Siah2 protein levels as detected by immunofluorescence microscopy (136, 137, 202). *H. pylori*-positive adenocarcinoma and metastatic gastric cancer biopsy samples collected from consenting patients also showed enhanced expression of Siah proteins. H&E staining of *H. felis*-infected C57BL/6 mice demonstrated various epidemiological evidences of gastric carcinogenesis including atrophic gastritis, inflammation with severe infiltration of macrophages, neoplasia, metaplasia and adenocarcinoma. This is the first report to show a positive correlation between enhanced expressions of Siah proteins and gastric cancer progression using animal model.

Sustained *H. pylori* infection leads to gastritis and induction of precancerous processes (7). In the present study, we found that human gastric adenocarcinoma and metastatic tissue samples were diagnosed positive for *H. pylori* and displayed a marked increase in expression of Siah1 and Siah2 proteins (Figure 2.1A and Figure 2.2A and B). In panel d of Figure 2.1A, gastric adenocarcinoma tissue samples showed excessive infiltrative cells with abundantly displaced nuclei to the periphery of the cells. The normal gastric cellular morphology was completely replaced with large mucinous cells, individual or in clusters floating around, giving a small microscopic tumor-like appearance. The sequential changes in the stomach caused by *H. pylori* infection leads to gastritis or atrophic gastritis with intestinal metaplasia, dysplasia which further progresses to metastatic adenocarcinoma. This model is only

applicable to intestinal type adenocarcinoma but not to the diffuse type. In our study, the metastatic sample also showed few developed glandular structures, an evidence of gastric carcinoma of diffusive type caused by *H. pylori* infection.

As per the Correa's and Lauren's classification systems on histological differentiation of gastrointestinal cancers, the well-differentiated intestinal-type of cancers are mostly influenced by *Helicobacter* infections which lead to formation of cohesive neoplastic cells forming glands-like tubular structures that frequently infiltrate into surrounding tissues and cause ulcerations (7, 205). We observed that *H. felis*-infected mouse gastric tissue samples were urease positive. In panel A and B of Figure 2.1 and panel C and D of Figure 2.2, infected samples showed inflammatory gastric atrophy characterized by thickening of gastric mucosa as compared to the uninfected tissue. Infected samples also displayed mucosal metaplasia. Fluidic secretions in the basal mucosal cells is a distinctive feature of mucosal metaplasia in *H. felis*-infected C57BL/6 mice. However, the gastric epithelial morphology did not change to the intestinal type indicating non-intestinal type of metaplasia which has higher risks of gastric carcinogenesis as compared to intestinal type metaplasia. The infected tissue was also predisposed to inflammatory infiltrations which marked the host responses to *Helicobacter* infections.

Siah proteins belong to RING type E3 ubiquitin ligase family of proteins which mark their targets by ubiquitination leading to their proteasomal degradation (173). These proteins have been found to be upregulated in breast, hepatic and colon cancers but their expression patterns and roles in *H. pylori*-mediated gastric epithelial pathophysiology was entirely unexplored. As the fate of cancer progression and metastasis is often essentially dependent on Siah protein's binding with their diversified targets and roles of these targets in cancer suppression or progression, the next part of this research was focused to understand the effect of *H. pylori* on Siah proteins and the effect of Siah proteins in gastric cancer progression.

**Siah2, but not Siah1 is acetylated by *H. pylori*
infection**

Chapter 3

Chapter 3: Siah2, but not Siah1 is acetylated by *H. pylori* infection

3.1. Siah2 undergoes acetylation in *H. pylori*-infected human GCCs

H. pylori-infected GCCs show significantly enhanced expression of Siah1 and Siah2 proteins (136, 137). However, PTMs of Siah1 and Siah2 in *H. pylori*-infected GC were not studied. Acetylation of proteins is one of the most crucial types of PTMs as it regulates protein stability, function, metabolism and interactions (206, 207). Role of phosphorylation in regulating various functions of Siah proteins is well established. As regulation of Siah proteins by acetylation is still unexplored, acetylation status of Siah proteins was examined in this thesis work. Siah1 and Siah2 proteins were overexpressed by transiently transfecting *siah1* and *siah2* plasmids in MKN45 cells followed by infection with *H. pylori* 26695 at 200 multiplicity of infection (MOI) (Figure 3.1A). *H. pylori* strain 26695 is a reference strain and is *cag* PAI (+). The induction of acetylation of Siah proteins was studied 12 h post-infection (p.i.). The isolated cell lysates were western blotted (n=3) and the acetylation status of Siah proteins was determined by probing the blots with pan acetylated lys (ac-lys) antibody followed by reprobing with Siah1 and Siah2-specific antibodies. respectively. Acetylation of Siah2 was substantially induced after *H. pylori* infection as those of the uninfected cells but to our surprise, we did not observe any acetylation of Siah1 protein (Figure 3.1A) although Siah1 and Siah2 proteins share 98% homology with each other. However, both Siah1 and Siah2 protein level increased after infection with *H. pylori* as previously reported with bands detected at 32 and 35 kDa, respectively (136, 137, 202). As acetylation of Siah1 was not observed, therefore, my thesis work focused on acetylation of Siah2, Siah2 functional regulation by acetylation and its effect on *H. pylori*-mediated invasiveness of GCCs. Human *siah2* (NCBI reference sequence: NP_005058.3, gi: 31982899) is a 975 nt long gene which codes for a 324 aa peptide with 11 lys (K) residues (Figure 3.1B).

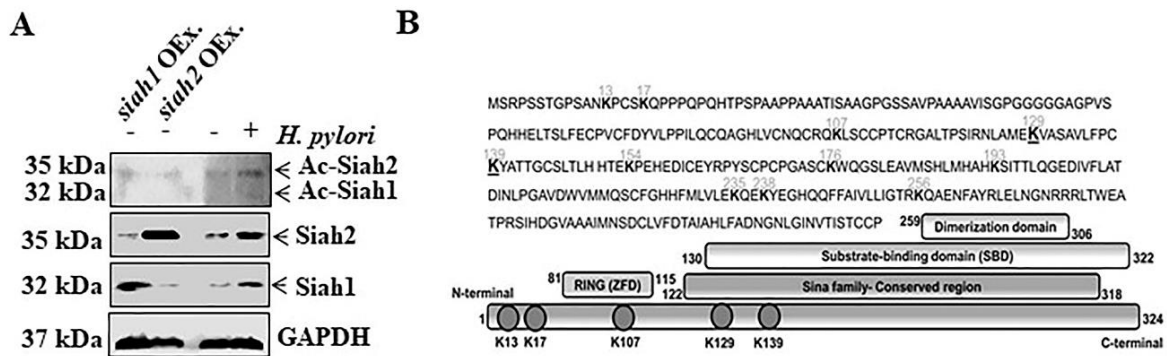


Figure 3.1: Siah2 undergoes acetylation in *H. pylori*-infected GCCs

(A) Immunoblotting (n=3) of cell lysates prepared from MKN45 cells transiently transfected with either *siah1* or *siah2* constructs and infected for 12 h with MOI 200 of *H. pylori* or left uninfected showed increased Siah1, Siah2 and ac-Siah2 proteins in infected cells. (B) Diagrammatic representation of Siah2 domain-structure.

Siah2 protein has 3 major domains, the N-terminal RING domain {a characteristic of Siah2 E3 Ub ligase family of proteins consisting of two identical zinc-finger domains (ZFD)} (208) (from 81- 115 aa), a C-terminal dimerization domain (from 259- 306 aa) which lies in a highly conserved region characteristic of *Sina* family proteins (from 122- 319 aa). This region also has another important domain known as the substrate binding domain (SBD, from 130- 322 aa). As Siah2 protein has many lys residues, the probability of Siah2 acetylation was predicted using GPS-PAIL online tool (209) (Figure 3.2A). Among these lys residues, lys 13, 17, 107, 129 and 139 showed probability of acetylation. Out of which, K¹²⁹ and K¹³⁹ had the highest probability to undergo acetylation. K¹³ and K¹⁷ are in the N-terminal region of Siah2, while K¹⁰⁷ in the ZFD and K¹²⁹ and K¹³⁹ are in the SBD. K¹²⁹ and K¹³⁹ correspond to K¹³⁰ and K¹⁴⁰ residues of mouse Siah2 (mouse Siah2 GenBank: NP_033200.2). As K¹²⁹ and K¹³⁹ showed the highest probability to undergo acetylation and as they belong to the SBD region, we investigated the effect of acetylation-null mutations at K¹²⁹ and K¹³⁹ residues on Siah2 function. By using site-directed mutagenesis kit,

acetylation-null *siah2* K129R and K139R constructs were generated. The empty vector, *siah2* WT, *siah2* K129R and *siah2* K139R constructs were transiently transfected in MKN45 cells and total Siah2 and its acetylation were accessed by immunoblotting (Figure 3.2B). Densitometric analysis from 3-independent experiments revealed that, *H. pylori*-mediated induction in total and ac-lys Siah2 was maximal in Siah2 WT-expressing cells. Siah2 K129R-expressing cells showed downregulation of Siah2 and its acetylation as compared to WT-transfected cells. Whereas, K139R mutation led to a significant decrease in Siah2 expression as well as its acetylation as compared to *siah2* WT and *siah2* K129R-transfected cells. This was indicative of probable degradation of Siah2 protein following K139R mutation. To avoid variations caused due to transient transfections, we generated stably-expressing MKN45 cells (Figure 3.2C) and AGS cells (Figure 3.2D) which were used for all future experimental studies.

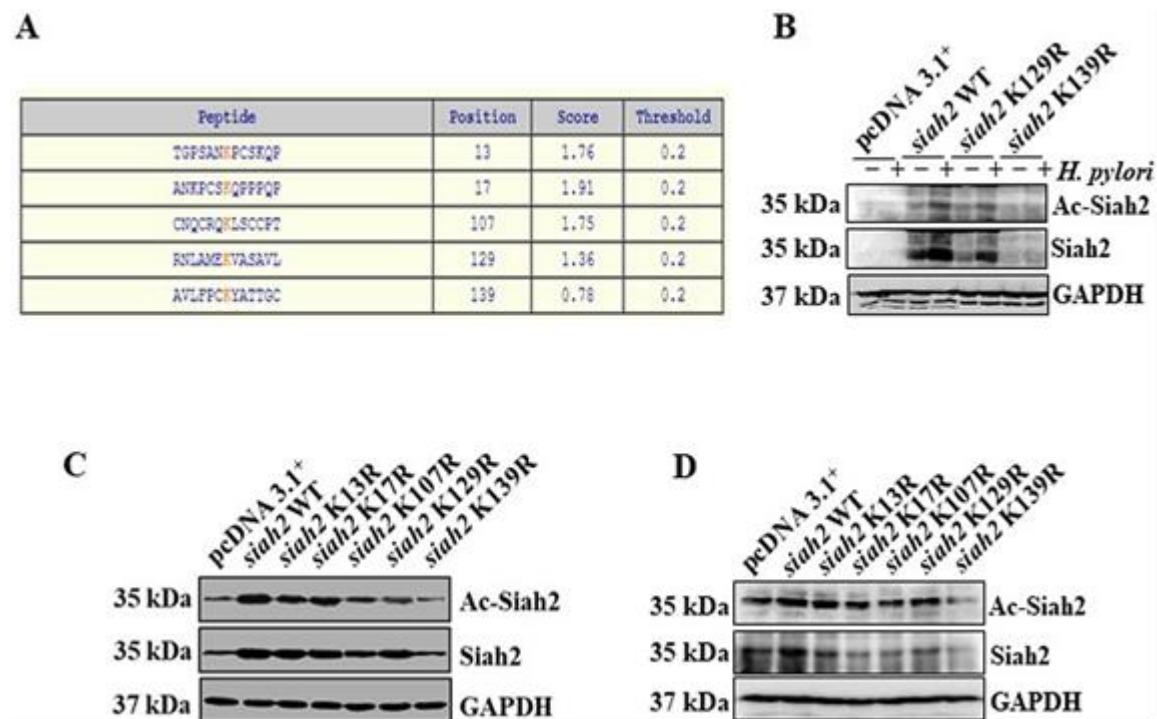


Figure 3.2: Siah2 undergoes acetylation at several residues in *H. pylori*-infected GCCs

(A) GPS PAIL 2.0 tool prediction of probable acetylated lys residues in Siah2. (B) Western blot analysis (n=3) performed using whole cell lysates of MKN45 cells that were transiently-

transfected with the empty vector pcDNA3.1⁺, *siah2* WT, *siah2* K129R and *siah2* K139R mutant constructs followed by infection with *H. pylori*. (C) Western blot (n=3) performed using whole cell lysates prepared from empty vector, *siah2* WT, K13R, K17R, K107R, K129R and K139R mutant construct stably-transfected MKN45 cells and (D) AGS cells.

Several classes of histone/lys acetyl transferases (HAT/KATs) are known to cause acetylation of target proteins that play crucial roles in various diseases including cancer. In order to predict the HAT/KAT protein(s) responsible for the acetylation of Siah2, *in-silico* analysis was performed using acetylation site enrichment based (ASEB) online tool (208) which indicated that CBP/p300 family of KATs were responsible for acetylation of Siah2 at K¹²⁹ and K¹³⁹ residues (Figure 3.3A). This prediction was further validated using GPS PAIL 2.0 tool which predicted 100% probability of Siah2 being acetylated by p300 (Figure 3.3B).

A

The shortest path between the lysine-acetyl-transferase and query protein:

CBP (CREBBP)	PINA	CREBBP -> PIAS1 -> SIAH2	network view
CBP (CREBBP)	STRING	CREBBP -> HIF1A -> SIAH2	network view
p300 (EP300)	PINA	EP300 -> PIAS3 -> SIAH2	network view
p300 (EP300)	STRING	EP300 -> SIAH2	network view

ASEB P-values for candidate sites:

KAT	Site	Sequence	P-value
CBP/p300	13	SSTG P SAN K P C SKQ P PP	0.0005
CBP/p300	17	P S AN K P C S K Q P PP Q P Q H	0.0369
CBP/p300	176	C P C P G A S C R W Q S L E A V	0.0451
CBP/p300	107	L V C N Q C R Q K L S C C P T C R	0.1664
CBP/p300	235	H H F M L V L E K Q E K Y E G H Q	0.4258
CBP/p300	139	A S A V L F P C K Y A T T G C S L	0.4341
CBP/p300	193	M S H L M H A H K S I T T L Q G E	0.8164
CBP/p300	238	M L V L E K Q E K Y E G H Q Q F F	0.8977
CBP/p300	256	I V L L I G T R K Q A E N F A Y R	0.9231
CBP/p300	129	S I R N L A M E K V A S A V L F P	0.9326
CBP/p300	154	S L T L H T E K P E H E D I C E	0.9348

B

Site distribution for HATs



Figure 3.3: p300 is predicted to acetylate Siah2 in *H. pylori*-infected GCCs

(A) *In-silico* analysis using ASEB online computer program for the prediction of HAT/KAT responsible for acetylation of Siah2 showed probable CBP/p300-Siah2 interaction and various acetylatable lys residues in Siah2 with their P-values. (B) Prediction using GPS

PAIL 2.0 revealed 100% probability of p300-mediated Siah2 acetylation. GAPDH was used as a loading control in all western blot analyses.

3.2. Discussion

Siah proteins are associated with various cancers including gastric cancer. This study showed for the first time that *H. pylori* infection can induce Siah acetylation. Although, both Siah1 and Siah2 have acetyltable lysine (K) residues, I found only Siah2 to undergo acetylation following infection with *H. pylori*. This might have further implications in imparting specific functions to Siah1 and Siah2 proteins, which are, otherwise, very similar in their properties.

In-silico analyses using GPS-PAIL 2.0 software (209) predicted that various lys residues in Siah2i.e. lys 13, 17, 107, 129 and 139 could be acetylated, out of which 129 and 139 residues had the highest probability to undergo acetylation. To experimentally determine the effect of acetylation at various lys residues, I generated several mutants of Siah2 at residues which were predicted as important residues for acetylation by ASEB or GPS-PAIL. K13R, K17R and K107R Siah2 did not show any significant change in either acetylation or stability as compared to the WT. Following K129R mutation, however, the Siah2 acetylation decreased significantly as compared to Siah2 WT and after K139R mutation, complete reduction in Siah2 acetylation and total Siah2 protein was observed indicating that acetylation at Siah2 K¹³⁹ might be important in regulating the stability of Siah2 protein.

Acetylation may induce the stability of proteins by either thermodynamically stabilizing the protein structure or preventing their interaction with other proteins which are responsible for their degradation (206, 210, 211) or may increase protein degradation (156). As K¹²⁹ and K¹³⁹ lie in the SBD, we presumed that these two residues might be very important in regulating the stability and activity of Siah2.

p300 is a transcriptional cofactor and has histone acetyltransferase (HAT) activity. It might also act as a cellular oncogene by activating several protooncogenic factors (72). p300 HAT activity is reported in the progression of cell cycle, cell survival and in cellular metabolism (212-214). Several acetyltransferases have been reported for acetylation of proteins. Using ASEB online tool (208) and GPS-PAIL 2.0, we found that p300 could play a role in acetylating Siah2 protein. This analysis data corroborated previous reports describing the role of p300 in regulating cellular acetylated protein pool (75, 76). As acetylation of proteins control various physiological processes, I experimentally investigated further the mechanism of Siah2 acetylation and studied the effect of acetylation on Siah2 stability and function in *H. pylori*-infected GCCs.

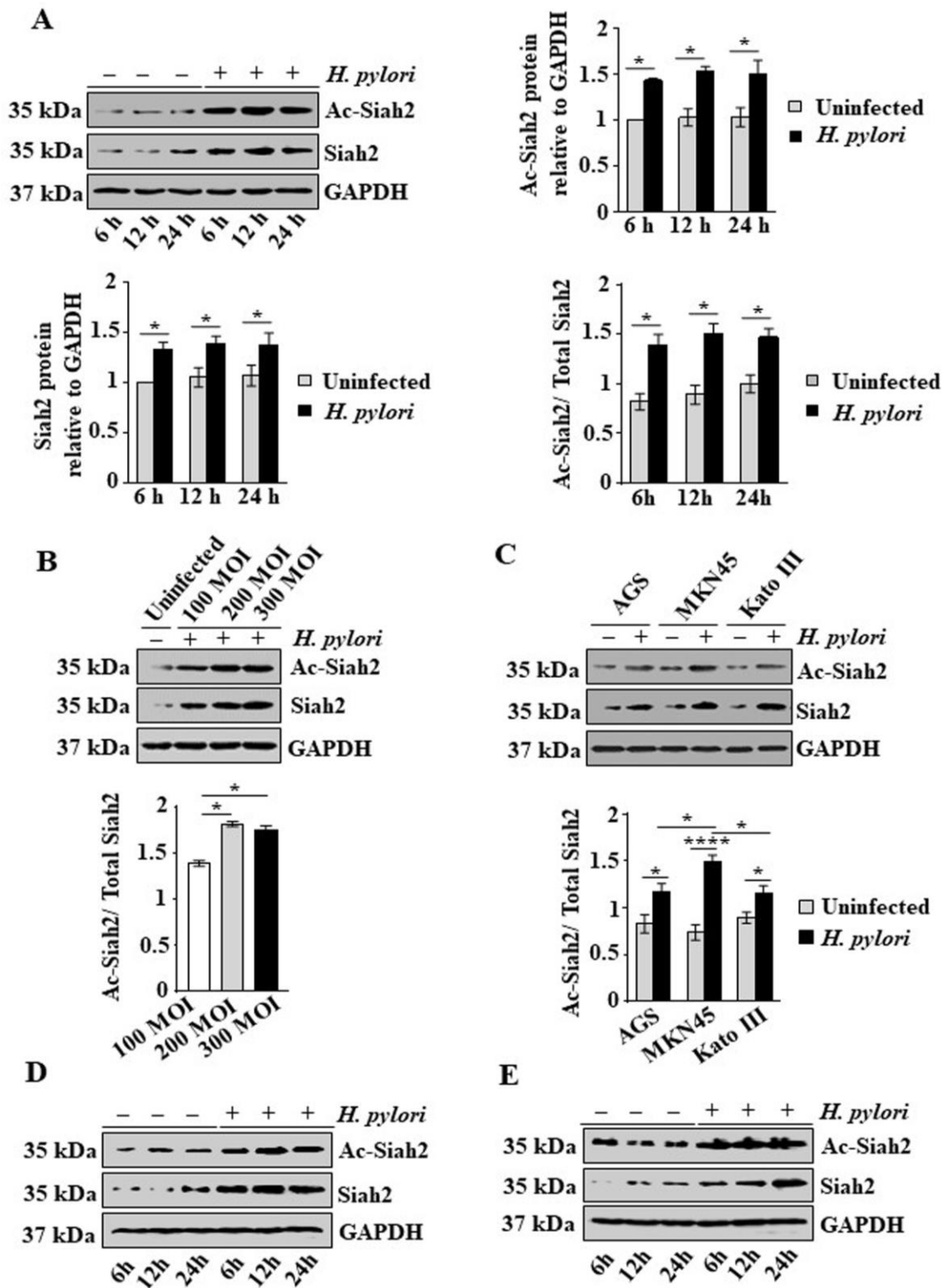
Acetylation at K¹³⁹ increases Siah2 stability

Chapter 4

Chapter 4: Acetylation at K¹³⁹ increases Siah2 stability

4.1. *H. pylori* induces Siah2 acetylation in the infected GCCs

In order to access the acetylation status of Siah2 protein, human GCC MKN45 was infected with *cag* PAI(+) strain 26695 at 200 MOI for 6 h, 12 h, and 24 h. Immunoblot analysis was performed using the cell lysates and blots were probed for Siah2 and lys acetylated Siah2 (ac-Siah2) proteins. Densitometric analysis showed that there was remarkable time-dependent increase in Siah2 and ac-Siah2 level in *H. pylori*-infected cells as compared to the uninfected cells, with 12 h showing the optimal time for Siah2 acetylation (Figure 4.1A). Although there was basal ac-Siah2 in uninfected cells, the ac-Siah2 to total Siah2 ratio was significantly higher in infected cells as compared to the uninfected cells indicating the importance of *H. pylori* in enhancing Siah2 acetylation. In order to access the optimal MOI for Siah2 acetylation, MKN45 cells were infected with 100, 200 and 300 MOI of *H. pylori* for 12 h and western blotting was performed. Densitometric analysis revealed that 200 MOI at 12 h optimally induced both Siah2 and ac-Siah2 (Figure 4.1B). Immunoblotting performed from cell lysates prepared from two other GCCs, AGS and Kato III, also showed significant increases in ac-Siah2 and Siah2 after *H. pylori* infection (Figure 4.1C). Western blot analysis further revealed that ac-Siah2 level was optimal at 12 h also in AGS (Figure 4.1D) and Kato III (Figure 4.1E) cells.



4.1 *H. pylori* induces Siah2 acetylation in the infected GCCs

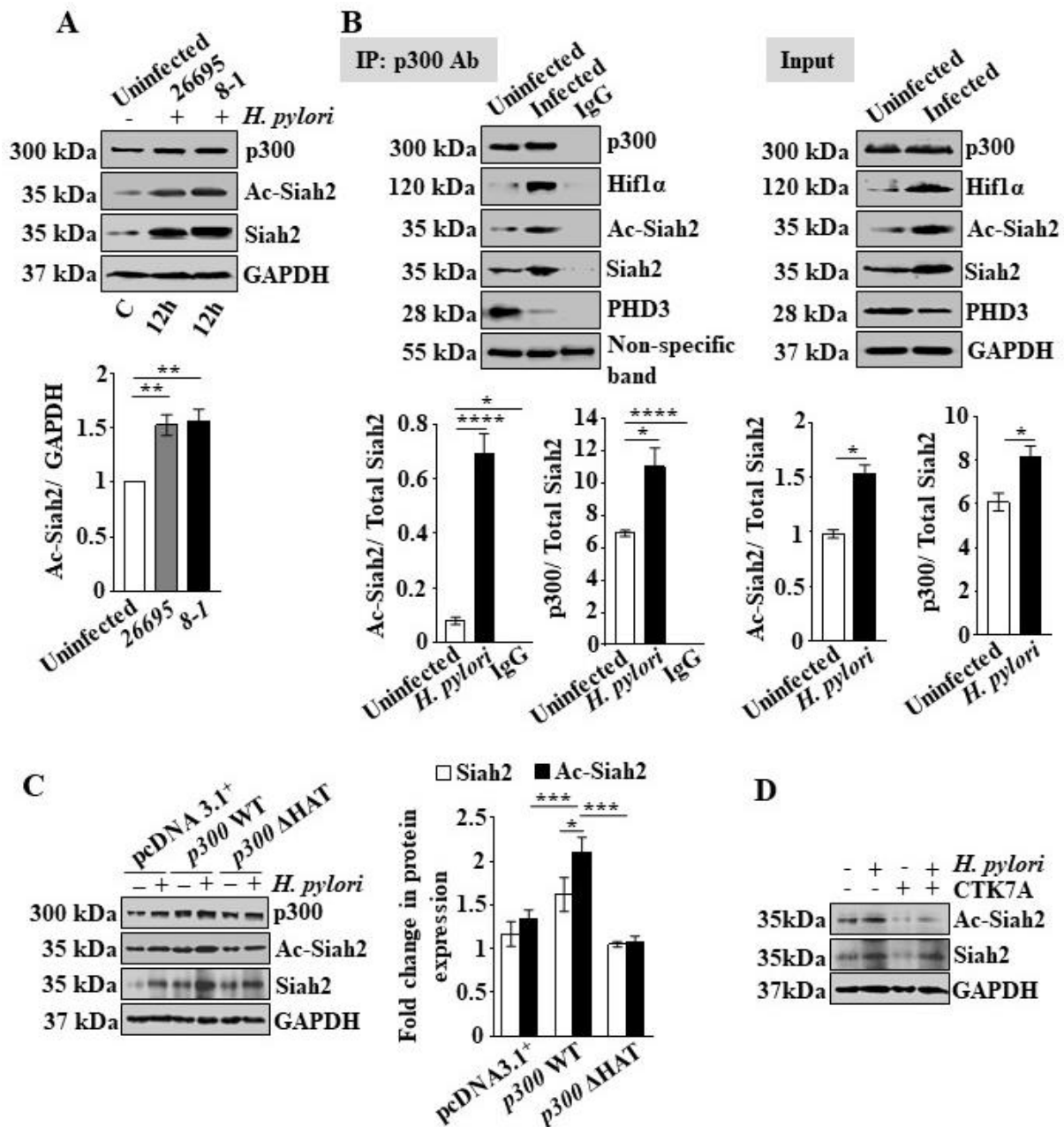
(A) Western blotting analysis performed using whole cell lysates prepared from uninfected or *H. pylori*-infected (with MOI 200 and at 6, 12 and 24 h) MKN45 cells showed increased expression of Siah2 and ac-Siah2 proteins in infected cells as compared to the uninfected

cells. Densitometric representations of the data indicated significant increase in ac-Siah2: total Siah2 ratio at all the time points, with optimal expression at 12 h. Data are mean, with $*P<0.05$. (B) Western blotting performed using MKN45 cell lysates infected with *H. pylori* (100 MOI, 200 MOI and 300 MOI) for 12 h. Graphical representation showed that MOI 200 was the optimal for inducing ac-Siah2. Data are mean \pm SEM, n=3, $*P<0.05$. (C) Immunoblot analysis was performed using 12 h MOI 200 *H. pylori*-infected AGS, MKN45 and Kato III cell lysates. Representative bar graph generated by performing 2-way ANOVA clearly indicated significant increment in ac-Siah2: total Siah2 ratio after *H. pylori* infection. Data are mean \pm SEM, n=3, $*P<0.05$, $****P<0.0001$. (D) Western blot analysis of AGS and (E) Kato III cell lysates prepared from either uninfected or *H. pylori*-infected cells (at 6 h, 12 h and 24 h with 200 MOI) showed similar results as with MKN45 cells (shown in panel A), further establishing that MOI 200 at 12 h of infection was optimal for Siah2 acetylation. GAPDH was used as the loading control in all western blot analyses.

4.2 p300 interacts with Siah2 and induces its acetylation in *H. pylori*-infected GCCs

p300 is upregulated in various tumors. p300-mediated acetylation is known to protect proteins from Ub-mediated proteasomal degradation as acetylation competes with ubiquitination and protects from undergoing degradation (194). We have earlier reported that Siah2 expression was uniformly induced in *cag* PAI(+) and (-) strains of *H. pylori*-infected GCCs (137). In order to assess the role of *cag* PAI on p300 and ac-Siah2, MKN45 cells were infected for 12 h with 200 MOI of *cag* PAI(+) strain 26695 and *cag* PAI(-) strain 8-1. Whole cell lysates were prepared and western blotted (Figure 4.2A). Blotted membrane was probed for Siah2, ac-Siah2 and p300 proteins. Both *cag* PAI(+) and *cag* PAI(-) strains were equally effective in inducing ac-Siah2 and establishing that *H. pylori*-mediated Siah2 acetylation was an *cag*-independent phenomenon. p300 was also found to be marginally

induced by both the strains. To investigate p300-Siah2 interaction, uninfected and *H. pylori*-infected (200 MOI at 12 h) MKN45 cell lysates were immunoprecipitated using p300 antibody, immunoblotted and probed for p300, Siah2, ac-Siah2, PHD3 and Hif1 α proteins (Figure 4.2B). Input lysates were also immunoblotted to understand the difference with p300 immunocomplex. The data showed marginal increase in p300, and significant increases in Siah2 and ac-Siah2 level following infection in the input whereas PHD3 level remained low in the infected cells. The immunoprecipitate showed that p300 interacted with Hif1 α , and ac-Siah2 or Siah2 with a much higher extent in the infected cells and PHD3 was low in the immunoprecipitate from the infected cell. Densitometric analysis showed that the difference between uninfected and infected cells with respect to the ratio of ac-Siah2 to total Siah2 was more prominent in pulled-down samples as compared to the input lysates indicating the importance of p300 in the interaction. To determine the effect of p300 HAT function on acetylation of Siah2, western blotting was performed using MKN45 cell lysates transiently transfected with empty vector pcDNA3.1⁺, *p300* WT and *p300* Δ HAT constructs followed by *H. pylori* infection for 12 h. The membrane was probed for Siah2 and ac-Siah2 expression was checked (Figure 4.2C). The data revealed that Siah2 and ac-Siah2 expression was significantly higher in *p300* WT-transfected group as compared to other two groups. To further ascertain p300 HAT function on Siah2 acetylation, MKN45 cells were co-incubated with 100 μ M conc. of CTK7A, a water-soluble derivative of curcumin and 200 MOI *H. pylori* (for 12 h). Western blot analysis further showed that *H. pylori*-mediated increase in Siah2 and ac-Siah2 expression drastically declined in CTK7A-treated group as compared with the untreated group (Figure 4.2D).



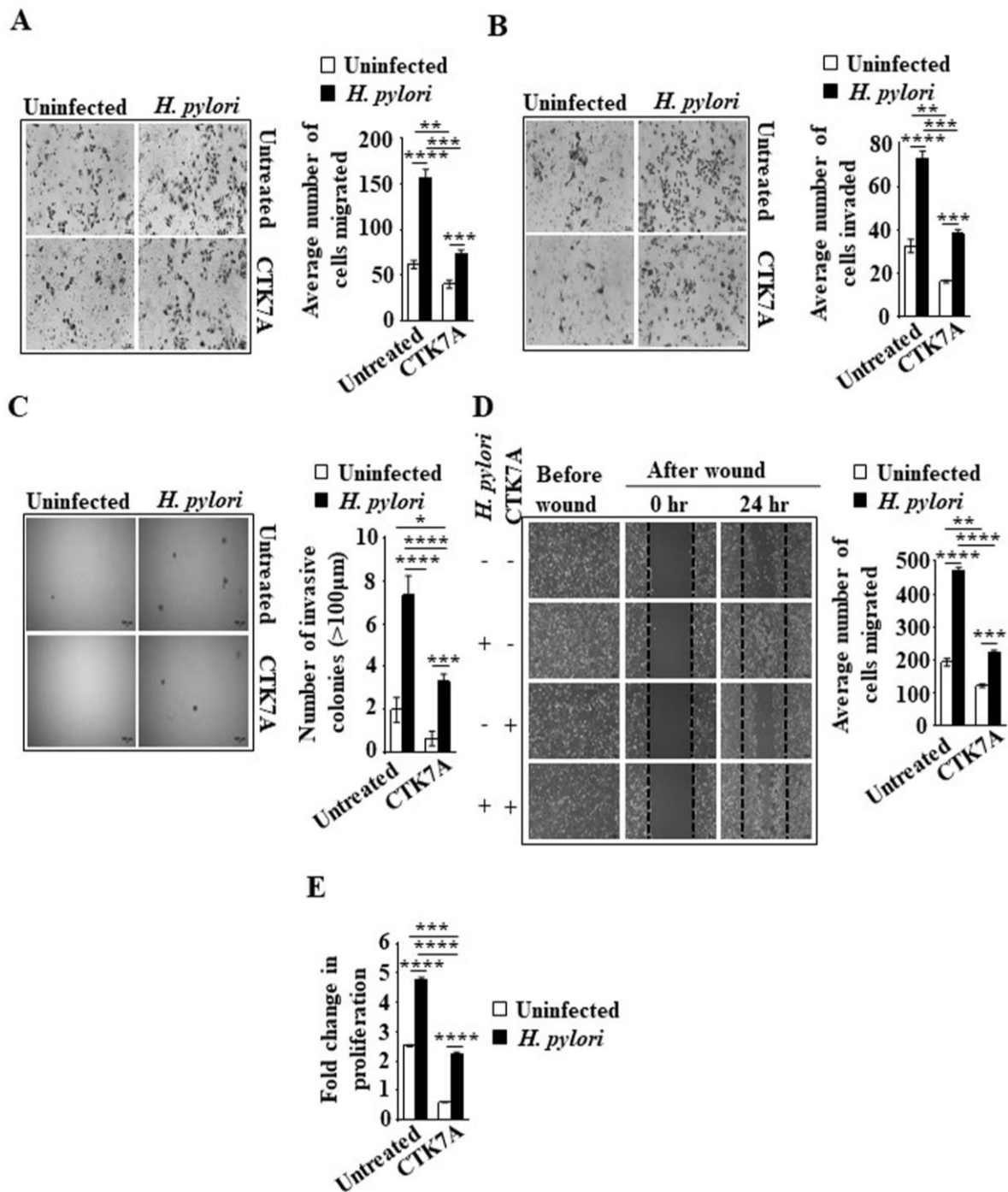
4.2 p300 interacts with Siah2 and induces its acetylation in *H. pylori*-infected GCCs

(A) Immunoblot analysis of cell lysates from MKN45 cells {either uninfected or infected with *H. pylori* *cag* PAI(+) strain 26695 or (-) strain 8-1 at 200 MOI for 12 h} revealed that p300, ac-Siah2 and Siah2 are equally induced by both the strains. (B) Western blot analysis and bar graphs of immunoprecipitation of protein lysates using p300-specific antibody to examine p300 interaction with Siah2, PHD3 and Hif1 α proteins showed significant increase in Siah2, and p300 interaction in infected cells when compared with uninfected cells. (C)

Western blot analysis for p300, ac-Siah2 and Siah2 protein levels in MKN45 cell lysates overexpressing empty vector, *p300* WT and *p300* Δ HAT plasmids and with *H. pylori* infection. Data showed decreased Siah2 and ac-Siah2 expression in Δ HAT plasmid-expressing cells. (D) Immunoblotting of MKN45 cells cotreated with *H. pylori* and 100 μ M HAT inhibitor CTK7A for 12 h showed that the HAT inhibitor decreased ac-Siah2 level in treated cells. GAPDH was used as a loading control in all western blot analysis experiments. All data were analyzed by 2-way ANOVA with Tukey's post-hoc analysis (Error bars represent mean \pm SEM, n=3). * P <0.05, ** P <0.01, *** P <0.003 and **** P <0.0001.

4.3 p300 HAT inhibitor CTK7A decreases the migration and invasiveness of *H. pylori*-infected GCCs

To examine the consequences of HAT inhibitor CTK7A treatment on cell migration and invasion of GCCs, *in-vitro* transwell migration (Figure 4.3A) and invasion assays (Figure 4.3B) were performed using AGS cells. MKN45 being semi adherent in nature were not selected for these experiments. CTK7A-treated AGS cells demonstrated reduced migration and invasive property as compared to untreated cells. Furthermore, the results were validated by soft agar colony formation assay (Figure 4.3C) using MKN45 cells and by wound healing assay (Figure 4.3D) using AGS cells. The ability of anchorage-independent growth of MKN45 cells leading to the formation of colonies was inhibited in CTK7A-treated cells. Also, the wound healing ability of AGS cells was reduced following the HAT inhibitor treatment. We performed the MTT assay to determine the effect of CTK7A on MKN45 cell proliferation. Cell proliferation was significantly reduced in CTK7A-treated group as compared to the untreated group (Figure 4.3E).



4.3 p300 HAT inhibitor CTK7A decreases the migration and invasiveness of *H. pylori*-infected GCCs

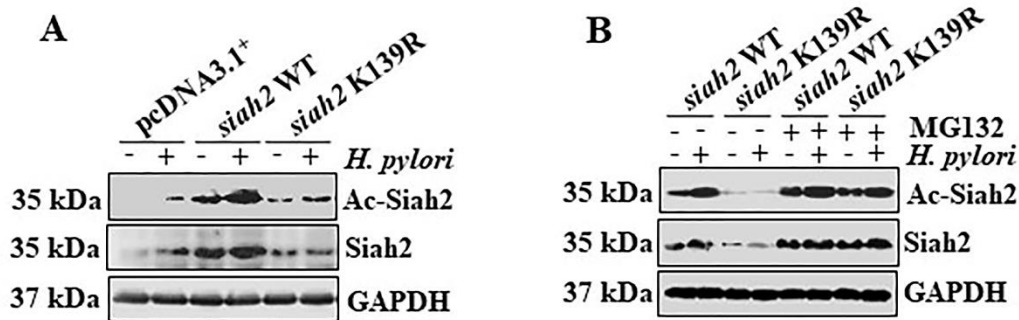
(A) Representative image (n=3) showing *in-vitro* cell migration assay and (B) *in-vitro* cell invasion assay performed using AGS cells co-treated with CTK7A (100 μ M for 24 h) and/or *H. pylori* (200 MOI for 12 h). Graphical data showing mean number of cells migrated clearly indicated reduced migration and invasion of AGS cells after CTK7A treatment.

Representative images (n=3) and graphical data of soft-agar assay (C) using semi-adherent MKN45 cells and wound healing/scratch assay using adherent AGS cells (D) showed that cell migration and invasiveness was reduced in cells treated with the HAT inhibitor CTK7A. (E) MTT assay performed using AGS cells either co-treated/ untreated with CTK7A (and *H. pylori* (200 MOI) for 12 h. Representative bar graph denoted the average number of colonies measured after MTT treatment. All data were analyzed by 2-way ANOVA with Tukey's post-hoc analysis (Error bars represent mean \pm SEM, n=3). * P <0.05, ** P <0.01, *** P <0.003 and **** P <0.0001.

4.4 Acetylation of Siah2 K¹³⁹ protects Siah2 from ubiquitination-mediated proteasomal degradation

Acetylation may either cause Ub-mediated proteasomal degradation of acetylated proteins (215) or may even inhibit the ubiquitination by acetylation to suppress their proteasomal degradation (216). Based on our data we presumed that acetylation might inhibit the degradation of Siah2 when acetylated at K¹³⁹ residue (ac-K¹³⁹ Siah2). The acetylation-null K139R mutated Siah2 showed reduced Siah2 protein level indicating further towards the importance of K139 acetylation in regulating Siah2 level. MKN45 cells stably expressing either the empty vector or *Siah2* WT or *Siah2* K139R mutant were infected with *H. pylori* (200 MOI for 12 h). Cell extracts were run to assess the expression of Siah2 and ac-Siah2 (Figure 4.4A). As observed before, K139R mutation led to significant decrease in Siah2 and ac-Siah2 level indicating that acetylation-null mutation at K¹³⁹ caused degradation of Siah2. In order to assess this phenomenon, MKN45 cells stably-expressing *siah2* K139R mutant construct were pre-treated with 50 μ M MG132 for 24 h prior to infection with 200 MOI *H. pylori* for 12 h. Cell lysates were western blotted and were probed for Siah2 and ac-Siah2 proteins (Figure 4.4B). The result showed that MG132 rescued Siah2 K139R mutant protein

from undergoing degradation. In other words, K¹³⁹ acetylation could protect Siah2 from ubiquitination-mediated proteasomal degradation.



4.4 Acetylation at Siah2 K¹³⁹ protects Siah2 from ubiquitination-mediated proteasomal degradation

(A) Immunoblot analysis (n=3) of MKN45 cells stably-expressing empty vector, *siah2* WT and *siah2* K139R constructs showed that Siah2 and ac-Siah2 were significantly downregulated in Siah2 K139R mutant-expressing cells as compared to the WT construct-expressing cells. (B) Western blotting (n=3) performed using MKN45 stable cells expressing pcDNA3.1⁺, Siah2 WT and Siah2 K139R proteins and treated with MG132 revealed that MG132 could protect Siah2 K139R protein and its acetylation level. GAPDH was used as a loading control.

4.5. Discussion

In this section, we showed that *H. pylori* induced Siah2 acetylation in infected GCCs and this phenomenon is *cag* PAI independent as both *cag* PAI(+) strain 26695 and *cag* PAI(-) strain 8-1 induced acetylation of Siah2. Induced expression of Siah2, its acetylation and Hif1 α was seen in infected cells and all of these proteins were found to form complex with p300. Furthermore, studies using *p300* WT and Δ HAT overexpression constructs and HAT/KAT inhibitor CTK7A proved that p300 HAT domain was crucial for acetylation of Siah2 in infected GCCs. Migration and invasiveness studies of infected GCCs using CTK7A displayed

that p300 HAT domain was essential for inducing migration and invasion of *H. pylori*-infected cells. Finally, proteasome inhibitor studies using MG132 proved that acetylation at K¹³⁹ residue was imperative to maintain the stability of Siah2 protein. Thus, this work concluded that p300 HAT/KAT activity plays significant roles in regulating *H. pylori*-mediated invasiveness of gastric cancer. The data further indicated that HAT/KAT p300-Siah2 K¹³⁹ axis could reveal more about the mechanisms regulating gastric cancer.

p300 is a bromodomain-containing protein and interacts with several non-histone proteins as well (217, 218). We found p300 to interact with Siah2, PHD3 and Hif1 α in GCCs. The specificity of interaction was higher for ac-Siah2 in *H. pylori*-infected GCCs. p300 is also a transcriptional activator of Hif1 α (71). So, apart from PTM of Siah2 by p300 HAT/KAT activity, the role of p300 in the transcriptional regulation of Siah2 should also be investigated in future.

CTK7A is a derivative of curcumin known to inhibit p300 HAT function in oral squamous cell carcinoma (OSCC) (203). Findings by *Rath et al.*, also suggested significant role of CTK7A in apoptosis induction in hypoxic gastric epithelia (204). CTK7A led to cell death in Hif1 α -independent manner and also reduced the migration and invasion of CTK7A-treated hypoxic GCCs. We studied invasiveness of *H. pylori*-infected GCCs after CTK7A treatment. However, the effect of CTK7A on apoptosis of *H. pylori*-infected GCCs is still unknown.

Acetylation can protect proteins from degradation by proteasome-mediated pathway and also stabilizes protein structure (187). p300 by virtue of its autoacetylation activity stabilizes itself in hypoxia (203). We found that K139R acetylation-null mutant of Siah2 was not stable in *H. pylori*-infected GCCs and identified a noticeable increase in its stability following MG132 treatment. This also highlighted the critical role of acetylation in the stabilization of Siah2. Siah2 is reported to self-ubiquitinate and degrade itself in cancer cells

(219). This study indicated that acetylation can rescue Siah2 possibly from self-ubiquitination but it needs to be studied further for confirmation. As Siah2 is known to induce migration and invasion of *H. pylori*-infected GCCs, the next section of this thesis elaborates on the mechanisms by which ac-K¹³⁹Siah2 enhance the invasiveness of infected GCCs.

**ac-K¹³⁹ Siah2 induces Hif1-mediated
invasiveness of *H. pylori*-infected GCCs**

Chapter 5

Chapter 5: ac-K¹³⁹ Siah2 induces Hif1-mediated invasiveness of *H. pylori*-infected GCCs

5.1. *H. pylori* causes ac-Siah2-mediated PHD3 degradation and Hif1 α accumulation in infected GCCs

Several reports suggest that *H. pylori* causes Hif1 α stabilization in GC (220-222) but the mechanism is not clearly known. PHD3 protein which causes degradation of Hif1 α in normoxia is a known target of Siah2 in hypoxia. I wanted to examine if Siah2 can target PHD3 for degradation in *H. pylori*-infected cells. In order to examine the role of ac-Siah2 on Hif1 α , the empty vector, *siah2* WT and *siah2* K139R-expressing stable MKN45 cells were used. Following *H. pylori* infection, cell lysates were prepared and western blotted. Densitometric analysis confirmed that WT Siah2-expressing cells had significantly high Hif1 α protein following *H. pylori* infection as compared to its counterparts in the other two transfection groups (Figure 5.1A). The expression of ac-K¹³⁹ Siah2 was detected using customized ac-K¹³⁹-specific Siah2 antibody. The specificity of the ac-K¹³⁹ antibody and dominance of acetylation at K¹³⁹ in infected MKN45 cells were verified by using another custom-prepared antibody, ac-K¹²⁹ Siah2 in western blotting (Figure 5.1B). Immunofluorescence (IF) microscopy (Figure 5.1C) using MKN45 empty vector, Siah2 WT and K139R mutant-expressing cells and the quantitative data further confirmed the effect of K139R mutation on PHD3 and Hif1 α expression. Siah2, ac-K¹³⁹Siah2 and Hif1 α proteins were significantly induced, whereas, PHD3 expression significantly decreased in WT cells as compared to the empty vector and K139R mutant-expressing cells. To ascertain the effect of ac-Siah2 on PHD3 and Hif1 α proteins was assessed by western blotting cell lysates from the above-mentioned stable cells (Figure 5.1D). Data confirmed that ac-K¹³⁹ Siah2 was effective in degrading PHD3 and in increasing Hif1 α stability in the infected cells.

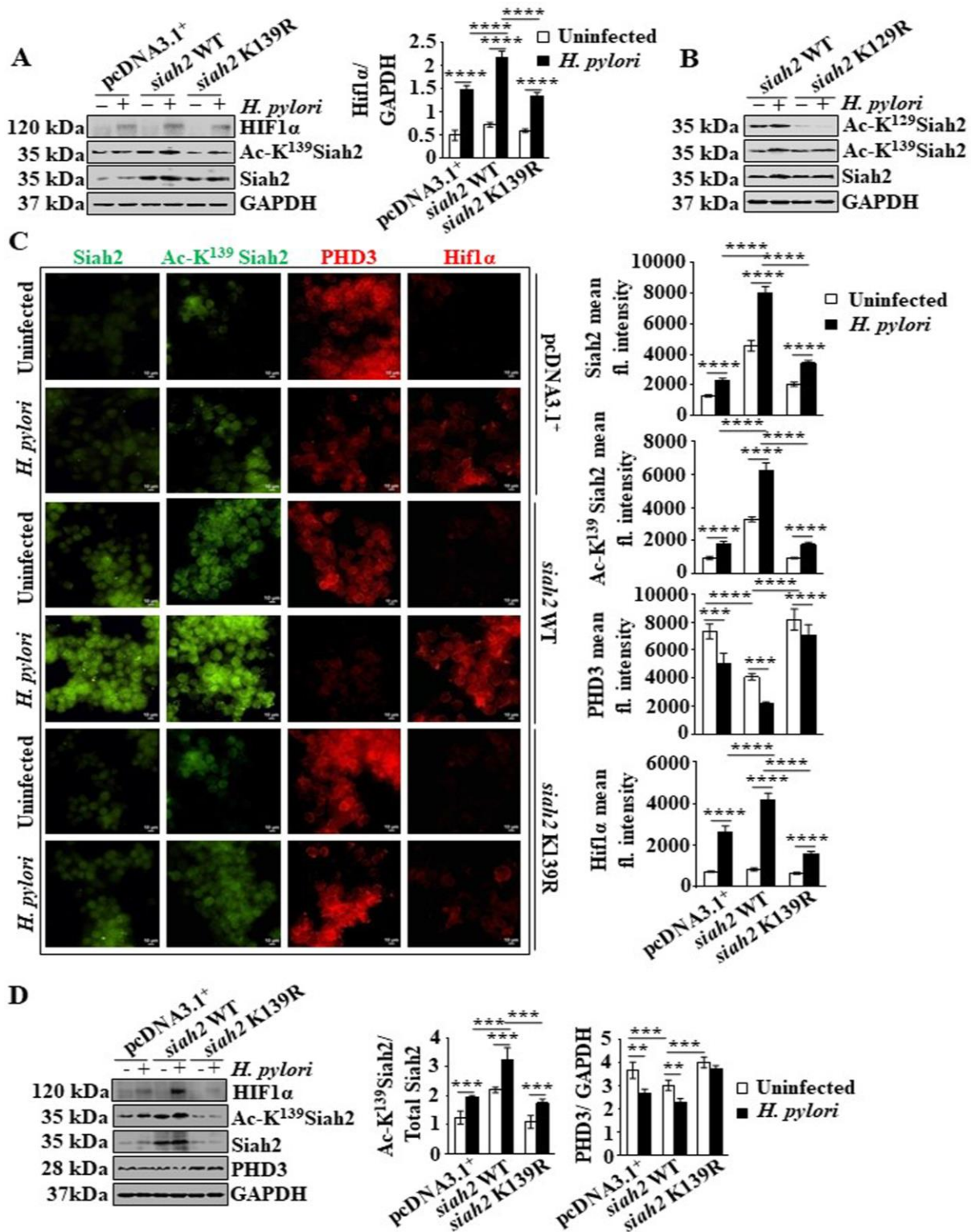


Figure 5.1: *H. pylori*-mediated Siah2 acetylation at K¹³⁹ causes PHD3 degradation and Hif1α accumulation in infected GCCs

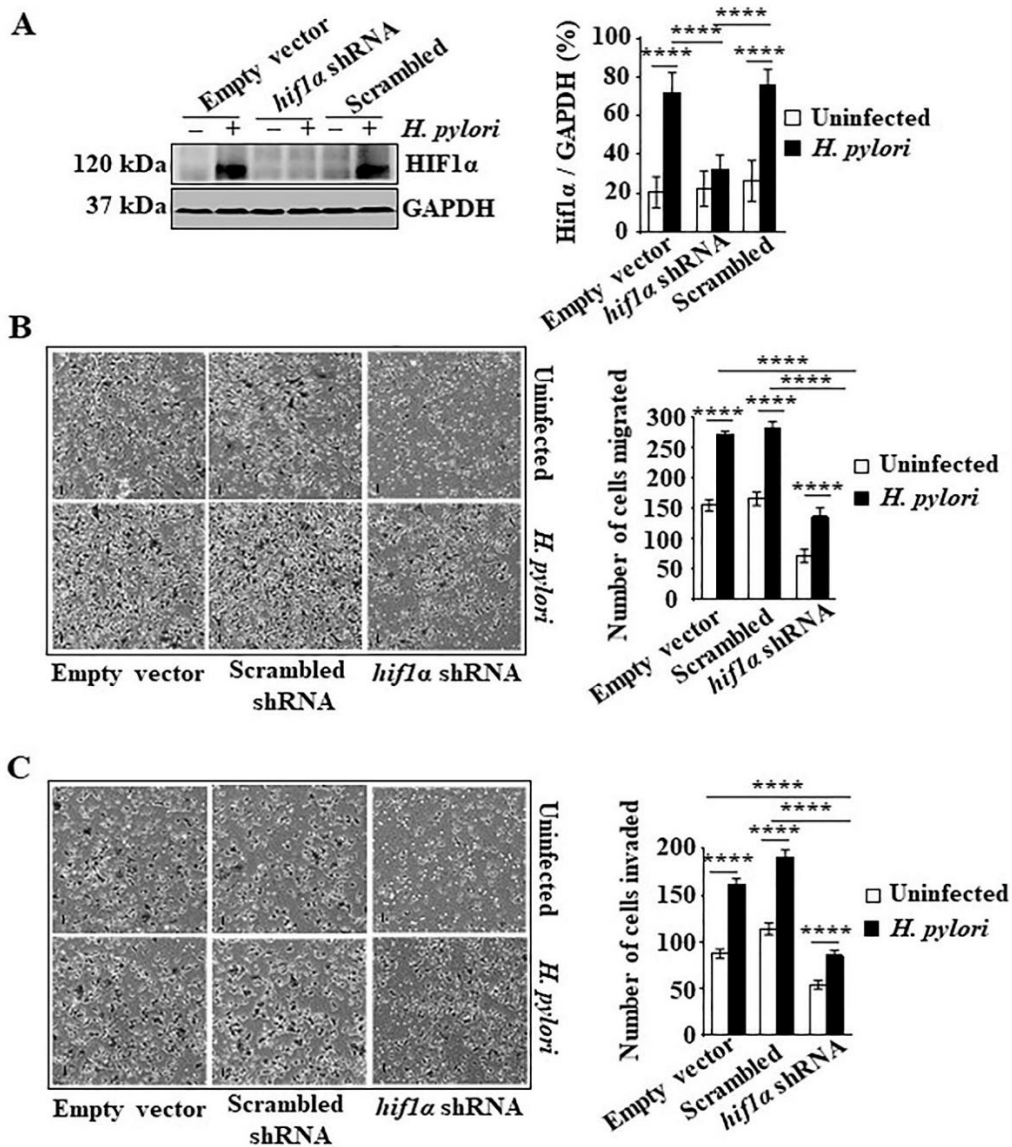
(A) Representative western blot (n=3) comparing expression of Hif1α, Siah2 and ac-K¹³⁹Siah2 in pcDNA3.1⁺, *siah2* WT and *siah2* K139R stably-transfected MKN45 cells with

and without infection with *H. pylori* (200 MOI, 12 h). (B) Immunoblot analysis of cell lysates showing the specificities of ac-K¹³⁹Siah2 custom-made antibody by using uninfected and infected WT and K129R stable cells. (C) Representative immunofluorescence microscopy images (n=3) illustrating Siah2, ac-K¹³⁹Siah2, PHD3 and Hif1 α protein level in MKN45 cells stably expressing empty vector, *siah2* WT and *siah2* K139R mutant constructs with or without *H. pylori* infection. At least 15 cells were selected from 3 different fields-stained for various proteins and their signals were recorded to plot mean fluorescence intensities. Images are captured by Nikon digital camera model DS Qi2 (Nikon Corporation) and the data is quantified using Nikon advanced analysis software. Scale shown= 10 μ m. Magnification= 600X. (D) Western blotting result (n=3) showing the importance of acetylation at K139 residue of Siah2 in degrading PHD3 and accumulation of Hif1 α protein in *H. pylori*-infected MKN45 stable cells. GAPDH was used as a loading control in all western blot analyses. Data were analyzed by 2-way ANOVA. Error bars represented mean \pm SEM, n=3. ** P <0.01, *** P <0.001, **** P <0.0001.

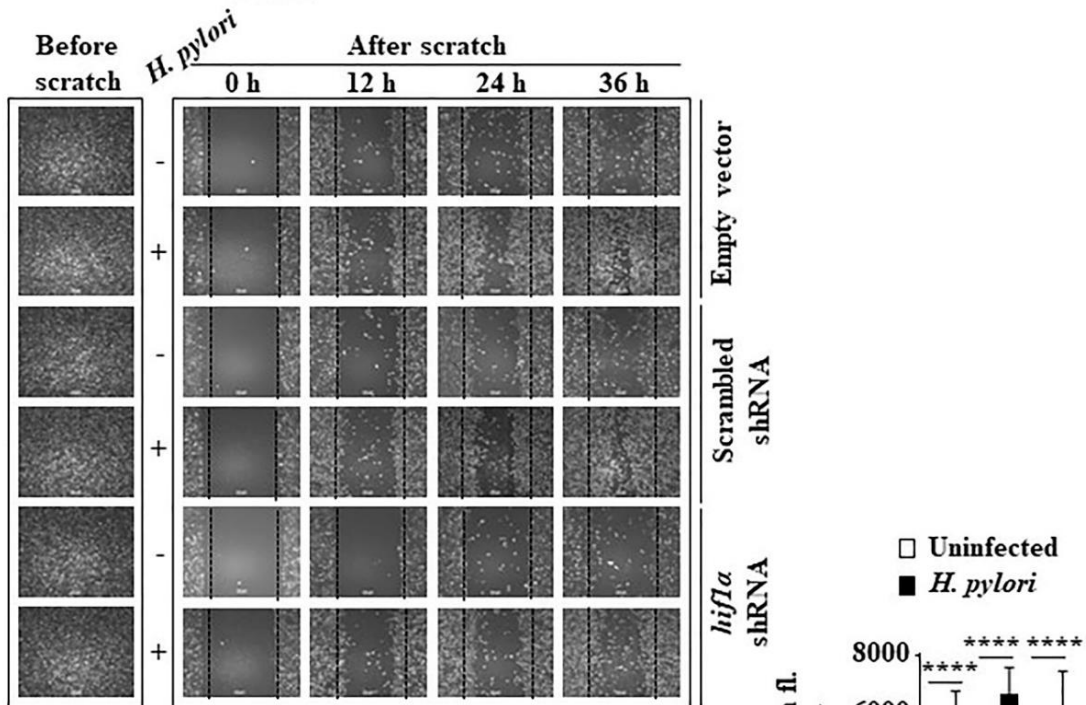
5.2. Hif1 α silencing decreases cell migration and invasiveness of *H. pylori*-infected GCCs

Hif1 α accumulation associates itself with metastasis of several cancers and also is known to upregulate cell migration, invasion and proliferation (202, 223, 224). To determine the effect of *hif1 α* knockdown on cell migration and invasive property of *H. pylori*-infected GCCs, AGS cells stably expressing *hif1 α* -shRNA were used in this study. Western blotting (Figure 5.2A) using cell lysates of infected or uninfected AGS cells stably transfected with empty vector, *hif1 α* scrambled shRNA and *hif1 α* -shRNA showed no Hif1 α expression in *shhif1 α* stable cells infected with *H. pylori* as compared to other two groups. The consequence of *hif1 α* silencing on cell migration ability of *H. pylori*-infected GCCs was studied by transwell

migration (Figure 5.2B) and matrigel assays (Figure 5.2C) using *hif1a*-shRNA stable cells. Cell migration and invasion were significantly affected in AGS cells transfected with *hif1a* shRNA as compared to the other two groups. A similar result was observed in scratch assay (Figure 5.2D) in which a marked reduction in *H. pylori* infection-induced cell migration was noticed in *hif1a*-knocked down cells with respect to the control and scrambled shRNA-expressing cells. Further, we studied the status of PHD3 and Siah2 proteins in *hif1a*-silenced cells by IF microscopy (Figure 5.2E). PHD3 level decreased whereas, Siah2 expression increased in all cells infected with *H. pylori* indicating that *H. pylori*-mediated regulation of PHD3 and Siah2 was independent of *hif1a* knockdown.



D



E

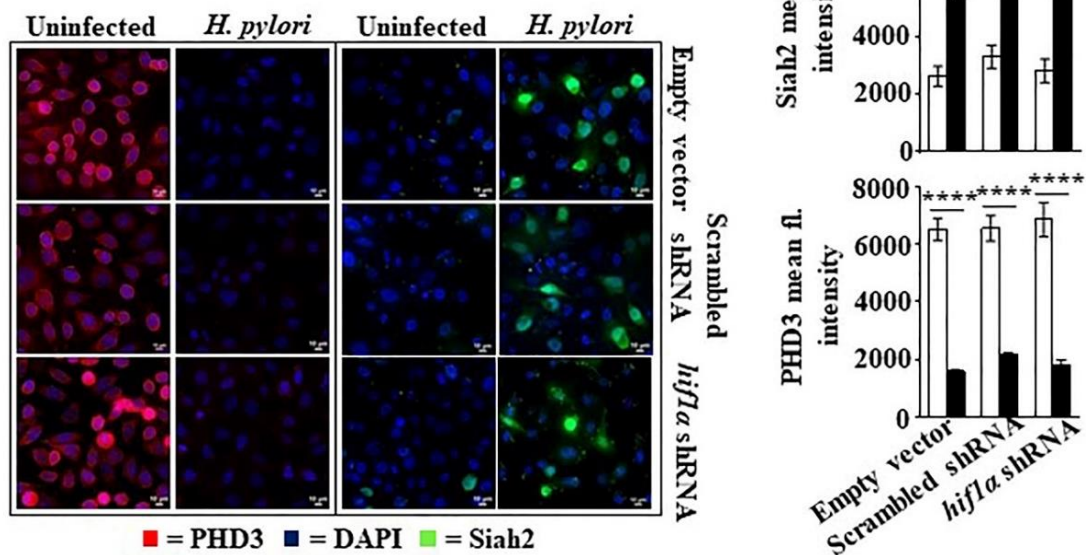


Figure 5.2: Hif1 α silencing decreases cell migration and invasiveness of *H. pylori*-infected GCCs

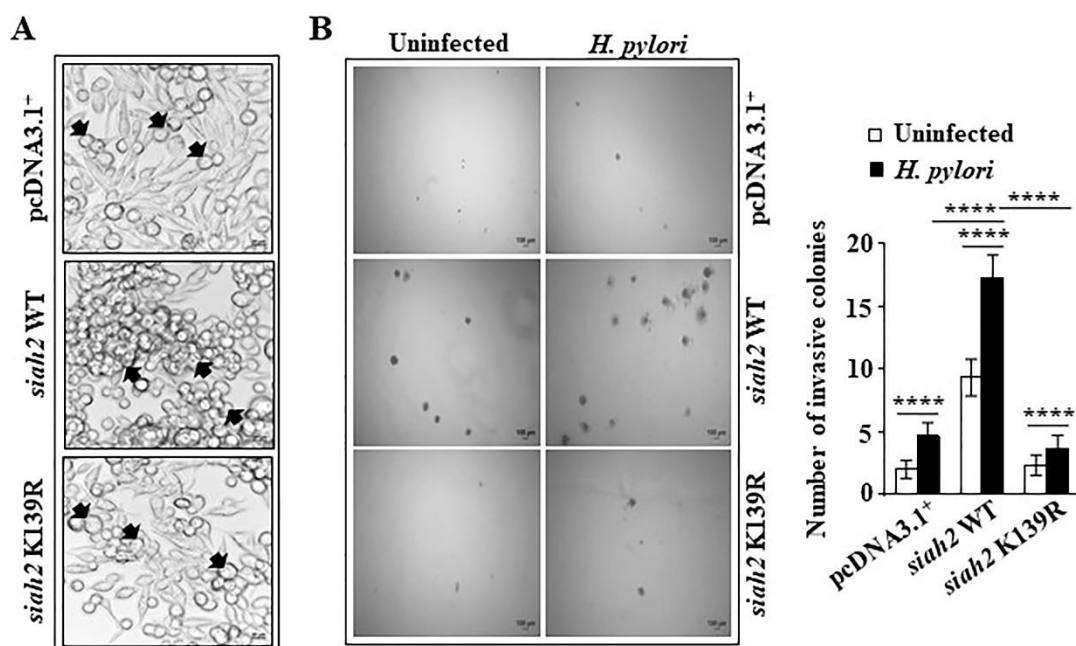
(A) Immunoblot and densitometry analysis performed using cell lysates isolated from AGS cells stably-expressing empty vector, scrambled shRNA and *hif1 α* -shRNA and infected with *H. pylori* (200 MOI for 12 h) showing significant downregulation of Hif1 α protein in *hif1 α* -shRNA stable cells. GAPDH was used as a loading control. (B) Representative (n=3) images of *in-vitro* migration assay and (C) matrigel assay comparing above-mentioned cells. The

number of cells was counted from 10 independent fields under the microscope and the mean number of cells were plotted graphically. Images were captured under in bright field using inverted microscope at 200X magnification. Scale bar= 50 μ m. (D) Wound-healing assay result (n=3) showing the extent of wound area covered by migrated cells (empty vector, *hif1 α* shRNA, and scrambled shRNA stably-expressing AGS cells). The number of migrated cells were counted by using inverted microscope from at least 5 different view fields and images were captured using camera attached to the microscope. Magnification= 100X. Scale bar=100 μ m. (E) Immunofluorescence microscopy images displaying Siah2 and PHD3 proteins in AGS cells stably-expressing the empty vector, *hif1 α* shRNA, and scrambled shRNA. Cells were visualized under inverted Nikon fluorescence microscope and at least 15 cells from 3 different fields were randomly selected for quantifying mean fluorescence intensities of Siah2 and PHD3 proteins. Quantification is done using Nikon analysis software and images are captured using Nikon digital color camera. All data were analyzed by 2-way ANOVA with Tukey's post-hoc analysis. Error bars represent (mean \pm SEM n=3, **** P <0.0001).

5.3. Siah2 K¹³⁹ acetylation enhances invasiveness of GCCs

The role Siah2 K¹³⁹ residue in regulating invasiveness of GCCs was investigated as already explained in the previous sections. In order to study the effect of K139R mutation on cell adhesiveness, MKN45 empty vector, WT *siah2* and *siah2* K139 mutant-expressing stable cells were visualized in bright field microscope for their property to adhere to the surface (Figure 5.3A). WT cells showed a more circular shape with majority of cells forming loosely adherent cell clusters while empty vector and K139 mutant cells displayed more adherent features. Soft agar assay was performed to determine the anchorage-independent clonogenic potential of *H. pylori*-infected cells (Figure 5.3B). Significantly higher number of colonies

were formed in the *H. pylori*-infected WT-expressing cells with respect to empty vector and K139R mutant-expressing cells. Similarly, the anchorage-dependent clonogenic potential of MKN45 stable cells infected with *H. pylori* showed similar results like soft agar assay (Figure 5.3C). The cell proliferation assay done using MTT reagent (Figure 5.3D) demonstrated that MKN45 cells stably-transfected with *siah2* WT plasmid infected with *H. pylori* had significantly higher proliferation rate than the other groups. Whereas, the K139R mutation in Siah2 led to significant reduction in cell proliferation. As AGS cells are more adherent in nature in comparison to semi-adherent MKN45 cells, wound healing assay was performed to assess the wound-healing ability of AGS cells stably-transfected AGS cells (Figure 5.4A). WT *siah2*-expressing cells was more migratory than K139R mutant and empty vector-expressing cells. In addition, we also confirmed the above-mentioned results obtained through traditional soft agar assay and wound-healing assay by employing *in-vitro* migration assay and matrigel assay using transwell inserts (Figure 5.4B and 5.4C, respectively). Indeed, K139R mutant stable cells displayed very less cell migration and cell invasion as compared to WT cells, further confirming our belief that ac-K¹³⁹ increases invasiveness of *H. pylori*-infected GCCs.



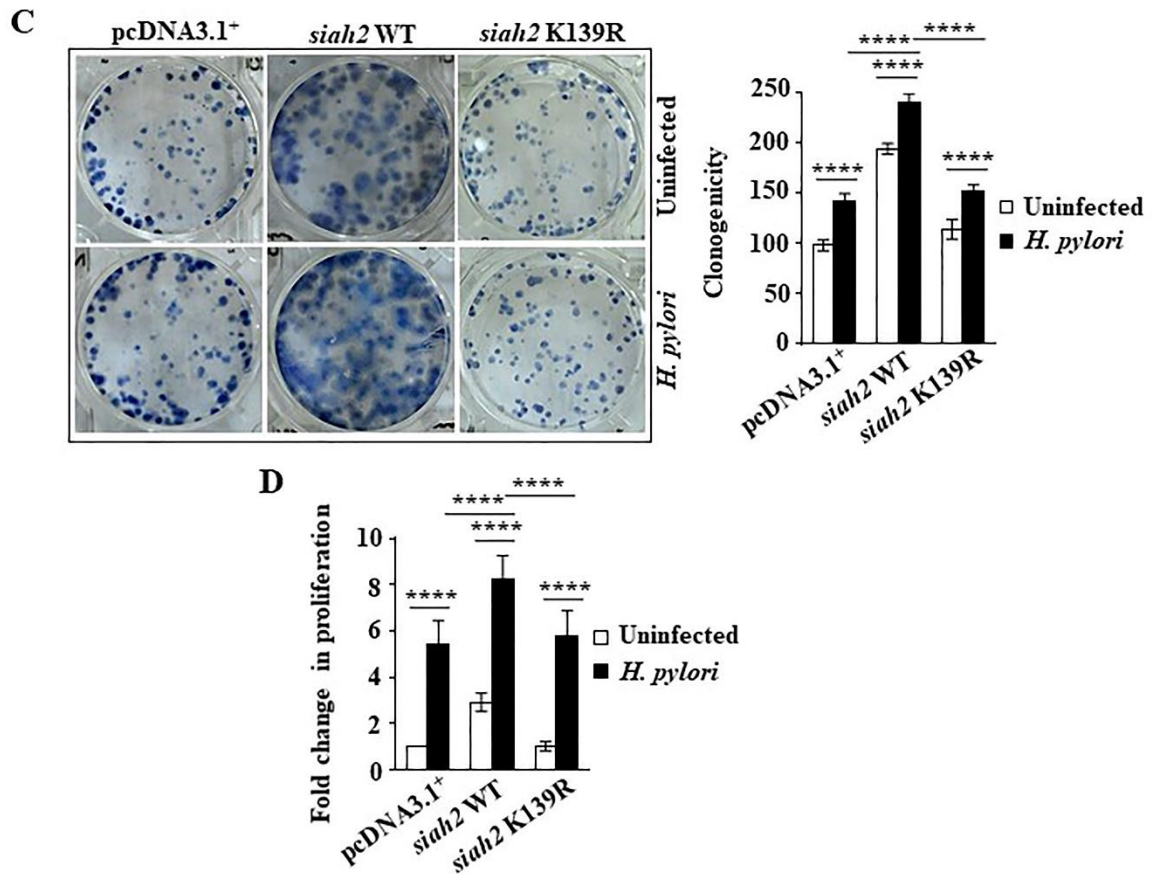


Figure 5.3: *Siah2* K¹³⁹ acetylation leads to invasion and migration of GCCs

(A) Images of MKN45 pcDNA3.1+, *siah2* WT and *siah2* K139R stably-transfected cells showing the change in cell morphology after *H. pylori* infection. Magnification 600X. Scale bar 20 μ m. (B) Representative soft agar assay images of MKN45 cells stably-transfected with above-mentioned constructs showing decreased foci formation by K139R mutant cells even after infection. Mean number of invaded colonies counted from 5 different fields were represented graphically. Magnification 100X. Scale bar 100 μ m. (C) Representative images of MKN45 stable cells showing increased clonogenic potential of *siah2* WT cells than the other transfected groups. Graphs corresponded to mean number of colonies formed. (D) Representative bar graph of MTT assay demonstrated the pro-proliferative ability of *H. pylori*-infected *siah2* WT stable cells in comparison to its counterparts in other groups. All data were analyzed by 2-way ANOVA with Tukey's post-hoc analysis. Bar graphs represented mean \pm SEM, n=3. *** P <0.001, **** P <0.0001.

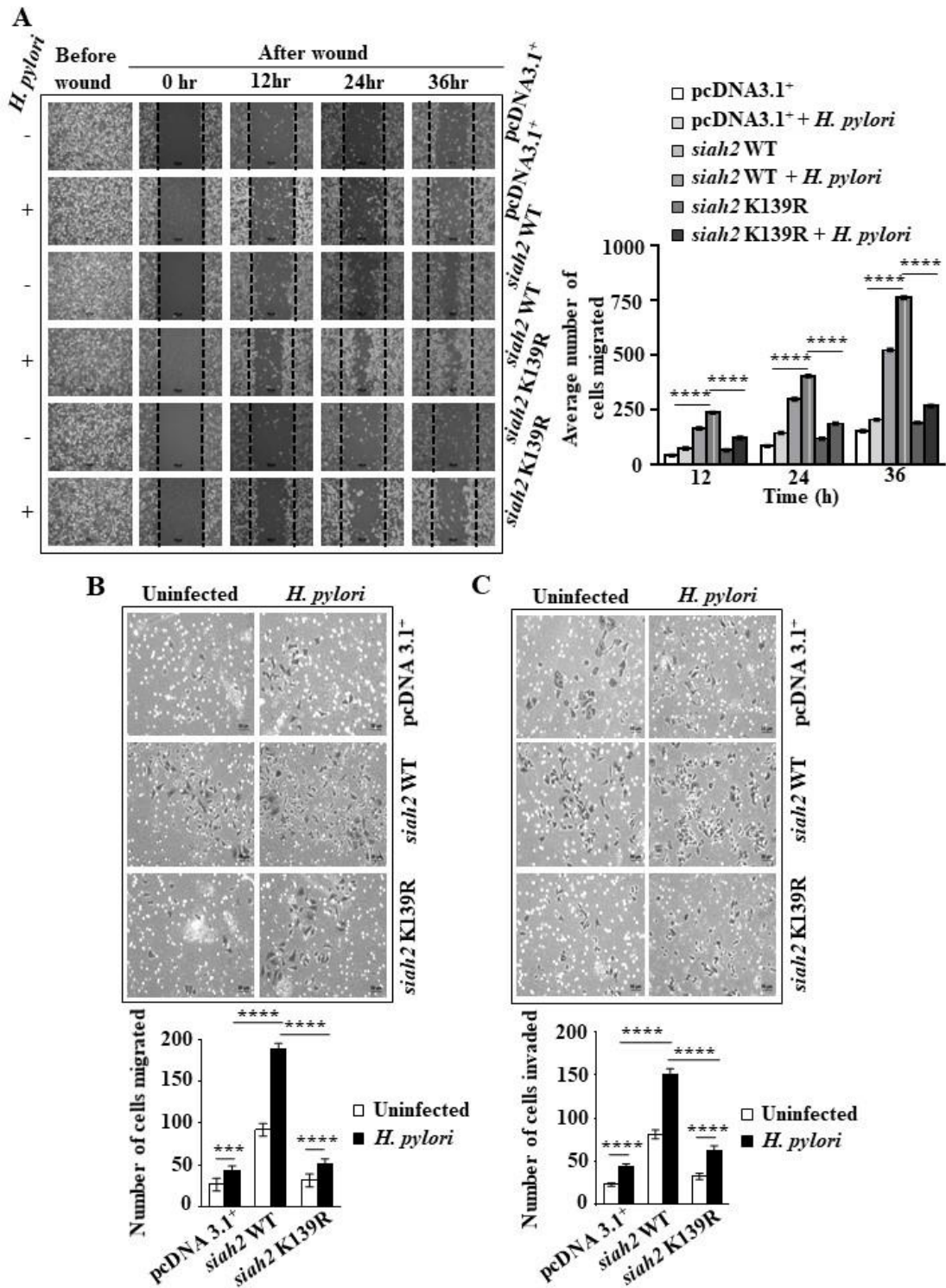


Figure 5.4: *Siah2* K¹³⁹ acetylation enhances invasiveness of GCCs

(A) Wound healing assay was performed using AGS pcDNA3.1+, *siah2* WT and *siah2* K139R stable cells and infected with *H. pylori*. Corresponding graphs of the assay showing mean number of cell migrated clearly highlighted the diminished wound healing ability of K139R mutant cells observed in *H. pylori*-infected WT cells. Magnification 100X. Scale bar

shown 100 μm . (B) Representative images of transwell migration assay and (C) Matrigel assay results of AGS cells stably-expressing empty vector, Siah2 WT and Siah2 K139R mutant proteins. The bar graph generated comparing the mean number of cell migrated and invaded after infection showed high migration and invasion potential of WT group as compared to the empty vector and K139R groups. Magnification 200X. Scale bar 50 μm . All data were analyzed by 2-way ANOVA with Tukey's post-hoc analysis. Bar graphs represented mean \pm SEM, n=3. *** P <0.001, **** P <0.0001.

5.4. *Helicobacter*-infected mouse and human gastric epithelia have remarkably low PHD3 but high ac-K¹³⁹ Siah2, Siah2 and Hif1 α protein level

Although the severity of inflammation, immune response and disease outcome in *H. felis*-infected mouse models is higher in comparison to *H. pylori*-driven human gastric carcinogenesis, but the *H. felis*-infected mice highly mimic the carcinogenic events occurring in *H. pylori*-infected humans (7, 225, 226). In order to examine the events observed *in-vitro*, we performed immunofluorescence microscopy and H&E staining of the tissue samples from C57BL/6 mice (n=20) infected for 12 months with *H. felis*. The infected mice manifested splenomegaly (Figure 5.5A), a common feature of infection. Uninfected mice gastric mucosa showed normal physiology but, *H. felis*-infected mice showed enlarged gastric mucosa with marked hypertrophy and increased infiltration of mononuclear cells (Figure 5.5B). The uninfected and infected mice gastric tissue sections were stained for ac-K¹³⁹Siah2, Siah2, PHD3 and Hif1 α proteins and immunofluorescence microscopy was performed. Infected mouse gastric epithelia had very high ac-K¹³⁹Siah2, Siah2 and Hif1 α protein expression but low expression of PHD3 as compared to the uninfected gastric tissue. H&E staining of infected mice gastric tissue samples exhibited distinctive features of hypertrophy with extensive mononuclear cell infiltration, gastritis, mucus gland metaplasia,

dysplasia and invasive adenocarcinoma (Figure 5.6A). Infected murine tissue samples which had higher expression of ac-K¹³⁹Siah2, Siah2, Hif1 α and lower expression of PHD3 were tested positive for *H. pylori* CagA protein (Figure 5.6B) and urease enzyme (Figure 5.6C), thus, directly linking *H. felis* infection with ac-K139 Siah2-PHD3- Hif1 α axis.

Immunofluorescence staining of human GC biopsy samples (n=14) collected from consenting patients and their respective non-cancerous tissues also demonstrated similar results as observed in C57BL/6 mice with marked increase in ac-K¹³⁹Siah2, Siah2 and Hif1 α expression and decreased PHD3 expression (Figure 5.6D).

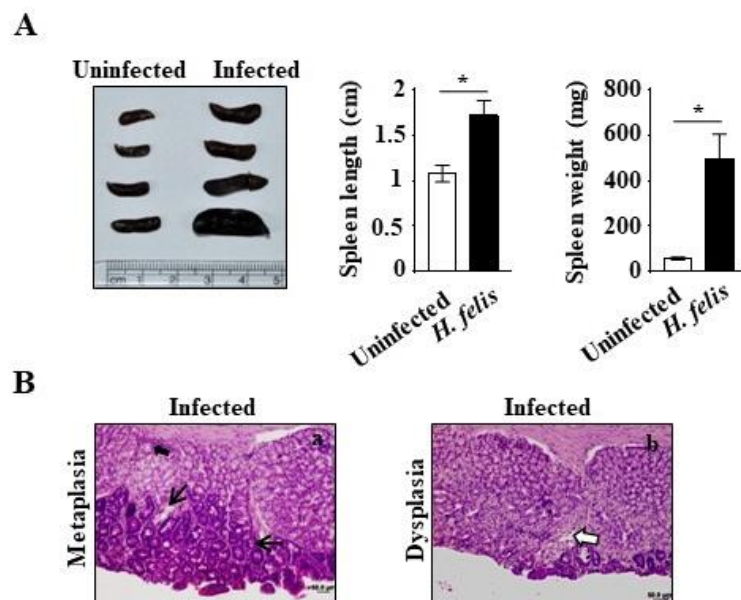


Figure 5.5 *Helicobacter*-infected mouse show splenomegaly and advanced stages of gastric carcinoma.

(A) Representative figure showing splenomegaly in infected C57BL/6 mice and corresponding bar graphs of average splenic-mass and average spleen length of uninfected and infected mice. (B) H&E staining of infected C57BL/6 gastric tissues showing (a) mucosal metaplasia (thin arrow) and (b) dysplasia (open arrow). Magnification 100X. Scale bar 50 μ m. Data were compared by Student's t-test. Error bars represented mean \pm SEM. * P <0.05.

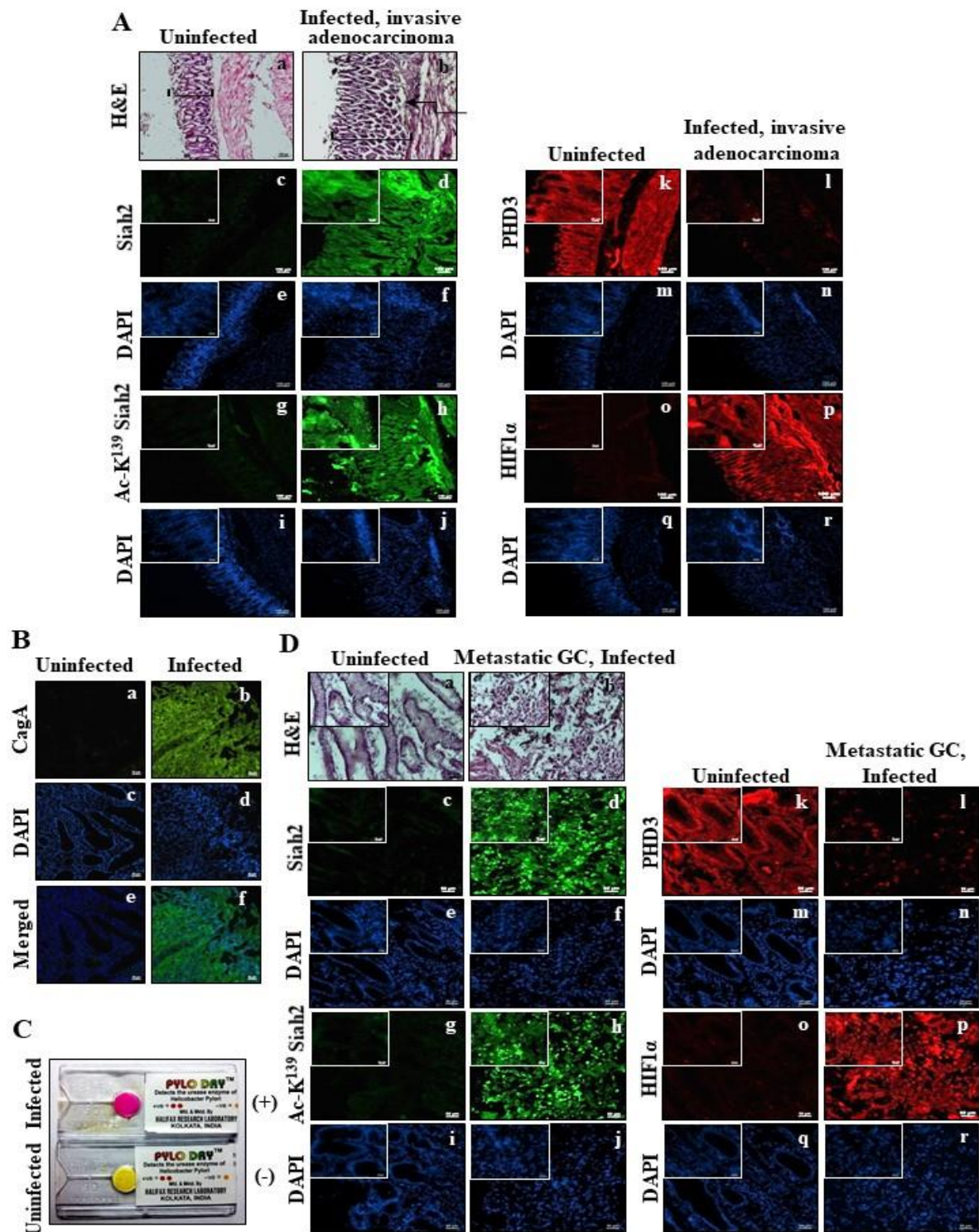


Figure 5.6 *Helicobacter*-infected mouse and human gastric epithelia have remarkably low PHD3 but high ac-K¹³⁹ Siah2, Siah2 and Hif1 α protein level

(A) H&E staining of infected C57BL/6 gastric tissues showing (a) mucosal metaplasia (thin arrow) and (b) dysplasia (open arrow). Magnification 100X. Scale bar 50 μ m. Antral stomach tissues from uninfected (a) and (b) *H. felis*-infected C57BL/6 mice were stained

with hematoxylin and eosin (H&E) showed mucosal thickening (bar) and sub-mucosal invasiveness (elbow arrow). Representative immunofluorescence microscopy results from uninfected and infected mouse gastric tissues showed expression of Siah2 (c and d), ac-K¹³⁹Siah2 (g and h), PHD3 (m and n), Hif1 α (q and r) and corresponding DAPI (e, f, i, j, o, p, s and t). Magnification 100X, inset 400X. Scale bar 100 μ m. (B) Fluorescence microscopy results of uninfected and infected murine antral gastric tissues showing expression of CagA (a and b), DAPI (c and d) and merged images (e and f). Magnification 200X. Scale shown 50 μ m. (C) Representative urease test image corresponding to infected and uninfected mouse gastric tissue. (D) Representative H&E staining data of human (a) non-cancerous and (b) metastatic gastric tissue biopsy samples. and immunofluorescence staining (c to r) for Siah2 (c and d), ac-K¹³⁹Siah2 (g and h), PHD3 (k and l), Hif1 α (o and p) and corresponding DAPI (e, f, i, j, m, n, q and r). Magnification 100X, inset 400X. Scale bar 50 μ m. Inset scale 25 μ m.

5.5. Discussion

In previous sections we have shown that *H. pylori* induces expression of Siah and acetylation of Siah2 protein in infected GCCs is responsible for preventing Siah2 protein from degradation. In this section we have shown that Siah2 acetylation (ac-K¹³⁹Siah2) enhances stability of Hif1 α by downregulating PHD3 thereby enhancing the invasiveness of *H. pylori*-infected epithelium. Phosphorylation and SUMOylation have been shown earlier to influence Siah2 activity and regulate Siah2 stability (138, 140, 141, 184). However, this is the first report on the impact of Siah2 acetylation in regulating Hif1 α stability. Our study authenticates previous reports which have emphasized on Siah2-PHD3 cascade known to regulate Hif1 α stability associated with tumorigenesis.

It is widely reported that hydroxylation causes normoxic degradation of Hif1 α regulated by prolyl hydroxylases (PHDs). E3 ubiquitin ligase von Hippel-Lindau (pVHL) has high affinity to hydroxylated proline residues of Hif1 α , which upon recognition, leads to Hif1 α degradation. However, in hypoxia, due to upregulation of Siah2, PHD proteins remain downregulated, ultimately stabilizing Hif1 α . Dimerization of Hif1 α with its constitutively expressed nuclear counterpart Hif1 β helps Hif1 to form a dimeric, functional transcriptional factor activating various downstream oncogenes (227). Our study reports the non-hypoxic regulation of Hif1 α influencing invasiveness in gastric cancer. Apart from hypoxic stabilization of Hif1 α , many other factors like bacterial sepsis, viruses, protozoan parasites, fungi also contribute to its accumulation (228). Recent studies suggest that, the role of Hif1 α is not just limited to hypoxic response in cancers, but it also orchestrates tissue barrier functions in response to numerous microbial infections (229-232). Even the regulation of PHDs is not explicitly linked to hypoxia. Carcinogenic metals, miRNAs, Vaccinia virus, ROS/ nitric oxide (NO) and cholesterol are also shown to regulate PHDs in varied physiological conditions (233-238). PHDs (PHD1, 2 and 3) are also involved in various biological processes affecting pathophysiological conditions (237). PHDs and Hif1 also regulate each-other in a feed-back loop manner (239).

We found acetylated Siah2 interacting with PHD3, which indicated that this modification did not affect their interaction. Stabilization of Siah2 by acetylation led to further effective downregulation of PHD3 by proteasome pathway contributing to increased Hif1 α accumulation. Our study confirmed that Hif1 α regulation by Siah2-PHD3 in *Helicobacter*-infected cases is independent of *cag* PAI status which indicates the possibility of other variants of *Helicobacter* species might also regulate Hif1 α expression in the same manner and hence, this need further investigation. As acetylation of Siah2 induced degradation of PHD3 and was upregulated in *H. pylori*-positive human GC biopsy samples or

H. felis-infected murine tissue samples, we speculate that targeting deacetylation of ac-Siah2 could help in reducing the severity of ac-Siah2 positive cancers and can be a strategy for therapeutic interventions for GC.

**TES and FLN-C degradation is promoted by
ac-K¹³⁹ Siah2 in *H. pylori*-infected GCCs**

Chapter 6

Chapter 6: TES and FLN-C degradation is promoted by ac-K¹³⁹ Siah2 in *H. pylori*-infected GCCs

6.1. *H. pylori* infection downregulates TES and FLN-C expression in GCCs

Siah2 induction and acetylation in gastric epithelia is associated with *H. pylori*-mediated gastric carcinogenesis. TES and FLN-C are scaffolding proteins, essential components of cell adhesion, spreading, proliferation, and are repressed in various tumors including GC (124, 240). Siah2 being an E3 Ub ligase, regulates the expressions of its numerous target proteins by ubiquitinating and degrading them. In order to identify novel targets of Siah2 in *H. pylori*-infected GCCs and their further implications in GC progression, we infected MKN45 cells that were stably expressing *siah2* WT and *siah2* K139R mutant constructs and infected with *H. pylori* (200 MOI for 12 h) while keeping one set uninfected. Whole cell lysates were immunoprecipitated with Siah2 antibody and the immunoprecipitate containing Siah2 binding-partners were resolved using SDS-PAGE. Gels were stained with CBB-R250 dye, washed with destaining buffer and the protein bands showing significant difference between uninfected and *H. pylori*-infected MKN45 stable cells were excised. The gel plugs were analyzed by LC-MS/MS analysis which revealed that TES and FLN-C can interact with Siah2. Western blotting performed using MKN45 cell lysates infected with *H. pylori* *cag* PAI(+) strain 26695 (at 200 MOI for 6 h, 12 h and 24 h) showed that the TES and FLN-C were downregulated in infected cells with maximal effect at 24 h p.i (Figure 6.1A). As TES and FLN-C are tumor suppressors and their expressions decreased in infected *siah2* stably-expressing GCCs, we were interested to understand the possible role of Siah2 in regulating their expression. To understand the effect of MOI on TES and FLN-C level, MKN45 cells were infected with 100, 200 and 300 MOI of *H. pylori* for 24 h. Western blotting of whole cell lysates revealed MOI-dependent decrease in TES and FLN-C proteins (Figure 6.1B). As 24 h infection with 200 and 300 MOI of *H. pylori* were most effective and

equivalent in downregulating TES and FLN-C, 200 MOI infection for 24 h was used for all future experiments unless mentioned specifically. In order to know whether this event was limited to only MKN45 or widespread across various GCCs, whole cell lysates from infected AGS and Kato III were immunoblotted. Similar trends were observed in both GCCs (Figure 6.1C). We did not see any difference in the downregulation of TES and FLN-C in MKN45 cells infected with *cag* PAI(+) and (-) strains 26695 and 8-1 as revealed by western blotting (Figure 6.1D).

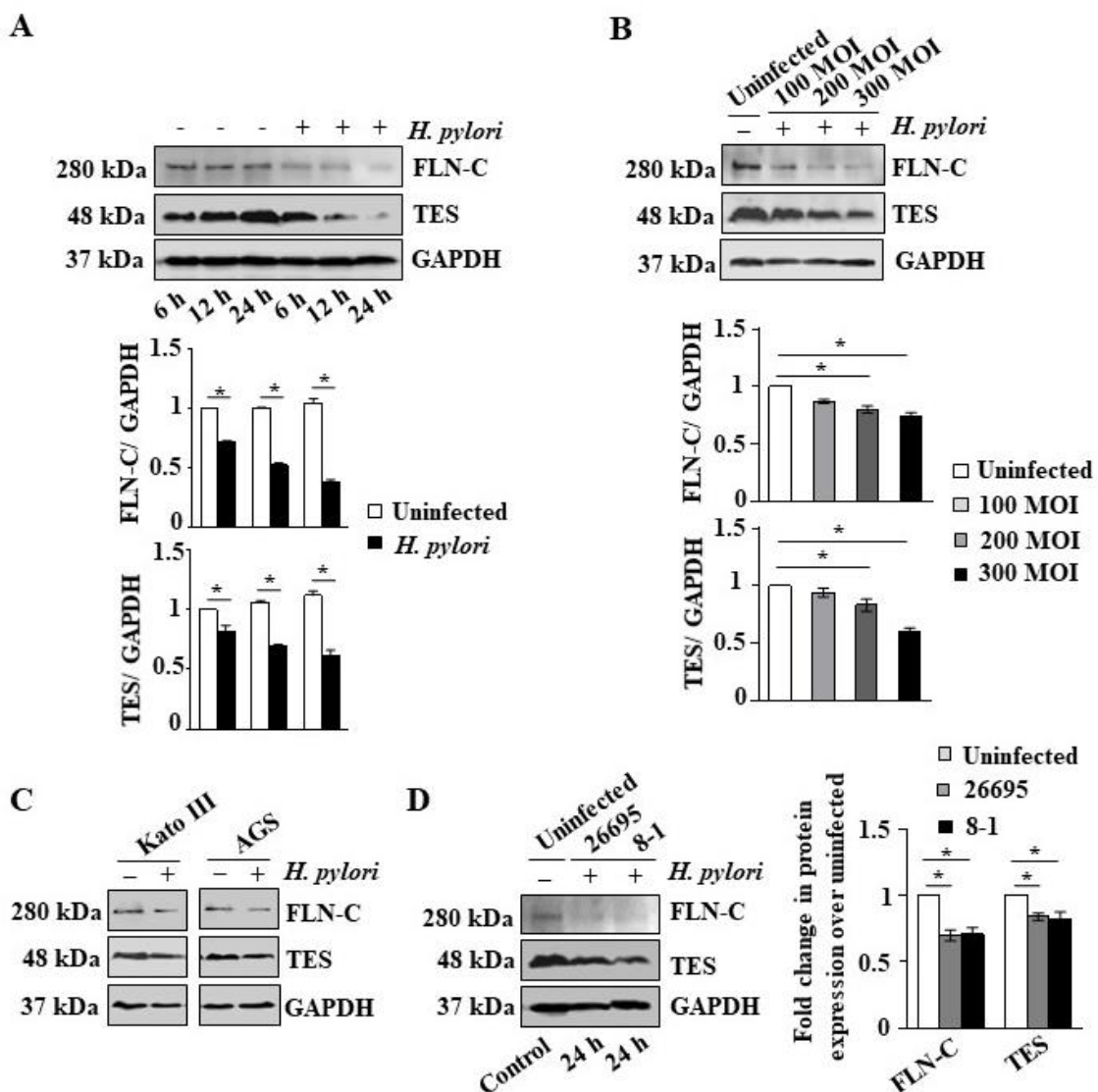


Figure 6.1: *H. pylori* infection downregulates TES and FLN-C expression in GCCs

(A) Representative western blot and graphical data showing expressions of FLN-C, and TES in MKN45 cells infected with *H. pylori cag* PAI(+) strain 26695 (200 MOI for 6 h, 12 h and

24 h). Data showed that FLN-C and TES expression decreased following *H. pylori* infection. (B) Western blotting performed using whole cell lysates of MKN45 cells infected with *H. pylori* (100, 200 and 300 MOI for 24 h). Densitometric graphs showed that TES and FLN-C expression were significantly decreased at 100, 200 and 300 MOI *H. pylori* infection. (C) Immunoblotting performed using Kato III and AGS cells also reveals that TES and FLN-C were downregulated in *H. pylori*-infected GCCs. (D) MKN45 cells were infected with *cag* PAI(+) and (-) strains of *H. pylori* (200 MOI for 24 h) and whole-cell lysates were blotted for TES and FLN-C proteins. Immunoblots revealed that both the strains were equally effective in reducing TES and FLN-C expression. Bars represented fold change in protein expressions over uninfected. Error bars, mean \pm SEM, n = 3, * P <0.05. GAPDH was used as a loading control in all western blots.

6.2. p300 causes downregulation of TES and FLN-C in *H. pylori*-infected GCCs

p300 mediates Siah2 acetylation in *H. pylori*-infected GCCs and enhances PHD3 degradation causing the accumulation of Hif1 α which further potentiates *H. pylori*-mediated gastric carcinogenesis (202). In order to assess the involvement of p300 in TES and FLN-C downregulation, we performed immunoprecipitation assays with Siah2 antibody and found that TES and FLN-C to significantly decrease in the immunocomplex from *H. pylori*-infected cells at 24 h p.i. whereas, p300 expression was found to be increased in the infected group (Figure 6.2A). Western blotting performed using infected immortalized normal gastric epithelial cell lysates HFE145 also displayed significantly decreased TES and FLN-C proteins as compared to uninfected cells (Figure 6.2B). To study the role of p300 HAT domain in the downregulation of TES and FLN-C in *H. pylori*-infected GCCs, MKN45 cell lysates transiently transfected with empty vector pcDNA3.1⁺, p300 WT and p300 Δ HAT constructs were immunoblotted and probed for p300, TES and FLN-C proteins. The data

showed that TES and FLN-C protein level was substantially decreased in *p300* WT-transfected group as compared to their counterparts (Figure 6.2C). TES and FLN-C expression was found to be increased in HAT/KAT acetyltransferase inhibitor CTK7A treated cells infected with *H. pylori* as compared to untreated cells establishing the role of HAT/KAT acetyltransferase p300 in Siah2 acetylation (Figure 6.2D).

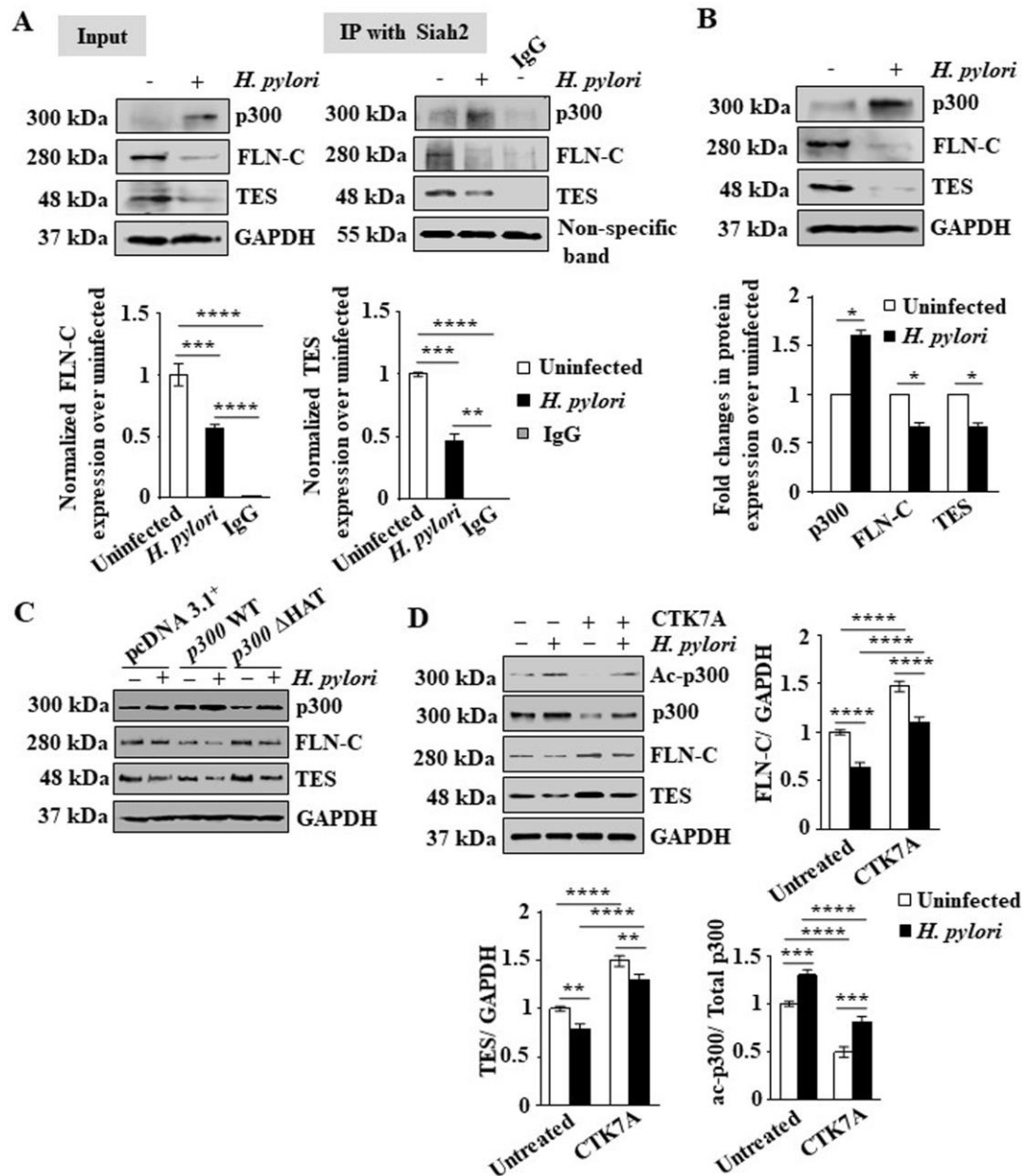


Figure 6.2: p300 causes downregulation of TES and FLN-C in *H. pylori*-infected GCCs

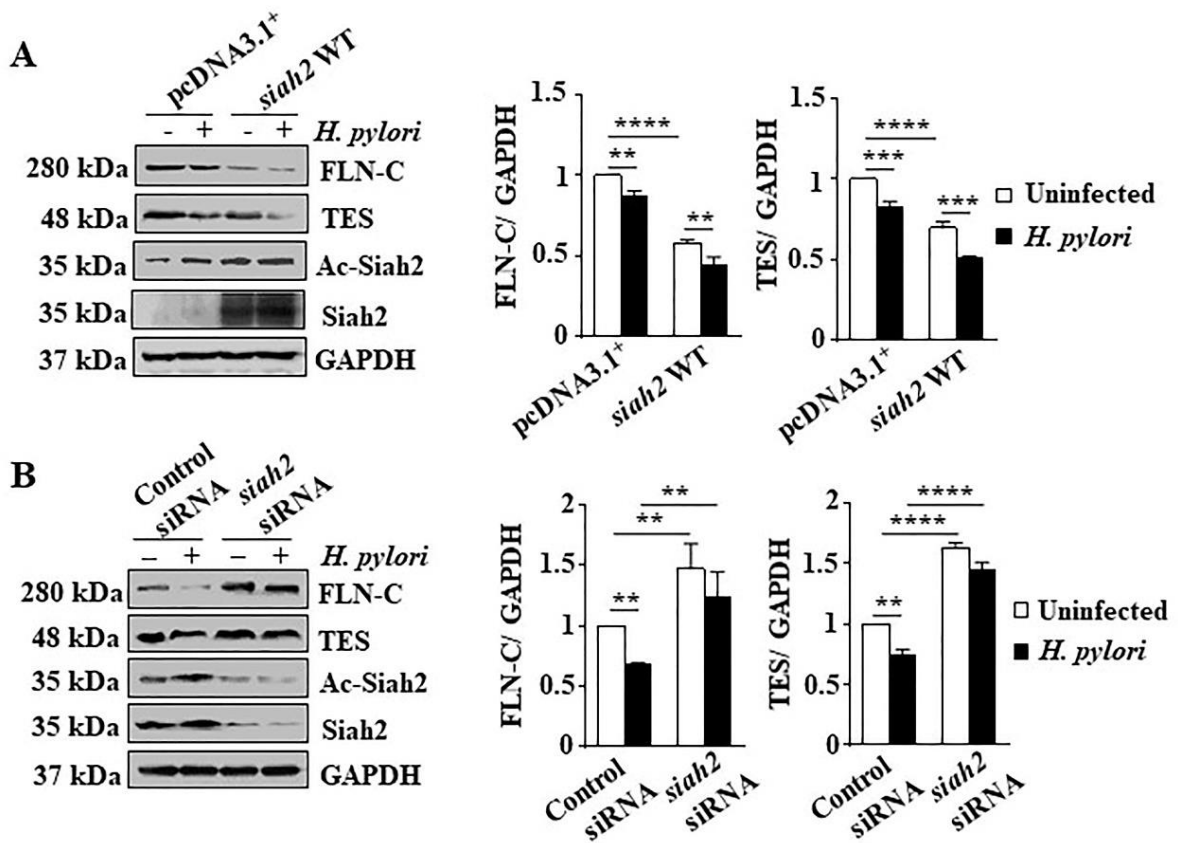
(A) Representative western blot of immunoprecipitation assay (n=3) performed using Siah2 antibody to pull down Siah2 immunocomplexes from uninfected or infected MKN45 (200

MOI, 24 h) to study the interaction of Siah2 with p300, TES and FLN-C. The result indicated that Siah2 interacted with p300, TES and FLN-C proteins. Data also showed the decrease in TES and FLN-C level in infected cells. (B) Immunoblot analysis image of HFE145 cells and corresponding densitometric graphs showing fold change in expressions of p300, TES and FLN-C with and without *H. pylori* infection. (C) Western blotting performed using whole cell lysates of MKN45 cells overexpressed with empty vector, p300 WT and p300 Δ HAT constructs either infected with *H. pylori* (200 MOI for 24 h) or left uninfected clearly showed downregulated TES and FLN-C proteins in p300 WT-expressing cells as compared to Δ HAT and empty vector-expressing cells. (D) Western blotting of whole cell lysates prepared from MKN45 cells double-transfected with *siah2* WT-K139R mutant constructs and p300 WT- Δ HAT plasmids and infected (200 MOI *H. pylori* for 24 h), showing expressions of p300, ac-K¹³⁹Siah2, Siah2, TES and FLN-C. All the graphical data represented fold change in protein expressions over uninfected control. GAPDH was the loading control in all western blot analysis. Error bars, mean \pm SEM, n = 3, * P <0.05; ** P <0.01; *** P <0.003; **** P <0.0001.

6.3. Siah2 K¹³⁹ acetylation enhances TES and FLN-C degradation

To establish the role of Siah2 on the degradation of TES and FLN-C proteins, western blotting was performed using MKN45 cells overexpressing pcDNA3.1⁺ and *siah2* WT constructs. After *H. pylori* infection, TES and FLN-C protein expression significantly decreased in cells expressing *siah2* WT compared to pcDNA3.1⁺-expressing cells (Figure 6.3A). To further confirm the downregulation of TES and FLN-C by Siah2, Siah2 siRNA-mediated knockdown methodology was applied in which MKN45 cells were transfected with *siah2* siRNA and later infected with *H. pylori*. The isolated cell lysates were western blotted for TES and FLN-C. Due to silencing of *siah2*, TES and FLN-C expression did not

decrease in *siah2*-transfected group as compared to control vector. As the silencing abrogated the effect of *H. pylori*, thus reconfirming Siah2-mediated TES and FLN-C downregulation (Figure 6.3B). Acetylation at K¹³⁹ residue protected Siah2 from undergoing proteasome-mediated degradation. To assess whether the inhibition of proteasome pathway could restore Siah2 K139R protein expression and its effect on TES and FLN-C, MKN45 cells-expressing *siah2* K139R mutant were treated with 50 μM MG132 for 24 h prior to *H. pylori* infection. Siah2 K139R protein expression was restored following MG132 treatment but ac-K¹³⁹Siah2 expression did not increase. TES and FLN-C expression was also rescued in MG132-treated cells indicating that acetylation at K¹³⁹ was crucial for Siah2 stabilization as well as TES and FLN-C degradation.



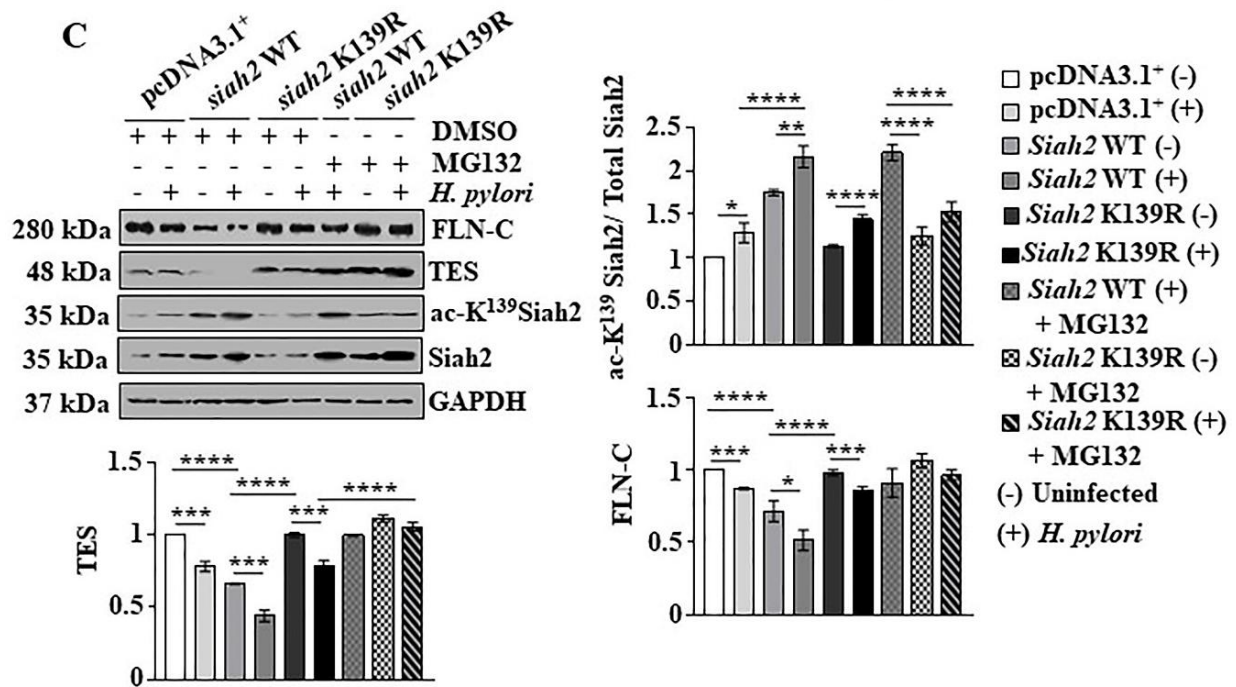
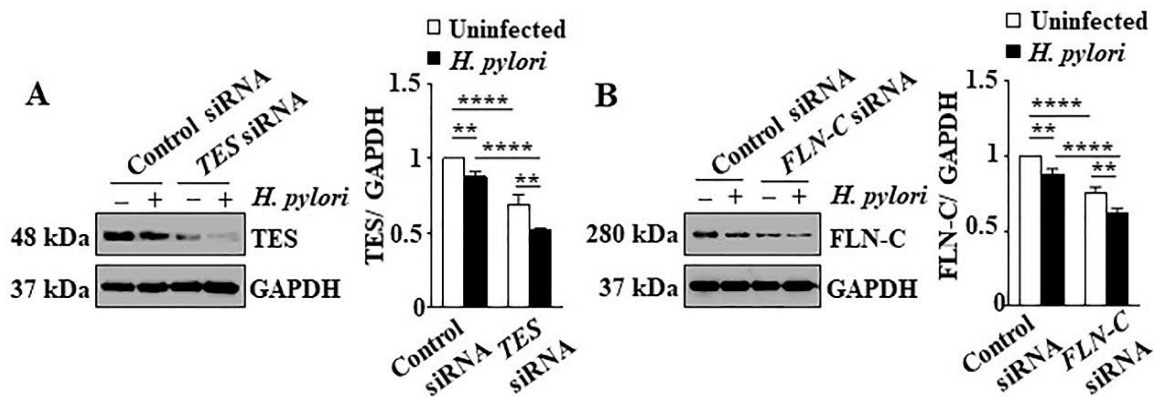


Figure 6.3: *Siah2* K¹³⁹ acetylation enhances TES and FLN-C degradation

(A) Representative immunoblotting image of MKN45 cells expressing empty vector and *siah2* WT constructs and infected with *H. pylori* (200 MOI for 24 h) showed that TES and FLN-C expression decreased in *siah2* WT-infected cells. Bar graphs representing fold change in normalized TES and FLN-C expression. (B) Western blotting of cell lysates prepared from MKN45 cells transfected with control siRNA and *siah2* siRNA showing significant increase in TES and FLN-C expression in *siah2*-transfected group in comparison to control siRNA group. Accompanying graphs showed TES and FLN-C normalized expression. (C) Representative western blot image of MKN45 cells stably-expressing empty vector, *siah2* WT and K139R mutant constructs treated with MG132 showing expressions of Siah2, ac-K¹³⁹Siah2, TES and FLN-C. Densitometric analysis of TES, FLN-C and ac-K¹³⁹Siah2: total Siah2 normalized to uninfected control. GAPDH was used as a loading control in all of the above immunoblotting. Error bars, mean±SEM, n=3, *P<0.05; **P<0.01; ***P<0.003; ****P<0.0001.

6.4. TES and FLN-C silencing leads to enhanced invasion and migration of GCCs

As the role of TES and FLN-C proteins in *H. pylori*-infected gastric epithelia invasiveness is unknown, we investigated the role of TES and FLN-C on migration and invasion ability of *H. pylori*-infected GCCs. In order to study this, we knocked-down the expressions of TES and FLN-C proteins in AGS cells as they are more suitable for migration and invasion assays. The effect of *TES* and *FLN-C* silencing at protein level was confirmed in AGS cells (Figure 6.4A). These cells were further utilized for *in vitro* migration and matrigel assays. *TES* and *FLN-C* silencing lead to remarkable increase in cell migration (Figure 6.4B and Figure 6.4C) and invasion (Figure 6.4D and Figure 6.4E) as compared to control groups. The increased-migration ability of *TES* and *FLN-C*-suppressed AGS cells infected with *H. pylori* was also examined by wound-healing assay. Result showed that wound area was almost entirely covered by *TES* and *FLN-C*-suppressed cells and *H. pylori* infection further enhanced this effect (Figure 6.5A and Figure 6.5B). The anchorage-independent colony-forming ability of *TES* and *FLN-C*-silenced cells was assessed by soft agar assay. For this assay, *TES* and *FLN-C* was knocked-down in MKN45 cells. *TES* and *FLN-C* suppression was determined by western blotting (Figure 6.5C and Figure 6.5D) prior to be used in the soft agar assay. Both, *TES* and *FLN-C* silencing promoted foci formation by suppressed cells as compared to control cells (Figure 6.5E and Figure 6.5F).



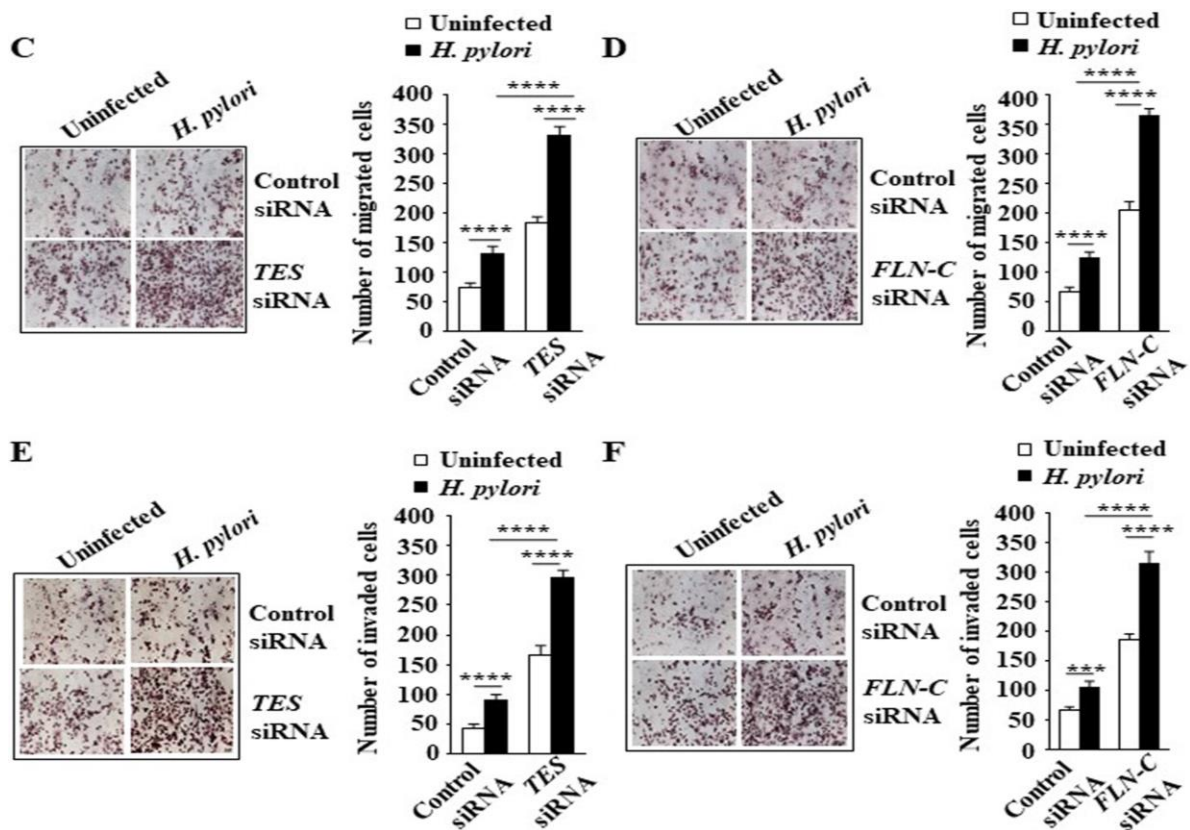


Figure 6.4: TES and FLN-C silencing leads to enhanced invasion and migration of GCCs

(A) Representative immunoblotting image of AGS cells (n=3) showing the effect of siRNA mediated-silencing of *FLN-C* and (B) *TES*. Bar graphs showed marked reduction in *FLN-C* and *TES* expression siRNA-transfected groups with respect to control group. GAPDH was used as a loading control. (C) Microscopic images of *in-vitro* cell migration assay performed using si*FLN-C* and (D) si*TES*-silenced AGS cells showing significantly increased migration of infected cells expressing si*FLN-C* and si*TES* as compared to their counterparts in siControl group. Magnification 200X. Scale bar 50 μ m. Representative graphs showing the mean number of migrated cells. (E) Microscopic images of matrigel assay performed using *FLN-C* and *TES*-knocked down AGS cells indicating significantly enhanced invasive property of si*FLN-C* and si*TES*-expressing cells. Magnification 200X. Scale bar 50 μ m. Representative bar graphs denoted the mean number of cells invaded. Data were analyzed by two-way ANOVA with Tukey's post hoc test. Bar graphs represented error bars, mean \pm SEM, n=3, ** P <0.01, *** P <0.003, **** P <0.0001.

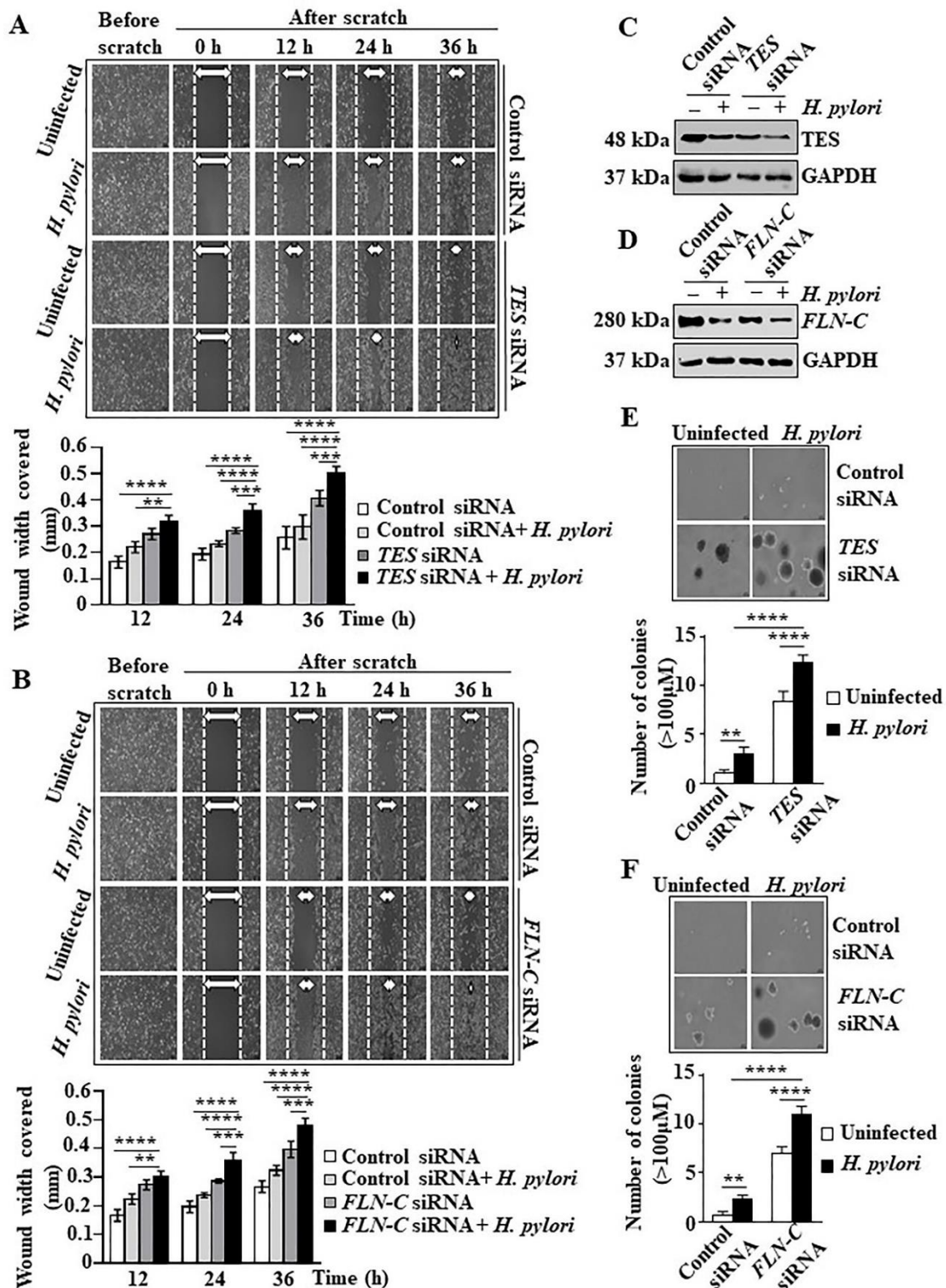


Figure 6.5: TES and FLN-C silencing increases invasiveness of GCCs

(A) Representative wound healing assay result (n=3) showing effect of siTES and (B) siFLN-C on the wound healing ability of siRNA-transfected AGS cells as compared to siControl cells. Magnification 100X. Scale bars shown 100 µm. Representative graphs shows average

area covered by transfected cells. (C) Representative western blot images (n=3) of MKN45 cells transfected with siControl and *siTES* and (D) *siFLN-C* showed marked decrease in TES and FLN-C expression in siRNA-transfected cells as compared to control siRNA cells. GAPDH was used as a loading control. (E) Soft agar colony formation assay performed using MKN45 cells showed that *siTES*-transfected cells had significant increase in colony formation p.i. as compared to siControl-transfected cells. Bar graphs representing the average number of colonies formed. (F) Soft agar assay data of MKN45 cells transfected with siControl and *siFLN-C* showing a substantial increase in colony forming ability of *FLN-C*-suppressed cells. Magnification 100X. Scales shown in (E) and (F) 200 μ m. Data were analyzed by two-way ANOVA with Tukey's post hoc test. Bar graphs represented mean \pm SEM, n=3. ** P <0.01; **** P <0.0001.

6.5. TES and FLN-C are stabilized in K139R acetylation-null Siah2-expressed GCCs

The importance of acetylation at Siah2 K¹³⁹ residue on TES and FLN-C degradation in *H. pylori*-infected GCCs was further investigated by confocal microscopy in empty vector, *siah2* WT and *siah2* K139R mutant construct stably-expressing MKN45 cells (Figure 6.6A) and AGS cells (Figure 6.6B). WT *siah2*-transfected and infected cells showed marked downregulation of TES and FLN-C when compared with the other transfected groups.

As TES and FLN-C are actin-binding proteins, we were interested to investigate the effect of Siah2 K¹³⁹ acetylation on actin rearrangement and polymerization. In order to assess this phenomenon, empty vector, *siah2* WT and *siah2* K139R-transfected AGS cells were infected with *H. pylori* followed by staining with phalloidin-FITC. In comparison to the other two transfection groups, WT cells infected with *H. pylori* showed remarkable decrease in the length of filopodia but lamellipodia were found to be well-developed (Figure 6.6C).

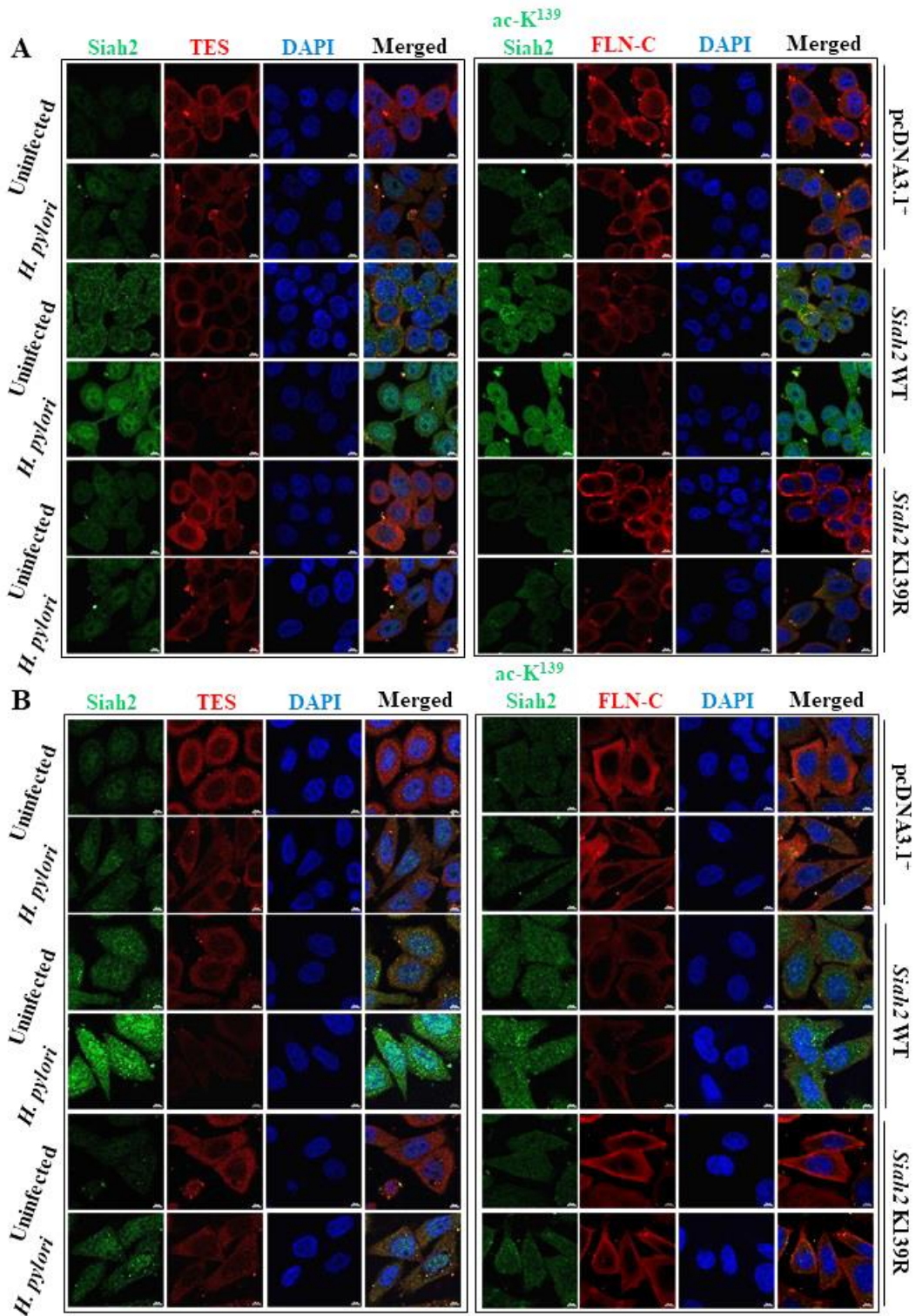
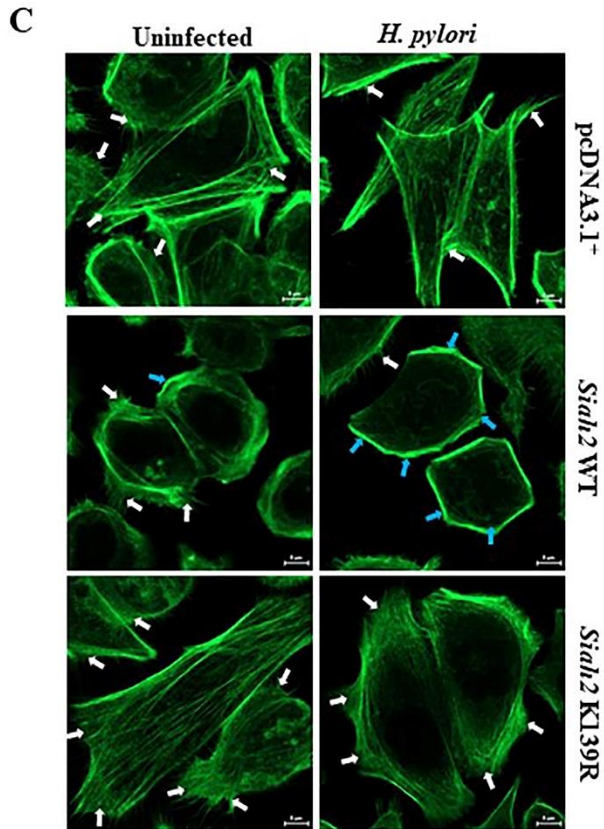


Figure 6.6: TES and FLN-C are stabilized in K139R acetylation-null Siah2 mutant-expressed GCCs

(A) Representative confocal microscopy images of MKN45 and (B) AGS cells stably-transfected with empty vector, *siah2* WT and *siah2* K139R mutant constructs showing

expression of Siah2, ac-K¹³⁹Siah2, TES and FLN-C. TES and FLN-C were significantly reduced in *H. pylori*-infected *siah2* WT stably-transfected MKN45 and AGS cells as compared to empty vector and K139R-transfected groups. Original magnification X630. Scale shown 10 μ m.



(C) F-actin was immunostained using phalloidin-FITC conjugate probe in AGS cells stably transfected with empty vector, *siah2* WT and *siah2* K139R constructs with or without *H. pylori* infection. Filopodia formation (white arrow) is found to be decreased and lamellipodia formation (blue arrow) increased in *siah2* WT-expressing AGS cells as compared to their counterparts. Magnification 630X. Scale shown 5 μ m.

6.6. TES and FLN-C expression is decreased in infected mouse and human gastric epithelia after *Helicobacter* infection

In order to validate the results *in-vivo*, TES and FLN-C protein level was determined in *Helicobacter*-infected C57BL/6 mice and in gastric biopsy samples obtained from consenting patients suffering from GC. Male or female C57BL/6 mice (n=16 for both control and infected groups) were infected with *H. felis*. Following 12 months of infection, antral gastric tissue sections were made and were immunostained for TES and FLN-C

proteins. Protein expression was assessed by immunofluorescence microscopy. Expression of TES and FLN-C was decreased in infected gastric tissues as compared to the uninfected tissues (Figure 6.7A and Figure 6.7B).

The metastatic gastric tissue samples obtained from consenting patients (n=10, and *H. pylori*-infected) showed TES and FLN-C downregulation as compared to the uninfected non-cancerous tissues (Figure 6.7C and Figure 6.7D).

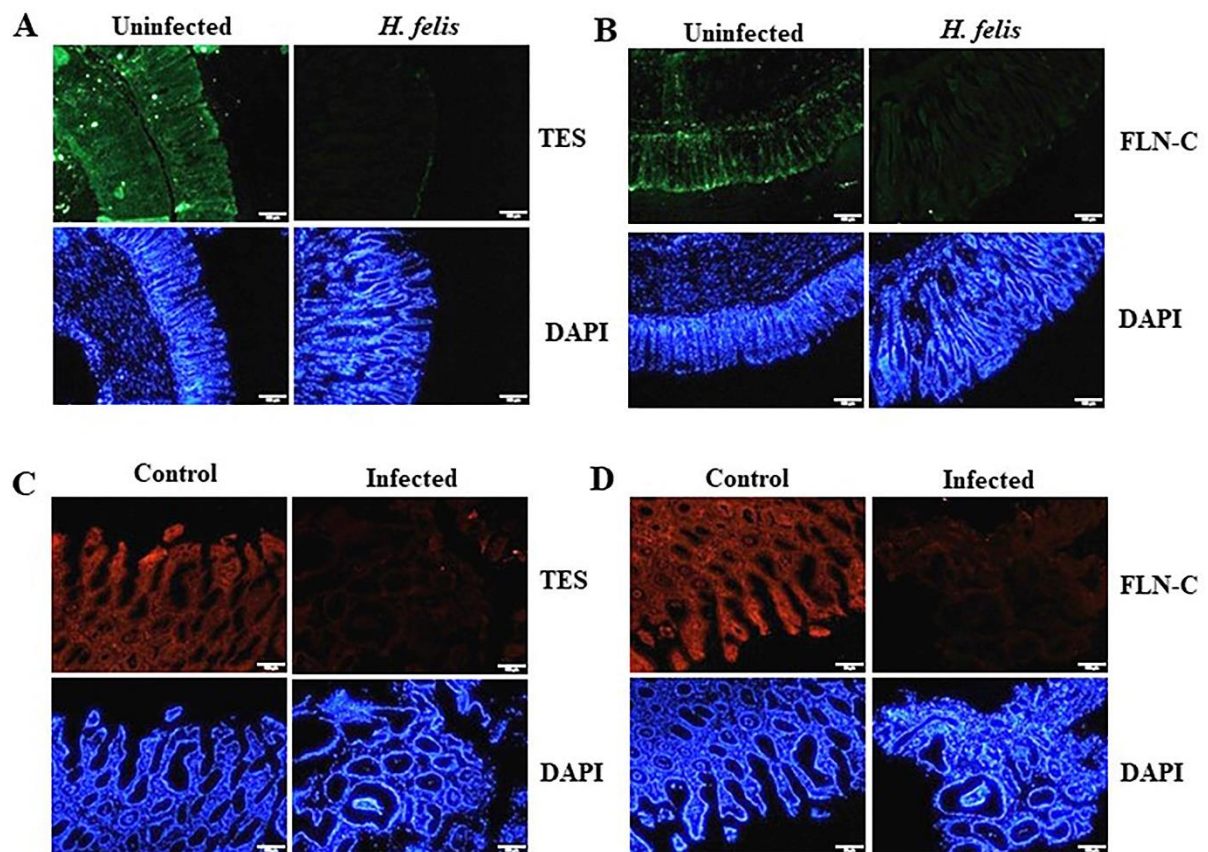


Figure 6.7: TES and FLN-C expression is decreased in infected mouse and human gastric epithelia following *Helicobacter* infection

(A) Representative fluorescence microscopic images of antral gastric mucosa from *H. felis*-infected and uninfected C57BL/6 mice (n=16) and stained for TES and (B) FLN-C proteins showed that TES and FLN-C were decreased in infected gastric epithelia as compared to uninfected tissue. (C) Representative fluorescence microscopic images of *H. pylori*-infected metastatic GC biopsy samples and uninfected non-cancerous tissue obtained from

consenting patients (n=10) showing expression of TES and (D) FLN-C proteins. The immunofluorescence data shows that TES and FLN-C proteins were downregulated in *Helicobacter*-infected human metastatic GCs. Magnification 100X. Scale bar shown 100 μm .

6.7. Discussion

Proteasomal degradation of tumor suppressor proteins is common in cancer (241-243). Siah2 is upregulated in various cancers including gastric cancer (137, 244). In the previous chapters we have shown that Siah2 acetylation downregulated PHD3 expression, thereby helping in the accumulation of Hif1 α which promotes the invasive property of infected GCCs. Here, we established that p300-mediated acetylation and stabilization of Siah2 was responsible for the degradation of actin-binding proteins TES and FLN-C, resulting in increased invasiveness of *H. pylori*-infected GCCs. High expression of ac-Siah2 and decreased expression of TES and FLN-C was observed in *H. felis*-infected mouse model and also in human stomach cancer biopsy tissues showing the therapeutic potential of targeting Siah2 acetylation to treat gastric cancer.

TES and FLN-C act as tumor suppressors in various cancers including gastric cancer where they affect the cell proliferation and motility (122, 130-133). They are involved in cytoskeletal rearrangement, adhesion structures and actin binding. Therefore, these proteins directly influence cell shape and cell-cell interactions (122, 123, 126). So, in order to become invasive, cancer cells often downregulate these adhesion proteins. This is also proved by the fact that *H. pylori* CagA protein causes modulation of signaling events which lead to cytoskeletal rearrangements in gastric cancer (118, 245, 246). However, this study is the first ever investigation to study the role of acetylation of an E3 ubiquitin ligase in disrupting cell

adhesion-related molecules TES and FLN-C by proteasomal degradation in *H. pylori*-infected gastric epithelia.

TES and FLN-C silencing by promoter hypermethylation is reported in advanced stages of gastric cancer (125, 130). It is interesting to highlight that many tumor suppressors like cell cycle regulators, E3 ubiquitin ligases, signaling molecules, etc. undergo silencing by promoter hypermethylation as well as by degradation through proteasome-mediated pathways in various cancers (93, 247-251). We could not determine the extent of TES and FLN-C hypermethylation and its relation with Siah2-mediated proteasome degradation in *H. pylori*-infected GCCs. The sequential or simultaneous occurrence of hypermethylation and proteasomal degradation of TES and FLN-C warrant further investigation.

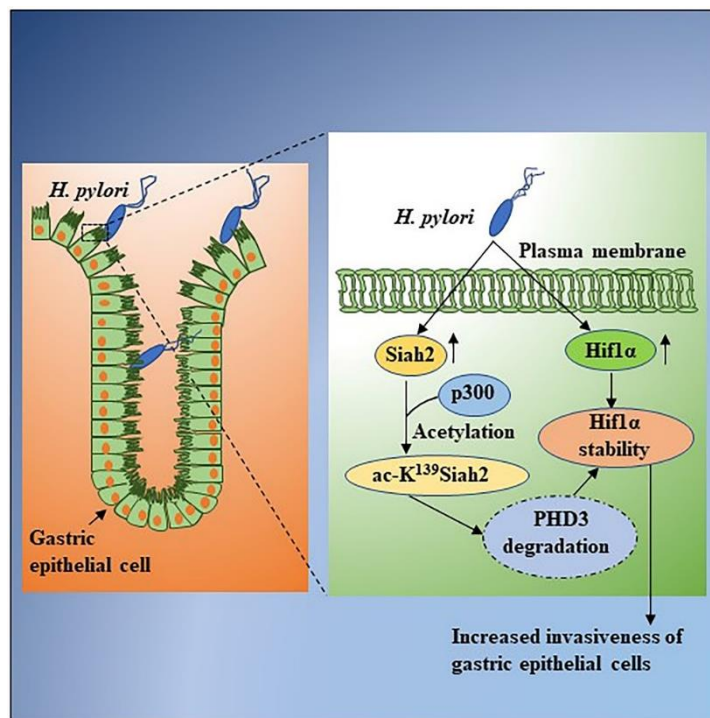
Actin cytoskeletal rearrangement involving filopodia, lamellipodia, stress fibers which regulate the cell elasticity are usually observed during *H. pylori* infection. Filopodia imparts cell-cell, cell-matrix attachments helping in invasive behaviour of cells during carcinogenesis (252-254). Lamellipodia, another component of cell motility is involved in the sheet-like cell edge formation at the protruding ends (255). FLNs help in forming the filopodial arrangement (245, 256) whereas, TES in association with its interacting proteins regulate filopodia formation (129). Out of several widely-distributed actin-binding proteins (ABPs) actin-related proteins (ARPs) like ARP2/3 are essential ones regulating the actin motor-driven processes known to be present from yeasts to humans (257). ARP2/3 along with other accessory factors regulating actin polymerization-depolymerization process are distributed differentially in between lamellipodia and filopodia which help them regulate cellular movements. We have shown that TES and FLN-C promote formation of filopodia and their reduction led to the formation of lamellipodia. However, the exact mechanism of TES and FLN-C regulating actin assembly in *H. pylori*-infected cells needs to be studied in detail.

Overall, this study advanced our understanding of the effect of Siah2 in promoting *H. pylori*-mediated GC invasiveness. Data presented here confirmed that down regulation of actin-binding proteins TES and FLN-C and increased Hif1 α -accumulation in the infected gastric epithelium were the resultant effect of Siah2 acetylation and these processes contributed in increasing invasiveness of *H. pylori*-infected GCCs.

SUMMARY AND CONCLUSION

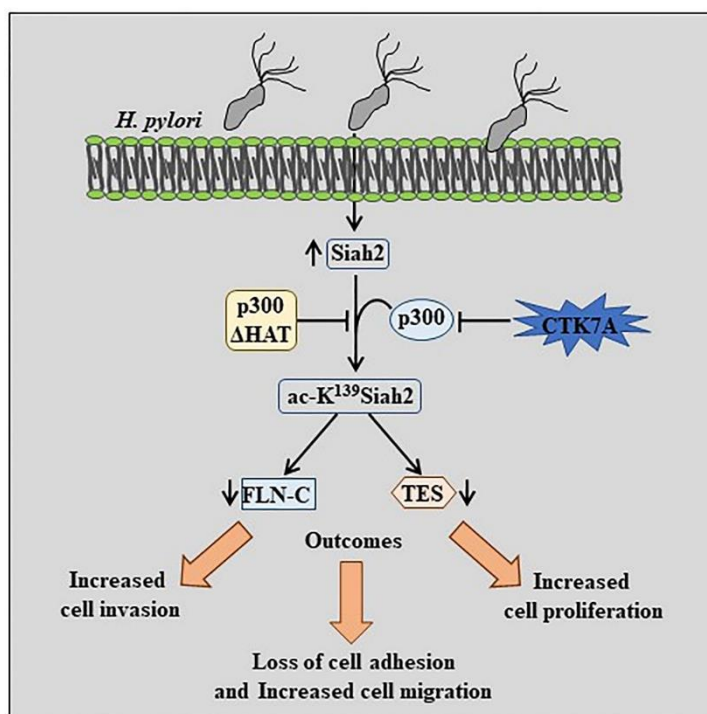
Chapter 7

Major conclusions from this study are summarily presented here.



Summary figure 7.1: Regulation of p300-mediated Siah2 acetylation enhances PHD3 degradation and Hif1 α accumulation in *H. pylori*-infected GCCs

- ❖ *H. pylori* infection induces Siah2 and p300 expression in GC cells. p300 HAT function promotes Siah2 K¹³⁹ residue acetylation in infected GCCs.
- ❖ Acetylation of Siah2 (ac-K¹³⁹Siah2) stabilizes Siah2 and protects it from undergoing proteasome-mediated degradation.
- ❖ Thus, ac-K139Siah2 enhances degradation of PHD3 leading to accumulation of Hif1 α which increases invasiveness of GCCs.



Summary figure 7.2: Acetylated Siah2 elevates GC invasiveness by degrading TES and FLN-C

- ❖ *H. pylori*-induced Siah2 acetylation at K¹³⁹ residue increases degradation of tumor suppressor proteins TES and FLN-C in infected GCCs.
- ❖ Silencing of *TES* and *FLN-C* enhances invasiveness of infected GCCs.
- ❖ Ac-K¹³⁹Siah2-mediated downregulation of TES and FLN-C increases lamellipodia formation however disrupts filopodia formation resulting in enhanced migration and invasion of *H. pylori*-infected GCCs.

In conclusion, this thesis demonstrates the critical role of *H. pylori* in acetylation of Siah2 which is characterized by enhanced migration and invasion behaviour of *H. pylori*-infected GCCs. Our findings elucidate a novel pathway regulated by p300 HAT domain in acetylating Siah2 primarily at the K¹³⁹ residue that rescues Siah2 from proteasome-mediated degradation in the infected GCCs. Our work elaborates further on the mechanisms through which Siah2 acetylation enhances the degradation of tumor suppressor proteins like PHD3, TES and FLN-C intensifying the invasive property of *H. pylori*-infected GCCs. Our

investigation adds to the present knowledge of factors that enhance Hif1 α expression in *H. pylori*-infected gastric epithelia. Thus, the above mechanisms highlight on the importance of acetylation in functional regulation of Siah2 apart from known PTM like phosphorylation.

MATERIALS AND METHODS

Chapter 8

8. MATERIALS AND METHODS

8.1. MATERIALS USED

8.1.1. Cell lines

The human gastric epithelial cancer cells (GCCs) MKN45, AGS and Kato III were procured from the University of Virginia, USA. The immortalized human GCC HFE145 was received as a gift from Prof. Hassan Ashktorab, Department of Medicine, Howard University, USA. Details of several stable cell lines generated in our lab are described later.

8.1.2. Helicobacter strains

Strains of *Helicobacter* used in this study: *H. pylori* 26695, a *cag* PAI (+) strain; strain 8-1, a *cag* PAI (-) strain and mouse gastric pathogen *H. felis* strain 49179 (ATCC, #49179) (received from the University of Virginia, USA).

8.1.3. DH5α and XL10 competent cells

For cloning of plasmids, subcloning efficiency DH5α competent cells (#18265-017, Invitrogen, Carlsbad, California, USA) were used. During site-directed mutagenesis for cloning purpose, XL10-Gold ultracompetent cells (#200514, Agilent, Santa Clara, California, USA) were used.

8.1.4. Biopsy samples

GC patients, diagnosed for different stages of cancer were studied and gastric biopsy samples (from the antral gastric mucosa) were collected from patients undergoing diagnostic esophagogastroduodenoscopy test following a National Institute of Science Education and Research (NISER) Review Board-approved protocol. Written informed consent was obtained from all patients prior to the study. Tissue samples obtained were further processed for immunofluorescence microscopy as described later.

8.1.5. Antibodies, siRNAs and plasmid constructs

List of all antibodies, siRNAs and plasmid constructs used in this research are mentioned in appendix I, II, III and IV, respectively.

8.2. METHODOLOGY

8.2.1. Cloning, site-directed mutagenesis and expression

8.2.1.1. Cloning of human *siah2* acetylation-null lysine to arginine (K-R) mutants

Primer designing: Cloning and mutagenesis primers were designed to generate human *siah2* K13R, K17R, K107R, K129R and K139R mutant constructs by using Integrated DNA Technology (IDT) software (appendix V for details).

Generation of *siah2* K13R, K17R, K107R, K129R and K139R mutants by site-directed mutagenesis: Site-directed mutagenesis was carried out by QuikChange multisite-directed mutagenesis kit (#200517, Agilent technologies) using a single primer for inserting a single point mutation in *siah2* gene construct (163).

The amino acid sequence of Siah2 is as follows:

E3 Ub-protein ligase SIAH2 [Homo sapiens]

NCBI Reference Sequence: NP_005058.3

>gi|31982899|ref|NP_005058.3| E3 ubiquitin-protein ligase SIAH2 [Homo sapiens]

MSRPSSTGPSANK*PCSK*QPPPQPQHTPSPAAPPAAATISAAGPGSSAVPAAAAVIS
GPGGGGGAGPVSPQHHELTSLFECPVCFDYVLPPILQCQAGHLVCNQCRQK*LSCCP
TCRGALTPSIRNLAMEK*VASAVLFPCK*YATTGCSLTLHHTEKPEHEDICEYRPYSC
PCPGASCKWQGSLEAVMSHLMHAHKSITTLQGEDIVFLATDINLPGAVDWVMMQS
CFGHHFMLVLEKQEKYEGHQFFAIVLLIGTRKQAENFAYRLELNGNRRRLTWEAT
PRSIHDGVAAAIMNSDCLVFDTAIAHLFADNGNLTGINVTISTCCP

The corresponding nucleotide sequence is:

Nucleotide sequence: Homo sapiens Siah2 mRNA

ACCESSION NM_005067 REGION: 628.1602

VERSION NM_005067.5 GI:55925659

1 atgagccgcc cgtcctccac cggccccage gctaataaac cctgcagcaa gcagccgccg
61 ccgcagcccc agcacactcc gtccccggct gcgccccgg ccgcccgcac catctcggct
121 gggggccccg gctcgtccgc ggtgccccgc gggcgggcgg tgatctcggg ccccggcggc
181 gggggcgggg ccggcccgg gtccccgcag caccacgagc tgacctcgt cttcagatgt
241 ccggtctgct ttgactatgt cctgcctcct attctgcagt gccaggccgg gcacctggtg
301 tgtaaccaat gccgccagaa gttgagctgc tgcccgcagc gcagggggcgc cctgacgccc
361 agcatcagga acctggctat ggagaagggtg gcctcggcag tctgtttcc ctgtaagat
421 gccaccacgg gctgttcct gacctgcac catacggaga aaccagaaca tgaagacata
481 tgtgaatacc gtcctactc ctgccatgt cctggtgctt cctgcaagt gcaggggtcc
541 ctggaagctg tgatgtccca tctcatgcac gccacaaga gcattaccac cctcagga
601 gaagacatg tctttctage tacagacatt aactgccag gggctgtcga ctgggtgatg
661 atgcagtcac gttttggcca tcaactcatg ctggtgctgg agaaacaaga gaagtacgaa
721 ggccaccage agtttttgc catcgtcctg ctattggca cccgcaagca agccgagaac
781 tttgctaca gactggagtt gaatgggaac cggcggagat tgacctggga ggccacgccc
841 cgttcgattc atgacggtgt ggctcggcc atcatgaaca gcgactgcct tgtttcgac
901 acagccatag cacatctttt tgcagataat gggaacctg gaatcaatgt tactatttct
961 acatgttgc catga

The 13th, 17th, 107th, 129th and 139th lysine residues (marked with *) of Siah2 wild type (WT) protein were replaced with arginine residue to form Siah2 K13R, K17R, K107R, K129R and K139R constructs, respectively. Codons AAA or AAG which represent lysine, was mutated to AGA or AGG representing arginine (primers used are listed in Appendix V).

The mutagenesis reaction mix (25 μ l) was prepared with following components:

Table 1. Components for site-directed mutagenesis

Components	Amount	Final conc.
10X QuikChange multi-reaction buffer	2.5 μ l	1X
Quik solution	0.75 μ l	NA
dNTP mix	1 μ l	2 mM/ reaction

Primer (10 μ M)	1 μ l	100 ng/ reaction
Plasmid DNA template	1 μ l	100 ng/ reaction
QuikChange multi enzyme	1 μ l	2-5 units/ reaction
Mole. grade H ₂ O	17.75 μ l	NA
Final volume	25 μ l	

The PCR reaction (PCR Master cycler provapo. protect, Eppendorf, Hamburg, Germany) conditions for site-directed mutagenesis are mentioned in Appendix VI.

After completion of the site-directed mutagenesis, the amplified products were treated with 1 μ l (10 U/ reaction) of Dpn I restriction enzyme (an endonuclease; targeted sequence: 5'-Gm6ATC-3' and is specific for methylated and hemi-methylated DNAs) and was incubated at 37 °C in PCR machine for 2 h. This enzyme digests the parental strands of DNA at specific sites leaving the daughter strands intact. After digestion, the Dpn I-treated ssDNA strands from mutagenesis reaction were transformed into XL10-Gold ultracompetent cells (#200515, Agilent) where the mutant closed-circle ssDNA was converted into a duplex form *in vivo*. The mutants generated were further confirmed by agarose gel electrophoresis (AGE), restriction digestion, sequencing and positive clones were further amplified by maxi prep method (#43776, Qiagen, Hilden, Germany). For the primers used for sequencing and the sequencing results, please refer appendix VII and VIII.

Transformation: 5 μ l site-directed mutagenesis product was mixed with gently-thawed 45 μ l XL10-Gold ultracompetent cells in 1.5 ml microcentrifuge tube. 2 μ l of beta-mercapto ethanol (β -ME) was added to the mix. The mix was mixed by swirling and incubated on ice for 10 min with intermittent gentle swirling every 2 min. Heat-shock was given to the tubes in a 42°C preset water bath (Model No. CD-200F refrigerated circulator, JULABO, Seelbach, Germany) for 30 seconds. Tubes were incubated on ice for 2 min. Pre-warmed

450 µl SOC media (#15544034, Invitrogen) was added to the tube quickly, mixed and incubated (Model No. Innova 42R, New Brunswick™, Eppendorf) for 1 h at 37 °C with shaking at 225-250 rpm. After incubation, appropriate volume of reaction mix was spread on Luria-Bertani agar, Miller {(LB), #M1151, HiMedia, Mumbai, India} plates containing 100 µg/ml Sodium-Ampicillin salt (#A022, HiMedia) using L-shaped spreader gently and uniformly till the bacterial suspension gets absorbed completely and the plate was incubated for overnight at 37 °C. In order to verify the transformation efficiency of XL10-Gold ultracompetent cells, transformation using 1 µl pUC18 control plasmid (0.01 ng/µl) was also performed (as positive control).

Selection of positive clones: After 24 h of transfection, 4-5 isolated colonies were selected from the plate using a sterile toothpick or inoculation needle. A master plate was prepared at first and the same toothpick was inoculated into 5 ml LB broth, Miller (#M1245-500G, HiMedia) with 100 µg/ml of Sodium-Ampicillin salt and incubated O/N at 37 °C with 225-250 rpm shaking. Plasmid DNA was isolated from bacterial culture next day using miniprep kit.

Miniprep plasmid isolation: For the plasmid miniprep isolation, QIAprep Spin Miniprep Kit (#27106, Qiagen) was used. O/N-grown 5 ml bacterial culture was pelleted at 6800xg for 3 min at 4 °C. The bacterial pellet was resuspended in pre-chilled 250 µl buffer P1 (RNase A added). The bacterial pellet was broken by vortexing for a short span or by using a micropipette. 250 µl buffer P2 was added and the tube was inverted several times till the color of solution turned evenly blue and was kept for 5 min at RT for bacterial lysis. Precaution was taken not to lyse for more than 5 min as it would lead to plasmid shearing. 350 µl buffer N3 was mixed immediately and thoroughly mixed by 4-6 times by inverting the tube till the solution turned cloudy. The suspension was spun-down at RT for 10 min and the supernatant was applied to the QIAprep spin column by decanting or pipetting. After a

30-60 sec spin, the flow-through was discarded and the column was washed with 500 µl buffer PB followed by 750 µl buffer PE and spun down for 1 min. An additional 1 min spin was given to remove residual buffers. 30 µl of pre-warmed EB buffer was added on the column, followed by a 1 min stand and centrifugation for 1 min at top speed to elute plasmids. The concentrations of the isolated plasmids were measured (Model-NanoDrop™2000 Spectrophotometer, ThermoFisher Scientific, Waltham, Massachusetts, USA) using TE buffer as blank/ control.

In order to select the plasmid with mutation, agarose gel electrophoresis (AGE) was performed before confirmation by restriction digestion using Hind III/Xho I enzymes and DNA sequencing.

Agarose gel electrophoresis of the mutant plasmids: Agarose gel electrophoresis was performed to verify proper isolation of plasmids and further confirmation by double digestion and sequencing. 1% agarose gel (#0219398425, MP Biomedicals, Santa Ana, California, USA) was prepared in 1X Tris acetate-EDTA buffer {(TAE) (#ML016-500ML, HiMedia)}, 0.5 µg/ml concentration of ethidium bromide {(EtBr) (#MB074-10ML, HiMedia)} and was allowed to polymerize for 20 min. The gel was run at 50-100 V in a horizontal mini-electrophoresis unit (#170-4467, Bio-Rad Laboratories, Hercules, California, USA) till the loading dye reached 3/4th of the gel and band position of plasmids along with its corresponding molecular weight markers (#N3232L-1 ml, New England Biolabs Inc., Ipswich, Massachusetts, USA) were visualized and image was captured using an ultraviolet (UV) trans-illuminator (ChemiDoc XRS plus, Model No. 1708265, Bio-Rad Laboratories Laboratories). The plasmids that showed the same band size as that of *siah2* WT plasmid were only selected for double digestion confirmation.

Restriction digestion of *siah2* WT and mutant constructs: Hind III (#R0104S, New England Biolabs Inc.) and Xho I (#R0146S, New England Biolabs Inc.) were used for confirmation

of mutants by double digestion. Double digestion was done using 1 μg amount of the plasmids in a 37 °C water bath for 3 h. For restriction digestion, the following components were used:

Table 2. Components for restriction digestion

Components	Amount	Final conc.
10X buffer 2.1	5 μl	1X
Xho I	0.5 μl	20,000 U/ml
Hind III	0.5 μl	20,000 U/ml
Plasmid DNA	2 μl	1 μg
Mole. Grade H ₂ O	42 μl	NA
Final volume	50 μl	

The digested products were run on 1% agarose gel and visualized using UV trans-illuminator as described previously. Positive clones were amplified by maxiprep method and finally confirmed by DNA sequencing.

Maxiprep of plasmid: Maxiprep kit (#43776, Qiagen) was used to amplify the selected positive clones. Positive clones were picked from the master plate and inoculated in 10 ml LB broth with 100 $\mu\text{g}/\text{ml}$ of ampicillin sodium salt and were incubated for 10-12 h at 37°C and 225-250 rpm shaking till sufficient growth occurred. This bacterial suspension was inoculated into 100 ml LB broth containing 100 $\mu\text{g}/\text{ml}$ of ampicillin sodium salt followed by incubation in a shaker incubator for 16 h at 37 °C. 1-2 ml of the culture was removed to prepare glycerol stocks. The culture was pelleted at 6000xg for 15 min at 4 °C. The supernatant was discarded and the bacterial pellet was resuspended in 10 ml of prechilled buffer P1 (containing RNase A and lyseblue reagent as per the manufacturer's instruction). 10 ml of buffer P2 was added, mixed vigorously by inverting 4-6 times till the mix turned blue and incubated for 5 min at RT. 10 ml of prechilled buffer P3 was added, mixed

thoroughly by vigorous mixing 4-6 times. The lysate was poured into the barrel of the Qiafilter cartridge with a cap fitted on the nozzle to prevent loss of the content as flow-through. The mix was then incubated for 10 min at RT without disturbance. While the incubation proceeded, Hispeed maxi tip was equilibrated by adding 10 ml Buffer QBT and the column was allowed to drain by gravity flow into a discard bowl. The cap fitted to the Qiafilter cartridge was removed and the bacterial lysate was filtered into the previously equilibrated Hispeed tip. The clear lysate was allowed to enter the resin through gravity flow. The Hispeed tip was washed with 60 ml Buffer QC. DNA was eluted into a 50 ml of centrifuge tube by adding 15 ml Buffer QF to the Hispeed tip. 10.5 ml of isopropanol was added to the eluate for precipitating DNA, mixed properly and incubated at RT for 5 min. The mixture was transferred to a 30 ml syringe attached to a Qiaprecipitator and filtered applying uniform pressure by the plunger provided. 2 ml 70% molecular grade ethanol was added to the 30 ml syringe and was filtered through Qiaprecipitator. This procedure was repeated once or twice to remove residual ethanol. The outlet nozzle of Qiaprecipitator was also air-dried to prevent ethanol carryover. The Qiaprecipitator was attached to a 5 ml syringe and 500 µl of prewarmed TE buffer was added to the syringe. The plunger was inserted to collect DNA from the other side in a DNase/RNase free microcentrifuge tube.

Glycerol stock preparation:

2 ml bacterial culture was used to prepare glycerol stocks. 2 ml of grown culture was taken in a sterile test tube, to which 2 ml of autoclaved 50% glycerol (#RM1027-1LTR, HiMedia) was added and mixed thoroughly by pipetting several times. 500 µl of the bacterial mix was transferred to sterile, labelled 1.5 ml cryovials and the cryovials were stored at -80°C.

8.2.2. Culture of MKN45, AGS, Kato III and HFE145

MKN45, AGS, Kato III and HFE 145 were maintained in Roswell park memorial institute (RPMI)-1640 media containing L-Glutamine and Sodium bicarbonate (#AL028A,

HiMedia) media supplemented with 10 % fetal bovine serum (heat-inactivated) (FBS, #RM9970, HiMedia) in a CO₂ incubator (New Brunswick Galaxy 170R, Eppendorf) at 37 °C temperature, 5% CO₂ and 95% humidity. All cells were routinely maintained by sub culturing.

All the cell culture-related work was performed in clean and sterile biosafety cabinets (Model No. Cell Gard ES NU-480-400E Class II, Nuair, Minneapolis, USA). During sub culturing, spent media was removed by decanting from the T-25/T-75 flasks (#430639, #430641, Corning, New York, USA) and adherent/ semi-adherent GCCs were treated with pre-warmed 0.25% Trypsin-EDTA solution (#TCL007, HiMedia). After 5 min of incubation in preset incubator, cells were dislodged using sterile serological pipette from the flask. Cells were suspended in fresh RPMI 1640 + 10% FBS in a sterile centrifuge tube, counted and seeded into new flasks in recommend numbers as suggested by the size chart of cell culture flasks. The procedure for cell counting was as mentioned below.

Cells were counted using a Neubauer hemocytometer (#0640010, Paul Marienfeld GmbH & Co. KG, Germany) under an inverted microscope (Primo vert, Carl Zeiss, Oberkochen, Germany) followed by centrifugation (Model No. 5415-R, Eppendorf) at 150xg (Rotations/minute) for 8 min at room temperature (RT). Cell number was counted as per the standard formula: Total no. of cells/4x10⁴ x total volume of cell suspension. Cell pellet was resuspended in the calculated volume of medium and were plated as per the requirement of any particular experiment.

8.2.3. Freezing and revival of cells

Cell freezing was done after cells in a cell culture flask containing cells reached 70-80% confluency. Cells were trypsinized with pre-warmed trypsin-EDTA solution and were suspended in a centrifuge tube containing fresh complete media. Cells were spun down at 150xg for 8 min at RT. Supernatant was discarded and cell pellet was resuspended in

freezing mix containing 20% dimethyl sulfoxide (DMSO) in FBS (163, 166). Cell suspension was aliquoted in cryovials and were first kept overnight at -80°C followed by storage in liquid nitrogen (-196 °C) for longer preservation. Frozen cells were revived by quickly transferring the cryovials from liquid nitrogen to a water bath preset at 37 °C. Then the thawed cells were gently transferred to T-25/T-75 cm² cell culture flasks containing prewarmed complete media and put back to the incubator.

8.2.4. Transient transfection of cell lines

Lipofectamine 3000 reagent (#L3000015, Invitrogen) was used for transient transfection of various plasmid constructs and siRNAs. The cell: DNA: lipofectamine ratios for different sizes of cell-culture plates are mentioned in Table 3.

Table 3. Parameters for transient transfection (Adapted from Invitrogen)

Culture plate	Cell No. per plate	Volume of plating media (µl)	DNA amount (µg)	P300 Reagent (µl)	Lipofectamine 3000 (µl)	DNA-lipid complex to cells (µl)
6 well	1 X 10 ⁶	2000	2.5	5	7.5	250
12 well	4 X 10 ⁵	1000	1.75	3.5	2.5	150
24 well	2 X 10 ⁵	500	1	2	1.5	50
48 well	1 X 10 ⁵	250	0.5	1	0.5	25
96 well	4 X 10 ⁴	100	0.25	0.5	0.3	10

GCCs were plated in cell culture plates with an appropriate volume of complete growth media 24 h prior to the transfection and were incubated at 37 °C and 5% CO₂. 1 h prior to transfection, spent growth media was gently aspirated from the wells and fresh complete growth media was added. Mix A and mix B were prepared in two separate sterile 1.5 ml micro-centrifuge tubes. An appropriate amount of DNA and P3000 reagent was added to mix A tube containing serum free media (SFM) or dilution medium whereas, in mix B tube Lipofectamine 3000 reagent was mixed in SFM. Tubes were incubated for 5 minutes at RT.

Then both the components were mixed together gently by pipetting 4-5 times and the mix was incubated at RT for 15-20 min to allow the Lipofectamine-DNA complex formation. The reaction mixture was added to respective wells containing cells drop-wise while swirling the plate gently to ensure uniform distribution of the complex. Cells were incubated with the complex in the incubator for 48-72 h at 37 °C, 5% CO₂. After completion of the incubation period, cells were treated accordingly as per the requirement of experiment.

8.2.5. Generations of stable cell lines overexpressing empty vector, *siah2* WT and *siah2 ac-lys* mutants

Empty vector (pcDNA3.1⁺), *siah2* WT and *siah2* mutant construct-expressing stable cells were generated using MKN45 and AGS cells. 24 h prior to transfection, cells were seeded in two 96-well plates with 4x10⁴ cells/well and 150 µl of RPMI-140 complete media. Cells were transfected and 48 h post-transfection, cells were trypsinized using 50 µl trypsin/well. From that, 15 µl of trypsinized cells were transferred in 6-well plates. Initially, 200 µg/ml of G418 (#G8168-10ML, Sigma-Aldrich, St. Louis, Missouri, USA) was added to select cells expressing the desired protein. Spent media along with floating non-transfected cells were removed and replaced by fresh complete media containing 200 µg/ml of G418 every third day. After 10-12 days, G418 concentration was increased to 300 µg/ml. This selection-pressure was maintained till visible isolated colonies were obtained from single cells. These colonies were marked and isolated using cloning discs (#Z374458-100EA, Sigma-Aldrich). Cloning discs were placed in a 12-well plate and were kept under the 300 µg/ml G418 selection pressure. After the cells settled to the bottom of the plate, cloning discs were removed. After a few days, confluent cultures were trypsinized, and cells were transferred to T-75 cm² flask with 300 µg/ml G418 selection pressure some cells were taken in a micro-centrifuge tube for confirmation of overexpression of a protein by immunoblotting and immunofluorescence (IF) techniques. After confirming the protein's overexpression, cells in

the T-75 cm² flask were grown till 70-80% confluency was attained. Flasks were trypsinized and cells were frozen in freezing mix and stored in liquid nitrogen (Liq. N₂, -196°C) as explained earlier.

8.2.6. Maintenance of *Helicobacter* strains and cell infections

Various strains of *Helicobacter* were maintained on trypticase soy agar (TSA) plates containing 5% sheep blood (#221239, Becton Dickinson and Company, New Jersey, USA) and incubated at 37 °C in a microaerophilic atmosphere containing 10 % CO₂ for 48-72 h. After incubation, uniform lawn of colonies grown on plate were scraped using a sterile inoculation loop and were introduced in membrane-filtered Brucella broth (#211088, BD BBL, New Jersey, USA) supplemented with 10% heat-inactivated FBS. The inoculated culture was grown with shaking (Tarsons, West Bengal, India) at 180 rpm for 14-16 h. Next, 1ml of bacterial suspension was used to measure bacterial growth in a UV-visible spectrophotometer (Model No. DU-720, Beckman Coulter, California, USA) at 600 nm. The growth was calculated as per the given formula: Optical density (OD₆₀₀) 0.3 was equivalent to 2x10⁸ colony forming units/ml (CFU/ml). Culture with OD between 0.5-1.2 was considered optimal for cell infection and was pelleted at 300xg (Model No. D35720, Sorvall Biofuge Stratos, Thermo Scientific, Massachusetts, USA) for 8 min at RT. The bacterial pellet was dissolved in complete RPMI-1640 media to reach desirable multiplicity of infection (MOI) of 100MOI/10µl. The cultured cells were infected as per the requirement of the experiment. After 72 h of incubation, the bacteria were passaged on a fresh TSA plate using sterile cotton swab and the plate was replaced back in the incubator.

8.2.7. Maintenance of C57BL/6 mice and *H. felis* infection

C57BL/6 mice (both male and female) aged between 4-5 weeks were procured from the National Centre for Laboratory Animal Sciences (NCLAS) of the National Institute of Nutrition (NIN, Hyderabad, India). Animal rooms were maintained at 22.2°C with a relative

humidity of 50-65%. A 12 h light-dark cycle (12:12 h L/D cycle) was strictly followed with automatic timers in the animal facility registered under Committee for the Purpose of Control and Supervision of Experiments (CPCSEA), Ministry of Environment & Forest, Government of India. All experiments performed were as per the CPCSEA and Institutional Animal Ethics Committee (IAEC) guidelines for laboratory animals. The average numbers of mice maintained were 2-3/cage. Mice were kept in cages containing sterilized corn and husk bedding. Cage lids were fitted with replacement filters to avoid cross-contamination due to infections. Polypropylene water bottles and food pellets were supplied through the top grid. Mice were kept in isolation for 1-2 weeks in order to assess existing infections before starting experiments. O/N-grown *H. felis* growth was measured at O.D₆₀₀ and the bacterium was suspended in 1X PBS such that 1 ml of suspension contained 1 X 10¹⁰ CFU of bacterium. The mice from infected group were orally fed with 0.5 ml of *H. felis* suspension each using 20 mm oral gavage needles whereas, mice from control group were orally fed with 0.5 ml of 1X PBS solution each. Animals were maintained for the duration of 12 months.

8.2.8. Infection of GCCs with *H. pylori*

Cells were infected with *H. pylori* at 100, 200 and 300 MOI for 6 h, 12 h and 24 h time points.

8.2.9. Treatment of cells with a proteasomal inhibitor MG132 and a p300 HAT inhibitor (CTK7A)

24 h after cell seeding or 48 h of transfection, cells were pretreated with 50 µM proteasomal inhibitor MG132 (#M7449-200UL, Sigma-Aldrich) for 24 h before infecting cells. MG132 is available as ready solution with a concentration of 10 mM in DMSO. Sodium-4-(3,5-bis(4-hydroxy-3-methoxystyryl)-1H-pyrazol-1-yl) benzoate {(CTK7A) (#382115-10MGCN, Merck Millipore, Darmstadt, Germany)}, a derivative of curcumin which inhibits HAT

activity of p300/CBP was used for co-treatment of cells at 100 μ M concentrations along with *H. pylori* infection. CTK7A was dissolved in DMSO in order to make a stock solution with 2 mM. The stock solution was stored at -20 °C.

8.2.10. Whole cell lysate preparation

After completion of *H. pylori* infection time points, cells were dislodged from plates by either trypsinization or scraping. Samples were collected in pre-chilled 1.5 ml microcentrifuge tubes. Then, cells were centrifuged at 250xg for 5 min at 4 °C and the supernatant was discarded. Cell pellets were kept on ice and required amount of 2X protease inhibitor cocktail (#ML051-1 ml, 100X protease inhibitor cocktail, HiMedia) was added to the pellets and vortexed for 15-30 sec. 2X Laemmli sample buffer (#ML-021, HiMedia) with β -mercaptoethanol {(β -ME) (#MB041-500ML, HiMedia)} was added to the mix in 1:1 ratio and vortexed. Samples were finally boiled at 100 °C (dry bath) for 8 min to prepare the whole cell lysate and stored lysates at -80 °C for future use.

8.2.11. Sodium dodecyl sulfate polyacrylamide gel electrophoresis (SDS-PAGE)

Protein samples were separated by SDS-PAGE following cell lysates preparation by Laemmli method (1970).

Gel components (stock solutions):

Acrylamide-bisacrylamide (solution A): (29:1) 30 % acrylamide: bis-acrylamide solution (#161-0156-500ML, Bio-Rad Laboratories).

Resolving gel buffer (solution B): 1.5 M Tris-HCl buffer solution, pH 8.8. Resolving/separation gel buffer (161-0798-500ML, Bio-Rad Laboratories)

Stacking gel buffer (solution C): 0.5 M Tris-HCl buffer solution, pH 6.8. Stacking gel buffer (161-0799-500ML, Bio-Rad Laboratories)

Glycerol (Molecular grade): A 50% glycerol solution was made by mixing glycerol (#MB060-500ML, HiMedia) and molecular grade water (#ML024-10X100ML, HiMedia) in 1:1 proportion.

TEMED: N, N, N', N'-Tetramethyl ethylenediamine {(TEMED) (#1610800, Bio-Rad Laboratories)} was used as an essential catalyst for polymerization of gels.

Ammonium persulfate (APS): A 10% solution was prepared by dissolving 100 mg of APS (#161-0700, Bio-Rad Laboratories) in 1000 µl molecular grade water. It acts an oxidizing agent, used with TEMED for polymerization of gels. TEMED and APS were prepared fresh for quick polymerization.

Working solutions:

Resolving gel solution: The stock solutions were mixed in the proportions given in the table below to obtain one resolving gel of 5-15%. To prepare more number of gels, the volume of solution was multiplied appropriately with the number of gels required keeping the percentage of gels constant.

Table 4. Components for the resolving gel

Components	5%	7.5%	10%	12.5%	15%
Acrylamide: bisacrylamide solution (Solution A)	0.75 ml	1.125 ml	1.5 ml	1.875 ml	2.25 ml
1.5 M Tris-HCl buffer, pH 8.8 (Solution B)	1.125 ml	1.125 ml	1.125 ml	1.125 ml	1.125 ml
Distilled water	1.375 ml	1 ml	1.25 ml	0.5 ml	Nil
50% glycerol solution	1.25 ml	1.25 ml	1.25 ml	1.25 ml	1.25 ml
TEMED	2.5 µl	2.5 µl	2.5 µl	2.5 µl	2.5 µl
10% APS	35 µl	35 µl	35 µl	35 µl	35 µl

Stacking gel solutions: The stock solutions were mixed in the following proportions (for 1 gel):

Table 5. Components for stacking gel

Components	Volume
Acrylamide: bisacrylamide solution (Solution A)	0.45 ml
1.5 M Tris-HCl buffer, pH 6.8 (Solution C or stacking gel buffer)	0.75 ml
Distilled water	1.8 ml
TEMED	3 μ l
10% APS	18 μ l

Freshly prepared 10% APS and TEMED were added to each solution just before polymerization.

Electrophoresis buffer: Gel running buffer (1X Tris-HCl/Glycine/Sodium Dodecyl Sulfate or TGS buffer containing 25 mM Tris-HCl, 190 mM glycine and 0.1% SDS) was prepared from 10X TGS buffer (#1610732, Bio-Rad Laboratories) by adding 100 ml of 10X TGS to 900 ml of double distilled water.

Sample denaturing (Laemmli) buffer: Ready to use 2X Laemmli buffer (#ML-021, HiMedia) was used to prepare sample denaturing buffer and 5% (v/v) β -ME (37.5 μ l β -ME + 750 μ l 2X Laemmli buffer) was added to it. It was saved at -20°C .

Protease inhibitor cocktail: 100X protease inhibitor cocktail mix (#ML-051, HiMedia) was used to prepare 2X protease inhibitor cocktail mix by adding 3.6 μ l 100X protease inhibitor cocktail to 176.4 μ l molecular biology grade water.

Casting of the SDS-PAGE gel (polymerization process):

SDS-PAGE was performed using Mini-PROTEAN tetra-system gel assembly (#165-8003, Bio-Rad Laboratories). As per the manufacturer's guidelines, a clean pair of thin glass plates

and thick spacer glass plate (1 mm) were fitted inside the gel casting stand. The resolving gel solution was poured in between the assembled glass plates up to the three-fourth spacer plate height. Stacking gel solution was slowly added on top of resolving gel without disturbing the level of the resolving gel. A 1 mm thick 10/15-well comb was inserted into the stacking gel solution and the solutions were allowed to polymerize for 20-30 min at RT. After gel polymerization, the comb was gently removed and the glass plates were fitted into SDS-PAGE running electrode. Electrophoresis buffer was poured on the upper surface of the gel plates and the whole glass plate assembly was kept inside the Mini-PROTEAN gel apparatus. Inner chamber of the apparatus was filled with chilled electrophoresis buffer which also removed bubbles trapped inside wells and unpolymerized acrylamide. Next, chilled electrophoresis buffer was poured in the outer chamber to fill it halfway.

Sample preparation:

Samples prepared as per previously-explained protocol and stored at -80°C were taken out, thawed at room temperature before loading on gel.

Sample loading and electrophoresis:

Samples were loaded into individual wells of the stacking gel. Standard molecular weight protein marker (#BM008-500, BLUelf pre-stained protein ladder, BR Biochem, New Delhi, India) was used to identify the molecular masses of sample proteins. The electrophoresis chamber was connected to a power pack and electrophoresis was carried at a constant voltage of 130 volts for 15 min for proper stacking of proteins followed by gel running at 180 volts till the bromophenol blue dye front was about to exit from the gel.

8.2.12. Immunoblotting

Immunoblotting was performed to identify proteins of interest by employing the method designed by Towbin *et al.* (1979)

Buffers and solutions:

Tris-buffered saline (TBS):

Table 6. Components for 10X TBS solution

Components	Amount	Final conc.
Tris	48.4 gm	20 mM
NaCl	584.8 gm	500 mM
pH (Adjusted with 1N HCl)	x ml	7.5
Final volume (Distilled water)	2 L	

1X TBS was prepared from 10X TBS by taking 100 ml of 10X TBS in a measuring cylinder and adjusting the final volume to 1000 ml by adding double-distilled water (NaCl; Sodium chloride, HCl; Hydrochloric acid).

Phosphate-buffered saline (PBS):

Table 7. Components for 10X PBS solution

Components	Amount	Final conc.
Na ₂ HPO ₄	14.4 gm	10 mM
KH ₂ PO ₄	2.4 gm	2 mM
NaCl	80 gm	137 mM
KCl	2 gm	2.7 mM
pH adjusted to 7.4 with 1 N HCl and final volume was made up to (with double-distilled water)	1L	

1X PBS was prepared from 10X PBS by taking 100 ml of 10X PBS in a measuring cylinder and adjusting the final volume to 1000 ml by adding double-distilled water (Na₂HPO₄; Disodium, hydrogen phosphate, KH₂PO₄; Potassium di-hydrogen phosphate KCl; Potassium chloride).

TBS-Tween-20 wash solution (TBST): 0.1% (v/v) Tween-20 (RM156-500G, HiMedia) was dissolved in 1X TBS.

Blocking buffer and antibody dilution buffer: 5% non-fat-dry-milk {(NFDM) (#RM1254, HiMedia)} dissolved in TBST and 3% (w/v) bovine serum albumin {(BSA, Cohn fraction V) (#RM3151, HiMedia)} dissolved in TBST, respectively. Sometimes, both primary and secondary antibodies were diluted in blocking buffer as suggested by antibody manufacturers.

Transfer buffer for polyvinylidene (PVDF) membrane (10X):

100 ml of 10X TG buffer (#161-0772, Bio-Rad Laboratories) was dissolved in 700 ml of double distilled water and 200 ml of methanol. 0.0375 gm of SDS was added to 1X TG buffer.

Procedure for transfer of protein onto PVDF membrane (wet transfer method): Wet transfer methodology was employed to transfer high molecular weight proteins. The transfer of protein onto PVDF membrane was performed in mini trans-blot cell wet transfer apparatus (Model No. 170-3940, Bio-Rad Laboratories). Protein samples were resolved using SDS-PAGE. After the run, the gel was immediately transferred into pre-chilled transfer buffer for 5 min. Hydrophobicity of PVDF membrane (#PVH00010, EMD Millipore) was reduced by treating it with pre-chilled methanol for 5 min and then washed with water followed by soaking in pre-chilled transfer buffer. All other components to prepare the wet transfer sandwich were also kept soaked in pre-chilled transfer buffer. Mini gel holder cassette was placed inside the casserole with the gray-side down. Pre-wetted foam pad was placed on the gray side of the cassette, followed by a sheet of Mini trans-blot pre-cut thin filter paper (#1703933, Bio-Rad Laboratories), the electrophoresed gel, the pre-soaked PVDF membrane, filter paper and a foam pad. A roller was used to make the whole assembly bubble-free. The cassette was closed and placed inside the transfer module and immersed in the tank with gray-side towards the black-side (anode) and transparent-side towards the red-side (cathode) of the module. A magnetic stir bar was placed inside the tank. The tank was

filled completely with chilled transfer buffer. The transfer unit lid was closed which was connected with cables to a power pack (Model No. 1645050, PowerPac™ Basic Power Supply, Bio-Rad Laboratories). Transfer was carried out at a “constant volt” of 40 V for 240 min. To keep the whole set up cool, the entire module was placed on an ice-filled tray and the tray was placed on magnetic stirring surface.

Semi-dry Transfer: The immunoblotting semi-dry transfer method, used to transfer low molecular weight proteins, was performed in mini trans-blot semi-dry blot apparatus (Model No. 170-3940, Bio-Rad Laboratories). After completion of SDS-PAGE, the PVDF membrane and the gel were treated in the same manner as mentioned for the wet transfer. Before starting the transfer, the semi-dry apparatus kept on a flat, horizontal surface. The level was adjusted using a bubble-inclinometer provided. A pre-cut thick filter paper (#1703932, Bio-Rad Laboratories), soaked in transfer buffer was placed over the transfer assembly (anode), followed by a PVDF membrane, the electrophoresed gel and a thick paper (towards the cathode). After removal of air bubbles from the stack using a roller, semi-dry transfer was performed at “constant volt” of 25 V for 35 min.

After the transfer process, the PVDF membrane was washed once with TBS for 5 min and then incubated at RT in blocking buffer (5% NFDM in 0.1% TBST on shaker for 1 h, to prevent non-specific binding of antibodies. The membrane was probed with a specific primary antibody solution (diluted in blocking buffer in a specific ratio as per the instruction from antibody manufacturer) and incubated at RT for 1 h on static condition or constant shaking, followed by O/N incubation at 4 °C at either the static or shaking condition. After incubation, the membrane was washed three times with 1X TBST/ PBST, and then kept into the secondary antibody solution, a horse-radish peroxidase (HRP)-conjugated IgG specific to the primary antibody. It was incubated in the secondary antibody solution at RT for 1-2 h with constant shaking. The membrane was washed three times with 1X TBST/ PBST for 5

min each and finally with 1X TBS/ PBS. For HRP signal detection on immunoblots, SuperSignal West Femto Chemiluminescent Maximum Sensitivity Substrate kit (#34094, ThermoFisher Scientific) was used for the detection of proteins with low expressions and Immobilon™ Western Chemiluminescent HRP Substrate kit (#WBKLS-0050, Merck Millipore) was used for the detection of proteins with high-expressions. Luminol and stable peroxide solutions provided in the kit were mixed in equal ratio and were uniformly applied on the immunoblot. The developed blots were imaged using ChemiDoc XRS plus (Model No. 170-8265, Bio-Rad Laboratories) and analyzed with Quantity 1-D analysis software version 4.6.9 (Bio-Rad Laboratories) equipped with the instrument.

Reprobing of the PVDF membrane: Reprobing was performed using ready-to-use Restore Plus Western Blot Stripping Buffer (#46430, ThermoFisher Scientific) for the removal of primary and secondary antibodies bound on the blotted membrane to detect other proteins with similar molecular size. After the detection, the blot was incubated in reprobing buffer for 30 min with constant shaking at RT. The blot was washed three times with 1X TBST for 15 min each followed by blocking, primary antibody incubation, washing with 1X TBST, secondary antibody incubation and washing. Finally, membranes were developed as mentioned previously to visualize bands. Refer appendix I and II for the dilutions of primary and secondary antibodies.

8.2.13. Immunoprecipitation (IP) assay

Immunoprecipitation (IP) assay was performed to study protein-protein interactions. It was mainly performed to identify various Siah2-binding partners. 1×10^6 cells were seeded in 6-well cell culture plates 24 h prior to transfection and/or infection. 48 h after transfection and/or 12 h and 24 h of infection, GCCs were lifted off the cell culture plates by scraping as mentioned earlier. Cells were centrifuged at 300xg for 5 min at 4 °C and to the cell pellet, 200 µl of triton-buffer was added (composition mentioned in table 8).

Table 8. Components of TEN + Triton X-100 buffer

Components	Concentration	
	Stock	Working
NaCl	5 M	150 mM
Tris, pH- 7.5	1 M	50 mM
EDTA	5 M	1 mM
Triton X-100	10%	1%
Protease Inhibitor cocktail (PIC)	100X	1X with 10 µl/ml of buffer

The cell pellet was resuspended properly by vortexing for 30-40 sec and was kept on ice for 30 min with intermittent vortexing (at every 10 min interval for thorough cell lysis). Then the cell lysate was centrifuged at 850xg for 10 min at 4 °C to clear cell debris and the supernatant was transferred to a clean 1.5 ml microcentrifuge tube. 800 µl TEN buffer without Triton X-100 with the composition mentioned below was added to each tube.

Table 9. Components of TEN – Triton X-100 buffer

Components	Concentration	
	Stock	Working
NaCl	5 M	150 mM
Tris, pH- 7.5	1 M	50 mM
EDTA	5 M	1 mM
Protease Inhibitor cocktail (PIC)	100X	1X with 10 µl/ml of buffer

10 µl of protein A/G plus-agarose (#SC-2003, Santa Cruz Biotechnology) was added in each tube to precipitate the debris and incubated at 4 °C for 30 min. Tubes were centrifuged at 850xg for 5 min at 4 °C and the supernatants were transferred to a clean microcentrifuge tube. Specific protein antibodies using which interaction was studied and equivalent normal/ control IgG were added to the respective samples as per the

recommended dilutions. Tubes were incubated O/N at 4 °C with shaking. After incubation, tubes were centrifuged at 230xg for 2 min at 4 °C and 15 µl of 50% protein A/G plus-agarose was added to each tube followed by incubation with shaking for 3 h at 4 °C. Agarose bead-attached immunocomplex was pulled-down at 230xg for 5 min at 4 °C and then the immunocomplex was washed twice with chilled 1X PBS (230xg, 5 min, 4 °C). Finally, agarose was boiled in 25 µl of sample buffer containing 5% β-ME at 100 °C for 10 min. Lysates were then loaded onto SDS gel and proteins were separated based on their molecular weight followed by immunoblotting, antibody probing and detection as previously described. Otherwise, gel was stained with coomassie brilliant blue-R250 dye {(CBB-R250) (#161-0436, Bio-Rad Laboratories)} for the identification of Siah2-binding partners by mass spectrometry. Refer to appendix I and II for the dilutions of proteins-specific primary antibodies and IgG.

8.2.14. Identification of proteins by mass spectrometry

For the identification of novel binding partners of Siah2 protein, 1 X 10⁶ MKN45 cells were seeded in 6-well plates 24 prior to transfection, transiently transfected with *siah2* WT and *siah2* acetylated lysine (ac-lys) mutant constructs *siah2* K129R and *siah2* K139R following infection with 200 MOI *H. pylori* for 12 h. Immunoprecipitation was carried out using Siah2 antibody and SDS-PAGE-based separation of proteins as described in the previous section. The SDS gel was stained O/N using ready to use CBB-R250 staining solution followed by destaining with gel destaining solution of following composition:

Table 10. Components of gel destaining solution

Components	Volume
Glacial acetic acid	500 ml
Methanol	400 ml

Distilled water	100 ml
Final volume	1 L

Visibly different band patterns were marked in order to identify new protein bands after comparing bands from infected-sample lane with uninfected sample-lane. Bands were excised using a new scalpel blade in a clean area to avoid keratin contamination and placed in labelled new and sterile (to avoid keratin contamination) 1.5 ml microcentrifuge tube. 50 μ l sterile, molecular biology grade water was added to each tube to avoid gel plug drying and were sealed firmly using parafilm. Gel samples were sent to the University of Texas Medical Branch, Biomolecular Resource Facility (UTMB BRF) Mass Spectrometry Core Lab, Texas, USA for Liquid Chromatography-Mass Spectrometry/ Mass Spectrometry (LC-MS/MS) analysis. Gel piece from protein free area was also analyzed by LC/MS/MS and was used as a control. From the obtained results those proteins detected in control sample were summarily rejected whereas only those proteins with minimum two peptides having ion score threshold value above 40 were shortlisted.

8.2.15. Soft-agar colony formation assay or anchorage-independent growth assay

The soft-agar assay was the method employed to study anchorage-independent growth of MKN45 and AGS cells in 4 different experimental conditions as follows:

8.2.15.1. MKN45 *siah2* WT and *siah2* ac-lys mutant stable cells with or without *H. pylori* infection were used to find out the effect of ac-lys mutation on anchorage-independent growth of cells.

8.2.15.2. MKN45 cells co-treated 100 μ M CTK7A and *H. pylori* were used to study the effect of CTK7A treatment on cell invasiveness.

8.2.15.3. MKN45 cells transiently transfected with siRNA for Siah2 (*siSiah2*), *siTES* and *siFLN-C* were used to study the effect of *siah2*, *TES* and *FLN-C* knockdown on anchorage-independent growth of cells.

8.2.15.4. AGS empty vector, scrambled shRNA and *hif1 α* -shRNA expressing stable cells were used to study the effect of *hif1 α* knockdown on colony forming ability of cells.

In this technique, cells trapped in between agar were allowed to come to the surface and form colonies on the top agar.

Preparation of the bottom agar/ hard agar (0.6%):

1.2 gm of Bacto Agar (#199835, MP Biomedicals) was dissolved in 100 ml of distilled water and was autoclaved at 121 °C for 20 min to prepare 1.2% agar. After autoclaving, the agar was maintained at 50-60 °C to avoid solidification. 0.2 gm of Dulbecco's Modified Eagle Medium/ Nutrient Mixture F-12 Ham's media {(DMEM/ F-12, 1:1 mixture) (#AT140A, HiMedia)}, 0.06 gm of L-Glutamine {(Q) (#TC243-10G, HiMedia)}, 0.6 gm of Sodium bicarbonate {(NaHCO₃) (#TC230-100G, HiMedia)} and 500 μ l of Penicillin-Streptomycin solution (#P0781, Sigma-Aldrich) were dissolved in 50 ml distilled water (v/v) and the media was membrane-filtered to make 2X DMEM: F-12 media. 500 μ l of 1.2% Bacto Agar and 2X DMEM: F-12 Ham's media were mixed in equal proportion and poured in per well of a 6-well plate, followed by incubation at 37 °C, 5% CO₂ for 30 min.

Preparation of cell suspension:

After completion of *H. pylori* infection, the spent media was discarded, cells were washed once using 1X PBS buffer (#SH30256.02, HyClone, South Logan, Utah, USA) and were incubated in RPMI complete media containing 50 μ g/ml gentamycin sulfate (#A010-10mg/ml, HiMedia) for 2 h at 37 °C, 5% CO₂ to kill extracellular bacteria. Then, cells were trypsinized and taken in a sterile 1.5 ml microcentrifuge tube. Cell counting was performed using the Neubauer chamber and centrifuged at 150xg for 8 min at RT. Cells were resuspended in appropriate amount of RPMI complete media to make cell density 1x10⁶ cells/ ml.

Preparation of top agar:

Top agar was prepared by adding 2X (DMEM/ F-12 Ham, 1:1 mixture) media, 1.2% agar, 10 μ l cell suspension (containing 10000 cells) and distilled water. Then the mix was poured slowly on solidified bottom agar by swirling the plate. Plates were placed back inside incubators containing 5% CO₂ at 37 °C for 3-4 weeks. 500 μ l fresh complete media was added thrice every week. After 3 weeks of incubation, visible colonies formed on the top agar were counted and the colony size was compared between various treatment groups. All components are summarized below:

Table 11. Components for soft-agar assay (For single well)

Components	Top Agar	Bottom Agar
1.3% Agar	0.5 ml	1 ml
2X DMEM: F-12 Ham's media	1 ml	1 ml
Cell suspension	10 μ l	-
Distilled water	0.5 ml	-
Final volume	~2 ml	2 ml

8.2.16. Wound-healing assay or scratch assay

Wound-healing assay was performed to study the wound-healing property of AGS *siah2* WT and various *siah2* ac-lys mutant stable cells. It was also used to study the effect of p300 HAT activity inhibitor, CTK7A on migration of AGS cells. The wound healing ability of AGS cells transiently transfected with empty vector, *shHif1 α* , scrambled shRNA, *siTES*, and *siFLN-C* was also studied using this assay. 1×10^6 AGS cells were seeded in 6-well cell culture plates and incubated for 16-24 h to get monolayer of cells. Next day, before making wound, images were captured. Wound was created by scraping cells from the 6-well using a 200 μ l micropipette tip and floating cells were discarded followed by addition of 1.5 ml of fresh complete media. When required, cells were co-treated with CTK7A and *H. pylori*. Images were captured at 6 h, 12 h and 24 h time points using an inverted microscope

(Model- Primo Vert, Carl Zeiss). The number of cells migrated were counted and the extent of wound healing with time was measured using ImageJ 1.50i software (National Institute of Health-NIH, Bethesda, Maryland, USA).

8.2.17. Transwell migration and invasion assay

Transwell migration and invasion assay as were performed to study invasive properties of GCCs overexpressing Siah2 WT, Siah2 ac-lys mutant constructs or TES siRNA and FLN-C siRNA or control siRNAs. Cell migration and invasion assays were performed using 8 µm pore size Transwell Bio coat control inserts (#353097, Becton Dickinson and Company) and transwell invasion assay was performed using 8 µm pore size transwell Bio coat matrigel-coated inserts (#354483, Becton Dickinson and Company) as per manufacturer's guidelines. AGS cells were seeded in a 24-well cell culture plate 24 h prior to transfection. Next, cells were either transfected with overexpression plasmids of *siah2* WT, *siah2* ac-lys mutants, pcDNA3.1⁺. In another experiment, cells were transfected with either siRNA of TES, FLN-C and control duplex. 48 h post transfection, cells were trypsinized and 5x10⁴ cells (suspended in complete RPMI media) were seeded on top of transwell control inserts or coated matrigel inserts were placed inside a 24-well plate. The upper chamber was filled with RPMI media containing 0.1% FBS whereas, the lower chamber was filled with 20% FBS containing RPMI media in order to create an increasing gradient of nutrient concentration. Cells were then infected with *H. pylori* or left uninfected and was incubated in a humidified incubator at 37 °C and 5% CO₂ for 24 h. After completion of incubation, inserts were taken out and cells on the top of transwell surface were scraped off twice by using a moist cotton swab. Inserts were washed with 1X PBS and the cells attached to the lower side of inserts were fixed with 4% paraformaldehyde for 30 min at RT followed by O/N fixation. Inserts were washed with 1X PBS followed by permeabilization with 0.5% Triton X-100 in PBS. Cells were then stained with hematoxylin (#S034, Hematoxylin

(Harris), HiMedia)} for 30 min and washed with 1X PBS. After final wash with 1X PBS, inserts were dried for 60 min, membrane was cut from the insert using scalpel blade and mounted over glass slide keeping the lower side down. Images were captured, migrated and invaded cells were counted under a bright field microscope.

8.2.18. Clonogenicity or cell proliferation assay

MKN45 cells stably expressing pcDNA3.1⁺, *siah2* WT and *siah2* ac-lys mutant constructs were analyzed for their viability following *H. pylori* infection for 12 h. 2x10⁵ cells were seeded in a 24 well plate 24 h prior to *H. pylori* infection and were incubated in a humidified incubator at 37 °C and 5% CO₂. After infection with *H. pylori* for 12 h, the cells washed with 1X PBS followed by 50 µg/ml gentamicin treatment for 2 h. The cells were trypsinized and seeded in a 6 well plate with 500 cells per well and incubated again in the incubator for 3 weeks. 500 µl RPMI complete media was given in each well thrice every week. After 3 weeks of incubation, colonies formed and those were fixed with 4% PFA in PBS for 30 min, permeabilized with 0.1% Triton X-100 in PBS for 20 min and washed with 1X PBS twice. The permeabilized-colonies were stained with Gram's Crystal Violet stain (#S012, HiMedia) for 10 min and finally washed with 1X PBS twice. Plates were dried for 1 h, colonies were counted and images were taken using brightfield microscope as described previously.

8.2.19. Tetrazolium dye 3-[4, 5- dimethylthiazol-2-yl]-2, 5-diphenyl tetrazolium bromide (MTT) assay

Proliferation and viability of MKN45 cells stably expressing pcDNA3.1⁺, *siah2* WT and *siah2* ac-lys mutants were assessed by using EZcount™ MTT Assay kit (#CCK003-1000, HiMedia). In another experiment, proliferation ability of MKN45 cells treated with CTK7A was also determined. This assay used the quantitative method for measurement of reduction in the extracellular yellow colored water soluble MTT dye to insoluble formazan crystals by

mitochondrial enzyme lactate dehydrogenase in metabolically active cells. These formazan crystals exhibited a purple color upon dissolving in an appropriate solvent. The intensity of the purple color formation was proportional to the number of viable cells which could be measured spectrophotometrically (Model No. 168-1135, iMark™ Microplate Absorbance Reader, Bio-Rad) at 570nm.

Preparation of MTT reagent:

6 ml of cell assay buffer was added aseptically to a vial containing 30 mg MTT reagent powder and vigorously mixed pipetting up and down 10-15 times with a serological pipette to completely dissolve the reagent, forming a bright yellow-colored 5mg/ ml MTT reagent solution. It was then filter sterilized and stored at -20°C in aliquots till further use.

Preparation of cells:

MKN45 cells were seeded in a 96-well cell culture plate 24 h before treatment with CK7A and/or infection with *H. pylori* for 24 h and incubated at 37 °C in a 5% CO₂ incubator as previously described.

Assay procedure:

Post infection (p.i), spent media was removed, cells were washed with 1X PBS and MTT reagent was added to a final concentration of 10% of the total volume of fresh RPMI complete media. The plate was wrapped with an aluminum foil to avoid exposure to light and was again incubated at 37 °C in a 5% CO₂ atmosphere for 2 to 4 h depending on the progression of formation crystal formation. Cells were observed at periodic intervals under the brightfield microscope for the presence of intracellular needle-shaped, dark purple colored precipitate. When the purple precipitate was clearly visible, 100 µl of solubilization buffer was added to each well and the plate was gently stirred by placing it on a nutating shaker (Model No. SBS500-3, MiniTwist™ nutating mixer, Select BioProducts, GE Healthcare, Edison, New Jersey, USA). The absorbance was measured using an enzyme-

linked immunosorbent assay (ELISA) reader at 570 nm and a reference wavelength higher than 650 nm. Specific absorbance was calculated using the formula: Absorbance of test sample_(570 nm) – Absorbance of blank sample_(570 nm) – Absorbance of test sample_(>650 nm). Data were analyzed by plotting absorbance values on Y-axis and experimental parameter on X-axis.

8.2.20. Peptide synthesis and custom antibody generation

To determine the *H. pylori*-mediated Siah2 acetylation at K¹²⁹ and K¹³⁹ residues, custom synthesized rabbit monoclonal antibodies were generated against acetylated K¹²⁹ and K¹³⁹ residues (ac-K¹²⁹Siah2 and ac-K¹³⁹Siah2) using the target-specific native ac-Siah2 protein peptide sequence. These antibodies were also specific for ac-K¹³⁰ and ac-K¹⁴⁰ residues of mouse Siah2, respectively. Two-step affinity purified antibodies were purchased from Bioklone Biotech Pvt. Ltd., Chennai, India. The company determined antibody titers by ELISA assay from the first and second bleeds. Peptide sequences used for generating antibodies are listed in appendix VIII. Antibodies were used for the detection of Siah2 acetylation in *H. pylori*-treated cell lysates by western blotting and immunoprecipitation assays as described earlier. Antibodies were also used for immunofluorescence staining of human gastric antral metastatic tissue sections and C57BL/6 mouse stomach tissue sections which are discussed below.

8.2.21. C57BL/6 mouse experiments

7-8 weeks old male and female mice were blindly divided into two groups: “uninfected” and “infected”. *H. felis* infection was given as per the following protocol (200). 0.5 ml PBS was fed orally three times at two-day intervals to the “uninfected group” and 0.5 ml 10¹⁰ CFU/ml in PBS of O/N-grown *H. felis* suspension to the “infected group”. Mice were maintained for a period of 10-12 months. After 12 months, weight of mice was measured and animals were euthanized. Metastases were examined in gastrointestinal (GI) tract, other vital organs and

adjoining lymph nodes. Weight of spleen from both the uninfected and infected mice was measured to study splenomegaly, a very common symptom of infection. Gastric tissue was collected from the antral portion of the stomach and was preserved in 4% paraformaldehyde solution (PFA) at 4 °C for further use.

8.2.22. Embedding and sectioning of gastric biopsy samples

Antral portion of the C57BL/6 mouse stomach and human gastric biopsies stored overnight in 4% PFA were transferred in 25% sucrose solution for at least 48 h before sectioning. The cryostat instrument (Model No. LEICA CM3050 S, Leica Biosystems, Wetzlar, Germany) was set to -20 °C, 24 h prior to sectioning. Just before the start of sectioning, poly-l-lysine (#P8920-100ML, Sigma Aldrich) uniform coating was made on glass slides where tissue sections would be mounted and incubated in 37 °C incubator for 30 min. Tissue sample was embedded on specimen holder using optimal cutting temperature compound {(OCT) (#3808609E, Leica Biosystems)} followed by fixing it inside the cryostat instrument in order to freeze the tissue embedded in OCT. Sections with 5 µm thickness were cut from tissues of human biopsies and C57BL/6 mouse antral gastric mucosa. Tissue section-mounted glass slides were kept in slide storage box and were stored at -20 °C until further use. Tissue sections were processed for hematoxylin and eosin staining and immunofluorescence microscopy as described in the next section.

8.2.23. Hematoxylin and eosin (H&E) staining

Tissue sections were stained with H&E to study the morphological differences between uninfected and human adenocarcinoma tissue from infected patients. Likewise, *H. felis*-infected antral gastric mucosa of mouse was compared with uninfected tissues to identify the extent of cancer induction in *H. felis*-infected gastric tissue samples. The H&E was performed as per the standard protocol (258). Tissue-mounted glass slides were removed from -20 °C and were kept at RT for 30 min. Sections were washed with 1X PBS thrice to

remove OCT followed by hematoxylin (#S058, Mayer's Hematoxylin solution, HiMedia) staining for 3 min. Sections were washed under running tap water for 5 min followed by eosin Y (#S007, 2% w/v Eosin Y stain, HiMedia) staining for 2 min. Sections were washed with 1X PBS thrice and mounted with antifade mounting reagent (#P36930, ProLong™ gold antifade mountant, ThermoFisher Scientific) by placing a coverslip over the slide. Images were captured under inverted brightfield microscope (Carl Zeiss).

8.2.24. Immunofluorescence microscopy

Immunofluorescence (IF) staining was performed to study the expression of Siah2, ac-K¹³⁹ Siah2, PHD3 and Hif1 α in MKN45, AGS cells and also in gastric tissue sections of patients and C57BL/6 mice. TES and FLN-C expression were also studied in human metastatic gastric tissue sections and mouse antral gastric mucosa tissue sections.

For immunofluorescence staining of AGS and MKN45 cells, 0.2×10^6 cells were seeded on coverslips 24 h prior to infection as described earlier. After *H. pylori* infection time point, old spent media was discarded, fresh complete media was given and uninfected or *H. pylori*-infected cells were fixed with 4% PFA in PBS and permeabilized with 0.1% Triton-X-100 as described earlier. Cells were kept in blocking buffer (3% BSA in PBST) for 1 h, followed by O/N incubation with respective primary antibodies diluted in blocking buffers as per the manufacturer's instructions. Next day, cells were washed in PBST for two times and kept in secondary antibody incubation for 2 h on RT in dark condition to avoid bleaching. Cells were washed twice with 1X PBST followed by staining with 4', 6-Diamidino-2-phenylindole dihydrochloride (DAPI) for 15 min. Finally, cells were washed with 1X PBS twice and mounted on Fluoromount G (#0100-01, Southern Biotech-ThermoFisher Scientific). Images were captured at 200X and 600X magnification using digital camera models DS Ri2 and DS Qi2 attached to inverted microscope (Model- Eclipse Ti-U, Nikon Corporation Tokyo, Japan).

Human gastric adenocarcinoma biopsy tissues and C57BL/6 antral gastric tissue sections were processed to study the expression of Siah2, ac-K¹³⁹ Siah2, PHD3, Hif1 α , TES and FLN-C by immunostaining following procedure as mentioned above. These tissue section consist of multilayer of cells, so, the sections were permeabilized with 0.5% Triton X-100 in PBS for 20 min. Imaging was done using inverted research microscope (Nikon Corporation) (Refer to appendix I and II for details of antibodies used).

8.2.25. Confocal microscopy

Empty vector, *siah2* WT and *siah2* K139R-expressing MKN45 and AGS stable cells and *siah2* siRNA-expressing AGS cells were used for confocal microscopy. Cells were seeded, transfected and infected as per the protocols described previously. Cells were processed and stained with Siah2, Siah2 ac-K¹³⁹, TES, FLN-C specific antibodies, followed by DAPI and Phalloidin-FITC conjugate probe (#A12379, Invitrogen) treatments. Imaging was done using a laser scanning confocal microscope (Model No. LSM- 800, Carl Zeiss). Images were captured using LSM-TPMT camera system (Carl Zeiss), analyzed using LSM software (Carl Zeiss) and were processed using Adobe Photoshop (Version- 7.0, Adobe Systems, San Jose, California, USA).

8.2.26. Densitometric and statistical analysis

Except for the *in-vivo* studies, all experiments were performed in a non-randomized and non-blinded manner. Densitometric analyses of western blot images were done by Quantity 1-D Analysis software (Version- 4.6.9, Bio-Rad Laboratories). All *in-vitro* experiments were performed at least three times with three technical repeats and the results were graphically expressed as means \pm SEM. Statistical analysis was performed using GraphPad Prism software (Version- 7.03, GraphPad, La Jolla, California, USA). Statistical significance between two groups was calculated by Student's t-tests or 1-way ANOVA at * P <0.05. 2-

way ANOVA was applied for comparing two or more independent groups with Tukey's post hoc analysis.

BIBLIOGRAPHY

1. Dikshit, R., Gupta, P. C., Ramasundarahettige, C., Gajalakshmi, V., Aleksandrowicz, L., Badwe, R., Kumar, R., Roy, S., Suraweera, W., and Bray, F. (2012) Cancer mortality in India: a nationally representative survey. *The Lancet* **379**, 1807-1816
2. Ferlay, J., Shin, H. R., Bray, F., Forman, D., Mathers, C., and Parkin, D. M. (2010) Estimates of worldwide burden of cancer in 2008: GLOBOCAN 2008. *International journal of cancer* **127**, 2893-2917
3. Rugge, M., Fassan, M., and Graham, D. Y. (2015) Epidemiology of gastric cancer. In *Gastric cancer* pp. 23-34, Springer
4. Pérez, M., García-Limones, C., Zapico, I., Marina, A., Schmitz, M. L., Muñoz, E., and Calzado, M. A. (2012) Mutual regulation between SIAH2 and DYRK2 controls hypoxic and genotoxic signaling pathways. *Journal of molecular cell biology* **4**, 316-330
5. Correa, P., and Piazuelo, M. B. (2012) The gastric precancerous cascade. *Journal of digestive diseases* **13**, 2-9
6. Fox, J. G., and Wang, T. C. (2007) Inflammation, atrophy, and gastric cancer. *The Journal of clinical investigation* **117**, 60-69
7. Correa, P., Haenszel, W., Cuello, C., Tannenbaum, S., and Archer, M. (1975) A model for gastric cancer epidemiology. *The Lancet* **306**, 58-60
8. Nagini, S. (2012) Carcinoma of the stomach: A review of epidemiology, pathogenesis, molecular genetics and chemoprevention. *World journal of gastrointestinal oncology* **4**, 156
9. Polekhina, G., House, C. M., Traficante, N., Mackay, J. P., Relaix, F., Sassoon, D. A., Parker, M. W., and Bowtell, D. D. (2002) Siah ubiquitin ligase is structurally related to TRAF and modulates TNF- α signaling. *Nature Structural and Molecular Biology* **9**, 68
10. Zabaleta, J. (2012) Multifactorial etiology of gastric cancer. In *Cancer Epigenetics* pp. 411-435, Springer
11. Berretta, M., Cappellani, A., Lleshi, A., Di Vita, M., Lo Menzo, E., Bearz, A., Galvano, F., Spina, M., Malaguarnera, M., and Tirelli, U. (2012) The role of diet in gastric cancer: still an open question. *Front Biosci* **17**, 1640-1647
12. Krejs, G. J. (2010) Gastric cancer: epidemiology and risk factors. *Digestive diseases* **28**, 600-603
13. Tsugane, S., and Sasazuki, S. (2007) Diet and the risk of gastric cancer: review of epidemiological evidence. *Gastric cancer* **10**, 75-83
14. Park, B., Shin, A., Park, S. K., Ko, K.-P., Ma, S. H., Lee, E.-H., Gwack, J., Jung, E.-J., Cho, L. Y., and Yang, J. J. (2011) Ecological study for refrigerator use, salt, vegetable, and fruit intakes, and gastric cancer. *Cancer causes & control* **22**, 1497
15. Tsugane, S., Sasazuki, S., Kobayashi, M., and Sasaki, S. (2004) Salt and salted food intake and subsequent risk of gastric cancer among middle-aged Japanese men and women. *British Journal of Cancer* **90**, 128
16. Wang, X.-Q., Terry, P. D., and Yan, H. (2009) Review of salt consumption and stomach cancer risk: epidemiological and biological evidence. *World journal of gastroenterology: WJG* **15**, 2204
17. Wogan, G. N., Hecht, S. S., Felton, J. S., Conney, A. H., and Loeb, L. A. (2004) Environmental and chemical carcinogenesis. In *Seminars in cancer biology* Vol. 14 pp. 473-486, Elsevier
18. Barber, M., Fitzgerald, R. C., and Caldas, C. (2006) Familial gastric cancer—etiology and pathogenesis. *Best Practice & Research Clinical Gastroenterology* **20**, 721-734

19. El-Omar, E. M., Carrington, M., Chow, W.-H., McColl, K. E., Bream, J. H., Young, H. A., Herrera, J., Lissowska, J., Yuan, C.-C., and Rothman, N. (2000) Interleukin-1 polymorphisms associated with increased risk of gastric cancer. *Nature* **404**, 398
20. Castaño-Rodríguez, N., Kaakoush, N. O., and Mitchell, H. M. (2014) Pattern-recognition receptors and gastric cancer. *Frontiers in immunology* **5**, 336
21. Dhillon, P. K., Farrow, D. C., Vaughan, T. L., Chow, W. H., Risch, H. A., Gammon, M. D., Mayne, S. T., Stanford, J. L., Schoenberg, J. B., and Ahsan, H. (2001) Family history of cancer and risk of esophageal and gastric cancers in the United States. *International journal of cancer* **93**, 148-152
22. Sjødahl, K., Lu, Y., Nilsen, T. I., Ye, W., Hveem, K., Vatten, L., and Lagergren, J. (2007) Smoking and alcohol drinking in relation to risk of gastric cancer: A population-based, prospective cohort study. *International journal of cancer* **120**, 128-132
23. González, C. A., Pera, G., Agudo, A., Palli, D., Krogh, V., Vineis, P., Tumino, R., Panico, S., Berglund, G., and Simán, H. (2003) Smoking and the risk of gastric cancer in the European Prospective Investigation Into Cancer and Nutrition (EPIC). *International journal of cancer* **107**, 629-634
24. Kreuzer, M., Straif, K., Marsh, J., Dufey, F., Grosche, B., Nosske, D., and Sogl, M. (2011) Occupational dust and radiation exposure and mortality from stomach cancer among German uranium miners, 1946–2003. *Occup Environ Med*, oemed-2011-100051
25. Santibañez, M., Alguacil, J., de la Hera, M. G., Navarrete-Muñoz, E. M., Llorca, J., Aragonés, N., Kauppinen, T., and Vioque, J. (2012) Occupational exposures and risk of stomach cancer by histological type. *Occup Environ Med* **69**, 268-275
26. Wroblewski, L. E., Peek, R. M., and Wilson, K. T. (2010) Helicobacter pylori and gastric cancer: factors that modulate disease risk. *Clinical microbiology reviews* **23**, 713-739
27. Howson, C. P., Hiyama, T., and Wynder, E. L. (1986) The decline in gastric cancer: epidemiology of an unplanned triumph. *Epidemiologic reviews* **8**, 1-27
28. Parsonnet, J. (1995) The incidence of Helicobacter pylori infection. *Alimentary pharmacology & therapeutics* **9**, 45-51
29. Goodwin, C., McCulloch, R., Armstrong, J., and Wee, S. (1985) Unusual cellular fatty acids and distinctive ultrastructure in a new spiral bacterium (Campylobacter pyloridis) from the human gastric mucosa. *Journal of medical microbiology* **19**, 257-267
30. Jones, D., Curry, A., and Fox, A. (1985) An Ultrastructural Study of the Gastric Campylobacter-like Organism 'Campylobacter pyloridis'. *Microbiology* **131**, 2335-2341
31. Eslick, G. D. (2006) Helicobacter pylori infection causes gastric cancer A? review of the epidemiological, meta-analytic, and experimental evidence. *World journal of gastroenterology: WJG* **12**, 2991
32. Catalano, V., Labianca, R., Beretta, G. D., Gatta, G., De Braud, F., and Van Cutsem, E. (2009) Gastric cancer. *Critical reviews in oncology/hematology* **71**, 127-164
33. Houghton, J., and Wang, T. C. (2005) Helicobacter pylori and gastric cancer: a new paradigm for inflammation-associated epithelial cancers. *Gastroenterology* **128**, 1567-1578
34. Sachs, G., and Scott, D. R. (2012) Helicobacter pylori: eradication or preservation. *F1000 medicine reports* **4**

35. Chan, J., Ng, C., Hui, P., Leung, T., Lo, E., Lau, W., and McGuire, L. (1989) Anaplastic large cell Ki-1 lymphoma. Delineation of two morphological types. *Histopathology* **15**, 11-34
36. Marshall, B., and Warren, J. R. (1984) Unidentified curved bacilli in the stomach of patients with gastritis and peptic ulceration. *The Lancet* **323**, 1311-1315
37. GOODWIN, C. S., ARMSTRONG, J. A., CHILVERS, T., PETERS, M., COLLINS, M. D., SLY, L., McCONNELL, W., and HARPER, W. E. (1989) Transfer of *Campylobacter pylori* and *Campylobacter mustelae* to *Helicobacter* gen. nov. as *Helicobacter pylori* comb. nov. and *Helicobacter mustelae* comb. nov., respectively. *International Journal of Systematic and Evolutionary Microbiology* **39**, 397-405
38. Donelli, G., Matarrese, P., Fiorentini, C., Dainelli, B., Taraborelli, T., Di Campi, E., Di Bartolomeo, S., and Cellini, L. (1998) The effect of oxygen on the growth and cell morphology of *Helicobacter pylori*. *FEMS microbiology letters* **168**, 9-15
39. Kusters, J., Gerrits, M., Van Strijp, J., and Vandenbroucke-Grauls, C. (1997) Coccoid forms of *Helicobacter pylori* are the morphologic manifestation of cell death. *Infection and immunity* **65**, 3672-3679
40. Vandenplas, Y. (2000) *Helicobacter pylori* infection. *World journal of gastroenterology* **6**, 20
41. Gao, D., and Mittal, V. (2009) The role of bone-marrow-derived cells in tumor growth, metastasis initiation and progression. *Trends in molecular medicine* **15**, 333-343
42. Houghton, J., Stoicov, C., Nomura, S., Rogers, A. B., Carlson, J., Li, H., Cai, X., Fox, J. G., Goldenring, J. R., and Wang, T. C. (2004) Gastric cancer originating from bone marrow-derived cells. *Science* **306**, 1568-1571
43. Quante, M., Tu, S. P., Tomita, H., Gonda, T., Wang, S. S., Takashi, S., Baik, G. H., Shibata, W., DiPrete, B., and Betz, K. S. (2011) Bone marrow-derived myofibroblasts contribute to the mesenchymal stem cell niche and promote tumor growth. *Cancer cell* **19**, 257-272
44. Pereira, M.-I., and Medeiros, J. A. (2014) Role of *Helicobacter pylori* in gastric mucosa-associated lymphoid tissue lymphomas. *World journal of gastroenterology: WJG* **20**, 684
45. Noto, J. M., and Peek Jr, R. M. (2012) The role of microRNAs in *Helicobacter pylori* pathogenesis and gastric carcinogenesis. *Frontiers in cellular and infection microbiology* **1**, 21
46. Morales-Guerrero, S. E., Mucito-Varela, E., Aguilar-Gutiérrez, G. R., Lopez-Vidal, Y., and Castillo-Rojas, G. (2013) The role of CagA protein signaling in gastric carcinogenesis—CagA signaling in gastric carcinogenesis. In *Current Topics in Gastritis-2012*, InTech
47. Noto, J. M., and Peek, R. M. (2012) The *Helicobacter pylori* cag pathogenicity island. In *Helicobacter Species* pp. 41-50, Springer
48. Tegtmeyer, N., Wessler, S., and Backert, S. (2011) Role of the cag-pathogenicity island encoded type IV secretion system in *Helicobacter pylori* pathogenesis. *The FEBS journal* **278**, 1190-1202
49. Selbach, M., Moese, S., Hauck, C. R., Meyer, T. F., and Backert, S. (2002) Src is the kinase of the *Helicobacter pylori* CagA protein in vitro and in vivo. *Journal of Biological Chemistry* **277**, 6775-6778
50. Allen, L.-A. H., Schlesinger, L. S., and Kang, B. (2000) Virulent strains of *Helicobacter pylori* demonstrate delayed phagocytosis and stimulate homotypic phagosome fusion in macrophages. *Journal of Experimental Medicine* **191**, 115-128

51. Amieva, M. R., and El-Omar, E. M. (2008) Host-bacterial interactions in *Helicobacter pylori* infection. *Gastroenterology* **134**, 306-323
52. Torres, V. J., VanCompernelle, S. E., Sundrud, M. S., Unutmaz, D., and Cover, T. L. (2007) *Helicobacter pylori* vacuolating cytotoxin inhibits activation-induced proliferation of human T and B lymphocyte subsets. *The Journal of Immunology* **179**, 5433-5440
53. Evans, D., Evans, D. G., Takemura, T., Nakano, H., Lampert, H. C., Graham, D. Y., Granger, D. N., and Kvietyts, P. R. (1995) Characterization of a *Helicobacter pylori* neutrophil-activating protein. *Infection and immunity* **63**, 2213-2220
54. Bode, G., Malfertheiner, P., Lehnhardt, G., Nilius, M., and Ditschuneit, H. (1993) Ultrastructural localization of urease of *Helicobacter pylori*. *Medical microbiology and immunology* **182**, 233-242
55. Phadnis, S. H., Parlow, M. H., Levy, M., Ilver, D., Caulkins, C. M., Connors, J. B., and Dunn, B. E. (1996) Surface localization of *Helicobacter pylori* urease and a heat shock protein homolog requires bacterial autolysis. *Infection and immunity* **64**, 905-912
56. Kao, C.-Y., Sheu, B.-S., and Wu, J.-J. (2016) *Helicobacter pylori* infection: An overview of bacterial virulence factors and pathogenesis. *Biomedical journal* **39**, 14-23
57. Suerbaum, S., and Michetti, P. (2002) *Helicobacter pylori* infection. *New England Journal of Medicine* **347**, 1175-1186
58. Harris, A. W., Douds, A., Meurisse, E., Dennis, M., Chambers, S., and Gould, S. R. (1995) Seroprevalence of *Helicobacter pylori* in residents of a hospital for people with severe learning difficulties. *European journal of gastroenterology & hepatology* **7**, 21-23
59. Kimura, A., Matsubasa, T., Kinoshita, H., Kuriya, N., Yamashita, Y., Fujisawa, T., Terakura, H., and Shinohara, M. (1999) *Helicobacter pylori* seropositivity in patients with severe neurologic impairment. *Brain and Development* **21**, 113-117
60. Lambert, J. R., Lin, S.-K., Sievert, W., Nicholson, L., Schembri, M., and Guest, C. (1995) High Prevalence of *Helicobacter pylori* Antibodies in an Institutionalized Population: Evidence for Person-to-Person Transmission. *American Journal of Gastroenterology* **90**
61. Goodman, K. J., and Correa, P. (2000) Transmission of *Helicobacter pylori* among siblings. *The Lancet* **355**, 358-362
62. Li, C., Ha, T., Ferguson, D. A., Chi, D. S., Zhao, R., Patel, N. R., Krishnaswamy, G., and Thomas, E. (1996) A newly developed PCR assay of *H. pylori* in gastric biopsy, saliva, and feces. *Digestive diseases and sciences* **41**, 2142-2149
63. Kelly, S. M., Pitcher, M. C., Farmery, S. M., and Gibson, G. R. (1994) Isolation of *Helicobacter pylori* from feces of patients with dyspepsia in the United Kingdom. *Gastroenterology* **107**, 1671-1674
64. Bhattacharyya, A., Chattopadhyay, R., Burnette, B. R., Cross, J. V., Mitra, S., Ernst, P. B., Bhakat, K. K., and Crowe, S. E. (2009) Acetylation of Apurinic/Apyrimidinic Endonuclease-1 Regulates *Helicobacter pylori*-Mediated Gastric Epithelial Cell Apoptosis. *Gastroenterology* **136**, 2258-2269
65. Ding, S.-Z., Minohara, Y., Fan, X. J., Wang, J., Reyes, V. E., Patel, J., Dirden-Kramer, B., Boldogh, I., Ernst, P. B., and Crowe, S. E. (2007) *Helicobacter pylori* infection induces oxidative stress and programmed cell death in human gastric epithelial cells. *Infection and immunity* **75**, 4030-4039
66. Ding, S.-Z., O'Hara, A. M., Denning, T. L., Dirden-Kramer, B., Mifflin, R. C., Reyes, V. E., Ryan, K. A., Elliott, S. N., Izumi, T., and Boldogh, I. (2004) *Helicobacter*

- pylori and H₂O₂ increase AP endonuclease-1/redox factor-1 expression in human gastric epithelial cells. *Gastroenterology* **127**, 845-858
67. O'Hara, A. M., Bhattacharyya, A., Mifflin, R. C., Smith, M. F., Ryan, K. A., Scott, K. G.-E., Naganuma, M., Casola, A., Izumi, T., and Mitra, S. (2006) Interleukin-8 induction by *Helicobacter pylori* in gastric epithelial cells is dependent on apurinic/aprimidinic endonuclease-1/redox factor-1. *The Journal of Immunology* **177**, 7990-7999
 68. Schieber, M., and Chandel, N. S. (2014) ROS function in redox signaling and oxidative stress. *Current biology* **24**, R453-R462
 69. Semenza, G. L. (2003) Targeting HIF-1 for cancer therapy. *Nature reviews cancer* **3**, 721
 70. Masoud, G. N., and Li, W. (2015) HIF-1 α pathway: role, regulation and intervention for cancer therapy. *Acta Pharmaceutica Sinica B* **5**, 378-389
 71. Freedman, S. J., Sun, Z.-Y. J., Poy, F., Kung, A. L., Livingston, D. M., Wagner, G., and Eck, M. J. (2002) Structural basis for recruitment of CBP/p300 by hypoxia-inducible factor-1 α . *Proceedings of the National Academy of Sciences* **99**, 5367-5372
 72. Goodman, R. H., and Smolik, S. (2000) CBP/p300 in cell growth, transformation, and development. *Genes & development* **14**, 1553-1577
 73. Clarke, A. S., Lowell, J. E., Jacobson, S. J., and Pillus, L. (1999) Esa1p is an essential histone acetyltransferase required for cell cycle progression. *Molecular and cellular biology* **19**, 2515-2526
 74. Kawamura, T., Hasegawa, K., Morimoto, T., Iwai-Kanai, E., Miyamoto, S., Kawase, Y., Ono, K., Wada, H., Akao, M., and Kita, T. (2004) Expression of p300 protects cardiac myocytes from apoptosis in vivo. *Biochemical and biophysical research communications* **315**, 733-738
 75. Ishihama, K., Yamakawa, M., Semba, S., Takeda, H., Kawata, S., Kimura, S., and Kimura, W. (2007) Expression of HDAC1 and CBP/p300 in human colorectal carcinomas. *Journal of clinical pathology* **60**, 1205-1210
 76. Yang, W.-Y., Gu, J.-L., and Zhen, T.-M. (2014) Recent advances of histone modification in gastric cancer. *Journal of cancer research and therapeutics* **10**, 240
 77. Leber, M. F., and Efferth, T. (2009) Molecular principles of cancer invasion and metastasis. *International journal of oncology* **34**, 881-895
 78. Gupta, G. P., and Massagué, J. (2006) Cancer metastasis: building a framework. *Cell* **127**, 679-695
 79. Nguyen, D. X., Bos, P. D., and Massagué, J. (2009) Metastasis: from dissemination to organ-specific colonization. *Nature reviews cancer* **9**, 274
 80. Housman, G., Byler, S., Heerboth, S., Lapinska, K., Longacre, M., Snyder, N., and Sarkar, S. (2014) Drug resistance in cancer: an overview. *Cancers* **6**, 1769-1792
 81. Reymond, N., d'Água, B. B., and Ridley, A. J. (2013) Crossing the endothelial barrier during metastasis. *Nature reviews cancer* **13**, 858
 82. Sonoshita, M., Aoki, M., Fuwa, H., Aoki, K., Hosogi, H., Sakai, Y., Hashida, H., Takabayashi, A., Sasaki, M., and Robine, S. (2011) Suppression of colon cancer metastasis by Aes through inhibition of Notch signaling. *Cancer cell* **19**, 125-137
 83. Valastyan, S., and Weinberg, R. A. (2011) Tumor metastasis: molecular insights and evolving paradigms. *Cell* **147**, 275-292
 84. Yao, D., Dai, C., and Peng, S. (2011) Mechanism of the mesenchymal-epithelial transition and its relationship with metastatic tumor formation. *Molecular cancer research* **9**, 1608-1620

85. Renjini, A., Titus, S., Narayan, P., Murali, M., Jha, R. K., and Laloraya, M. (2014) STAT3 and MCL-1 associate to cause a mesenchymal epithelial transition. *J Cell Sci* **127**, 1738-1750
86. Bessede, E., Staedel, C., Amador, L. A., Nguyen, P., Chambonnier, L., Hatakeyama, M., Belleanne, G., Megraud, F., and Varon, C. (2014) Helicobacter pylori generates cells with cancer stem cell properties via epithelial–mesenchymal transition-like changes. *Oncogene* **33**, 4123
87. Lamouille, S., Xu, J., and Derynck, R. (2014) Molecular mechanisms of epithelial–mesenchymal transition. *Nature reviews Molecular cell biology* **15**, 178
88. Li, Y., Tan, B., Zhao, Q., Fan, L., Wang, D., and Liu, Y. (2014) ZNF139 promotes tumor metastasis by increasing migration and invasion in human gastric cancer cells. *Neoplasia* **61**, 291-298
89. Zhao, H., Wang, Y., Yang, L., Jiang, R., and Li, W. (2014) MiR-25 promotes gastric cancer cells growth and motility by targeting RECK. *Molecular and cellular biochemistry* **385**, 207-213
90. Yan, S.-y., Chen, M.-m., Li, G.-m., Wang, Y.-q., and Fan, J.-g. (2015) MiR-32 induces cell proliferation, migration, and invasion in hepatocellular carcinoma by targeting PTEN. *Tumor Biology* **36**, 4747-4755
91. Buti, L., Spooner, E., Van der Veen, A. G., Rappuoli, R., Covacci, A., and Ploegh, H. L. (2011) Helicobacter pylori cytotoxin-associated gene A (CagA) subverts the apoptosis-stimulating protein of p53 (ASPP2) tumor suppressor pathway of the host. *Proceedings of the National Academy of Sciences* **108**, 9238-9243
92. Lamb, A., Yang, X. D., Tsang, Y. H. N., Li, J. D., Higashi, H., Hatakeyama, M., Peek, R. M., Blanke, S. R., and Chen, L. F. (2009) Helicobacter pylori CagA activates NF- κ B by targeting TAK1 for TRAF6-mediated Lys 63 ubiquitination. *EMBO reports* **10**, 1242-1249
93. Tsang, Y., Lamb, A., Romero-Gallo, J., Huang, B., Ito, K., Peek Jr, R., Ito, Y., and Chen, L. (2010) Helicobacter pylori CagA targets gastric tumor suppressor RUNX3 for proteasome-mediated degradation. *Oncogene* **29**, 5643
94. Mani, S. A., Guo, W., Liao, M.-J., Eaton, E. N., Ayyanan, A., Zhou, A. Y., Brooks, M., Reinhard, F., Zhang, C. C., and Shipitsin, M. (2008) The epithelial-mesenchymal transition generates cells with properties of stem cells. *Cell* **133**, 704-715
95. Franke, W. W. (2009) Discovering the molecular components of intercellular junctions—a historical view. *Cold Spring Harbor perspectives in biology* **1**, a003061
96. Jeanes, A., Gottardi, C., and Yap, A. (2008) Cadherins and cancer: how does cadherin dysfunction promote tumor progression? *Oncogene* **27**, 6920
97. Tian, X., Liu, Z., Niu, B., Zhang, J., Tan, T. K., Lee, S. R., Zhao, Y., Harris, D. C., and Zheng, G. (2011) E-cadherin/ β -catenin complex and the epithelial barrier. *BioMed Research International* **2011**
98. King, N. (2004) The unicellular ancestry of animal development. *Developmental cell* **7**, 313-325
99. Heisenberg, C.-P., and Bellaïche, Y. (2013) Forces in tissue morphogenesis and patterning. *Cell* **153**, 948-962
100. Harris, T. J., and Tepass, U. (2010) Adherens junctions: from molecules to morphogenesis. *Nature reviews Molecular cell biology* **11**, 502
101. Perez-Moreno, M., Jamora, C., and Fuchs, E. (2003) Sticky business: orchestrating cellular signals at adherens junctions. *Cell* **112**, 535-548
102. Berx, G., and Van Roy, F. (2009) Involvement of members of the cadherin superfamily in cancer. *Cold Spring Harbor perspectives in biology* **1**, a003129

103. Fukagawa, A., Ishii, H., Miyazawa, K., and Saitoh, M. (2015) δ EF1 associates with DNMT1 and maintains DNA methylation of the E-cadherin promoter in breast cancer cells. *Cancer medicine* **4**, 125-135
104. Shargh, S. A., Sakizli, M., Khalaj, V., Movafagh, A., Yazdi, H., Hagigatjou, E., Sayad, A., Mansouri, N., Mortazavi-Tabatabaei, S. A., and Khorshid, H. R. K. (2014) Downregulation of E-cadherin expression in breast cancer by promoter hypermethylation and its relation with progression and prognosis of tumor. *Medical oncology* **31**, 250
105. Nagaishi, M., Nakata, S., Ono, Y., Hirata, K., Tanaka, Y., Suzuki, K., Yokoo, H., and Hyodo, A. (2017) Tumoral and stromal expression of Slug, ZEB1, and ZEB2 in brain metastasis. *Journal of Clinical Neuroscience* **46**, 124-128
106. Garg, M. (2013) Epithelial-mesenchymal transition-activating transcription factors-multifunctional regulators in cancer. *World journal of stem cells* **5**, 188
107. Katoh, Y., and Katoh, M. (2008) Hedgehog signaling, epithelial-to-mesenchymal transition and miRNA. *International journal of molecular medicine* **22**, 271-275
108. Gregory, P. A., Bert, A. G., Paterson, E. L., Barry, S. C., Tsykin, A., Farshid, G., Vadas, M. A., Khew-Goodall, Y., and Goodall, G. J. (2008) The miR-200 family and miR-205 regulate epithelial to mesenchymal transition by targeting ZEB1 and SIP1. *Nature cell biology* **10**, 593
109. Gialeli, C., Theocharis, A. D., and Karamanos, N. K. (2011) Roles of matrix metalloproteinases in cancer progression and their pharmacological targeting. *The FEBS journal* **278**, 16-27
110. Nieman, M. T., Prudoff, R. S., Johnson, K. R., and Wheelock, M. J. (1999) N-cadherin promotes motility in human breast cancer cells regardless of their E-cadherin expression. *The Journal of cell biology* **147**, 631-644
111. Loges, S., Roncal, C., and Carmeliet, P. (2009) Development of targeted angiogenic medicine. *Journal of Thrombosis and Haemostasis* **7**, 21-33
112. Nagafuchi, A., and Takeichi, M. (1989) Transmembrane control of cadherin-mediated cell adhesion: a 94 kDa protein functionally associated with a specific region of the cytoplasmic domain of E-cadherin. *Cell regulation* **1**, 37-44
113. Clevers, H. (2006) Wnt/ β -catenin signaling in development and disease. *Cell* **127**, 469-480
114. Zhan, T., Rindtorff, N., and Boutros, M. (2017) Wnt signaling in cancer. *Oncogene* **36**, 1461
115. Peifer, M., Hertwig, F., Roels, F., Dreidax, D., Gartlgruber, M., Menon, R., Krämer, A., Roncaioli, J. L., Sand, F., and Heuckmann, J. M. (2015) Telomerase activation by genomic rearrangements in high-risk neuroblastoma. *Nature* **526**, 700
116. Mao, J., Fan, S., Ma, W., Fan, P., Wang, B., Zhang, J., Wang, H., Tang, B., Zhang, Q., and Yu, X. (2015) Roles of Wnt/ β -catenin signaling in the gastric cancer stem cells proliferation and salinomycin treatment. *Cell death & disease* **5**, e1039
117. Gonzalez-Mariscal, L., Lechuga, S., and Garay, E. (2007) Role of tight junctions in cell proliferation and cancer. *Progress in histochemistry and cytochemistry* **42**, 1-57
118. Wessler, S., Gimona, M., and Rieder, G. (2011) Regulation of the actin cytoskeleton in Helicobacter pylori-induced migration and invasive growth of gastric epithelial cells. *Cell Communication and Signaling* **9**, 27
119. Mimuro, H., Suzuki, T., Nagai, S., Rieder, G., Suzuki, M., Nagai, T., Fujita, Y., Nagamatsu, K., Ishijima, N., and Koyasu, S. (2007) Helicobacter pylori dampens gut epithelial self-renewal by inhibiting apoptosis, a bacterial strategy to enhance colonization of the stomach. *Cell host & microbe* **2**, 250-263

120. Alzahrani, S., Lina, T. T., Gonzalez, J., Pinchuk, I. V., Beswick, E. J., and Reyes, V. E. (2014) Effect of *Helicobacter pylori* on gastric epithelial cells. *World journal of gastroenterology: WJG* **20**, 12767
121. Backert, S., Bernegger, S., Skórko-Glonek, J., and Wessler, S. (2018) Extracellular HtrA serine proteases: an emerging new strategy in bacterial pathogenesis. *Cellular microbiology*, e12845
122. Saarikangas, J., Zhao, H., and Lappalainen, P. (2010) Regulation of the actin cytoskeleton-plasma membrane interplay by phosphoinositides. *Physiological reviews* **90**, 259-289
123. Zhou, A.-X., Hartwig, J. H., and Akyürek, L. M. (2010) Filamins in cell signaling, transcription and organ development. *Trends in cell biology* **20**, 113-123
124. Qiao, J., Cui, S.-J., Xu, L.-L., Chen, S.-J., Yao, J., Jiang, Y.-H., Peng, G., Fang, C.-Y., Yang, P.-Y., and Liu, F. (2015) Filamin C, a dysregulated protein in cancer revealed by label-free quantitative proteomic analyses of human gastric cancer cells. *Oncotarget* **6**, 1171
125. Qu, Y., Dang, S., and Hou, P. (2013) Gene methylation in gastric cancer. *Clinica chimica acta* **424**, 53-65
126. Tanabe, K., Shinsato, Y., Furukawa, T., Kita, Y., Hatanaka, K., Minami, K., Kawahara, K., Yamamoto, M., Baba, K., and Mori, S. (2017) Filamin C promotes lymphatic invasion and lymphatic metastasis and increases cell motility by regulating Rho GTPase in esophageal squamous cell carcinoma. *Oncotarget* **8**, 6353-6363
127. Nakamura, F., Stossel, T. P., and Hartwig, J. H. (2011) The filamins: organizers of cell structure and function. *Cell adhesion & migration* **5**, 160-169
128. Adachi-Hayama, M., Adachi, A., Shinozaki, N., Matsutani, T., Hiwasa, T., Takiguchi, M., Saeki, N., and Iwadate, Y. (2014) Circulating anti-filamin C autoantibody as a potential serum biomarker for low-grade gliomas. *BMC cancer* **14**, 452
129. Coutts, A. S., MacKenzie, E., Griffith, E., and Black, D. M. (2003) TES is a novel focal adhesion protein with a role in cell spreading. *Journal of cell science* **116**, 897-906
130. Ma, H., Weng, D., Chen, Y., Huang, W., Pan, K., Wang, H., Sun, J., Wang, Q., Zhou, Z., and Wang, H. (2010) Extensive analysis of D7S486 in primary gastric cancer supports TESTIN as a candidate tumor suppressor gene. *Molecular cancer* **9**, 190
131. Xia, J., Weng, D., Ma, H., Chen, Y., Huang, W., and Pan, K. (2010) Analysis of D7S486 in primary gastric cancer and evaluation of TESTIN as a candidate tumor suppressor gene. *Journal of Clinical Oncology* **28**, 4129-4129
132. Steponaitis, G., Kazlauskas, A., Skiriute, D., Valiulyte, I., Skauminas, K., Tamasauskas, A., and Vaitkiene, P. (2016) Testin (TES) as a candidate tumour suppressor and prognostic marker in human astrocytoma. *Oncology letters* **12**, 3305-3311
133. Zhu, J., Li, X., Kong, X., Moran, M. S., Su, P., Haffty, B. G., and Yang, Q. (2012) Testin is a tumor suppressor and prognostic marker in breast cancer. *Cancer science* **103**, 2092-2101
134. Luo, Z.-Q., and Qiu, J. (2017) Hijacking of the host ubiquitin network by *Legionella pneumophila*. *Frontiers in cellular and infection microbiology* **7**, 487
135. Eguchi, H., Herschenhous, N., Kuzushita, N., and Moss, S. F. (2003) *Helicobacter pylori* increases proteasome-mediated degradation of p27kip1 in gastric epithelial cells. *Cancer research* **63**, 4739-4746
136. Das, L., Kokate, S., Dixit, P., Rath, S., Rout, N., Singh, S., Crowe, S., and Bhattacharyya, A. (2017) Membrane-bound β -catenin degradation is enhanced by

- ETS2-mediated Siah1 induction in Helicobacter pylori-infected gastric cancer cells. *Oncogenesis* **6**, e327
137. Das, L., Kokate, S. B., Rath, S., Rout, N., Singh, S. P., Crowe, S. E., Mukhopadhyay, A. K., and Bhattacharyya, A. (2016) ETS2 and Twist1 promote invasiveness of Helicobacter pylori-infected gastric cancer cells by inducing Siah2. *Biochemical Journal* **473**, 1629-1640
 138. Calzado, M. A., De La Vega, L., Möller, A., Bowtell, D. D., and Schmitz, M. L. (2009) An inducible autoregulatory loop between HIPK2 and Siah2 at the apex of the hypoxic response. *Nature cell biology* **11**, 85
 139. Carbia-Nagashima, A., Gerez, J., Perez-Castro, C., Paez-Pereda, M., Silberstein, S., Stalla, G. K., Holsboer, F., and Arzt, E. (2007) RSUME, a small RWD-containing protein, enhances SUMO conjugation and stabilizes HIF-1 α during hypoxia. *Cell* **131**, 309-323
 140. Richard, D. E., Berra, E., Gothié, E., Roux, D., and Pouyssegur, J. (1999) p42/p44 mitogen-activated protein kinases phosphorylate hypoxia-inducible factor 1 α (HIF-1 α) and enhance the transcriptional activity of HIF-1. *Journal of Biological Chemistry* **274**, 32631-32637
 141. Khurana, A., Nakayama, K., Williams, S., Davis, R. J., Mustelin, T., and Ronai, Z. e. (2006) Regulation of the ring finger E3 ligase Siah2 by p38 MAPK. *Journal of Biological Chemistry* **281**, 35316-35326
 142. Shabek, N., Herman-Bachinsky, Y., Buchsbaum, S., Lewinson, O., Haj-Yahya, M., Hejjaoui, M., Lashuel, H. A., Sommer, T., Brik, A., and Ciechanover, A. (2012) The size of the proteasomal substrate determines whether its degradation will be mediated by mono- or polyubiquitylation. *Molecular cell* **48**, 87-97
 143. Swatek, K. N., and Komander, D. (2016) Ubiquitin modifications. *Cell research* **26**, 399
 144. Dikic, I., Wakatsuki, S., and Walters, K. J. (2009) Ubiquitin-binding domains—from structures to functions. *Nature reviews Molecular cell biology* **10**, 659
 145. Kim, H. M., Yu, Y., and Cheng, Y. (2011) Structure characterization of the 26S proteasome. *Biochimica et Biophysica Acta (BBA)-Gene Regulatory Mechanisms* **1809**, 67-79
 146. Kowalski, J. R., and Juo, P. (2012) The role of deubiquitinating enzymes in synaptic function and nervous system diseases. *Neural plasticity* **2012**
 147. Rotin, D., and Kumar, S. (2009) Physiological functions of the HECT family of ubiquitin ligases. *Nature reviews Molecular cell biology* **10**, 398
 148. Zheng, N., and Shabek, N. (2017) Ubiquitin ligases: structure, function, and regulation. *Annual review of biochemistry* **86**, 129-157
 149. Yang, H., Landis-Piowar, K., Chen, D., Milacic, V., and Dou, Q. (2008) Natural compounds with proteasome inhibitory activity for cancer prevention and treatment. *Current Protein and Peptide Science* **9**, 227-239
 150. Buetow, L., and Huang, D. T. (2016) Structural insights into the catalysis and regulation of E3 ubiquitin ligases. *Nature reviews Molecular cell biology* **17**, 626
 151. Metzger, M. B., Hristova, V. A., and Weissman, A. M. (2012) HECT and RING finger families of E3 ubiquitin ligases at a glance. *J Cell Sci* **125**, 531-537
 152. Nethe, M., and Hordijk, P. L. (2010) The role of ubiquitylation and degradation in RhoGTPase signalling. *J Cell Sci* **123**, 4011-4018
 153. Paul, A., and Paul, S. (2014) The breast cancer susceptibility genes (BRCA) in breast and ovarian cancers. *Frontiers in bioscience (Landmark edition)* **19**, 605
 154. Moldovan, G.-L., and D'Andrea, A. D. (2009) How the fanconi anemia pathway guards the genome. *Annual review of genetics* **43**, 223-249

155. Dong, Q., Liu, Y., Qu, X., Hou, K., and Li, L. (2010) Expression of c-Cbl, Cbl-b, and epidermal growth factor receptor in gastric carcinoma and their clinical significance. *Chinese journal of cancer* **29**, 59-64
156. Jiang, W., Wang, S., Xiao, M., Lin, Y., Zhou, L., Lei, Q., Xiong, Y., Guan, K.-L., and Zhao, S. (2011) Acetylation regulates gluconeogenesis by promoting PEPCK1 degradation via recruiting the UBR5 ubiquitin ligase. *Molecular cell* **43**, 33-44
157. Kang, J. M., Park, S., Kim, S. J., Hong, H., Jeong, J., and Kim, H. (2012) CBL enhances breast tumor formation by inhibiting tumor suppressive activity of TGF- β signaling. *Oncogene* **31**, 5123
158. Lo, F. Y., Tan, Y. H. C., Cheng, H. C., Salgia, R., and Wang, Y. C. (2011) An E3 ubiquitin ligase: c-Cbl. *Cancer* **117**, 5344-5350
159. Xin, J., Bo, J., Shunchao, Y., Kezuo, H., Yunpeng, L., and Xuejun, H. (2011) Expressions of c-Cbl, Cbl-b and EGFR and Its Role of Prognosis in NSCLC. *Chinese Journal of Lung Cancer* **14**
160. Genschik, P., Sumara, I., and Lechner, E. (2013) The emerging family of CULLIN3-RING ubiquitin ligases (CRL3s): cellular functions and disease implications. *The EMBO journal* **32**, 2307-2320
161. Rankin, E. B., and Giaccia, A. J. (2016) Hypoxic control of metastasis. *Science* **352**, 175-180
162. Gossage, L., Eisen, T., and Maher, E. R. (2015) VHL, the story of a tumour suppressor gene. *Nature reviews cancer* **15**, 55
163. Krämer, O., Stauber, R., Bug, G., Hartkamp, J., and Knauer, S. (2013) SIAH proteins: critical roles in leukemogenesis. *Leukemia* **27**, 792
164. Kim, H., Jeong, W., Ahn, K., Ahn, C., and Kang, S. (2004) Siah-1 interacts with the intracellular region of polycystin-1 and affects its stability via the ubiquitin-proteasome pathway. *Journal of the American Society of Nephrology* **15**, 2042-2049
165. Gopalsamy, A., Hagen, T., and Swaminathan, K. (2014) Investigating the molecular basis of Siah1 and Siah2 E3 ubiquitin ligase substrate specificity. *PloS one* **9**, e106547
166. House, C. M., Hancock, N. C., Möller, A., Cromer, B. A., Fedorov, V., Bowtell, D. D., Parker, M. W., and Polekhina, G. (2006) Elucidation of the substrate binding site of Siah ubiquitin ligase. *Structure* **14**, 695-701
167. Zhang, Q., Wang, Z., Hou, F., Harding, R., Huang, X., Dong, A., Walker, J. R., and Tong, Y. (2017) The substrate binding domains of human SIAH E3 ubiquitin ligases are now crystal clear. *Biochimica et Biophysica Acta (BBA)-General Subjects* **1861**, 3095-3105
168. Wong, C. S., and Möller, A. (2013) Siah-a promising anti-cancer target. *Cancer research*, canres. 4348.2012
169. Habelhah, H., Frew, I. J., Laine, A., Janes, P. W., Relaix, F., Sassoon, D., Bowtell, D. D., and Ronai, Z. e. (2002) Stress-induced decrease in TRAF2 stability is mediated by Siah2. *The EMBO journal* **21**, 5756-5765
170. Matsuzawa, S.-i., and Reed, J. C. (2001) Siah-1, SIP, and Ebi collaborate in a novel pathway for β -catenin degradation linked to p53 responses. *Molecular cell* **7**, 915-926
171. Brauckhoff, A., Malz, M., Tschaharganeh, D., Malek, N., Weber, A., Riener, M.-O., Soll, C., Samarin, J., Bissinger, M., and Schmidt, J. (2011) Nuclear expression of the ubiquitin ligase seven in absentia homolog (SIAH)-1 induces proliferation and migration of liver cancer cells. *Journal of hepatology* **55**, 1049-1057
172. Hara, M. R., Agrawal, N., Kim, S. F., Cascio, M. B., Fujimuro, M., Ozeki, Y., Takahashi, M., Cheah, J. H., Tankou, S. K., and Hester, L. D. (2005) S-nitrosylated GAPDH initiates apoptotic cell death by nuclear translocation following Siah1 binding. *Nature cell biology* **7**, 665

173. House, C. M., Möller, A., and Bowtell, D. D. (2009) Siah proteins: novel drug targets in the Ras and hypoxia pathways. *Cancer research* **69**, 8835-8838
174. Nagano, Y., Fukushima, T., Okemoto, K., Tanaka, K., Bowtell, D. D., Ronai, Z. e., Reed, J. C., and Matsuzawa, S.-i. (2011) Siah1/SIP regulates p27kip1 stability and cell migration under metabolic stress. *Cell Cycle* **10**, 2592-2602
175. Wong, C. S., Sceneay, J., House, C. M., Halse, H. M., Liu, M. C., George, J., Hunnam, T. C. P., Parker, B. S., Haviv, I., and Ronai, Z. e. (2012) Vascular normalization by loss of Siah2 results in increased chemotherapeutic efficacy. *Cancer research* **72**, 1694-1704
176. Nagano, Y., and Matsuzawa, S.-I. (2013) SIAH1 (siah E3 ubiquitin protein ligase 1).
177. Ma, B., Chen, Y., Chen, L., Cheng, H., Mu, C., Li, J., Gao, R., Zhou, C., Cao, L., and Liu, J. (2015) Hypoxia regulates Hippo signalling through the SIAH2 ubiquitin E3 ligase. *Nature cell biology* **17**, 95
178. Zhao, Y., Lu, S., Wu, L., Chai, G., Wang, H., Chen, Y., Sun, J., Yu, Y., Zhou, W., and Zheng, Q. (2006) Acetylation of p53 at lysine 373/382 by the histone deacetylase inhibitor depsipeptide induces expression of p21Waf1/Cip1. *Molecular and cellular biology* **26**, 2782-2790
179. Hsieh, S.-C., Kuo, S.-N., Zheng, Y.-H., Tsai, M.-H., Lin, Y.-S., and Lin, J.-H. (2013) The E3 ubiquitin ligase SIAH2 is a prosurvival factor overexpressed in oral cancer. *Anticancer research* **33**, 4965-4973
180. Chan, P., Möller, A., Liu, M. C., Sceneay, J. E., Wong, C. S., Waddell, N., Huang, K. T., Dobrovic, A., Millar, E. K., and O'Toole, S. A. (2011) The expression of the ubiquitin ligase SIAH2 (seven in absentia homolog 2) is mediated through gene copy number in breast cancer and is associated with a basal-like phenotype and p53 expression. *Breast Cancer Research* **13**, R19
181. Hayes, J. D., and Dinkova-Kostova, A. T. (2014) The Nrf2 regulatory network provides an interface between redox and intermediary metabolism. *Trends in biochemical sciences* **39**, 199-218
182. Xu, Z., Sproul, A., Wang, W., Kukekov, N., and Greene, L. A. (2006) Siah1 interacts with the scaffold protein POSH to promote JNK activation and apoptosis. *Journal of Biological Chemistry* **281**, 303-312
183. Winter, M., Sombroek, D., Dauth, I., Moehlenbrink, J., Scheuermann, K., Crone, J., and Hofmann, T. G. (2008) Control of HIPK2 stability by ubiquitin ligase Siah-1 and checkpoint kinases ATM and ATR. *Nature cell biology* **10**, 812
184. Nakayama, K., Qi, J., and Ronai, Z. e. (2009) The ubiquitin ligase Siah2 and the hypoxia response. *Molecular Cancer Research* **7**, 443-451
185. Schmidt, R. L., Park, C. H., Ahmed, A. U., Gundelach, J. H., Reed, N. R., Cheng, S., Knudsen, B. E., and Tang, A. H. (2007) Inhibition of RAS-mediated transformation and tumorigenesis by targeting the downstream E3 ubiquitin ligase seven in absentia homologue. *Cancer research* **67**, 11798-11810
186. Scortegagna, M., Subtil, T., Qi, J., Kim, H., Zhao, W., Gu, W., Kluger, H., and Ze'ev, A. R. (2011) USP13 enzyme regulates Siah2 ligase stability and activity via noncatalytic ubiquitin-binding domains. *Journal of Biological Chemistry* **286**, 27333-27341
187. Verdin, E., and Ott, M. (2015) 50 years of protein acetylation: from gene regulation to epigenetics, metabolism and beyond. *Nature reviews Molecular cell biology* **16**, 258
188. Sang, Y., Ren, J., Qin, R., Liu, S., Cui, Z., Cheng, S., Liu, X., Lu, J., Tao, J., and Yao, Y.-F. (2017) Acetylation Regulating Protein Stability and DNA-Binding Ability of HILD, thus Modulating Salmonella Typhimurium Virulence. *The Journal of infectious diseases* **216**, 1018-1026

189. Ishfaq, M., Maeta, K., Maeda, S., Natsume, T., Ito, A., and Yoshida, M. (2012) Acetylation regulates subcellular localization of eukaryotic translation initiation factor 5A (eIF5A). *FEBS letters* **586**, 3236-3241
190. Drazic, A., Myklebust, L. M., Ree, R., and Arnesen, T. (2016) The world of protein acetylation. *Biochimica et Biophysica Acta (BBA)-Proteins and Proteomics* **1864**, 1372-1401
191. Dai, C., Shi, D., and Gu, W. (2013) Negative regulation of the acetyltransferase TIP60-p53 interplay by UHRF1 (ubiquitin-like with PHD and RING finger domains 1). *Journal of Biological Chemistry* **288**, 19581-19592
192. Holmlund, T., Lindberg, M., Grander, D., and Wallberg, A. (2013) GCN5 acetylates and regulates the stability of the oncoprotein E2A-PBX1 in acute lymphoblastic leukemia. *Leukemia* **27**, 578
193. Kong, X., Lin, Z., Liang, D., Fath, D., Sang, N., and Caro, J. (2006) Histone deacetylase inhibitors induce VHL and ubiquitin-independent proteasomal degradation of hypoxia-inducible factor 1 α . *Molecular and cellular biology* **26**, 2019-2028
194. Jin, Y.-H., Jeon, E.-J., Li, Q.-L., Lee, Y. H., Choi, J.-K., Kim, W.-J., Lee, K.-Y., and Bae, S.-C. (2004) Transforming growth factor- β stimulates p300-dependent RUNX3 acetylation, which inhibits ubiquitination-mediated degradation. *Journal of Biological Chemistry* **279**, 29409-29417
195. Chamberlain, W., Gonnella, P., Alamdari, N., Aversa, Z., and Hasselgren, P.-O. (2012) Multiple muscle wasting-related transcription factors are acetylated in dexamethasone-treated muscle cells. *Biochemistry and Cell Biology* **90**, 200-208
196. di Bari, M. G., Ciuffini, L., Mingardi, M., Testi, R., Soddu, S., and Barilà, D. (2006) c-Abl acetylation by histone acetyltransferases regulates its nuclear-cytoplasmic localization. *EMBO reports* **7**, 727-733
197. Wang, Z., Inuzuka, H., Zhong, J., Liu, P., Sarkar, F. H., Sun, Y., and Wei, W. (2012) Identification of acetylation-dependent regulatory mechanisms that govern the oncogenic functions of Skp2. *Oncotarget* **3**, 1294
198. Ventura, M., Mateo, F., Serratos, J., Salaet, I., Carujo, S., Bachs, O., and Pujol, M. J. (2010) Nuclear translocation of glyceraldehyde-3-phosphate dehydrogenase is regulated by acetylation. *The international journal of biochemistry & cell biology* **42**, 1672-1680
199. Sen, N., Hara, M. R., Kornberg, M. D., Cascio, M. B., Bae, B.-I., Shahani, N., Thomas, B., Dawson, T. M., Dawson, V. L., and Snyder, S. H. (2008) Nitric oxide-induced nuclear GAPDH activates p300/CBP and mediates apoptosis. *Nature cell biology* **10**, 866
200. Cai, X., Carlson, J., Stoicov, C., Li, H., Wang, T. C., and Houghton, J. (2005) *Helicobacter felis* eradication restores normal architecture and inhibits gastric cancer progression in C57BL/6 mice. *Gastroenterology* **128**, 1937-1952
201. Backert, S., Clyne, M., and Tegtmeyer, N. (2011) Molecular mechanisms of gastric epithelial cell adhesion and injection of CagA by *Helicobacter pylori*. *Cell Communication and Signaling* **9**, 28
202. Kokate, S. B., Dixit, P., Das, L., Rath, S., Roy, A. D., Poirah, I., Chakraborty, D., Rout, N., Singh, S. P., and Bhattacharyya, A. (2018) Acetylation-mediated Siah2 stabilization enhances PHD3 degradation in *Helicobacter pylori*-infected gastric epithelial cancer cells. *The FASEB Journal*, fj. 201701344RRR
203. Arif, M., Vedamurthy, B. M., Choudhari, R., Ostwal, Y. B., Mantelingu, K., Kodaganur, G. S., and Kundu, T. K. (2010) Nitric oxide-mediated histone

- hyperacetylation in oral cancer: target for a water-soluble HAT inhibitor, CTK7A. *Chemistry & biology* **17**, 903-913
204. Rath, S., Das, L., Kokate, S. B., Ghosh, N., Dixit, P., Rout, N., Singh, S. P., Chattopadhyay, S., Ashktorab, H., and Smoot, D. T. (2017) Inhibition of histone/lysine acetyltransferase activity kills CoCL2-treated and hypoxia-exposed gastric cancer cells and reduces their invasiveness. *The international journal of biochemistry & cell biology* **82**, 28-40
 205. Ma, J., Shen, H., Kapesa, L., and Zeng, S. (2016) Lauren classification and individualized chemotherapy in gastric cancer. *Oncology letters* **11**, 2959-2964
 206. Spange, S., Wagner, T., Heinzl, T., and Krämer, O. H. (2009) Acetylation of non-histone proteins modulates cellular signalling at multiple levels. *The international journal of biochemistry & cell biology* **41**, 185-198
 207. Zhao, S., Xu, W., Jiang, W., Yu, W., Lin, Y., Zhang, T., Yao, J., Zhou, L., Zeng, Y., and Li, H. (2010) Regulation of cellular metabolism by protein lysine acetylation. *Science* **327**, 1000-1004
 208. Wang, L., Du, Y., Lu, M., and Li, T. (2012) ASEB: a web server for KAT-specific acetylation site prediction. *Nucleic acids research* **40**, W376-W379
 209. Xue, Y., Li, A., and Yao, X. (2006) PAIL: prediction of acetylation on internal lysines.
 210. Choudhary, C., Kumar, C., Gnad, F., Nielsen, M. L., Rehman, M., Walther, T. C., Olsen, J. V., and Mann, M. (2009) Lysine acetylation targets protein complexes and co-regulates major cellular functions. *Science* **325**, 834-840
 211. Das, C., and Kundu, T. (2005) Transcriptional Regulation by the Acetylation of Nonhistone Proteins in Humans-A New Target for Therapeutics. *IUBMB life* **57**, 137-149
 212. Wan, W., You, Z., Xu, Y., Zhou, L., Guan, Z., Peng, C., Wong, C. C., Su, H., Zhou, T., and Xia, H. (2017) mTORC1 Phosphorylates Acetyltransferase p300 to Regulate Autophagy and Lipogenesis. *Molecular cell* **68**, 323-335. e326
 213. Ono, H., Basson, M. D., and Ito, H. (2016) P300 inhibition enhances gemcitabine-induced apoptosis of pancreatic cancer. *Oncotarget* **7**, 51301
 214. Yan, G., Eller, M. S., Elm, C., Larocca, C. A., Ryu, B., Panova, I. P., Dancy, B. M., Bowers, E. M., Meyers, D., and Lareau, L. (2013) Selective inhibition of p300 HAT blocks cell cycle progression, induces cellular senescence, and inhibits the DNA damage response in melanoma cells. *Journal of Investigative Dermatology* **133**, 2444-2452
 215. Du, Z., Song, J., Wang, Y., Zhao, Y., Guda, K., Yang, S., Kao, H.-Y., Xu, Y., Willis, J., and Markowitz, S. D. (2010) DNMT1 stability is regulated by proteins coordinating deubiquitination and acetylation-driven ubiquitination. *Sci. Signal.* **3**, ra80-ra80
 216. Li, M., Luo, J., Brooks, C. L., and Gu, W. (2002) Acetylation of p53 inhibits its ubiquitination by Mdm2. *Journal of Biological Chemistry* **277**, 50607-50611
 217. Dyson, H. J., and Wright, P. E. (2016) Role of intrinsic protein disorder in the function and interactions of the transcriptional coactivators CREB-binding protein (CBP) and p300. *Journal of Biological Chemistry* **291**, 6714-6722
 218. Mujtaba, S., He, Y., Zeng, L., Yan, S., Plotnikova, O., Sanchez, R., Zeleznik-Le, N. J., Ronai, Z. e., and Zhou, M.-M. (2004) Structural mechanism of the bromodomain of the coactivator CBP in p53 transcriptional activation. *Molecular cell* **13**, 251-263
 219. Fan, L., Peng, G., Hussain, A., Fazli, L., Guns, E., Gleave, M., and Qi, J. (2015) The steroidogenic enzyme AKR1C3 regulates stability of the ubiquitin ligase Siah2 in prostate cancer cells. *Journal of Biological Chemistry* **290**, 20865-20879

220. Do Yeon Lee, D. E. J., Yu, S. S., Lee, Y. S., Choi, B. K., and Lee, Y. C. (2017) Regulation of SIRT3 signal related metabolic reprogramming in gastric cancer by Helicobacter pylori oncoprotein CagA. *Oncotarget* **8**, 78365
221. Canales, J., Valenzuela, M., Bravo, J., Cerda-Opazo, P., Jorquera, C., Toledo, H., Bravo, D., and Quest, A. F. (2017) Helicobacter pylori Induced Phosphatidylinositol-3-OH Kinase/mTOR Activation Increases Hypoxia Inducible Factor-1 α to Promote Loss of Cyclin D1 and G0/G1 Cell Cycle Arrest in Human Gastric Cells. *Frontiers in cellular and infection microbiology* **7**, 92
222. Bhattacharyya, A., Chattopadhyay, R., Hall, E. H., Mebrahtu, S. T., Ernst, P. B., and Crowe, S. E. (2010) Mechanism of hypoxia-inducible factor 1 α -mediated Mcl1 regulation in Helicobacter pylori-infected human gastric epithelium. *American Journal of Physiology-Gastrointestinal and Liver Physiology* **299**, G1177-G1186
223. Lin, M., Lin, J., Hsu, C., Juan, H., Lou, P., and Huang, M. (2017) GATA3 interacts with and stabilizes HIF-1 α to enhance cancer cell invasiveness. *Oncogene* **36**, 4243
224. Majmundar, A. J., Wong, W. J., and Simon, M. C. (2010) Hypoxia-inducible factors and the response to hypoxic stress. *Molecular cell* **40**, 294-309
225. Martin, M. E., and Solnick, J. V. (2014) The gastric microbial community, Helicobacter pylori colonization, and disease. *Gut microbes* **5**, 345-350
226. Zhang, S., and Moss, S. F. (2012) Rodent models of Helicobacter infection, inflammation, and disease. In *Helicobacter Species* pp. 89-98, Springer
227. Appelhoff, R. J., Tian, Y.-M., Raval, R. R., Turley, H., Harris, A. L., Pugh, C. W., Ratcliffe, P. J., and Gleadle, J. M. (2004) Differential function of the prolyl hydroxylases PHD1, PHD2, and PHD3 in the regulation of hypoxia-inducible factor. *Journal of Biological Chemistry* **279**, 38458-38465
228. Kuschel, A., Simon, P., and Tug, S. (2012) Functional regulation of HIF-1 α under normoxia—is there more than post-translational regulation? *Journal of cellular physiology* **227**, 514-524
229. Saeedi, B. J., Kao, D. J., Kitzenberg, D. A., Dobrinskikh, E., Schwisow, K. D., Masterson, J. C., Kendrick, A. A., Kelly, C. J., Bayless, A. J., and Kominsky, D. J. (2015) HIF-dependent regulation of claudin-1 is central to intestinal epithelial tight junction integrity. *Molecular biology of the cell* **26**, 2252-2262
230. Kelly, C. J., Zheng, L., Campbell, E. L., Saeedi, B., Scholz, C. C., Bayless, A. J., Wilson, K. E., Glover, L. E., Kominsky, D. J., and Magnuson, A. (2015) Crosstalk between microbiota-derived short-chain fatty acids and intestinal epithelial HIF augments tissue barrier function. *Cell host & microbe* **17**, 662-671
231. Kelly, C. J., Glover, L. E., Campbell, E. L., Kominsky, D. J., Ehrentraut, S. F., Bowers, B. E., Bayless, A. J., Saeedi, B. J., and Colgan, S. P. (2013) Fundamental role for HIF-1 α in constitutive expression of human β defensin-1. *Mucosal immunology* **6**, 1110
232. Glover, L. E., Bowers, B. E., Saeedi, B., Ehrentraut, S. F., Campbell, E. L., Bayless, A. J., Dobrinskikh, E., Kendrick, A. A., Kelly, C. J., and Burgess, A. (2013) Control of creatine metabolism by HIF is an endogenous mechanism of barrier regulation in colitis. *Proceedings of the National Academy of Sciences* **110**, 19820-19825
233. Chen, T., Zhou, Q., Tang, H., Bozkanat, M., Yuan, J. X. J., Raj, J. U., and Zhou, G. (2016) miR-17/20 Controls Prolyl Hydroxylase 2 (PHD2)/Hypoxia-Inducible Factor 1 (HIF1) to Regulate Pulmonary Artery Smooth Muscle Cell Proliferation. *Journal of the American Heart Association* **5**, e004510
234. Anavi, S., Hahn-Obercyger, M., Madar, Z., and Tirosh, O. (2014) Mechanism for HIF-1 activation by cholesterol under normoxia: a redox signaling pathway for liver damage. *Free Radical Biology and Medicine* **71**, 61-69

235. Mazzon, M., Peters, N. E., Loenarz, C., Krysztofinska, E. M., Ember, S. W., Ferguson, B. J., and Smith, G. L. (2013) A mechanism for induction of a hypoxic response by vaccinia virus. *Proceedings of the National Academy of Sciences* **110**, 12444-12449
236. Niecknig, H., Tug, S., Reyes, B. D., Kirsch, M., Fandrey, J., and Berchner-Pfannschmidt, U. (2012) Role of reactive oxygen species in the regulation of HIF-1 by prolyl hydroxylase 2 under mild hypoxia. *Free radical research* **46**, 705-717
237. Fong, G., and Takeda, K. (2008) Role and regulation of prolyl hydroxylase domain proteins. *Cell death and differentiation* **15**, 635
238. Salnikow, K., Donald, S. P., Bruick, R. K., Zhitkovich, A., Phang, J. M., and Kasprzak, K. S. (2004) Depletion of intracellular ascorbate by the carcinogenic metals nickel and cobalt results in the induction of hypoxic stress. *Journal of Biological Chemistry* **279**, 40337-40344
239. Aprelikova, O., Chandramouli, G. V., Wood, M., Vasselli, J. R., Riss, J., Maranchie, J. K., Linehan, W. M., and Barrett, J. C. (2004) Regulation of HIF prolyl hydroxylases by hypoxia-inducible factors. *Journal of cellular biochemistry* **92**, 491-501
240. Wang, M., Wang, Q., Peng, W.-J., Hu, J.-F., Wang, Z.-Y., Liu, H., and Huang, L.-N. (2017) Testin is a tumor suppressor in non-small cell lung cancer. *Oncology reports* **37**, 1027-1035
241. Liu, S., Fei, W., Shi, Q., Li, Q., Kuang, Y., Wang, C., He, C., and Hu, X. (2017) CHAC2, downregulated in gastric and colorectal cancers, acted as a tumor suppressor inducing apoptosis and autophagy through unfolded protein response. *Cell death & disease* **8**, e3009
242. Chaugule, V. K., and Walden, H. (2016) Specificity and disease in the ubiquitin system. *Biochemical Society Transactions* **44**, 212-227
243. Liang, Y., Hu, J., Li, J., Liu, Y., Yu, J., Zhuang, X., Mu, L., Kong, X., Hong, D., and Yang, Q. (2015) Epigenetic Activation of TWIST1 by MTDH Promotes Cancer Stem-like Cell Traits in Breast Cancer. *Cancer research* **75**, 3672-3680
244. Qi, J., Kim, H., Scortegagna, M., and Ze'ev, A. R. (2013) Regulators and effectors of Siah ubiquitin ligases. *Cell biochemistry and biophysics* **67**, 15-24
245. Yamaguchi, H., and Condeelis, J. (2007) Regulation of the actin cytoskeleton in cancer cell migration and invasion. *Biochimica et Biophysica Acta (BBA)-Molecular Cell Research* **1773**, 642-652
246. Bagnoli, F., Buti, L., Tompkins, L., Covacci, A., and Amieva, M. R. (2005) Helicobacter pylori CagA induces a transition from polarized to invasive phenotypes in MDCK cells. *Proceedings of the National Academy of Sciences of the United States of America* **102**, 16339-16344
247. Hu, X.-T., and He, C. (2013) Recent progress in the study of methylated tumor suppressor genes in gastric cancer. *Chinese journal of cancer* **32**, 31
248. Lopez-Serra, P., and Esteller, M. (2012) DNA methylation-associated silencing of tumor-suppressor microRNAs in cancer. *Oncogene* **31**, 1609
249. Tsang, Y. H. N., Lamb, A., and Chen, L. F. (2011) New insights into the inactivation of gastric tumor suppressor RUNX3: the role of H. pylori infection. *Journal of cellular biochemistry* **112**, 381-386
250. Roberti, A., Rizzolio, F., Lucchetti, C., de Leval, L., and Giordano, A. (2011) Ubiquitin-mediated protein degradation and methylation-induced gene silencing cooperate in the inactivation of the INK4/ARF locus in Burkitt lymphoma cell lines. *Cell Cycle* **10**, 127-134

251. Ozenne, P., Eymin, B., Brambilla, E., and Gazzeri, S. (2010) The ARF tumor suppressor: structure, functions and status in cancer. *International journal of cancer* **127**, 2239-2247
252. Zhao, Y., Shapiro, S. S., and Eto, M. (2015) F-actin clustering and cell dysmotility induced by the pathological W148R missense mutation of filamin B at the actin-binding domain. *American Journal of Physiology-Cell Physiology* **310**, C89-C98
253. Davis, J. R., Luchici, A., Mosis, F., Thackery, J., Salazar, J. A., Mao, Y., Dunn, G. A., Betz, T., Miodownik, M., and Stramer, B. M. (2015) Inter-cellular forces orchestrate contact inhibition of locomotion. *Cell* **161**, 361-373
254. Petrie, R. J., and Yamada, K. M. (2012) At the leading edge of three-dimensional cell migration. *J Cell Sci* **125**, 5917-5926
255. Fleischer, F., Ananthakrishnan, R., Eckel, S., Schmidt, H., Käs, J., Svitkina, T., Schmidt, V., and Beil, M. (2007) Actin network architecture and elasticity in lamellipodia of melanoma cells. *New Journal of Physics* **9**, 420
256. Leijnse, N., Oddershede, L. B., and Bendix, P. M. (2015) An updated look at actin dynamics in filopodia. *Cytoskeleton* **72**, 71-79
257. Dos Remedios, C., Chhabra, D., Kekic, M., Dedova, I., Tsubakihara, M., Berry, D., and Nosworthy, N. (2003) Actin binding proteins: regulation of cytoskeletal microfilaments. *Physiological reviews* **83**, 433-473
258. Cardiff, R. D., Miller, C. H., and Munn, R. J. (2014) Manual hematoxylin and eosin staining of mouse tissue sections. *Cold Spring Harbor protocols* **2014**, pdb. prot073411

APPENDIX I

PRIMARY ANTIBODIES USED

Antibodies	Dilution	Catalogue	Company
ac-K129Siah2 (CUSTOMIZED)	1:250 (WB), 1:50 (IF)	#ac-KLS	Bioklone Biotech, Chennai, India
ac-K139Siah2 (CUSTOMIZED)	1:250 (WB), 1:50 (IF)	#ac-KYS	Bioklone Biotech, Chennai, India
EGLN3/PHD3	1:1000 (WB), 1:50 (IF)	#NB100- 139SS	Novus Biologicals, CO, USA
GAL-4	1:500 (WB), 1:50 (IF)	#sc-19286	Santa Cruz Biotechnology, CA, USA
GAPDH	1:500 (WB)	#10100-11	Abgenex, Odisha, India
FLN-A	1:500 (WB), 1:50 (IF)	#sc-7565	Santa Cruz Biotechnology, CA, USA
FLN-C	1:500 (WB), 1:50 (IF)	#sc-48495	Santa Cruz Biotechnology, CA, USA
Hif1 α	1:2000 (WB), 1:50 (IF)	#ab1066	Abcam, MD, USA
KAT3B/p300	1:1000 (WB), 1:50 (IF)	#ab3164	Abcam, MD, USA
Pan-ac lysine	1:1000 (WB), 1:300 (IP)	#9441	Cell Signaling Technology, MA, USA
Siah1	1:1000 (WB), 1:50 (IF)	#NB300-974	Novus Biologicals, CO, USA
Siah2	1:500 (WB), 1:100 (IP)	#sc-5507	Santa Cruz Biotechnology, CA, USA
Siah2	1:50 (IF)	#ab208642	Abcam, MD, USA
TES	1:500 (WB), 1:50 (IF)	#sc-34737	Santa Cruz Biotechnology, CA, USA
CagA	1:1000 (WB), 1:100 (IF)	#sc-28368	Santa Cruz Biotechnology, CA, USA

Normal goat IgG	1:2000 (IP)	#sc2028	Santa Cruz Biotechnology, CA, USA
Normal mouse IgG	1:2000 (IP)	#sc2025	Santa Cruz Biotechnology, CA, USA
Normal rabbit IgG	1:2000 (IP)	#sc2027	Santa Cruz Biotechnology, CA, USA

WB- western blotting, IP- Immunoprecipitation, IF- Immunofluorescence

APPENDIX II

SECONDARY ANTIBODIES USED (FOR WESTERN BLOTTING)

Antibodies	Conjugate	Dilution	Catalogue	Company
Anti-goat	HRP-conjugated IgG	1:3000	#ab6741	Abcam, MD, USA
Anti-mouse	HRP-conjugated IgG	1:2000	#7076S	Cell Signaling Technology, MA, USA
Anti-rabbit	HRP-conjugated IgG	1:2000	#7074S	Cell Signaling Technology, MA, USA

**SECONDARY ANTIBODIES USED (FOR IMMUNOFLUORESCENCE
MICROSCOPY)**

Antibodies	Conjugate	Dilution	Catalogue	Company
Anti-goat IgG (H+L)	Alexa flour 488	1:500	#A-11055	Thermo Fisher Scientific, Waltham, MA USA
Anti-goat IgG (H+L)	Alexa flour 594	1:500	#A-11058	Thermo Fisher Scientific, Waltham, MA USA
Anti-mouse IgG (H+L)	Alexa flour 488	1:500	#A-11001	Thermo Fisher Scientific, Waltham, MA USA
Anti-mouse IgG (H+L)	Alexa flour 594	1:500	#A-11005	Thermo Fisher Scientific, Waltham, MA USA
Anti-rabbit IgG (H+L)	Alexa flour 488	1:500	#A-21206	Thermo Fisher Scientific, Waltham, MA USA
Anti-rabbit IgG (H+L)	Alexa flour 594	1:500	#A-11012	Thermo Fisher Scientific, Waltham, MA USA
Phalloidin-FITC	FITC (488)	1:3000	#F432	Thermo Fisher Scientific, Waltham, MA USA
DAPI	Dye	1:2000	#D3571	Thermo Fisher Scientific, Waltham, MA USA

APPENDIX III

PLASMID CONSTRUCTS USED

Constructs	Description	Source
pcDNA3.1+	Empty vector construct	#28128, Addgene, MA, USA
<i>p300</i> WT	Wild type construct	Gastroenterology. 2009 June; 136(7): 2258–2269
<i>p300</i> ΔHAT	HAT region is deleted from WT <i>p300</i>	Gastroenterology. 2009 June; 136(7): 2258–2269
<i>siah2</i>	WT construct	#RG203802, Origene, Maryland, USA
<i>siah2</i> K13R	13th lysine (K) mutated to Arginine (R) in WT <i>siah2</i>	Generated from WT <i>siah2</i>
<i>siah2</i> K17R	17th lysine (K) mutated to Arginine (R) in WT <i>siah2</i>	Generated from WT <i>siah2</i>
<i>siah2</i> K107R	107th lysine (K) mutated to Arginine (R) in WT <i>siah2</i>	Generated from WT <i>siah2</i>
<i>siah2</i> K129R	129th lysine (K) mutated to Arginine (R) in WT <i>siah2</i>	Generated from WT <i>siah2</i>
<i>siah2</i> K139R	139th lysine (K) mutated to Arginine (R) in WT <i>siah2</i>	Generated from WT <i>siah2</i>

APPENDIX IV***siRNAs USED***

siRNA	Catalogue No.	Company
Control siRNA	#sc-37007	Santa Cruz Biotechnology, CA, USA
<i>siah2</i> siRNA	#SR-304370	Origene, Maryland, USA
<i>FLN-C</i> siRNA	#sc-60639	Santa Cruz Biotechnology, CA, USA
<i>TES</i> siRNA	#sc-45509	Santa Cruz Biotechnology, CA, USA

APPENDIX V***CONDITIONS USED FOR SIAH2 SITE-DIRECTED MUTAGENESIS***

Phase	Temperature	Time	Cycle
Initial denaturation	95 °C	1 min	--
Final denaturation	95 °C	1 min	30 cycles
Annealing	55 °C	1 min	
Extension	65 °C	13 min	
Final extension	65 °C	13 min	--
Hold	4 °C	∞	--

APPENDIX VI

PRIMERS USED FOR SIAH2 SITE-DIRECTED MUTAGENESIS

Primer	Sequence
K13R mutation	5'-CGGCCCCAGCGCTAATAGACCCTGCAGCAAGCAGC-3'
K17R mutation	5'-AATAGACCCTGCAGCAGGCAGCCGCCGCCGCAG-3'
K107R mutation	5'-AACCAATGCCGCCAGAGGTTGAGCTGCTGCCCG-3'
K129R mutation	5'-AACCTGGCTATGGAGAGGGTGGCCTCGGCAGTC-3'
K139R mutation	5'-GTCCTGTTTCCCTGTAGGTATGCCACCACGGGC-3'

AGA/ AGG- Arginine (R)-specific codons.

APPENDIX VII

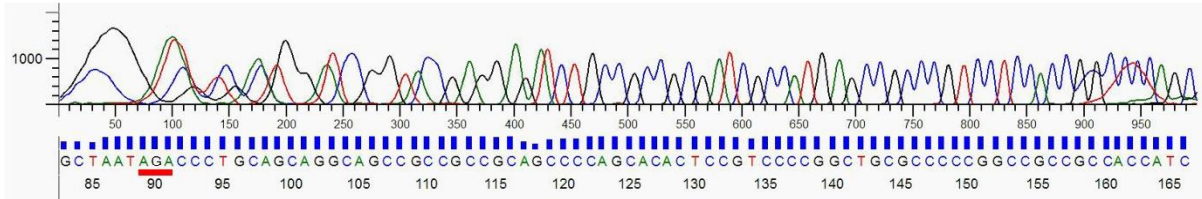
PRIMERS USED FOR SIAH2 SITE-DIRECTED MUTAGENESIS SEQUENCING

Primer	Sequence
T7 promoter-specific primer	5'-TAATACGACTCACTATAGGG-3'

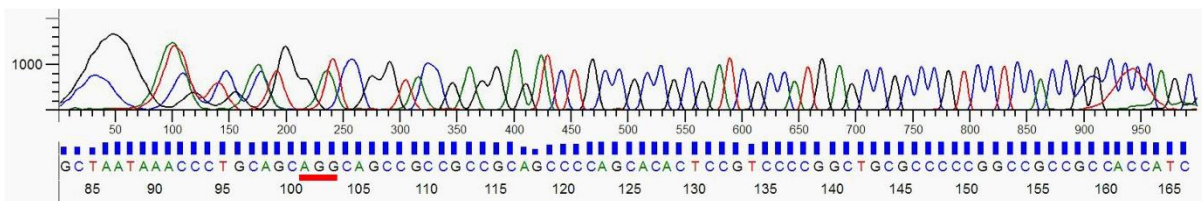
APPENDIX VIII

SIAH2 SITE-DIRECTED MUTAGENESIS SEQUENCING RESULTS

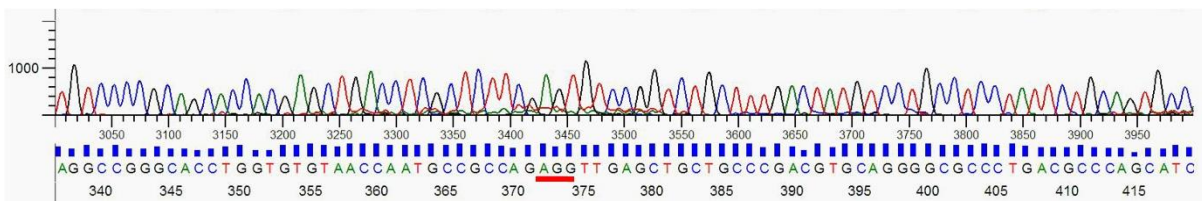
1. K13R mutation



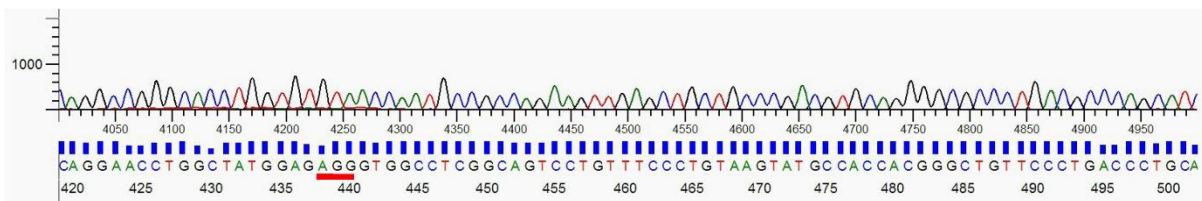
2. K17R mutation



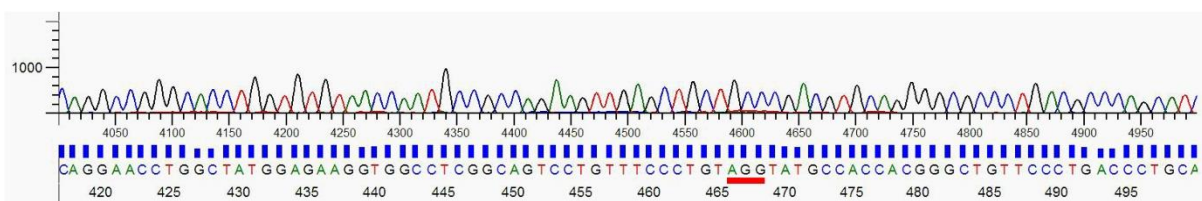
3. K107R mutation



4. K129R mutation



5. K139R mutation



APPENDIX IX

PEPTIDES USED FOR CUSTOMIZED ANTIBODY GENERATION

Primer	Sequence
ac-K ¹²⁹ Siah2	KLSCCPTCRGALTPSIRNLAMEK (acetylated)
ac-K ¹³⁹ Siah2	(acetylated) KYATTGCSLTLHHTEKPEHEDI

ORIGINAL ARTICLE

Membrane-bound β -catenin degradation is enhanced by ETS2-mediated Siah1 induction in *Helicobacter pylori*-infected gastric cancer cells

L Das^{1,5}, SB Kokate^{1,5}, P Dixit¹, S Rath¹, N Rout², SP Singh³, SE Crowe⁴ and A Bhattacharyya¹

β -catenin has two different cellular functions: intercellular adhesion and transcriptional activity. The E3 ubiquitin ligase Siah1 causes ubiquitin-mediated degradation of the cytosolic β -catenin and therefore, impairs nuclear translocation and oncogenic function of β -catenin. However, the effect of Siah1 on the cell membrane bound β -catenin has not been studied. In this study, we identified that the carcinogenic bacterium *H. pylori* increased ETS2 transcription factor-mediated Siah1 protein expression in gastric cancer cells (GCCs) MKN45, AGS and Kato III. Siah1 protein level was also noticeably higher in gastric adenocarcinoma biopsy samples as compared to non-cancerous gastric epithelia. Siah1 knockdown significantly decreased invasiveness and migration of *H. pylori*-infected GCCs. Although, Siah1 could not increase degradation of the cytosolic β -catenin and its nuclear translocation, it enhanced degradation of the membrane-bound β -catenin in the infected GCCs. This loss of membrane-bound pool of β -catenin was not associated with the proteasomal degradation of E-cadherin. Thus, this work delineated the role of Siah1 in increasing invasiveness of *H. pylori*-infected GCCs.

Oncogenesis (2017) 6, e327; doi:10.1038/oncsis.2017.26; published online 8 May 2017

INTRODUCTION

Siah family of E3 ubiquitin ligases are involved in the proteasome-dependent degradation of target proteins. These proteins modulate several cellular functions including angiogenesis, inflammation, cell proliferation, cell migration and apoptosis.^{1–5} Humans have *siah1*, *siah2* and *siah3* genes whereas, mice have *siah1a*, *siah1b* and *siah2* genes.^{6,7} Animal model-based studies support oncogenic functions of both Siah1 and Siah2 while tumor-promoting roles of Siah2 and apoptosis-inducing role of Siah1 are mostly reported from cell line-based assays.⁸

Siah1 is involved in the p53-mediated degradation of the oncogene β -catenin in the cytosol.^{9–11} β -catenin is involved in the cell–cell adhesion, as well as Wnt-signaling in epithelial cells.^{12,13} Two separate pools of β -catenin maintain these two very different functions—a nonmembranous cytoplasmic-nuclear pool and a cell membrane pool bound with E-cadherin.¹⁴ In the absence of Wnt-signaling, the cytoplasmic β -catenin is degraded by the ubiquitin-proteasomal degradation pathway. This results in the accumulation and translocation of β -catenin to the nucleus and causes transcriptional activation of its target genes.¹⁵

Siah1-mediated degradation of cytoplasmic β -catenin is a phosphorylation-independent mechanism. While several studies reported about proteasomal degradation of β -catenin in the cytosolic compartment, very little is known about its proteasomal degradation in the cell membrane adherens junction. However, this is clear that cell membrane-bound β -catenin degradation is associated with the loosening of the cell–cell attachment. The E3 ubiquitin ligase Hakai ubiquitinates cell membrane-bound

E-cadherin and β -catenin leading to the internalization of the E-cadherin complex and enhanced epithelial cell migration.^{16,17} What happens to the cadherin-bound β -catenin after the complex is dissociated from the adherens junction is not clearly known but it is considered to be either degraded or recycled.¹⁸ Another E3 ubiquitin ligase, Ozz-E3, ubiquitinates β -catenin and causes its proteasomal degradation.¹⁹ Since there is only one report of a rare inactivating mutation of *siah1* in gastric cancer²⁰ and none in any other cancers,²¹ the cellular function of Siah1 in regulating gastric cancer possibly is not limited to its tumor-suppressive role. This notion is further supported by animal studies, which have shown Siah1 as a tumor-promoter.⁸

We sought to investigate the effect of *H. pylori* infection on the expression and activity of Siah1 protein in the infected gastric cancer cells (GCCs). Our findings reveal a novel mechanism of *H. pylori* pathogenesis wherein *H. pylori*-mediated upregulation of ETS2 induces *siah1* transcription. We observe that Siah1 causes membrane-bound β -catenin degradation and induces invasiveness and migration of infected GCCs.

RESULTS

Siah1 mRNA and protein levels in *H. pylori*-infected human GCCs To study the Siah1 protein level in *H. pylori*-infected gastric cancer cells (GCCs), MKN45 cells were infected with a cytotoxin-associated gene pathogenicity island-positive {*cag* PAI(+)} *H. pylori* strain 26695 at a multiplicity of infection (MOI) 100 and 200 for 3 h and 6 h. Western blot analysis revealed that although MOI 100 at

¹School of Biological Sciences, National Institute of Science Education and Research (NISER) Bhubaneswar, Jatni, Odisha, India; ²Department of Oncopathology, Acharya Harihar Regional Cancer Centre, Cuttack, Odisha, India; ³Department of Gastroenterology, SCB Medical College, Cuttack, Odisha, India and ⁴School of Medicine, Division of Gastroenterology, UC San Diego, California, USA. Correspondence: Dr A Bhattacharyya, School of Biological Sciences, National Institute of Science Education and Research (NISER) Bhubaneswar, HBNI, P.O. Bhubaneswar-Padanpur, Via Jatni, Dist. Khurda, Jatni, Odisha 752050, India.

E-mail: asima@niser.ac.in

⁵These authors contributed equally to this work.

Received 17 October 2016; revised 16 February 2017; accepted 20 March 2017

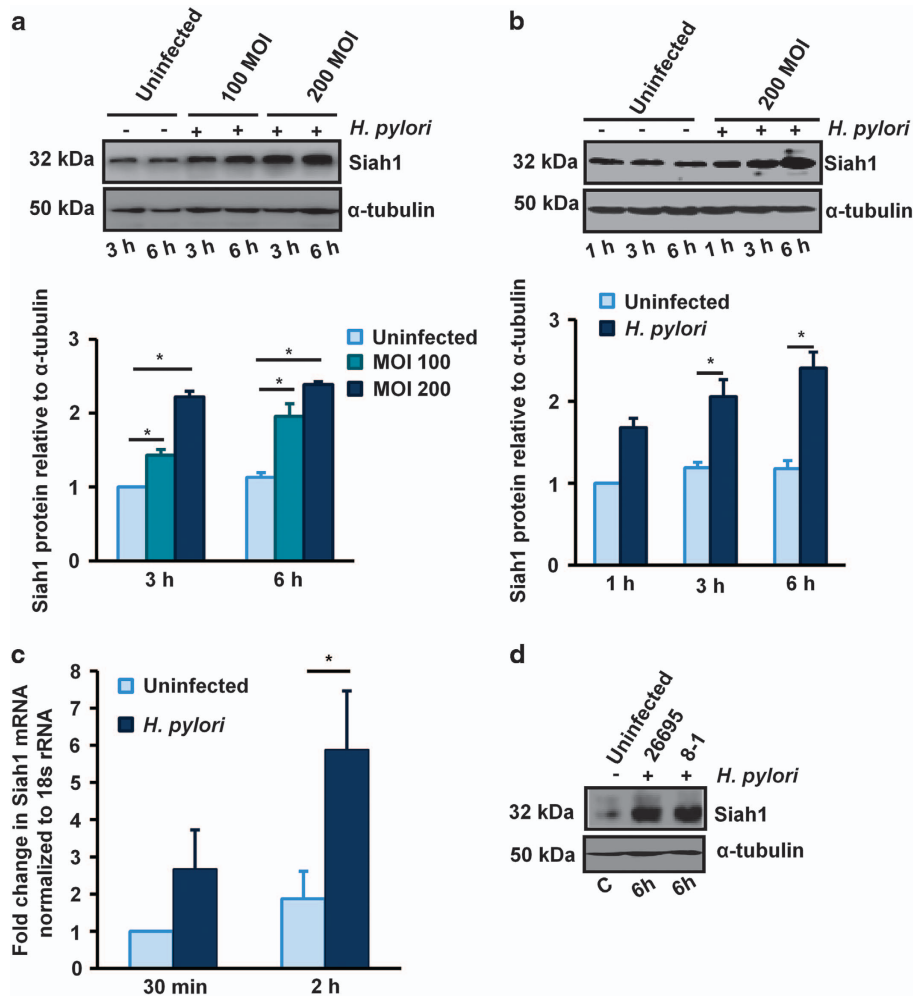


Figure 1. *H. pylori* enhance Siah1 expression in GCCs. (a) Western blotting of whole cell lysates from uninfected and *H. pylori*-infected (3 h and 6 h with MOI 100 and 200) MKN45 cells show increased Siah1 protein levels in infected cell lysates. α -tubulin is the loading control. (b) Time kinetics of Siah1 protein induction (1–6 h) in *H. pylori*-infected MKN45 cells. (c) Real time RT-PCR shows increased Siah1 mRNA expression in *H. pylori*-infected MKN45 cells. Bars shown in panels A–C represent normalized data (mean \pm s.e.m., $n = 3$), $*P < 0.05$. (d) Western blot results of showing Siah1 protein levels from cell lysates isolated from uninfected and *H. pylori*-infected MKN45 cells. Two different strains of *H. pylori* compared are *cag* PAI(+) strain 26695 and *cag* PAI(-) strain 8-1.

6 h post infection (p.i) and MOI 200 at both 3 h and 6 h significantly induced Siah1 protein, MOI 200 at 6 h was maximally effective (Figure 1a). To identify the optimal time for Siah1 protein induction with 200 MOI of *H. pylori* infection, MKN45 cells were infected for 1 h, 3 h and 6 h. Representative western blot results ($n = 3$) showed that 6 h was the optimal time required for Siah1 protein induction (Figure 1b). To assess the effect of *H. pylori* infection on Siah1 transcription, MKN45 cells were infected with MOI 200 of *H. pylori*. The real-time RT-PCR data ($n = 3$) confirmed that Siah1 messenger RNA (mRNA) was significantly ($*P < 0.05$) enhanced after 2 h p.i. as compared to the uninfected control (Figure 1c). Comparison of the *cag* PAI(+) strain with an isogenic *cag* PAI(-) mutant strain 8-1 revealed that Siah1 protein induction was a *cag* PAI-independent event (Figure 1d). So, all future experiments used only strain 26695, unless specified differently.

ETS2 binds with *siah1* 5' UTR and enhances Siah1 transcription in the *H. pylori*-infected GCCs

To identify the transcription factor responsible for Siah1 upregulation in the *H. pylori*-infected human GCCs, *siah1* promoter and 5' UTR analysis was done using the Genomatix Suite of sequence analysis tool MatInspector (professional version 6.2.2). We identified

the presence of an E26 transformation-specific (ETS) binding site (EBS) in the *siah1* 5' UTR (core element GGAA located between +92 and +95, GenBank: AJ400626.1)²² (Figure 2a).

In vitro binding assay was performed to study ETS2 binding with the EBS of the 5' UTR of *siah1* in uninfected and infected MKN45 cells. WT and EBS-mut oligonucleotides were 5' biotinylated (Supplementary Figure 1). Nuclear extracts prepared from uninfected or 3 h *H. pylori*-infected MKN45 cells were incubated with biotinylated-oligonucleotides coated over magnetic beads. Western blots of bead-bound proteins showed ETS2 binding with the *siah1* promoter EBS only in the infected cells (Figure 2b). Western blot of input nuclear lysates showed ETS2 protein level in the nuclear fraction. HDAC1 was used as a nuclear loading control. *In vivo* binding of ETS2 with *siah1* EBS was further confirmed by chromatin immunoprecipitation (ChIP) assay. Uninfected and *H. pylori*-infected MKN45 cells were immunoprecipitated using ETS2 specific antibody. PCR products obtained from the immunocomplex represented the *siah1* promoter and 5' UTR flanking the EBS (S=specific PCR product). PCR product was not obtained from the 5' far upstream sequence (NS=non-specific PCR product) (Figure 2c).

Next, dual luciferase assays were performed to study the effect of ETS2 on *siah1* transactivation. WT or EBS-Mut *siah1* reporter constructs were co-transfected with *Renilla* luciferase construct

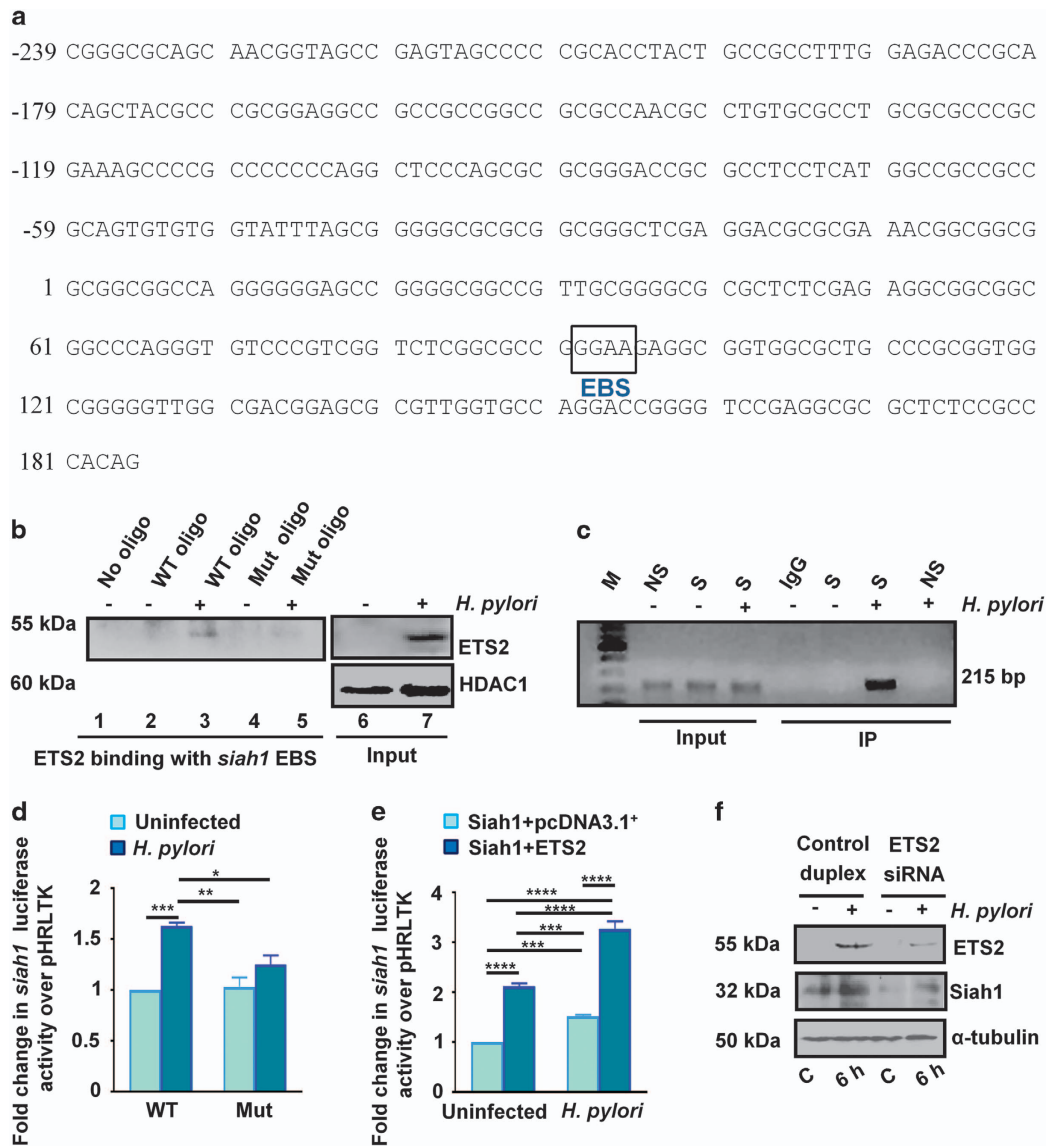


Figure 2. ETS2 binds to EBS in the 5' UTR and induces *siah1* transcription and protein expression in the *H. pylori*-infected GCCs. (a) Promoter and 5' UTR analysis of human *siah1* gene shows that an EBS located between +92 and +95 (represented by a box). We assume that the most upstream exon 1 of the Siah1 cDNA is at position +1²². (b) Western blot results showing the status of ETS2 binding with the *siah1* 5' UTR ($n = 3$) in the presence or absence of *H. pylori*. ETS2 binds to the WT EBS only but not with the EBS-Mut oligo. Western blot of nuclear lysates shows the levels of ETS2 protein expression in the input lanes. HDAC1 is the loading control for nuclear lysates. (c) ChIP assay of ETS2 immunocomplex for *siah1* EBS. IgG = immunoglobulin G; M = MW marker; NS = non-specific primer, S = specific primer. (d) Figure shows dual luciferase assay involving WT and ETS2-Mut *siah1* 5' UTR-transfected and uninfected or uninfected MKN45 cells. Data are analyzed by two-way ANOVA with Tukey's post hoc test ($n = 3$). Error Bars, s.e.m. **** $P < 0.001$, ** $P < 0.01$, * $P < 0.05$. (e) Bar graph of dual luciferase assay result showing transcriptional activation of WT *siah1* 5' UTR with ectopic ETS2 expression and *H. pylori* infection. Data are analyzed by two-way ANOVA with Tukey's post hoc test. Error bars, s.e.m. **** $P < 0.003$; **** $P < 0.0001$. (f) Transient transfection of ETS2 siRNA followed by western blotting shows Siah1 suppression in the ETS2-suppressed MKN45 cells.

phRLTK in MKN45 cells followed by infection with *H. pylori* for 1 h. Data confirmed that *H. pylori* significantly increased *siah1* transactivation in the WT *siah1* EBS-expressing cells as compared to the mut EBS-expressing cells (Figure 2d). Reduced *siah1* transactivation in EBS-mut *H. pylori*-infected MKN45 cells compared with WT EBS-expressing *H. pylori*-infected cells further confirmed the positive effect of ETS2 on *siah1* transcription in *H. pylori*-infected GCCs. Further, dual luciferase assay was performed with co-transfection of empty vector or ETS2 overexpression plasmid along with the WT *siah1* promoter construct and the *Renilla* luciferase construct pRLTK followed by infection for 1 h. Results (Figure 2e) confirmed that ETS2 could significantly enhance *H. pylori*-mediated *siah1* transcription.

To find out the role of ETS2 knockdown on Siah1 protein level, we transfected MKN45 cells with siETS2 or control duplex and infected with *H. pylori* or left uninfected. A noticeable decrease in *H. pylori*-induced Siah1 protein level was observed in ETS2-suppressed cells after *H. pylori* infection as compared to the control duplex-transfected cells. This confirmed the role of ETS2 in inducing Siah1 protein during *H. pylori* infection (Figure 2f).

ETS transcription factors are crucial for cancer progression.²³ We also studied the status of ETS2 along with Siah1 proteins after infection with 100 and 200 MOI at 3 and 6 h. *H. pylori* MOI and time-dependently increased ETS2 as well as Siah1 proteins in MKN45 cells and 200 MOI was optimal (Figure 3a). To find out the expression of Siah1 and ETS2 at 200 MOI, MKN45 cells were

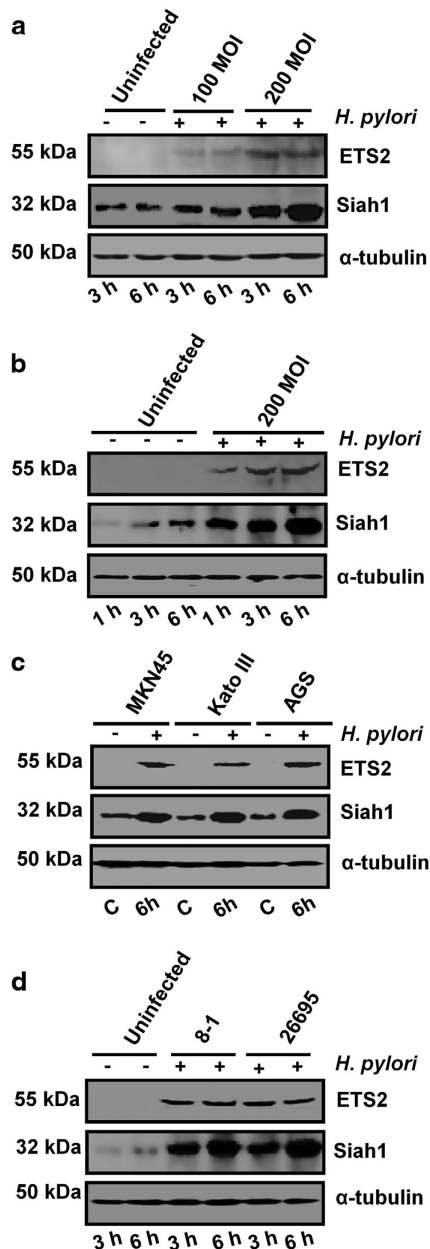


Figure 3. Parallel ETS2 and Siah1 induction occurs in *H. pylori*-infected GCCs, as well as in human gastric adenocarcinoma biopsy samples. (a) A representative western blot ($n=3$) showing optimal induction of ETS2 and Siah1 by 200 MOI of *H. pylori* at 3 h and 6 h p.i. (b) Cells infected for various time periods are analyzed for ETS2 and Siah1 protein expression ($n=3$). (c) Western blot ($n=4$) showing ETS2 and Siah1 proteins in uninfected and *H. pylori*-infected Kato III, MKN45 and AGS cells. (d) Western blot results ($n=3$) depicting equal effectiveness of 8-1 and 26695 in inducing ETS2 and Siah1 proteins. Graphical representations of panels A–D are shown in Supplementary Figure 2.

infected for 1, 3 and 6 h. Although ETS2 and Siah1 expressed from 1 h p.i., 3 and 6 h infection resulted in highly-induced expression of both of these proteins (Figure 3b). Like MKN45, other GCCs, that is, Kato III and AGS also showed ETS2 and Siah1 expression at 6 h of infection with MOI 200 (Figure 3c). Siah1 was earlier reported to be activated by p53.^{9,22,24} As Kato III cells are p53-null cells, our data confirmed that Siah1 expression in *H. pylori*-infected GCCs was p53-independent. In addition, 26695 and 8-1 strains equally induced ETS2 and Siah1 proteins in MKN45 cells

(Figure 3d) suggesting of *cag* PAI-independent regulation of Siah1. Figures 3a–d are graphically presented in Supplementary Figure 2.

Helicobacter-infected human and mouse gastric epithelia show enhanced expression of ETS2 and Siah1

ETS2 and Siah1 were assessed in gastric adenocarcinoma, antral biopsy samples (stage III, rapid urease test-positive) collected from consenting patients. H&E staining and fluorescence microscopy showed marked induction of ETS2 and Siah1 in adenocarcinoma samples ($n=10$) compared to non-cancer tissues ($n=10$) (Figure 4a). These data showed coexistence of ETS2 and Siah1 proteins in *H. pylori*-mediated gastric adenocarcinoma.

C57BL/6 mice were infected with *H. felis* as this model represents the classical cascade of *H. pylori*-driven carcinomatous changes observed in humans.²⁵ Eight months p.i. all infected mice showed precancerous lesions represented by marked mucous-gland metaplasia, enhanced ETS2 and Siah1 expression ($n=16$) as compared to the uninfected tissues ($n=16$) (Figures 4b and c).

Siah1 enhances loss of membrane-bound β -catenin in the *H. pylori*-infected GCCs

Siah1 was previously reported to induce apoptosis and cell-cycle arrest by degradation of cytosolic β -catenin.^{9,10} Siah1 enhanced β -catenin degradation in the cytosolic compartment of hepatocytes and thereby reduced its nuclear localization and effectiveness as an oncogenic factor.²⁶ The same study, however, showed that the membrane-bound β -catenin was not affected by Siah1. Siah1 was also reported to degrade cytosolic β -catenin in the cervical epithelial cancer cells.²⁷ To find out the effect of *H. pylori* infection on β -catenin, we performed western blot of whole cell lysates prepared from *H. pylori*-infected (6, 14 and 20 h) or uninfected MKN45 cells. Data indicated that although Siah1 was significantly ($*P < 0.05$) induced by *H. pylori*, β -catenin level in the whole cell lysate did not change with *H. pylori* infection (Figure 5a). We next assessed the membrane-enriched, cytoplasmic and nuclear-fraction-enriched lysates by western blotting. Pan-cadherin, α -tubulin and histone-deacetylase 1 (HDAC1) served as loading controls for the membrane fractions, cytoplasmic fractions and nuclear fractions, respectively. Membranous β -catenin was significantly ($*P < 0.05$) downregulated only after 20 h of *H. pylori* infection (Figure 5b). However, no change in membrane-bound Siah1 was noted following *H. pylori* infection. Surprisingly, cytoplasmic fractions which showed significantly high ($*P < 0.05$) Siah1 protein levels after *H. pylori* infection at all time points, did not demonstrate any loss of β -catenin in infected cells. P.i., nuclear fractions also showed a time-dependent significant ($*P < 0.05$) increase in Siah1 but unchanged β -catenin protein level. Confocal microscopy performed on MKN45 cells further confirmed that expression of only the membrane-bound β -catenin was highly reduced 20 h p.i. (Figure 5c). To find out whether membrane β -catenin loss was a proteasome-dependent degradation process or not, we infected MKN45 cells with *H. pylori* in the presence or absence of 50 μ M MG132, a proteasome inhibitor. *H. pylori*-mediated downregulation of membrane-bound β -catenin was markedly rescued by MG132 treatment indicating that *H. pylori*-mediated membrane-bound β -catenin loss was due to proteasomal degradation (Figure 5d).

To assess the effect of *siah1* and *ETS2* on membrane β -catenin level, we performed a few assays. Siah1-overexpressed MKN45 cells showed no change in β -catenin in whole cell lysates even after 20 h of *H. pylori* infection (Figure 6a). With Siah1 overexpression, however, β -catenin loss in the membrane was significantly enhanced (Figure 6b). siSiah1 transfection had no impact on the β -catenin level in whole cell lysates (Figure 6c). However, siSiah1 transfection significantly ($*P < 0.05$) blocked *H. pylori*-mediated membrane β -catenin degradation (Figure 6d).

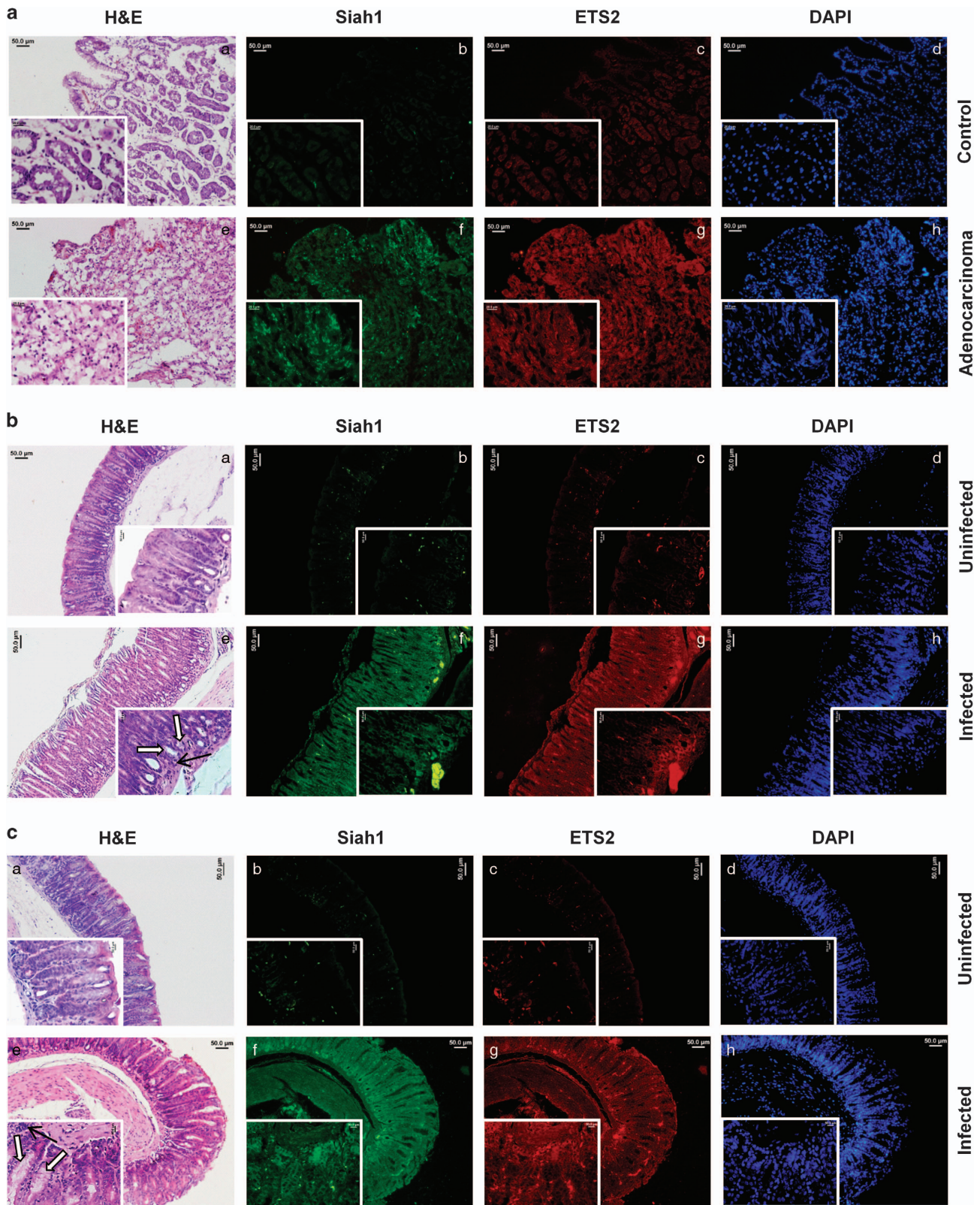


Figure 4. Induced ETS2 and Siah1 expression in *Helicobacter*-infected human and mouse gastric epithelia. (a) H&E staining of human non-cancer (a) and adenocarcinoma (e) biopsy samples ($n=10$ for each group) and fluorescence microscopy of the staining for Siah1 (b and f), ETS2 (c and g) and DAPI (d and h). Original magnification $\times 100$, inset $\times 400$. Scales shown $50\ \mu\text{m}$. Inset scale $20\ \mu\text{m}$. (b) H&E staining of uninfected ($n=16$) and infected ($n=16$) antral gastric tissues from C57BL/6 mice (a and e, respectively) and their corresponding fluorescence microscopy images showing Siah1 (b and f), ETS2 (c and g) and DAPI (d and h) staining. Infected mice show inflammation (thin arrow), mucus gland metaplasia (open arrow) in the mucosa. (c) Data representing similar observations in another set of uninfected and infected mice gastric tissues. Original magnification $\times 100$, inset $\times 400$. Scales shown in **b** and **c**: $50\ \mu\text{m}$.

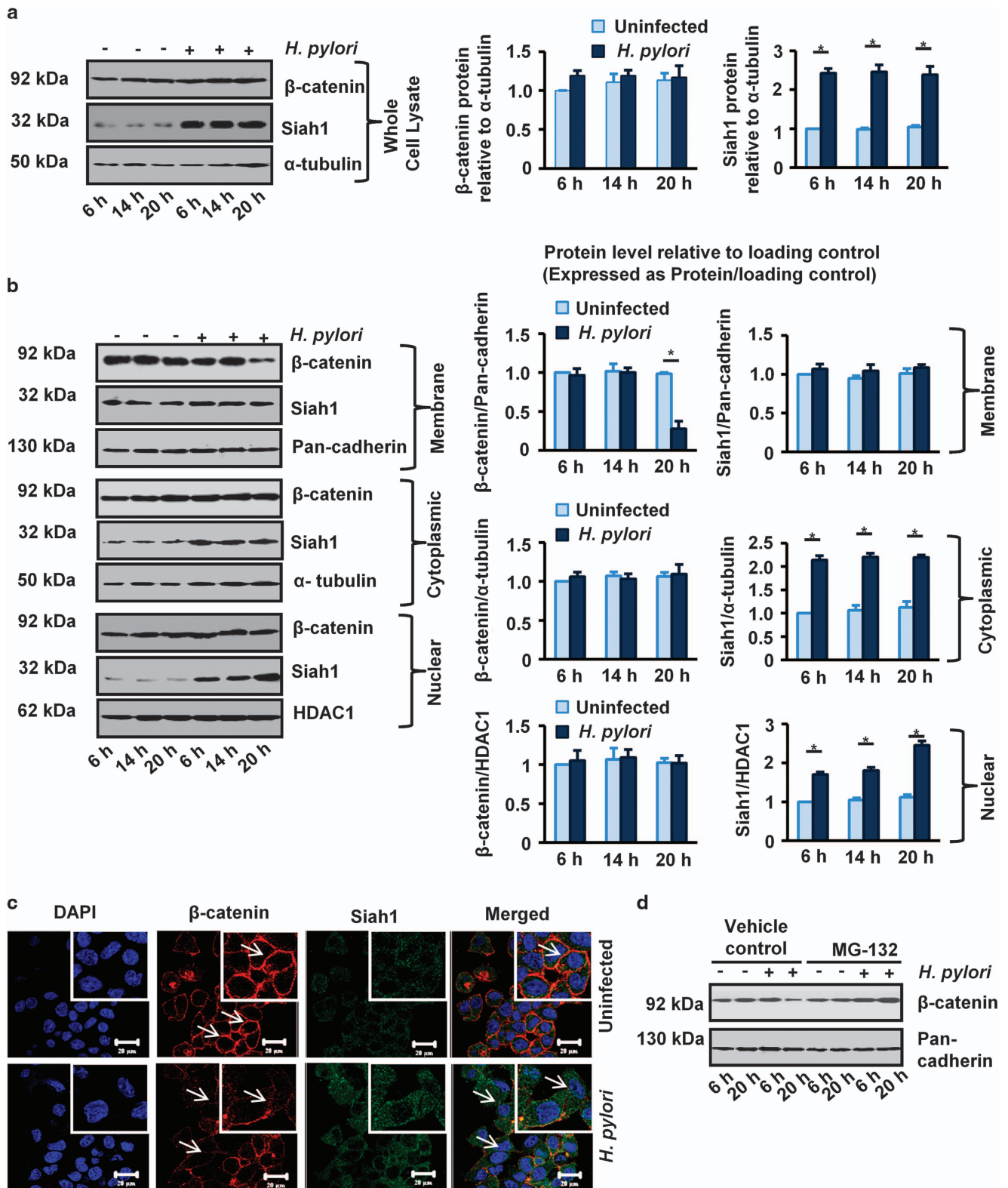


Figure 5. Membrane-bound β -catenin degradation in *H. pylori*-infected GCCs is proteasome-mediated. **(a)** Western blotting for Siah1 and β -catenin in uninfected and *H. pylori*-infected (6 h, 14 h and 20 h) MKN45 whole cell lysates ($n=3$). **(b)** Western blotting of membrane, cytoplasmic and nuclear fractions of uninfected or *H. pylori*-infected lysates for detection of Siah1 and β -catenin proteins ($n=3$). Pan-cadherin, α -tubulin and HDAC1 are used as respective loading controls. Bars depicting panels A–B represent normalized data (mean \pm s.e.m., $n=3$), $*P < 0.05$. **(c)** A representative confocal microscopy result ($n=3$) showing degradation of membrane-bound β -catenin in *H. pylori*-infected MKN45 cells. **(d)** Western blot ($n=3$) showing rescue of membrane-bound β -catenin from degradation by treatment with the proteasome inhibitor, MG132.

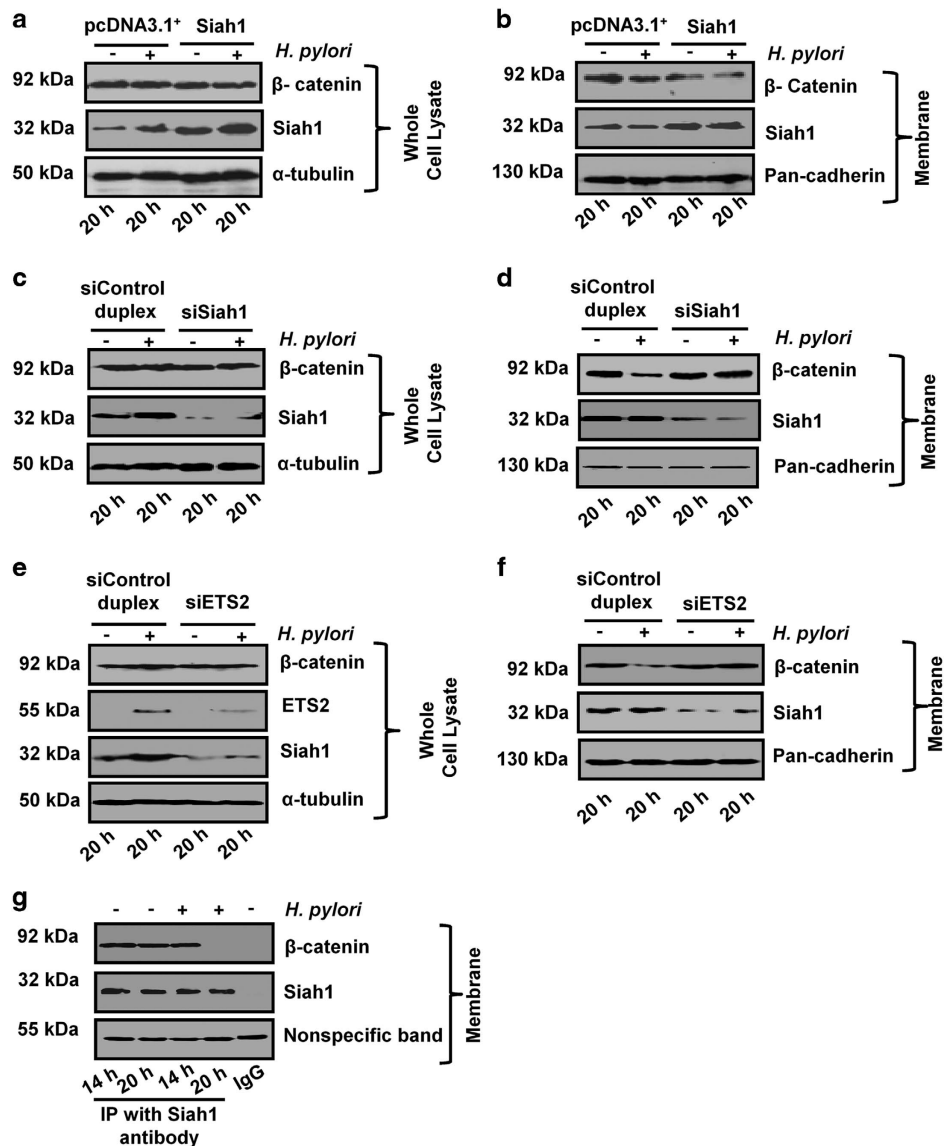


Figure 6. Siah1 promotes membrane-bound β -catenin degradation in *H. pylori*-infected GCCs. **(a)** Western blotting result ($n = 3$) of whole cell lysates prepared from Siah1 or empty vector (pcDNA3.1⁺)-transfected and *H. pylori*-infected or uninfected MKN45 cells. Blots are incubated with Siah1 and β -catenin primary antibodies. α -tubulin is the loading control. **(b)** Decreased membrane-bound β -catenin expression is detected by western blotting ($n = 3$) in Siah1-overexpressed and *H. pylori*-infected cells. **(c)** Western blotting result ($n = 3$) of whole cell lysates prepared from siSiah1 or siControl duplex-transfected and *H. pylori*-infected or uninfected MKN45 cells. Blots are incubated with Siah1 and β -catenin primary antibodies. α -tubulin is the loading control. **(d)** Decreased membrane-bound β -catenin expression is seen in Siah1-suppressed and *H. pylori*-infected cells. **(e)** Western blotting result ($n = 3$) of whole cell lysates prepared from siETS2 or siControl duplex-transfected and *H. pylori*-infected MKN45 cells. Blots are incubated with Siah1 and β -catenin primary antibodies. α -tubulin is the loading control. **(f)** Decreased membrane-bound β -catenin expression is detected in western blotting ($n = 3$) in ETS2-suppressed and *H. pylori*-infected cells. **(g)** Siah1 is immunoprecipitated with anti-Siah1 antibody from the membrane fraction and immunoblotted to detect β -catenin and Siah1 interaction. Non-specific band = immunoglobulin heavy chain. Graphical representations are shown in Supplementary Figure 3.

Next, we tried to assess the effect of *ETS2* knockdown on Siah1 protein. siETS2 significantly ($*P < 0.05$) reduced *ETS2*, as well as Siah1 protein levels in the whole cell lysates (Figure 6e). Post siETS2 transfection, cell membrane fractions showed significant reduction in membrane Siah1 level (Figure 6f). siETS2 could significantly ($*P < 0.05$) decrease *H. pylori*-driven membrane β -catenin degradation. Data shown in Figures 6a-f have been graphically presented in Supplementary Figure 3. Interaction of Siah1 with membrane-bound β -catenin was studied by immunoprecipitation assay of membrane-rich lysates. Result (Figure 6g) showed that although Siah1 interacted with β -catenin in uninfected or infected cells at 14 h and in uninfected cells at

20 h, β -catenin was completely lost in the immunoprecipitate only after 20 h of infection.

As both E-cadherin and β -catenin are degraded by E3 ubiquitin ligases¹⁶ and previous studies reported about loss of E-cadherin from the membrane in *H. pylori*-infected GCCs,^{28,29} we wanted to assess E-cadherin status in the membrane of Siah1-overexpressed cells in the presence or absence of *H. pylori*. For this, MKN45 cells were transfected with the empty vector (pcDNA3.1⁺) or Siah1 construct. Transfected cells were infected with *H. pylori* for 20 h in the presence or absence of either vehicle control or 50 μ M MG132. Data revealed that neither Siah1 overexpression nor *H. pylori* promoted membrane-bound E-cadherin loss in GCCs

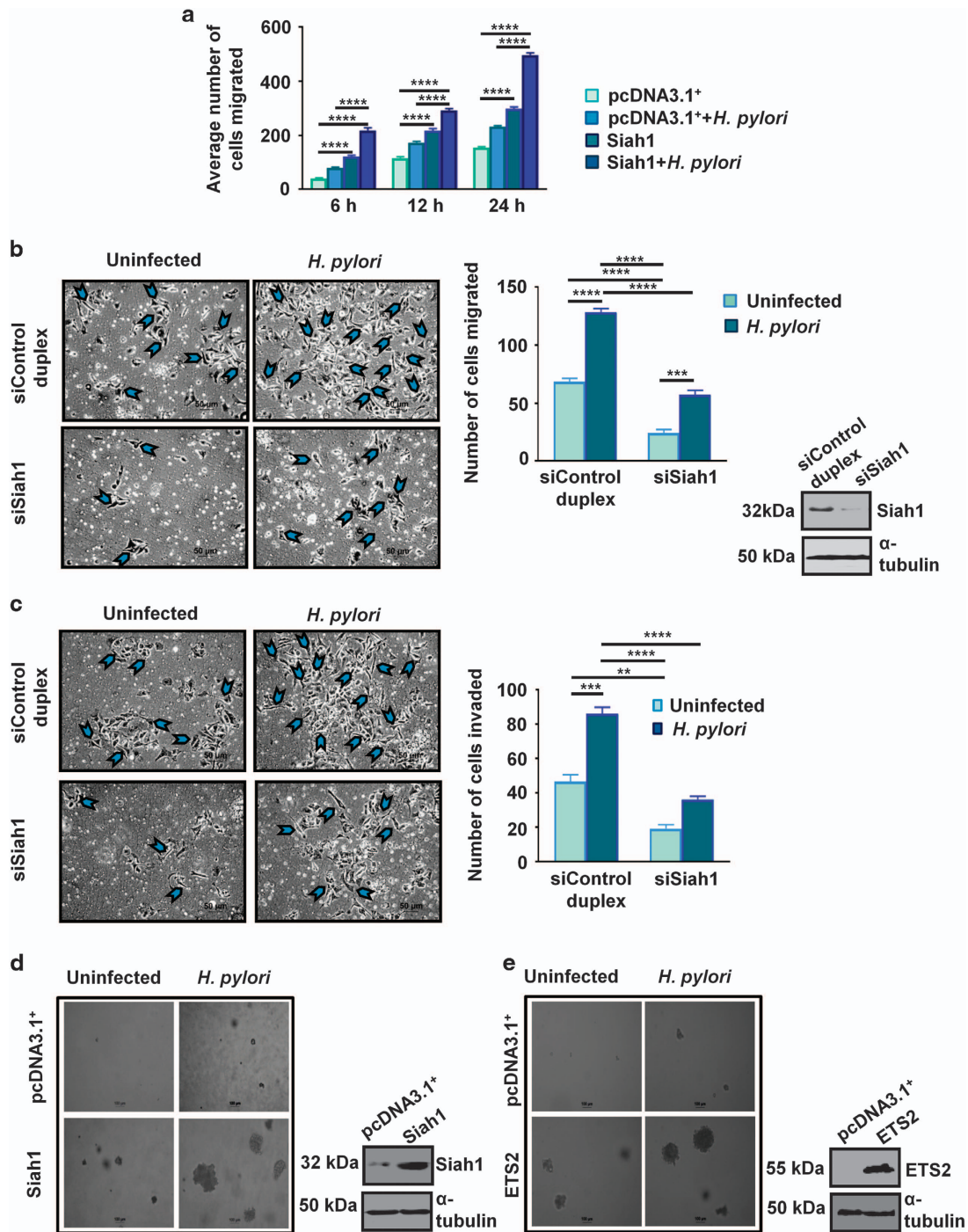


Figure 7. Siah1 increases the rate of cell migration in *H. pylori*-infected GCCs. **(a)** Graphical representations ($n=3$) of wound healing assay showing enhanced migration potential of Siah1-overexpressed and *H. pylori*-infected cells. 24 h post transfection, wound is marked and the scratched area is monitored from 6 h–24 h. Data have been analyzed by 2-way ANOVA with Tukey's post hoc test. Error bars, s.e.m. $****P < 0.0001$. **(b)** Cell migration assay performed in transwell chambers with AGS cells show decreased migration of infected cells expressing siSiah1 as compared to the siControl group. Arrowheads indicate migrated cells; scales shown: 50 μ m. Bar graphs denote the average number of migrated cells (mean \pm s.e.m., $n=3$). Data are analyzed by 2-way ANOVA with Tukey's post hoc test. Error bars, s.e.m. $***P < 0.003$; $****P < 0.0001$. Protein level of siSiah1 cells are shown in the accompanying western blot images. **(c)** Matrigel invasion assay with Siah1-suppressed AGS cells showing reduced invasiveness in *H. pylori*-infected GCCs. Bar graphs denote the average number of cells invaded through the Transwell matrigel ($n=3$). Arrowheads indicate invaded cells. Data are analyzed by two-way ANOVA with Tukey's post hoc test. Error bars, s.e.m. $**P < 0.01$; $***P < 0.003$; $****P < 0.0001$. Scales shown: 50 μ m. **(d)** Soft agar colony formation assay is performed on MKN45 cells. Siah1 stably-transfected cells show a substantial increase in colony forming ability post *H. pylori* infection as compared to cells expressing the empty vector. Siah1 level in Siah1-stable cells are shown in the accompanying western blot result. **(e)** Soft agar assay performed with uninfected or infected MKN45 cells that stably-express either ETS2 or empty vector show a substantial increase in colony forming ability of ETS2-expressing cells. Protein level of ETS2 stable cells are shown in the accompanying western blot images. Scales shown in **b** and **c**: 100 μ m.

(Supplementary Figure 4). Western blotting of the membrane-fraction showed E-cadherin expression under the above experimental conditions.

Siah1 promotes migration and invasiveness of *H. pylori*-infected GCCs

It is well established that loss of membrane-bound β -catenin enhances cancer invasiveness.^{30–32} Membrane-bound β -catenin loss is also frequent in metastatic gastric cancer cases.³³ As we found that Siah1 could increase membrane-bound β -catenin degradation and it is also well known that *H. pylori* induces invasiveness of infected cells,³⁴ we next wanted to assess the effect of Siah1 in increasing metastatic properties in GCCs. To evaluate the influence of Siah1 overexpression on the ability of migration of *H. pylori*-infected GCCs, we performed wound-healing assay. For this, the highly adherent gastric adenocarcinoma cell AGS was preferred over the partially adherent MKN45 cells (poorly-differentiated gastric adenocarcinoma cells) since MKN45 cells partly grow in clumps.³⁵ pcDNA3.1⁺ or Siah1 stably-expressing AGS cells were grown in monolayer, a wound was marked and cells were incubated in the presence or absence of *H. pylori* for various time periods. A significant time-dependent increase in cell migration was observed in Siah1-expressing *H. pylori*-infected AGS cells than empty-vector-expressing infected cells (Figure 7a). To further confirm the role of Siah1 in cell migration, Transwell migration assay was performed with Siah1-suppressed AGS cells. siSiah1-expressing cells showed significantly less *H. pylori*-induced cell migration (Figure 7b). Cell invasiveness was studied by Matrigel-invasion assay using exogenous siSiah1-expressing AGS cells. Significantly less ($*P < 0.05$) cell invasion was observed in siSiah1-expressing infected AGS cells as compared to control duplex-expressing infected AGS cells (Figure 7c). Western blot results alongside the Transwell migration assay data indicated status of siSiah1. Soft agar colony formation assay was performed to study anchorage-independent growth of *H. pylori*-infected cells. Both Siah1 or ETS2-expressing AGS cells showed markedly increased colony formation in soft agar plates as compared to empty vector-expressing *H. pylori*-infected cells (Figure 7d and e, respectively). Western blot results alongside the soft agar assay data indicated status of Siah1 and ETS2 proteins in the respective stable cells used for soft agar assays.

DISCUSSION

H. pylori colonization enhances inflammatory responses and neoplastic changes owing to the loss of the gastric epithelial cell barrier function. Loss of cell-to-cell adhesions takes place in the infected epithelium as disruption of the junctional cadherin-catenin complex occurs. Here, we report for the first time that ETS2 enhances *siah1* transcription in the *H. pylori*-infected GCCs. We prove that *H. pylori*-mediated Siah1 upregulation promotes invasiveness of *H. pylori*-infected GCCs by increasing degradation of the membrane-bound β -catenin. In addition, we also show that increased expression of Siah1 protein in *H. pylori*-infected GCCs does not cause E-cadherin loss from the cell membrane.

Cadherin-bound β -catenin is an integral component of the adherens junctions. An E3 ubiquitin ligase Hakai induces E-cadherin ubiquitination and internalization by endocytosis.¹⁶ Endocytosis possibly plays a role in releasing β -catenin from the internalized E-cadherin complex.³⁶ Otherwise, tyrosine phosphorylation of β -catenin can also disrupt the α -catenin-E-cadherin association.³⁷ It is believed that E-cadherin-bound β -catenin can accumulate at the perinuclear endocytic recycling compartment and translocate to the nucleus upon Wnt activation.³⁸ After internalization, Hakai-mediated E-cadherin ubiquitination redirects the latter from a recycling pathway to a lysosome-mediated degradation process.³⁹ Membrane-bound β -catenin is also

targeted for ubiquitin-mediated degradation by E3 ubiquitin ligases Hakai and Ozz.^{16,19} Other ubiquitin ligases such as MDM2 and K5, can also ubiquitinate and degrade E-cadherin.^{40,41} We show here that the E3 ubiquitin ligase Siah1 enhances degradation of the cell membrane-bound β -catenin in the *H. pylori*-infected GCCs which can be prevented by inhibiting proteasomal degradation.

This study reveals that Siah1 mediated membrane β -catenin degradation is independent of membrane E-cadherin status. Interestingly, *H. pylori* CagA can interact with E-cadherin and to disrupt the E-cadherin- β -catenin complex. Thereby, CagA increases cytoplasmic β -catenin degradation and its nuclear accumulation.⁴² In contrast to this, we notice no β -catenin loss in the cytosol and no nuclear β -catenin accumulation in MKN45 cells by the *cag* PAI(+) *H. pylori* strain. Our findings corroborate another report by Bebb *et al.* which shows that the reduction in membrane β -catenin occurs in *H. pylori*-infected cells without concomitant increase in its cytosolic and nuclear pool.⁴³ However, as only nonphosphorylated CagA interacts with E-cadherin^{42,44} while CagA gets phosphorylated in the infected host,^{45,46} cell disruption of E-cadherin- β -catenin interaction by CagA in our system is ruled out. We note that loss of membrane-bound β -catenin only takes place in *H. pylori*-infected GCCs but not in uninfected GCCs. This could be due to increased activity of Siah1 protein in *H. pylori*-infected GCCs. Research is currently underway in our laboratory to identify the possible role of posttranslational modification(s) in regulating Siah1 activity and whether that is restricted to the cell membrane.

Siah1-mediated cytosolic β -catenin degradation is thought to have an overall tumor-suppressive effect. We find that Siah1 protein is induced by ETS2 in *H. pylori*-infected GCCs but it does not cause any change in the cytosolic and nuclear pool of β -catenin. These observations are in complete contradiction with earlier findings which have shown that the cytosolic fraction of β -catenin is degraded by Siah1 and thus, Siah1 act as a tumor suppressor.^{9,10,47} As Siah1 can be upregulated in a p53-dependent manner,^{20,48,49} association of Siah1 with apoptosis is also widely accepted. Surprisingly, we find that the level of Siah1 protein in *H. pylori*-infected GCCs is not dependent on p53 as it is also induced in the p53-null Kato III cells. As basal expression of Siah1 is noticed in uninfected GCCs when ETS2 protein is not expressed, it is clear that p53 and ETS2-independent mechanisms of *siah1* transcription exist.

E3 ubiquitin ligases are involved in various cellular processes including cancer and inflammation.^{3,50} Recently we have shown that Siah2 was induced by ETS2 and Twist1 in *H. pylori*-infected GCCs.⁵¹ It is therefore evident from the current study that ETS2 can simultaneously induce both Siah1 and Siah2 proteins in *H. pylori*-infected GCCs. As Siah1 lacks Twist1-binding site, we speculate that these isotypes can still be differentially regulated since ETS2 and Twist1 expression might vary depending on the staging of gastric cancer. As we have not observed any role of Siah2 in membrane-bound β -catenin degradation in *H. pylori*-infected GCCs (unpublished data), target molecules of these Siah isotypes might very well be different. We believe that despite having a common transcription factor ETS2, Siah1 and Siah2 have unique roles in the cell and disease processes.

Since this work uncovers a new mechanism of *H. pylori*-induced degradation of cell membrane-associated β -catenin, we believe that Siah1 is a crucial factor regulating gastric cancer progression and metastasis. Stage-dependent variation in Siah1- β -catenin interaction might exist that can determine the course of treatment-outcome. For this, further studies with patient samples are required which will surely enrich our current knowledge of the molecular basis of *H. pylori*-mediated gastric cancer pathogenesis.

MATERIALS AND METHODS

Cells, plasmids, siRNAs and inhibitors

The human adenocarcinoma GCCs MKN45, Kato III, AGS were cultured and maintained, as described earlier.^{52,53} Full-length wild type (WT) human Siah1 cDNA was subcloned in HindIII/XhoI restriction sites of eukaryotic expression vector pcDNA3.1⁺ (Invitrogen, CA, USA). ETS2 construct (#28128) was procured from Addgene, MA, USA. The full length human *siah1* promoter was cloned into the pGL3 basic vector (Promega, WI, USA) using restriction sites KpnI and HindIII. The promoter construct *siah1* WT was used as a template to generate mutation at the ETS2-binding site (EBS) using Quik Change site-directed mutagenesis kit (Agilent Technologies, CA, USA). Constructs were confirmed by sequencing. Primer sequences are shown in Supplementary Figure 1. *siah1* were purchased from Santa Cruz Biotechnology, Texas, USA, whereas siETS2 was purchased from Origene, MD, USA. The proteasome inhibitor Z-Leu-Leu-Leu-al (MG132) was purchased from Sigma-Aldrich, WI, USA.

Bacterial infection, inhibitor treatment and human gastric mucosal biopsy specimen collection

H. pylori strains 26695, 8-1 and *H. felis* strain 49179 (#49179, ATCC, VA, USA) were cultured and maintained as reported previously.^{52,53} Unless otherwise specified, GCCs were infected with strain 26695 at 200 MOI for the indicated period. To study proteasome-mediated degradation, cells were co-treated with the proteasome inhibitor MG132 for 6 h at 50 μ M dose.

Endoscopic biopsy samples (from the antral region of the stomach) were collected from consenting patients who were suffering from stage III gastric adenocarcinoma following a National Institute of Science Education and Research (NISER) Review Board-approved protocol. Pathologically-confirmed gastric cancer cases with paired non-cancerous gastric tissues were included for the study. Patients with a history of previous *H. pylori* eradication therapy were excluded. The investigation was carried out in compliance with the Helsinki Declaration (2013) of the World Medical Association.

Transient transfection and generation of stable cells

To transiently express Siah1, 1×10^6 MKN45 cells were seeded in 6-well plates. On the next day, cells were transfected with 2.5 μ g of plasmid DNA, 5 μ l of P3000 reagent and 7.5 μ l of Lipofectamine3000 reagent (Invitrogen). After 36 h, cells were infected with *H. pylori*. To knockdown expression of ETS2 and *siah1*, 0.2×10^6 MKN45 cells were seeded in 6-well plates. On the next day, cells were transfected with 50 nM siRNA of ETS2 or Siah1 along with 10 μ l of Lipofectamine3000 reagent (Invitrogen). To generate stable cell lines, MKN45 or AGS cells were seeded in 96 well plates 18–24 h before transfection. Stable transfectants were established with G418 selection.

Real-time reverse transcription (RT)-PCR analysis

Total RNA was isolated from MKN45 cells after 30 min and 2 h of infection using an RNeasy kit (Qiagen, CA, USA). cDNA was synthesized and real-time RT-PCR was performed as described previously.⁵¹

In vitro binding assay

Nuclear lysates were incubated with 5' biotinylated double-stranded (ds) *siah1* EBS oligonucleotide (WT or Mut) coated on streptavidin-coated superparamagnetic beads (Dynabeads M-280 Streptavidin, Dynal, Invitrogen). Binding assays were performed as described previously.⁵¹ Oligos are shown in Supplementary Figure 1.

Chromatin immunoprecipitation (ChIP) assay

ChIP assay was performed using QuikChIP chromatin immunoprecipitation kit (Imgenex, CA, USA) according to the manufacturer's protocol.⁵¹ Chromatins were immunoprecipitated using ETS2 antibody (#22803, Santa Cruz Biotechnology, CA, USA). PCR amplification was performed to analyze the *in vivo* binding of ETS2 to *siah1* 5' UTR EBS. Primers used for ChIP assay are shown in Supplementary Figure 1.

Luciferase assay

Dual luciferase assays was performed to study activity of *siah1* promoter after *H. pylori* infection. Cells were co-transfected either with the WT or ETS2-Mut *siah1* luciferase constructs (cloned in pGL3 basic vector) and the

phRLTK *Renilla* luciferase constructs at a ratio of 50:1 using Lipofectamine 2000 reagent (Invitrogen). For another set of experiment, cells were co-transfected with WT *siah1* luciferase construct along with ETS2 overexpression plasmid and phRLTK *Renilla* luciferase construct at a ratio of 25:25:1 using Lipofectamine 2000 reagent (Invitrogen). At 36 h of transfection, uninfected or 2 h *H. pylori*-infected cells were lysed with passive lysis buffer (Promega) and analyzed for luciferase activity as described earlier.⁵¹

Immunoblotting and antibodies

Nuclear, cytoplasmic and membrane proteins were isolated from *H. pylori*-infected MKN45 cells using NE-PER Nuclear and Cytoplasmic Extraction Reagents (Pierce, Rockford, IL, USA). Around 2×10^6 MKN45 cells were seeded in 60 mm cell culture dish 24 h before infection. Postinfection, cytoplasmic and nuclear fractions were isolated as per manufacturer's instruction, whereas membrane proteins were isolated from the cytoplasmic extract after further centrifugation at 16000g for 45 min at 4 $^{\circ}$ C. Whole cell extracts were prepared from uninfected or *H. pylori*-infected GCCs. For immunoblotting, proteins were resolved on SDS-PAGE gel and blotted onto PVDF membranes. The following primary antibodies were used: Siah1 (1:250) (#300974, Novus Biologicals, CO, USA), ETS2 (1:1000) (#22803, Santa Cruz Biotechnology, CA, USA), E-cadherin (1:1000) (#3195, Cell Signalling Technology, MA, USA) and β -catenin (1:5000) (#32572, Abcam, MA, USA). α -tubulin (1:5000) (#52866, Abcam), histone-deacetylase 1 (HDAC1) (1:1000) (#2062, Cell Signalling Technology), Pan-cadherin (1:1000) (#4068, Cell Signalling Technology) antibodies were used for normalization of protein loading. Immunoreactive bands were detected as described earlier.⁵¹

Coimmunoprecipitation assay

For, coimmunoprecipitation assays, 5×10^6 MKN45 cells were seeded in 100 mm cell culture dish 24 h before infection. Membrane fractions were isolated and were incubated with Siah1 primary antibody (Novus) for overnight at 4 $^{\circ}$ C. The protein-antibody complex was pulled down using 50% A/G agarose followed by washing with ice-cold phosphate-buffered saline (PBS). Proteins were denatured by using Laemmli buffer (HiMedia, Mumbai, India) and analyzed by western blotting.

Cell migration and invasion assays

AGS cells were transfected with or control duplex RNA and siRNA of Siah1. Cell migration and invasion assay was performed following a previously-described protocol.⁵¹

Wound-healing assay

To study the effect of Siah1 on the wound-healing property of GCCs, adherent AGS cells were preferred than semi-adherent MKN45 cells. AGS cells stably-expressing *siah1* or pcDNA3.1⁺ were seeded and wound-healing assay was performed as described previously.⁵¹

Soft agar assay

Anchorage-independent growth was studied by performing soft-agar assay using the empty vector (pcDNA3.1⁺) or ETS2 or Siah1-expressing MKN45 stable cells following a previously-described method.⁵¹

H. felis infection in C57BL/6 mice

Four to five week-old both male and female C57BL/6 mice were procured from the National Centre for Laboratory Animal Sciences of the National Institute of Nutrition (Hyderabad, India). The study was performed after getting the institutional animal ethics committee (IAEC) approval provided by NISER (approval No SBS-AH/03/13/05). Male and female mice of 7–8 weeks of age were randomly and blindly divided into two groups- uninfected and infected (16 mice in each group) and infected with *H. felis* as mentioned earlier.²⁵ After 8 months of observation, mice were killed and the stomach was isolated from uninfected and infected animals. After fixation, antral sections (5 μ m) were either stained with H&E or processed for immunofluorescence microscopy as mentioned below.

Confocal and immunofluorescence microscopy and H&E staining MKN45 cells were seeded on glass coverslips 24 h before infection to study endogenous levels of various proteins. For transfection-based assays,

MKN45 cells were seeded on coverslips 24 h before transfection and were transfected using Lipofectamine3000 (Invitrogen). Nontransfected and transfected cells were either infected with *H. pylori* for 20 h or left uninfected followed by fixation and staining.⁵¹ Cells were incubated with Siah1 (1:100, #sc101252, Santa Cruz Biotechnology) or β -catenin (1:250, Abcam) or E-cadherin (1:100, Cell Signalling Technology) primary antibodies for overnight and images were taken using a confocal microscope.⁵¹

For immunostaining, 5 μ m thick gastric adenocarcinoma biopsy specimen were fixed as before.⁵¹ Fixed sections were incubated with primary antibodies against Siah1 (1:50, #ab49177, Abcam) or ETS2 (1:100, Santa Cruz Biotechnology) followed by incubation with secondary antibodies. Images were taken following a previously-described method.⁵¹ H&E staining was done following standard procedure.

Statistical analysis

In vitro experiments had a minimum of three independent experiments, each with three technical replicates. No statistical method was used to predetermine the sample size. Experiments were performed and analyzed in non-randomized and non-blinded fashion (except for animal studies). Statistical analysis of data was performed by Student's *t*-test for comparisons involving two groups. Values were given as mean \pm s.e.m. Statistical significance was determined at **P* < 0.05. Two-way ANOVA was performed to compare various transfection groups. Tukey's test was done for post hoc comparisons. There was no estimate of variation within each group.

ABBREVIATIONS

ChIP, Chromatin immunoprecipitation; *cag*, Cytotoxin-associated gene; DAPI, 4', 6-Diamidino-2-Phenylindole, Dilactate; EBS, E26 transformation-specific sequence 2-binding site; ETS2, E26 transformation-specific sequence 2; GCCs, Gastric cancer cells; H&E, Haematoxylin and eosin; HDAC1, Histone-deacetylase 1; *H. pylori*, *Helicobacter pylori*; MOI, Multiplicity of infection; MDM2, Mouse double minute 2 homolog; PAI, Pathogenicity island; PBS, Phosphate-buffered saline; PVDF, Polyvinylidene fluoride; Real-time RT-PCR, Real-time reverse transcription PCR; RING, Really interesting new gene; Siah, The seven in absentia homolog; SIP, Siah-interacting protein

CONFLICT OF INTEREST

The authors declare no conflict of interest.

ACKNOWLEDGEMENTS

This work was supported by two grants to A.B. (Sanction Nos BT/PR15092/GBD/27/311/2011, Department of Biotechnology, Govt. of India and SB/SO/BB-0015/2014, Science and Engineering Research Board, Govt. of India. S.R. is supported by an Indian Council of Medical Research (ICMR) fellowship; L.D., S.B.K and P.D. are supported by fellowships from Department of Atomic Energy (DAE), Govt. of India.

AUTHOR CONTRIBUTIONS

LD performed experiments and analyzed results; SBK generated stable cell lines; SBK and PD generated histology data, SBK, SR and PD performed a few important assays; NR and SPS helped with gastric cancer biopsy collection and analysis; SEC gave reagents and comments; AB conceived the work, designed experiments, analyzed the data, supervised the work and wrote the paper.

REFERENCES

- Wong CS, Sceneay J, House CM, Halse HM, Liu MC, George J *et al*. Vascular normalization by loss of Siah2 results in increased chemotherapeutic efficacy. *Cancer Res* 2012; **72**: 1694–1704.
- House CM, Moller A, Bowtell DD. Siah proteins: novel drug targets in the Ras and hypoxia pathways. *Cancer Res* 2009; **69**: 8835–8838.
- Brauckhoff A, Malz M, Tschaharganeh D, Malek N, Weber A, Riener MO *et al*. Nuclear expression of the ubiquitin ligase seven in absentia homolog (SIAH)-1 induces proliferation and migration of liver cancer cells. *J Hepatol* 2011; **55**: 1049–1057.

- Nagano Y, Fukushima T, Okemoto K, Tanaka K, Bowtell DD, Ronai Z *et al*. Siah1/SIP regulates p27(kip1) stability and cell migration under metabolic stress. *Cell Cycle* 2011; **10**: 2592–2602.
- Hara MR, Agrawal N, Kim SF, Cascio MB, Fujimuro M, Ozeki Y *et al*. S-nitrosylated GAPDH initiates apoptotic cell death by nuclear translocation following Siah1 binding. *Nat Cell Biol* 2005; **7**: 665–674.
- Hasson SA, Kane LA, Yamano K, Huang CH, Sliter DA, Buehler E *et al*. High-content genome-wide RNAi screens identify regulators of parkin upstream of mitophagy. *Nature* 2013; **504**: 291–295.
- Qi J, Kim H, Scortegagna M, Ronai ZA. Regulators and effectors of Siah ubiquitin ligases. *Cell Biochem Biophys* 2013; **67**: 15–24.
- Wong CS, Moller A. Siah: a promising anticancer target. *Cancer Res* 2013; **73**: 2400–2406.
- Liu J, Stevens J, Rote CA, Yost HJ, Hu Y, Neufeld KL *et al*. Siah-1 mediates a novel beta-catenin degradation pathway linking p53 to the adenomatous polyposis coli protein. *Mol Cell* 2001; **7**: 927–936.
- Matsuzawa SI, Reed JC. Siah-1, SIP, and Ebi collaborate in a novel pathway for beta-catenin degradation linked to p53 responses. *Mol Cell* 2001; **7**: 915–926.
- Frew IJ, Dickens RA, Cuddihy AR, Del Rosario M, Reinhard C, O'Connell MJ *et al*. Normal p53 function in primary cells deficient for Siah genes. *Mol Cell Biol* 2002; **22**: 8155–8164.
- Clevers H. Wnt/beta-catenin signaling in development and disease. *Cell* 2006; **127**: 469–480.
- Brembeck FH, Rosario M, Birchmeier W. Balancing cell adhesion and Wnt signaling, the key role of beta-catenin. *Curr Opin Genet Dev* 2006; **16**: 51–59.
- Maelandsmo GM, Holm R, Nesland JM, Fodstad O, Florenes VA. Reduced beta-catenin expression in the cytoplasm of advanced-stage superficial spreading malignant melanoma. *Clin Cancer Res: Off J Am Assoc Cancer Res* 2003; **9**: 3383–3388.
- Staal FJ, van Noort M, Strous GJ, Clevers HC. Wnt signals are transmitted through N-terminally dephosphorylated beta-catenin. *EMBO Rep* 2002; **3**: 63–68.
- Fujita Y, Krause G, Scheffner M, Zechner D, Leddy HE, Behrens J *et al*. Hakai, a c-Cbl-like protein, ubiquitinates and induces endocytosis of the E-cadherin complex. *Nat Cell Biol* 2002; **4**: 222–231.
- Tauriello DV, Maurice MM. The various roles of ubiquitin in Wnt pathway regulation. *Cell Cycle* 2010; **9**: 3700–3709.
- Bryant DM, Stow JL. The ins and outs of E-cadherin trafficking. *Trends Cell Biol* 2004; **14**: 427–434.
- Nastasi T, Bongiovanni A, Campos Y, Mann L, Toy JN, Bostrom J *et al*. Ozz-E3, a muscle-specific ubiquitin ligase, regulates beta-catenin degradation during myogenesis. *Dev Cell* 2004; **6**: 269–282.
- Kim CJ, Cho YG, Park CH, Jeong SW, Nam SW, Kim SY *et al*. Inactivating mutations of the Siah-1 gene in gastric cancer. *Oncogene* 2004; **23**: 8591–8596.
- Medhioub M, Vaury C, Hamelin R, Thomas G. Lack of somatic mutation in the coding sequence of SIAH1 in tumors hemizygous for this candidate tumor suppressor gene. *Int J Cancer* 2000; **87**: 794–797.
- Maeda A, Yoshida T, Kusuzaki K, Sakai T. The characterization of the human Siah-1 promoter(1). *FEBS Lett* 2002; **512**: 223–226.
- Seth A, Watson DK. ETS transcription factors and their emerging roles in human cancer. *Eur J Cancer* 2005; **41**: 2462–2478.
- Wang D, Wang Y, Kong T, Fan F, Jiang Y. Hypoxia-induced beta-catenin down-regulation involves p53-dependent activation of Siah-1. *Cancer Sci* 2011; **102**: 1322–1328.
- Cai X, Carlson J, Stoicov C, Li H, Wang TC, Houghton J. *Helicobacter felis* eradication restores normal architecture and inhibits gastric cancer progression in C57BL/6 mice. *Gastroenterology* 2005; **128**: 1937–1952.
- Yoshiyayashi H, Okabe H, Satoh S, Hida K, Kawashima K, Hamasu S *et al*. SIAH1 causes growth arrest and apoptosis in hepatoma cells through beta-catenin degradation-dependent and -independent mechanisms. *Oncol Rep* 2007; **17**: 549–556.
- Leung CO, Deng W, Ye TM, Ngan HY, Tsao SW, Cheung AN *et al*. miR-135a leads to cervical cancer cell transformation through regulation of beta-catenin via a SIAH1-dependent ubiquitin proteasomal pathway. *Carcinogenesis* 2014; **35**: 1931–1940.
- Weydig C, Starzinski-Powitz A, Carra G, Lower J, Wessler S. CagA-independent disruption of adherence junction complexes involves E-cadherin shedding and implies multiple steps in *Helicobacter pylori* pathogenicity. *Exp Cell Res* 2007; **313**: 3459–3471.
- Costa AM, Leite M, Seruca R, Figueiredo C. Adherens junctions as targets of microorganisms: a focus on *Helicobacter pylori*. *FEBS Lett* 2013; **587**: 259–265.
- Takayama T, Shiozaki H, Shibamoto S, Oka H, Kimura Y, Tamura S *et al*. Beta-catenin expression in human cancers. *Am J Pathol* 1996; **148**: 39–46.
- Chen KH, Tung PY, Wu JC, Chen Y, Chen PC, Huang SH *et al*. An acidic extracellular pH induces Src kinase-dependent loss of beta-catenin from the adherens junction. *Cancer Lett* 2008; **267**: 37–48.

- 32 Stanczak A, Stec R, Bodnar L, Olszewski W, Cichowicz M, Kozlowski W et al. Prognostic significance of Wnt-1, beta-catenin and E-cadherin expression in advanced colorectal carcinoma. *Pathol Oncol Res* 2011; **17**: 955–963.
- 33 Ebert MP, Yu J, Hoffmann J, Rocco A, Rocken C, Kahmann S et al. Loss of beta-catenin expression in metastatic gastric cancer. *J Clin Oncol Off J Am Soc Clin Oncol* 2003; **21**: 1708–1714.
- 34 Sougleri IS, Papadakos KS, Zadik MP, Mavri-Vavagianni M, Mentis AF, Sgouras DN. Helicobacter pylori CagA protein induces factors involved in the epithelial to mesenchymal transition (EMT) in infected gastric epithelial cells in an EPIYA- phosphorylation-dependent manner. *FEBS J* 2016; **283**: 206–220.
- 35 Schneider S, Carra G, Sahin U, Hoy B, Rieder G, Wessler S. Complex cellular responses of Helicobacter pylori-colonized gastric adenocarcinoma cells. *Infect Immun* 2011; **79**: 2362–2371.
- 36 Howard S, Deroo T, Fujita Y, Itasaki N. A positive role of cadherin in Wnt/beta-catenin signalling during epithelial-mesenchymal transition. *PLoS ONE* 2011; **6**: e23899.
- 37 Brembeck FH, Schwarz-Romond T, Bakkers J, Wilhelm S, Hammerschmidt M, Birchmeier W. Essential role of BCL9-2 in the switch between beta-catenin's adhesive and transcriptional functions. *Genes Dev* 2004; **18**: 2225–2230.
- 38 Kam Y, Quaranta V. Cadherin-bound beta-catenin feeds into the Wnt pathway upon adherens junctions dissociation: evidence for an intersection between beta-catenin pools. *PLoS ONE* 2009; **4**: e4580.
- 39 Palacios F, Tushir JS, Fujita Y, D'Souza-Schorey C. Lysosomal targeting of E-cadherin: a unique mechanism for the down-regulation of cell-cell adhesion during epithelial to mesenchymal transitions. *Mol Cell Biol* 2005; **25**: 389–402.
- 40 Yang JY, Zong CS, Xia W, Wei Y, Ali-Seyed M, Li Z et al. MDM2 promotes cell motility and invasiveness by regulating E-cadherin degradation. *Mol Cell Biol* 2006; **26**: 7269–7282.
- 41 Mansouri M, Rose PP, Moses AV, Fruh K. Remodeling of endothelial adherens junctions by Kaposi's sarcoma-associated herpesvirus. *J Virol* 2008; **82**: 9615–9628.
- 42 Murata-Kamiya N, Kurashima Y, Teishikata Y, Yamahashi Y, Saito Y, Higashi H et al. Helicobacter pylori CagA interacts with E-cadherin and deregulates the beta-catenin signal that promotes intestinal transdifferentiation in gastric epithelial cells. *Oncogene* 2007; **26**: 4617–4626.
- 43 Bebb JR, Leach L, Zaitoun A, Hand N, Letley DP, Thomas R et al. Effects of Helicobacter pylori on the cadherin-catenin complex. *J Clin Pathol* 2006; **59**: 1261–1266.
- 44 Wroblewski LE, Peek RM Jr. Helicobacter pylori in gastric carcinogenesis: mechanisms. *Gastroenterol Clin N Am* 2013; **42**: 285–298.
- 45 Wroblewski LE, Peek RM Jr., Wilson KT. Helicobacter pylori and gastric cancer: factors that modulate disease risk. *Clin Microbiol Rev* 2010; **23**: 713–739.
- 46 Rath S, Das L, Kokate SB, Pratheek BM, Chattopadhyay S, Goswami C et al. Regulation of Noxa-mediated apoptosis in Helicobacter pylori-infected gastric epithelial cells. *FASEB J* 2014; **29**: 796–806.
- 47 Sadot E, Geiger B, Oren M, Ben-Ze'ev A. Down-regulation of beta-catenin by activated p53. *Mol Cell Biol* 2001; **21**: 6768–6781.
- 48 Iwai A, Marusawa H, Matsuzawa S, Fukushima T, Hijikata M, Reed JC et al. Siah-1L, a novel transcript variant belonging to the human Siah family of proteins, regulates beta-catenin activity in a p53-dependent manner. *Oncogene* 2004; **23**: 7593–7600.
- 49 Matsuzawa S, Takayama S, Froesch BA, Zapata JM, Reed JC. p53-inducible human homologue of Drosophila seven in absentia (Siah) inhibits cell growth: suppression by BAG-1. *EMBO J* 1998; **17**: 2736–2747.
- 50 Elton L, Carpentier I, Verhelst K, Staal J, Beyaert R. The multifaceted role of the E3 ubiquitin ligase HOIL-1: beyond linear ubiquitination. *Immunol Rev* 2015; **266**: 208–221.
- 51 Das L, Kokate SB, Rath S, Rout N, Singh SP, Crowe SE et al. ETS2 and Twist1 promote invasiveness of Helicobacter pylori-infected gastric cancer cells by inducing Siah2. *Biochem J* 2016; **473**: 1629–1640.
- 52 Bhattacharyya A, Chattopadhyay R, Burnette BR, Cross JV, Mitra S, Ernst PB et al. Acetylation of apurinic/apyrimidinic endonuclease-1 regulates Helicobacter pylori-mediated gastric epithelial cell apoptosis. *Gastroenterology* 2009; **136**: 2258–2269.
- 53 Ding SZ, O'Hara AM, Denning TL, Dirden-Kramer B, Mifflin RC, Reyes VE et al. Helicobacter pylori and H2O2 increase AP endonuclease-1/redox factor-1 expression in human gastric epithelial cells. *Gastroenterology* 2004; **127**: 845–858.



Oncogenesis is an open-access journal published by Nature Publishing Group. This work is licensed under a Creative Commons Attribution 4.0 International License. The images or other third party material in this article are included in the article's Creative Commons license, unless indicated otherwise in the credit line; if the material is not included under the Creative Commons license, users will need to obtain permission from the license holder to reproduce the material. To view a copy of this license, visit <http://creativecommons.org/licenses/by/4.0/>

© The Author(s) 2017

Supplementary Information accompanies this paper on the Oncogenesis website (<http://www.nature.com/oncsis>).

Acetylation-mediated Siah2 stabilization enhances PHD3 degradation in *Helicobacter pylori*-infected gastric epithelial cancer cells

Shrikant Babanrao Kokate,* Pragyesh Dixit,* Lopamudra Das,* Suvasmita Rath,* Arjama Dhar Roy,*
 Indrajit Poirah,* Debashish Chakraborty,* Niranjan Rout,[†] Shivaram Prasad Singh,[‡]
 and Asima Bhattacharyya*¹

*School of Biological Sciences, National Institute of Science Education and Research (NISER) Bhubaneswar, Homi Bhabha National Institute (HBNI), Odisha, India; [†]Department of Oncopathology, Acharya Harihar Regional Cancer Centre, Odisha, India; and [‡]Department of Gastroenterology, Srirama Chandra Bhanja (SCB) Medical College, Odisha, India

ABSTRACT: Gastric epithelial cells infected with *Helicobacter pylori* acquire highly invasive and metastatic characteristics. The seven in absentia homolog (Siah)2, an E3 ubiquitin ligase, is one of the major proteins that induces invasiveness of infected gastric epithelial cells. We find that p300-driven acetylation of Siah2 at lysine 139 residue stabilizes the molecule in infected cells, thereby substantially increasing its efficiency to degrade prolyl hydroxylase (PHD)3 in the gastric epithelium. This enhances the accumulation of an oncogenic transcription factor hypoxia-inducible factor 1 α (Hif1 α) in *H. pylori*-infected gastric cancer cells in normoxic condition and promotes invasiveness of infected cells. Increased acetylation of Siah2, Hif1 α accumulation, and the absence of PHD3 in the infected human gastric metastatic cancer biopsy samples and in invasive murine gastric cancer tissues further confirm that the acetylated Siah2 (ac-Siah2)–Hif1 α axis is crucial in promoting gastric cancer invasiveness. This study establishes the importance of a previously unrecognized function of ac-Siah2 in regulating invasiveness of *H. pylori*-infected gastric epithelial cells.—Kokate, S. B., Dixit, P., Das, L., Rath, S., Roy, A. D., Poirah, I., Chakraborty, D., Rout, N., Singh, S. P., Bhattacharyya, A. Acetylation-mediated Siah2 stabilization enhances PHD3 degradation in *Helicobacter pylori*-infected gastric epithelial cancer cells. *FASEB J.* 32, 000–000 (2018). www.fasebj.org

KEY WORDS: E3 ubiquitin ligase · hypoxia-inducible factor · cancer invasiveness · post-translational modification · proteasomal degradation

Helicobacter pylori are the most potent causative agents for gastric cancer (1, 2). Strains possessing the cytotoxin-associated gene (*cag*) pathogenicity island (PAI) or *cag* PAI (+) strains are associated with greater disease severity (3, 4) despite its short lifespan in epithelial cells (5). *H. pylori* infection induces the expression of a number of inflammatory, neoplastic, and stress-inducible genes. Enhanced production of reactive oxygen species (ROS) in *H. pylori*-infected gastric epithelial cells (6) stabilizes hypoxia-inducible

factor 1 α (Hif1 α) in normoxic condition (7, 8). Hif1 α expression is positively correlated with gastric cancer progression (9), metastasis (10), treatment resistance (11, 12), and poor prognosis (13).

Stability of Hif1 α , a major factor responsible for the regulation of cancer progression and metastasis, is influenced by a seven in absentia homolog (Siah) family protein, Siah2. Siah proteins belong to the “really interesting new gene” (14) family, the largest family of E3 ubiquitin ligases. By targeting the degradation of its target molecules, Siah proteins can function as tumor suppressors and as oncogenic inducers (15–17). The oncogenic potential of Siah2 has been established by several recent studies (18–20), and it can increase the invasiveness of gastric epithelial cancer cells (GCCs) (18).

The degradation of the hypoxia-inducible α -residue of Hif1 under normoxia is regulated by hydroxylation of Hif1 α at proline residues (P⁴⁰² and P⁵⁶⁴ in humans and P⁴⁰² and P⁵⁶² in mice). The reaction is catalyzed by prolyl hydroxylases (PHDs). ROS generated in *H. pylori*-infected gastric epithelium can inactivate PHD enzymes (21) and contribute to Hif1 α accumulation in the infected gastric

ABBREVIATIONS: ac-K^{129/139} Siah2, acetylated K^{129/139} seven in absentia homolog 2; ac-Siah2, acetylated seven in absentia homolog 2; *cag*, cytotoxin-associated gene; GCC, gastric epithelial cancer cell; H&E, hematoxylin and eosin; HAT, histone acetyltransferase; Hif1 α , hypoxia-inducible factor 1 α ; MOI, multiplicity of infection; PAI, pathogenicity island; PHD, prolyl hydroxylase; ROS, reactive oxygen species; shRNA, short hairpin RNA; Siah, seven in absentia homolog; WT, wild type

¹ Correspondence: School of Biological Sciences, National Institute of Science Education and Research (NISER) Bhubaneswar, HBNI, P.O. Bhipur-Padanpur, Via Jatni, District Khurda 752050, Odisha, India. E-mail: asima@niser.ac.in

doi: 10.1096/fj.201701344RRR

This article includes supplemental data. Please visit <http://www.fasebj.org> to obtain this information.

epithelium. PHD3 is one of the major stress-related genes up-regulated during *H. pylori* infection (4). In hypoxia, PHD3 is targeted for degradation by Siah2 (22). It has been recently reported that the function and stability of the E3 ubiquitin ligase mouse double minute 2 are tightly regulated by p300-mediated acetylation (23), wherein acetylation results in reduced self-ubiquitination-mediated degradation of mouse double minute 2. However, the effect of acetylation in regulating Siah function and *H. pylori* pathogenesis is unknown.

Given the impact of Siah2 on PHD3, we investigated whether Siah2 is acetylated in *H. pylori*-infected GCCs and its effect on Hif1 α stability. This study shows that p300 acetylates Siah2 in the *H. pylori*-infected GCCs. Acetylation stabilizes Siah2, which causes PHD3 degradation and increases Hif1 α accumulation, resulting in enhanced invasiveness of *H. pylori*-infected cells. The presence of acetylated Siah2 (ac-Siah2) in murine gastric cancer tissue and in human gastric cancer biopsy samples suggests that ac-Siah2 might be useful as a therapeutic target.

MATERIALS AND METHODS

Cell culture, *Helicobacter*, and chemicals

Human GCCs MKN45, AGS, Kato III, and *H. pylori* strains 26695 [*cag* PAI (+)], 8-1 [*cag* PAI (-)], and *Helicobacter felis* strain 49179 (American Type Culture Collection, Manassas, VA, USA) were used in this study and were maintained as previously described (24, 25). GCCs were infected with strain 26695 at 200 multiplicity of infection (MOI) for the indicated period unless mentioned otherwise. When required, GCCs were treated with 100 μ M CTK7A (Merck Millipore, Burlington, MA, USA) along with *H. pylori* infection. Z-Leu-Leu-Leu-al (MG132; MilliporeSigma, Milwaukee, WI, USA) at 50 μ M concentration was used to study proteasomal degradation events.

Expression plasmids, site-directed mutagenesis, transfection, and stable cell line generation

p300 wild-type (WT) and histone acetyltransferase (HAT) mutant constructs have been reported by Bhattacharyya *et al.* (26). *siah2* WT plasmid was purchased from Origene Technologies (Beijing, China), and empty vector (pcDNA3.1⁺) was purchased from Thermo Fisher Scientific (Waltham, MA, USA). *siah2* acetyl lysine mutants K129R and K139R were generated from the *siah2* WT construct using the QuikChange Site-Directed Mutagenesis Kit (Agilent Technologies, Santa Clara, CA, USA). Primers used were as follows: K129R, 5'-GAACCTGGCTATGGAGAGGGTGGC-CTCGGCAGTCC-3' and K139R, 5'-CAGTCTGTTCCCTGT-AGGTATGCCACCACGGCTG-3' for K139R mutation. Mutations at specific sites were confirmed by sequencing.

Twenty-four hours after plating, cells were transfected with the recommended amount of DNA, P3000 reagent, and Lipofectamine 3000 (Thermo Fisher Scientific) following manufacturer's instructions and were incubated for 48 h. Stably transfected positive clones were selected using G418 solution (MilliporeSigma) following the standard protocol described by Das *et al.* (15).

Stable *hif1 α* knocked out AGS cells, scrambled negative-control AGS cells, and empty vector short hairpin RNA (shRNA) cells (8) were also used in this study.

Western blotting and immunoblotting

A total of 1×10^6 cells were seeded 24 h before treatment. Whole cell extracts were prepared, and proteins were separated on SDS-PAGE gel followed by immunoblotting onto the PVDF membranes. The primary antibodies used were Siah2 (Santa Cruz Biotechnology, Santa Cruz, CA, USA), acetylated lysine (Cell Signaling Technology, Danvers, MA, USA), p300 (Abcam, MD, USA), HIF1 α (Abcam), and PHD3 (Novus Biologicals, Littleton, CO, USA). Antibodies used as loading control were α -tubulin (Abcam) and GAPDH (Abgenex, Bhubaneswar, Odisha, India). Bands were detected as described by Das *et al.* (18).

Immunoprecipitation assay was performed by using p300 antibody (Abcam). Equivalent normal mouse IgG (Santa Cruz Biotechnology) was used to assess the specificity of immune interactions.

Customized acetylated K¹²⁹ and K¹³⁹ (ac-K¹²⁹ and ac-K¹³⁹) human Siah2 antibodies (anti-rabbit, polyclonal) were obtained from Bioklone Biotech Pvt. Ltd. (Chennai, India). These antibodies could also detect ac-K¹³⁰ and ac-K¹⁴⁰ of mouse Siah2, respectively.

Human and mouse gastric tissue collection

Antral endoscopic biopsy samples were collected from consenting patients who had a positive rapid urease test (Halifax Research Laboratory, Kolkata, India) and who had stage III metastatic adenocarcinoma following a protocol approved by the National Institute of Science Education and Research Review Board (Jatni, India). Noncancerous and uninfected gastric tissues were used as controls. Patients with a history of previous *H. pylori* eradication therapy were not included in the study. This study was performed in compliance with the Helsinki Declaration (2013), World Medical Association.

C57BL/6 mice (4–5 wk old) were procured from the National Centre for Laboratory Animal Sciences of the National Institute of Nutrition (Hyderabad, India). After reaching 7–8 wk of age, male and female mice were blindly divided into 2 groups (uninfected, $n = 16$; infected, $n = 16$) and orogastrically fed with *H. felis* following the standard protocol. After 12 mo, mice were killed, and stomachs were collected. Tissues were fixed and sectioned at 5 μ m thickness. The stomach mucosa was examined to detect mononuclear cell infiltration, hyperplasia, adenocarcinoma, and invasiveness of adenocarcinoma. Four out of 16 infected mice showed symptoms of invasive adenocarcinoma and splenomegaly. The study was performed in accordance with the Institutional Animal Ethics Committee approval of the National Institute of Science Education and Research.

Immunofluorescence microscopy

MKN45 or AGS cells were seeded on glass coverslips 1 d prior to transfection followed by infection or infection only. Tissues were processed for immunofluorescence microscopy and hematoxylin and eosin (H&E) staining as described by Das *et al.* (15). The following antibodies were used for immunofluorescence staining: Siah2 (Abcam), PHD3 (Novus Biologicals), HIF1 α (Abcam), custom-synthesized ac-K¹²⁹ and ac-K¹³⁹ Siah2 antibody (Bioklone Biotech), and CagA (A-10) (Santa Cruz Biotechnology). The following fluorophore-linked secondary antibodies were used: anti-rabbit IgG (H+L) Alexa Fluor 488 (Thermo Fisher Scientific), anti-mouse IgG (H+L) Alexa Fluor 594 (Thermo Fisher Scientific), and anti-rabbit IgG (H+L) Alexa Fluor 594 (Thermo Fisher Scientific). H&E staining was done following the standard procedure. An inverted research microscope (Eclipse Ti-U; Nikon Corp., Tokyo, Japan) was used, and images were captured at $\times 200$ and $\times 600$ magnification using digital cameras (DS Ri2 and DS Qi2; Nikon Corp.).

In vitro invasion and migration assays

To study the effect of Siah2 ac-lys mutation and the effect of HAT inhibitor CTK7A on the invasive and migratory properties of GCCs, cell culture inserts with 0.3 cm² polyethylene terephthalate membrane (8- μ m pore size and 6.4-mm diameter) (Falcon Corning, Tewksbury, MA, USA) were used with (invasion assay) and without (migration assay) growth factor-reduced standard Matrigel matrix (Becton Dickinson, Franklin Lakes, NJ, USA) following a previously reported method (27). Invaded and migrated cells were counted from at least 5 different fields, and the images were captured using the forementioned microscope and camera models.

Wound-healing assay

The stable cells (either shRNA-expressing stable cells or WT or ac-K139R *siah2* mutant or empty-vector overexpressing AGS cells) were seeded in 6-well plates and maintained for 24 h until 95% confluency was achieved followed by infection with *H. pylori*. Wound-healing assay was performed following the standard protocol (27) using a Nikon microscope and the camera systems described above.

To study the effect of HAT inhibitor CTK7A on the wound-healing property of GCCs, AGS cells were seeded in a 6-well plate 24 h prior to CTK7A treatment and *H. pylori* infection. CTK7A-treated and untreated cells were infected, and wound-healing assay was performed.

Soft agar assay

pcDNA3.1⁺, *siah2* WT, and *siah2* ac-K139R mutant-expressing stable MKN45 cells were seeded in a 24-well plate with 0.16×10^4 seeding density and were incubated for 24 h. Cells were infected with *H. pylori* for 12 h followed by gentamicin treatment for 2 h to kill extracellular *H. pylori*. When required, cells were treated with CTK7A along with *H. pylori* infection before performing the soft agar assay. The experiment was performed using the protocol of Das *et al.* (18). Images were captured from 4 to 5 marked places once in a week at regular intervals, and the number and size of the colonies were measured using ImageJ 1.50i software (National Institutes of Health, Bethesda, MD, USA).

MTT assay

Proliferation of transfected MKN45 cells and untreated or CTK7A-treated cells with or without *H. pylori* infection were assessed by using an MTT assay kit as described by Das *et al.* (18).

Clonogenicity assay

MKN45 cells expressing pcDNA3.1⁺, *siah2* WT, and *siah2* ac-K139R constructs were assessed for their viability after *H. pylori* infection. Cells were seeded in a 24-well plate with 0.16×10^4 seeding density and incubated for 24 h followed by gentamicin treatment for 2 h. The cells were trypsinized and seeded in a 6-well plate with 500 cells/well. After 3 wk of incubation, 4% paraformaldehyde-fixed colonies were washed with $1 \times$ PBS and stained with crystal violet (0.5%). Colonies were counted, and images were taken as described above.

Statistical analysis

All experiments were performed at least 3 times, and the results were graphically expressed as means \pm SEM. Statistical analysis was done using GraphPad Prism software v.7.03 (GraphPad, La

Jolla, CA, USA). Statistical significance between 2 groups was calculated by Student's *t* tests at $P < 0.05$. Two-way ANOVA was applied for comparing 2 or more independent groups.

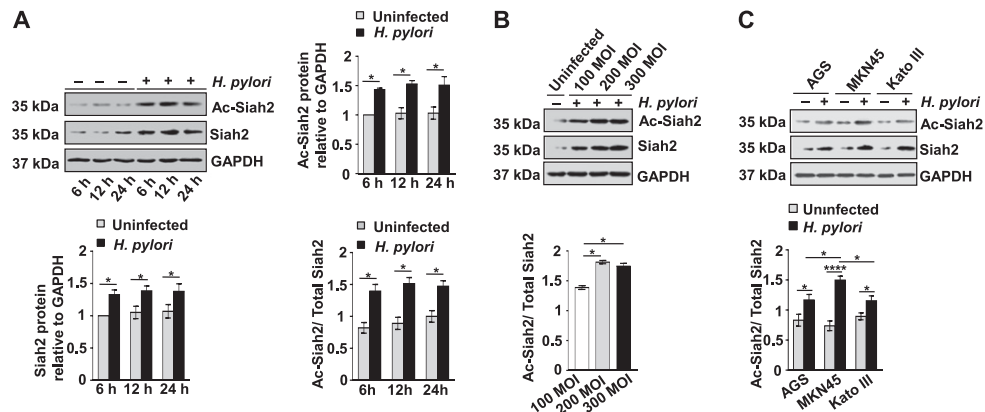
RESULTS

H. pylori increases acetylation of Siah2 in the infected GCCs

The specificity in ubiquitination-mediated proteasomal degradation is provided by E3 ligases. Deregulation of E3s has been reported in several diseases, including cancer (24, 28–30). Although phosphorylation-mediated regulation of E3 ligases is known (31), the effect of acetylation on E3 ligases is less understood. Siah2 enhances invasiveness of *H. pylori*-infected GCCs (18). Because GCCs also express p300, which by virtue of its HAT function plays an important role in regulating the lifespan of GCCs (26, 27, 32, 33), we examined the acetylation status of Siah2. MKN45 cells were infected with *cag* PAI (+) *H. pylori* strain 26695 at 200 MOI for 6, 12, and 24 h. Western blotting for ac-Siah2 and total Siah2 was performed on whole cell lysates. Densitometric analyses (ac-Siah2: GAPDH; Siah2: GAPDH; and ac-Siah2: total Siah2) revealed that Siah2 and its acetylation were significantly induced in the infected cells as compared with the uninfected cells at all time points, with 12-h infection being significant for Siah2 acetylation (Fig. 1A). To determine the optimal MOI for expression of ac-Siah2 protein, Western blotting was performed after infecting MKN45 cells with 100, 200, and 300 MOI for 12 h. The ratio of ac-Siah2 to total Siah2 was significantly high at 200 MOI and at 300 MOI (Fig. 1B). Because 200 MOI had an equivalent effect as that of 300 MOI in inducing ac-Siah2, we used 200 MOI for the rest of our experiments. Two other GCCs, Kato III and AGS, showed a similar trend of Siah2 acetylation after being infected with *H. pylori* (MOI 200 at 12 h), indicating that Siah2 acetylation by *H. pylori* is not limited to MKN45 cells (Fig. 1C).

Siah2 expression is increased in *H. pylori*-infected GCCs and *cag* PAI (+) as well as *cag* PAI (–) strains were equally effective in increasing Siah2 expression (18). To identify the role of *cag* PAI on Siah2 acetylation, we infected MKN45 cells with MOI 200 of *cag* PAI (+) strain 26695 and the *cag* PAI (–) strain 8-1 for 12 h. The *cag* PAI (+) and PAI (–) strains showed equal effectiveness in increasing Siah2 acetylation (Fig. 2A). *H. pylori* can strongly induce Hif1 α (8) and PHD3 (4). On one hand, normoxic degradation of Hif1 α is mediated by PHD proteins; on the other hand, PHD3 degradation in hypoxia is mediated by Siah2 (22). To determine whether p300 interacts with Siah2, Hif1 α , and PHD3 proteins in the *H. pylori*-infected epithelium, whole cell lysates were immunoprecipitated with p300 antibody, Western blotted, and probed with p300, Hif1 α , ac-lys, Siah2, and PHD3 antibodies (Fig. 2B). Input lysates were also Western blotted for these proteins. Data showed that p300 was not much altered after infection, but Hif1 α was highly induced and PHD3 level was decreased. These findings were also reflected in the p300-immunoprecipitates. Moreover, *H. pylori* infection resulted in significantly higher Siah2 and ac-Siah2 in the p300-immunoprecipitated

Figure 1. Siah2 acetylation is induced in *H. pylori*-infected human GCCs. **A)** Western blot analysis of cell lysates prepared from uninfected and *H. pylori*-infected MKN45 cells (6, 12, and 24 h with 200 MOI of *H. pylori* infection) shows induced expression of Siah2 and ac-Siah2. Graphical representations of the data clearly show a significant increment in Siah2 acetylation at all time points, with 12 h being the optimal time to detect ac-Siah2. GAPDH is used as a loading control. Data are means \pm SEM ($n = 3$). **B)** Western blotting analysis of cell lysates ($n = 3$) prepared from *H. pylori*-infected (100, 200, and 300 MOI for 12 h) MKN45 cells. A representative bar diagram indicates that MOI 200 is the optimum time point for Siah2 acetylation (means \pm SEM, $n = 3$). **C)** Western blot analysis ($n = 3$) showing the ratio of ac-Siah2 to total Siah2 in *H. pylori*-infected AGS, MKN45, and Kato III cells. Representative bar graph data generated by 2-way ANOVA (means \pm SEM, $n = 3$). * $P < 0.05$, **** $P < 0.0001$.



complex than in the noninfected cell. This was more apparent when immunoprecipitation results were compared with the expression of p300, Siah2, and ac-Siah2 in the input lanes. p300, being a bromodomain-containing protein, showed higher efficiency in pulling down ac-Siah2 in the infected cell. To further understand the importance of p300 HAT activity on Siah2 acetylation, MKN45 cells were transfected with the empty vector, p300 WT and p300 Δ HAT constructs. Western blot data revealed that p300 HAT deletion mutant significantly reduced Siah2 and ac-Siah2 protein levels (Supplemental Fig. 1A). Coincubation of MKN45 cells for 12 h with *H. pylori* and CTK7A, an inhibitor of p300 lysine/HAT activity (27), remarkably reduced Siah2 and ac-Siah2 proteins (Supplemental Fig. 1B). The effect of HAT inhibitor CTK7A on cell migration and invasion was studied by *in vitro* cell migration and invasion assays using adherent AGS cells (MKN45 cell is semi-adherent in nature) (Supplemental Fig. 1C, D). A wound-healing assay was performed to further evaluate the effect of CTK7A on AGS cell migration (Supplemental Fig. 1E). CTK7A significantly decreased AGS migration, invasion, and wound healing ability, as shown in the bar graphs in Fig. 1E. A similar result was detected in CTK7A-treated MKN45 cells after performing soft agar assay (Supplemental Fig. 1F). All data (Supplemental Fig. 1C–F) were analyzed by 2-way ANOVA with Tukey's *post hoc* analysis. We performed MTT assay to determine the effect of CTK7A on MKN45 cell proliferation (Supplemental Fig. 1G). *H. pylori*-mediated increase in cell proliferation was significantly down-regulated upon CTK7A treatment.

Human Siah2 protein (GenBank: CAA75557.1) has several lysine (K) residues (Fig. 2C). Acetylation of Siah2 was predicted using the GPS-PAIL tool (34). Among the predicted K residues with high probability for acetylation, K¹²⁹ and K¹³⁹ belong to the substrate-binding domain of Siah2. In mouse, the corresponding residues are K¹³⁰ and K¹⁴⁰ (mouse Siah2 GenBank: NP_033200.2). E3 ubiquitin ligase function depends on the acetylation of the "really interesting new gene" domain (23, 35). Therefore, we examined the effects of acetylation-null mutations at K¹²⁹ and K¹³⁹ of Siah2. Acetylation-null *siah2* K129R and K139R constructs were generated by site-directed mutagenesis.

The empty vector pcDNA3.1⁺, *siah2* WT, *siah2* K139R, and *siah2* K129R were overexpressed in MKN45 cells. Acetylation of Siah2 was examined by probing the Western blotted membrane with Siah2 and ac-lys antibodies. The *H. pylori*-mediated increase in Siah2 and ac-Siah2 was optimal in WT construct-transfected cells. The amount of these proteins was slightly less in K129R-transfected cells as compared with the WT construct-transfected cells (Fig. 2D). In K139R-expressing cells, Siah2 and ac-Siah2 were remarkably less compared to the other 2 transfected groups, which indicated probable instability of Siah2 when mutated at the K139 residue. Siah2 bands were not detected in empty vector-transfected lanes, and we believed that strong Siah2 band intensities in the WT lanes were masking the appearance of Siah2 bands in empty vector-overexpressed lanes. Therefore, stable cells expressing empty vector, Siah2 WT, and K139R constructs were generated, and Siah2 expression was compared by performing Western blot. Data ($n = 3$) confirmed that Siah2 was markedly decreased in K139R-stable cells when compared with WT cells even after *H. pylori* infection (Fig. 2E). Because stable cells consistently showed ($n = 3$) better Siah2 and ac-Siah2 bands than transient transfections, stable cells were used for future studies. Acetylation may compete with ubiquitination and suppress ubiquitination-mediated proteasomal degradation (36, 37). Acetylation can also mark proteins for ubiquitin-mediated degradation (38). Presuming that K139R Siah2 might undergo increased proteasomal degradation, K139R mutant-expressing MKN45 stable cells were treated with MG132 prior to *H. pylori* infection and compared with MG132-treated WT cells. MG132 rescued K139R Siah2 protein from being degraded, indicating that Siah2 acetylation at K¹³⁹ could protect Siah2 from ubiquitination-mediated proteasomal degradation (Fig. 2F).

***H. pylori*-mediated acetylation of Siah2 at K¹³⁹ enhances degradation of PHD3 and causes Hif1 α protein accumulation in GCCs**

H. pylori can induce Hif1 α as well as PHD3. Because PHD3 is responsible for Hif1 α degradation in normoxia and is a

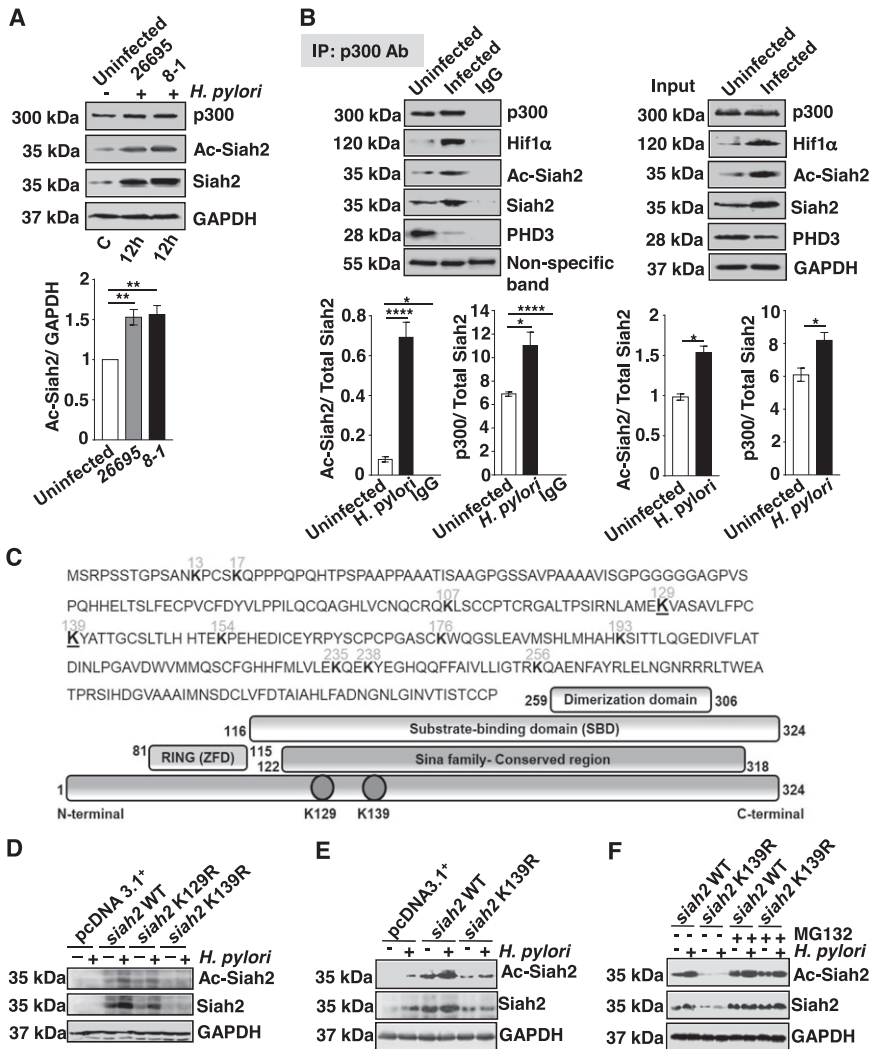


Figure 2. p300 regulates Siah2 acetylation in *H. pylori*-infected human GCCs. **A)** A representative immunoblot analysis ($n = 3$) from uninfected and infected [200 MOI of *cag* PAI (+) strain 26695 or (-) strain 8-1 for 12 h]. MKN45 cell lysates show the protein level of p300, ac-Siah2, and Siah2 (means \pm SEM, $n = 3$). **B)** Protein lysates were immunoprecipitated ($n = 3$) using p300 antibody to determine the interaction of p300 with Siah2, PHD3, and Hif1 α . Representative bar diagrams show significant increase in ac-Siah2 formation and p300-Siah2 interaction in infected cells when compared with uninfected cells (means \pm SEM, $n = 3$). **C)** Schematic depictions of different multi-domain structures of Siah2 protein from N- to C-terminal, dimerization domain, substrate-binding domain (SBD), really interesting new gene (RING), or zinc finger domain (ZFD) and Sina family-conserved region. **D)** Western blot analysis ($n = 3$) showing ac-Siah2 and Siah2 expression in cell lysates prepared from transiently transfected pcDNA3.1+, *siah2* WT, *siah2* K129R, and K139R cells after *H. pylori* infection. **E)** Western blot data ($n = 3$) showing ac-Siah2 and Siah2 bands in cell lysates prepared from pcDNA3.1+, *siah2* WT, *siah2* K129R, and K139R-expressing stable cells after *H. pylori* infection. **F)** Immunoblotting showing the effect of MG132 treatment (50 μ M, for 24 h) on WT or *siah2* K139R-expressing stable cells. GAPDH is used as a loading control. * $P < 0.05$, ** $P < 0.01$, *** $P < 0.0001$.

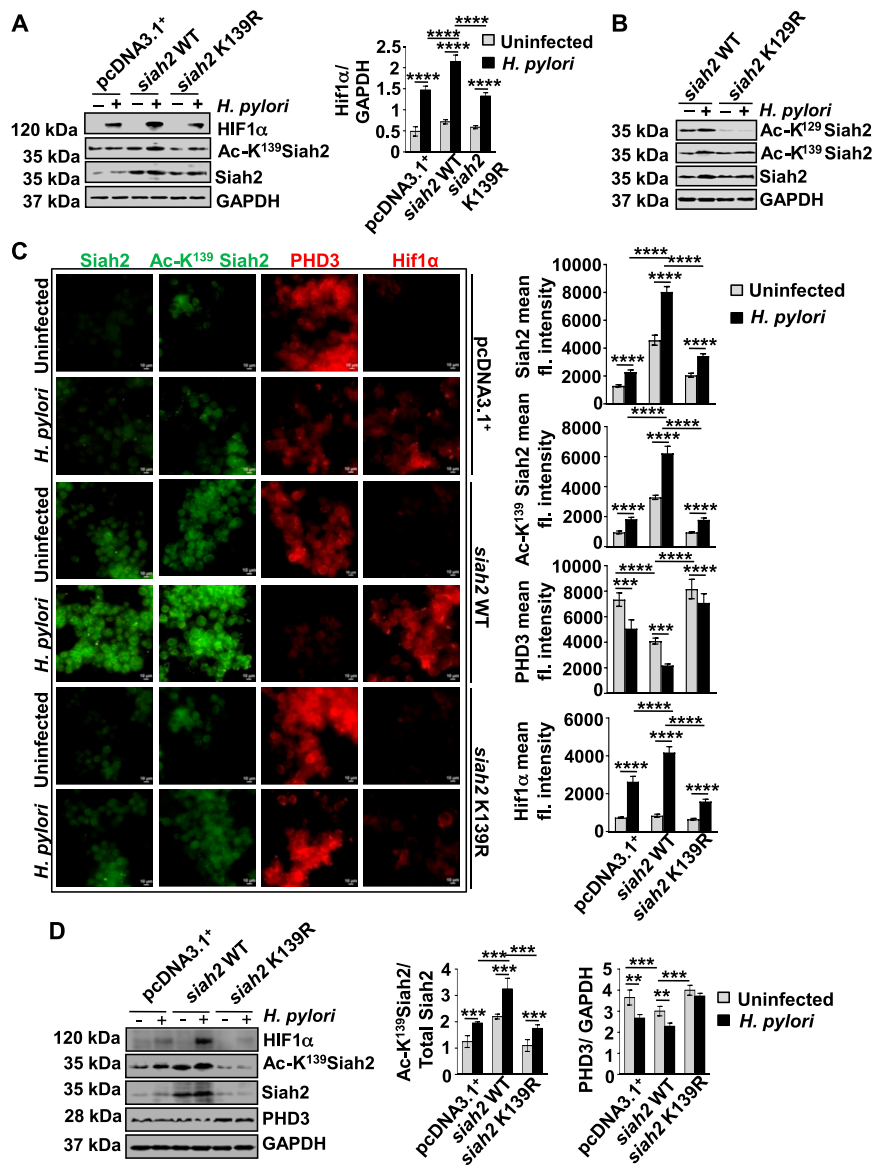
target of Siah2-mediated ubiquitination, we determined the effect of Siah2 K¹³⁹ acetylation on PHD3 and Hif1 α protein level in *H. pylori*-infected GCCs. To identify the specificity of acetylation, the Western blotted membrane was probed with customized ac-K¹³⁹ Siah2 antibody. Western blot results confirmed that overexpression of *siah2* markedly increased the level of Hif1 α protein in infected GCCs, whereas K139R mutant abrogated this effect (Fig. 3A). The specificity of ac-K¹³⁹ antibody was assessed by performing Western blotting of cell lysates prepared from uninfected and infected WT and K129R stable cells (Fig. 3B). To confirm the effect of K139R mutation on PHD3 protein, immunofluorescence microscopy was done using uninfected and *H. pylori*-infected MKN45 cells stably transfected with the empty vector, *siah2* WT, and *siah2* K139R constructs. WT *siah2*-transfected and infected cells showed significantly low PHD3 but significantly high Hif1 α protein when compared with the other transfected groups (Fig. 3C). K139R mutant-expressing infected cells, in contrast, showed significantly low immunofluorescence for Hif1 α but significantly high immunofluorescence for PHD3 among all of these *H. pylori*-infected groups. The effect of Siah2 acetylation on PHD3 was studied by performing Western blot using cell lysates prepared from the empty vector, WT *siah2*, or

K139R mutant-expressing cells. Results established that Siah2 acetylation at K¹³⁹ had significant effects on PHD3 degradation and Hif1 α accumulation in *H. pylori*-infected GCCs (Fig. 3D).

Hif1 α suppression reduces cell migration and invasiveness of *H. pylori*-infected GCCs

The relationship of PHD3 and Siah2 with Hif1 α is complex. In hypoxic cells, PHD3 can be induced by Hif1 α and might control Hif1 α in a negative-feedback manner (39–41). Siah2 can also get up-regulated in hypoxic cells (42). Therefore, we studied the effect of *hif1 α* suppression on PHD3 and Siah2 proteins in *H. pylori*-infected GCCs. In addition, we assessed the effect of *hif1 α* suppression in the infected GCCs. MKN45 cells were not used for stable *hif1 α* -suppressed cell generation due to their semiadherent and clumpy nature, which make them unsuitable for cell invasion and migration assays (18). Instead, more adherent AGS cells stably transfected with Hif1 α shRNA (43) were used. *H. pylori*-mediated down-regulation of PHD3 was equally effective in the empty vector, scrambled shRNA, and *hif1 α* shRNA-expressing stable cells, indicating that Hif1 α had no effect on PHD3 protein (Supplemental Fig. 2). Similarly, an *H. pylori*-mediated increase in Siah2 was

Figure 3. Siah2 acetylation at K¹³⁹ decreases PHD3 expression and increases Hif1 α expression in *H. pylori*-infected human GCCs. *A*) Expression of Siah2 WT or ac-K¹³⁹ Siah2 on Hif1 α was assessed by ($n = 3$) using cell lysates prepared from MKN45 cells stably transfected with pcDNA 3.1+, *siah2* WT, or *siah2* K139R constructs and infected with 200 MOI *H. pylori* for 12 h. Ac-K¹³⁹ Siah2 is detected using Ac-K¹³⁹ Siah2 custom-generated antibody. GAPDH is used as a loading control. *B*) The specificity of ac-K¹³⁹ antibody was assessed by Western blotting of cell lysates prepared from uninfected and infected WT and K129R stable cells. *C*) A representative immunofluorescence microscopy result ($n = 3$) derived from MKN45 cells overexpressing the above-mentioned constructs with or without *H. pylori* infection indicates low PHD3 but a high level of Hif1 α in *H. pylori*-infected WT-cells, whereas the K139R-expressing cells show high PHD3 and low Hif1 α in *H. pylori*-infected WT cells. Mean fluorescence intensities of various proteins were plotted after recording signals from at least 15 cells from 3 different fields. Quantitation was done by Nikon advanced analysis software, and images were captured using a digital camera (DS Qj2; Nikon Corp.). Data were analyzed by 2-way ANOVA. Error bars represent means \pm SEM ($n = 3$). Original magnification, $\times 600$. Scale bars, 10 μ m. *D*) A representative immunoblot ($n = 3$) result detects the level of PHD3 along with ac-Siah2, Siah2, and Hif1 α in the above-mentioned stable MKN45 cells after *H. pylori* infection. PHD3 degradation was significantly down-regulated in K139R cells in comparison to WT cells. Error bars indicate SEM ($n = 3$). ** $P < 0.01$, *** $P < 0.001$, **** $P < 0.0001$.



equally detected in these stable cells, establishing no effect of *hif1 α* knockdown in regulating Siah2 in *H. pylori*-infected GCCs. It is well established that Hif1 α is a determinant factor of metastasis in gastric adenocarcinoma (44).

We performed Transwell migration assay to evaluate the effect of *hif1 α* suppression on cell migration ability of *H. pylori*-infected GCCs. Migration ability of *hif1 α* shRNA-transfected AGS cells was significantly impaired in both the uninfected and infected cells in comparison to their counterparts in the empty vector or scrambled shRNA-transfected groups (Fig. 4A). Wound-healing assay showed a similar trend; *H. pylori*-induced wound healing ability was remarkably less in *hif1 α* -suppressed AGS cells in comparison to the empty vector and scrambled shRNA-expressing cells (Supplemental Fig. 3). Matrigel-invasion assay was performed to assess cell invasiveness of *hif1 α* shRNA-expressing AGS cells. Significantly less cell invasion was observed in *hif1 α* -suppressed and infected AGS cells as compared with the empty vector-expressing infected AGS cells (Fig. 4B). Western blotting showed significantly

suppressed Hif1 α protein in *hif1 α* shRNA-expressing cells (Fig. 4C).

Acetylation of Siah2 at K¹³⁹ enhances invasiveness of GCCs via up-regulation of Hif1 α

We found that *siah2* WT induced Hif1 α in the infected GCCs, whereas *siah2* K139R markedly reduced this effect (Fig. 3A). Because Hif1 α mediated the invasiveness and migration-inducing effect of *H. pylori* (Fig. 4 and Supplemental Fig. 3), we investigated the effect of K139R mutation on the adherence property of GCCs. MKN45 cells were stably transfected with the empty vector, WT *siah2*, or *siah2* K139R constructs. *siah2* WT construct-transfected cells were round and less adherent than the weakly adherent K139R-transfected or empty vector-expressing cells (Fig. 5A). The change in anchorage-independent clonogenic potential of *siah2*-expressing *H. pylori*-infected cells was assessed

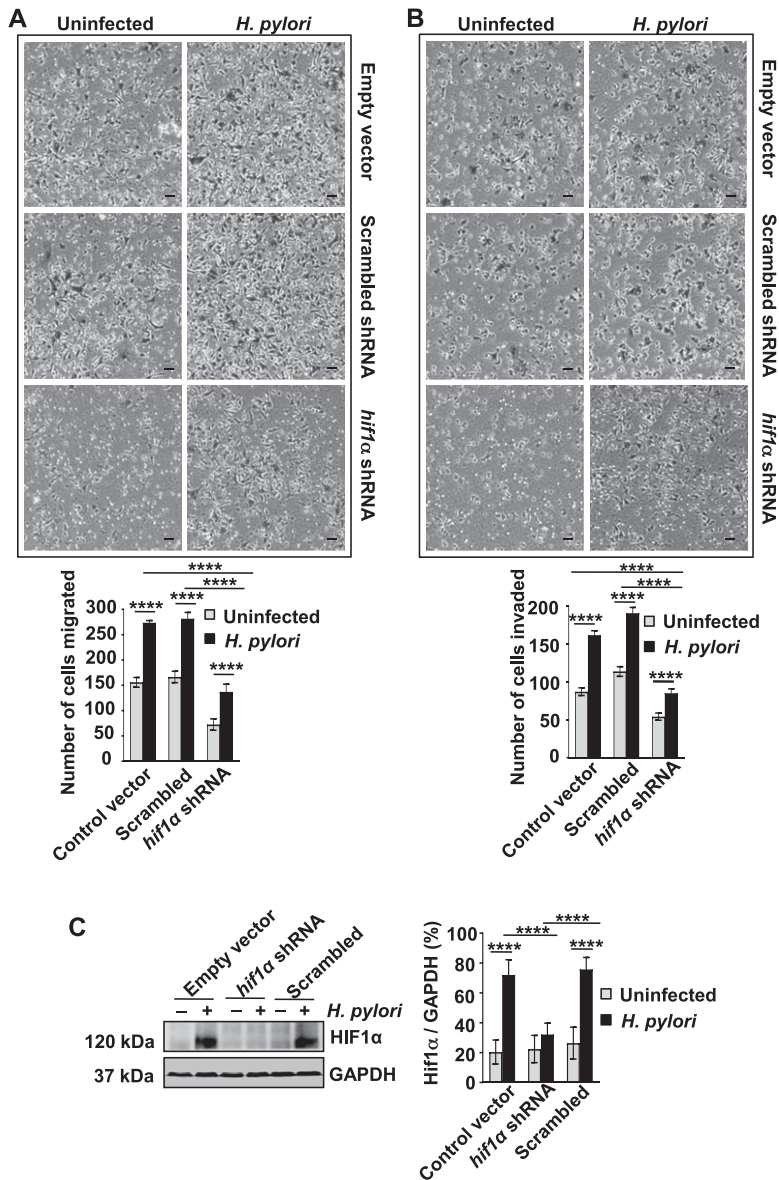


Figure 4. *hif1α* suppression reduces migration and invasion of *H. pylori*-infected human GCCs. **A)** Transwell migration assay shows the effect of *hif1α* silencing on migration ability of empty vector, scrambled shRNA, and *hif1α* shRNA stably transfected AGS cells. The migrated cells were counted under the microscope, and images were captured and plotted. The graph depicts means \pm SEM ($n = 3$). Original magnification, $\times 200$. Scale bars, 50 μ m. **B)** Result represents the invasive property of AGS *hif1α* stable cells. The graph represents means \pm SEM ($n = 3$). Scale bars, 50 μ m. **C)** Representative Western blot analysis ($n = 3$) from cell lysates of empty vector, scrambled shRNA, and *hif1α* shRNA-expressing AGS cells after 12 h of *H. pylori* infection. Bars depict Hif1 α expression over GAPDH control. Data were analyzed by 2-way ANOVA with Tukey's *post hoc* analysis. Error bars represent SEM ($n = 3$). **** $P < 0.0001$.

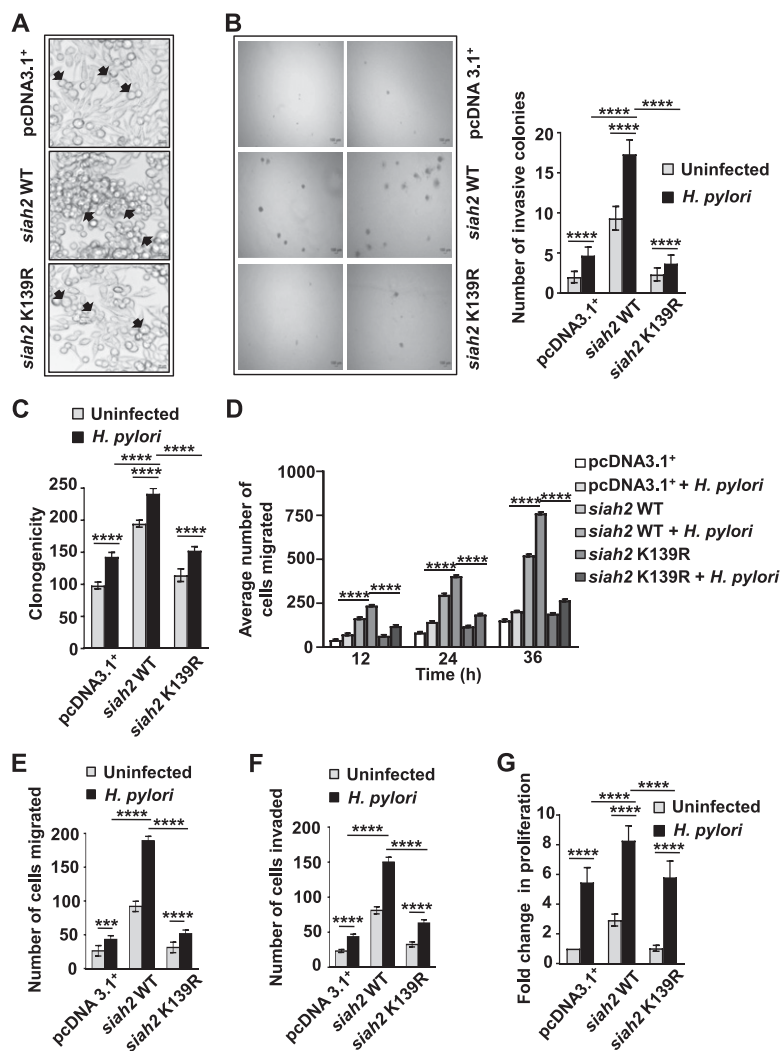
by soft-agar assay. The number of foci formed was significantly higher in the infected WT *siah2*-expressing cells as compared with the K139R and empty vector-expressing infected cells (Fig. 5B). Likewise, anchorage-dependent clonogenic potential was significantly higher in WT *siah2* construct-transfected cells (Fig. 5C). Due to the inherent semiadherent nature of MKN45 cells, a more adherent gastric adenocarcinoma cell line (AGS cells) was used to study the effect of *H. pylori* on the wound-healing property. For this, AGS cells were stably transfected with the empty vector, WT *siah2*, or *siah2* K139R constructs. WT *siah2*-expressing cells showed significantly more wound-healing ability than the empty vector and K139R-expressing cells (Fig. 5D). To evaluate the influence of Siah2 acetylation at K¹³⁹ on the ability of migration and invasion of *H. pylori*-infected GCCs, transwell migration, and invasion assays were performed using AGS pcDNA3.1⁺, *siah2* WT, and *siah2* K139R mutant stably transfected cells. *siah2* K139R mutant stable cells showed significantly less cell migration and cell invasion as

compared with their counterparts from the other 2 transfected groups (Fig. 5E, F). MKN45 cells were transfected with *siah2* WT and K139R overexpression plasmids, and the differences in their proliferation were assessed by MTT assay. The K139R mutation resulted in significantly decreased proliferation as compared with the WT *siah2*-transfected cells after 12 h *H. pylori* infection (Fig. 5G).

Helicobacter-infected mouse and human gastric epithelia have remarkably high ac-K¹³⁹ Siah2, Siah2, and Hif1 α proteins

C57BL/6 mice infected for 12 mo with *H. felis* manifested the classic events of *Helicobacter*-driven carcinogenic cascade. Immunofluorescence microscopy of the tissue samples that revealed features of invasive adenocarcinoma showed very high expression of ac-K¹³⁹ Siah2, Siah2, and Hif1 α as compared with the uninfected noncancer tissues.

Figure 5. *siah2* K139R mutation reduces cell migration and invasion. **A)** Images showing cellular morphology after *siah2* K139R mutation in MKN45 cells. Original magnification, $\times 600$. Scale bars, 20 μm . **B)** Soft agar colony formation assay performed with MKN45 *siah2* WT, *siah2* K139R, or empty vector stable cells shows a significant increase in colony forming ability of *siah2* WT cells, which was reduced significantly upon K139R mutation. Bar graph represents the mean of number of invaded cells (means \pm SEM, $n = 3$). **C)** Bar graph representing clonogenicity assay using MKN45 pcDNA3.1⁺, *siah2* WT, and *siah2* K139R stable cells showing increased anchorage-dependent growth of *siah2* WT cells than the other transfected groups ($n = 3$). **D)** Graphical representation of the wound-healing assay using MKN45 pcDNA3.1⁺, *siah2* WT, and *siah2* K139R stable cells shows that K139R mutation diminishes the wound-healing ability induced by *H. pylori*. The data represent the mean number of migrated cells from 3 independent experiments (means \pm SEM). **E)** The role of ac-K¹³⁹ Siah2 on the invasiveness of infected GCCs was assessed by Transwell migration and invasion assays using AGS pcDNA3.1⁺, *siah2* WT, and *siah2* K139R stable cells. Graphical representation of the data shows that *siah2* WT stable cells attain maximal migration ability after *H. pylori* infection than their counterparts in other transfection groups. Bar graph represents mean number \pm SEM of migrated cells ($n = 3$). **F)** Bar graph generated from the Transwell migration showing that the average number of cells invading the matrigel after infection was significantly higher in the *siah2* WT group as compared with the K139R stable cells. Bars indicate means \pm SEM. **G)** MTT assay graph shows *H. pylori*-mediated induction of cell proliferative ability of *siah2* WT-expressing cells as compared with K139R-expressing cells (means \pm SEM, $n = 3$). All data are analyzed by 2-way ANOVA with Tukey's *post hoc* analysis. Error bars represent SEM ($n = 3$). **** $P < 0.0001$.



Infected mice showed remarkably high mucus gland metaplasia, dysplasia, or invasive adenocarcinoma. All infected tissues showed marked infiltration of mononuclear cells in the submucosa or marked hypertrophy of the gastric mucosa (H&E staining) (Fig. 6A). Mice that showed invasive cancer also had significantly high splenomegaly (Fig. 6B).

Comparison of metastatic gastric cancer biopsy samples ($n = 14$, urease test positive) collected from consenting patients with noncancer tissues showed that cancer samples had high expression of ac-K¹³⁹ Siah2, Siah2, and Hif1 α in comparison to noncancerous samples ($n = 14$) (Fig. 6C). Accompanying H&E staining revealed the histologic features of normal gastric mucosa and metastatic gastric cancer. CagA protein expression was also compared between urease test-positive metastatic gastric biopsy samples collected from patients and uninfected tissues. The immunofluorescence data clearly showed that invasive gastric cancer samples were infected with CagA (+) *H. pylori* strains.

Overall, our data confirmed that Siah2 expression is induced in *H. pylori*-infected GCCs. p300 HAT-mediated acetylation of Siah2 at the K¹³⁹ position

increases its stability, promoting degradation of PHD3 and accumulation of Hif1 α . Hif1 α , in turn, increases invasiveness of *H. pylori*-infected GCCs. Figure 7 summarizes our findings.

DISCUSSION

We have reported previously that *H. pylori* increase Siah2 expression and enhance invasiveness in GCCs (18). Here, we show for the first time that Siah2 gets acetylated by p300 in *H. pylori*-infected GCCs and identify that acetylation of Siah2 is crucial to increase Hif1 α stability in the infected epithelium. Siah2 acetylation at K¹³⁹ stabilizes the protein and thereby promotes degradation of PHD3 and causes accumulation of Hif1 α in the infected GCCs. This study also establishes the significance of Siah2 acetylation in regulating Hif1 α -mediated metastasis. The novelty of this work lies in the fact that until now acetylation of Siah2 and its effect have not been reported, whereas SUMOylation and phosphorylation effects have been studied (45–49). Because ac-K¹³⁹ Siah2 is significantly induced in the infected and metastatic GCCs in comparison to the

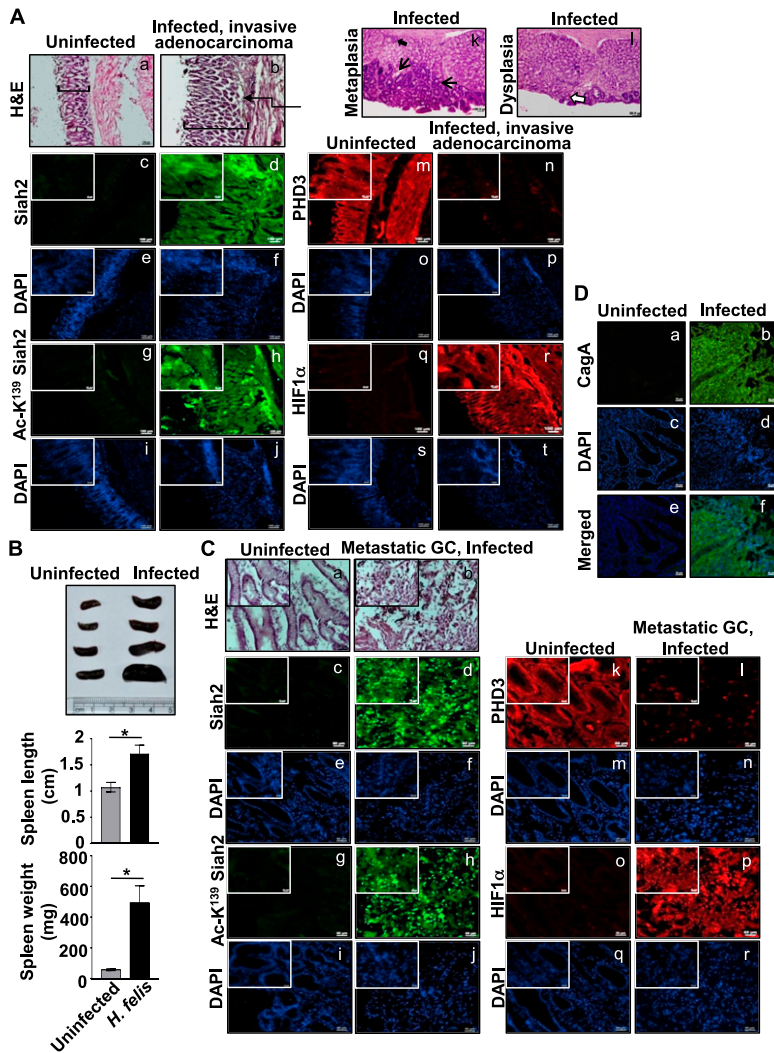


Figure 6. Enhanced Siah2 and Hif1 α expression and decreased PHD3 expression in *Helicobacter*-infected mouse and human gastric epithelia. **A)** H&E staining of uninfected (*a*) and infected (*b*, *k*, *l*) antral gastric tissues from C57BL/6 mice. Infected mice show thickening of mucosa (bar), inflammatory infiltrations (thick arrow), mucosal metaplasia (thin arrow), and dysplasia (open arrow). Mucosa to submucosal invasiveness is also observed in *b* (elbow arrow). Corresponding fluorescence microscopy data from tissues (*a*, *b*) showing Siah2 (*c*, *d*), ac-K¹³⁹ Siah2 (*g*, *h*), PHD3 (*m*, *n*), Hif1 α (*q*, *r*), and DAPI (*e*, *f*, *i*, *j*, *o*, *p*, *s*, *t*). Original magnification, $\times 100$ (inset, $\times 400$). Scale bars, 100 μm (50 μm ; *k*, *l*). **B)** Splenomegaly in infected mice. Data were analyzed by Student's *t* test. Error bars indicate SEM. $*P < 0.05$. **C)** H&E staining of human noncancer, uninfected (*a*), and metastatic gastric cancer (*b*) biopsy samples and fluorescence microscopy showing Siah2 (*c*, *d*), Ac-K¹³⁹ Siah2 (*g*, *h*), PHD3 (*k*, *l*), Hif1 α (*o*, *p*), and DAPI (*e*, *f*, *i*, *j*, *m*, *n*, *q*, *r*). Original magnification, $\times 100$; 400 (inset). Scale bar, 50 μm ; 25 μm (inset). **D)** Human noncancer and metastatic gastric cancer biopsy samples showing immunofluorescence microscopy data of CagA (*a*, *b*) and DAPI staining (*c*, *d*), merged images (*e*, *f*). Original magnification, $\times 200$. Scale bars, 50 μm .

uninfected GCCs, we believe that ac-Siah2–Hif1 α axis may be a good target for therapy.

Werth *et al.* (50) ascribe Hif1 activation as a “general phenomenon” in various human infections with bacteria, viruses, protozoa, and fungi and link enhanced Hif1 level with host defense strategies. A solid line of evidence supports this view (51–54). Myeloid cells phagocytose bacteria more efficiently under hypoxic conditions, and Hif1 contributes to this process (55). Hif1 has recently been implicated in maintaining the gut barrier function (56). The synergy between the hypoxic and immune response is established by the transcription factor NF- κ B. In macrophages, NF- κ B is induced in hypoxia and in bacterial infection, and it can transcriptionally up-regulate Hif1 α (57).

Post-translational modification in the form of hydroxylation, however, is responsible for normoxic degradation of Hif1 α . Hydroxylation of Hif1 α at specific proline residues is catalyzed by PHD proteins under normoxia. Hydroxylated Hif1 α attracts the tumor suppressor E3 ubiquitin ligase von Hippel-Lindau and leads to the proteasomal degradation of Hif1 α (58). Although this mode of post-translational regulation by PHDs under normoxia has been widely studied, the nonhypoxic

regulation of Hif1 α by PHD3 is less explored. Recent views indicate that many nonhypoxic stimuli, such as lipopolysaccharide, angiotensin II, thrombin, and vitamin D analog paricalcitol, can accumulate Hif1 α protein by mechanisms other than protein stability (59, 60). Inhibition of PHDs during hypoxia is one mechanism for hypoxic accumulation of Hif1 α (61). A few studies have identified the mechanism of suppression of PHD2 in normoxia. Vaccinia virus C16 protein can bind with PHD2 protein, thereby barring degradation of Hif1 α (62). In normoxia, NO and ROS can inhibit PHD2 activity (63). Cholesterol can also cause Hif1 α accumulation in normoxic hepatocytes in an ROS- and NO-dependent manner (64). However, the effect of ROS on PHD2-dependent Hif1 α degradation has been shown to be regulated by the duration of exposure (65). Siah2 can regulate PHD3 and PHD1 proteins in the range of normoxia to mild hypoxia and causes accumulation of Hif1 α protein (66).

Our study corroborates earlier findings that show the importance of the Siah2–PHD3 axis in regulating Hif1 α stability (67) and tumor development in normoxia (66). We confirm that, in *H. pylori*-infected GCCs, acetylation stabilizes Siah2 from being proteasomally degraded.

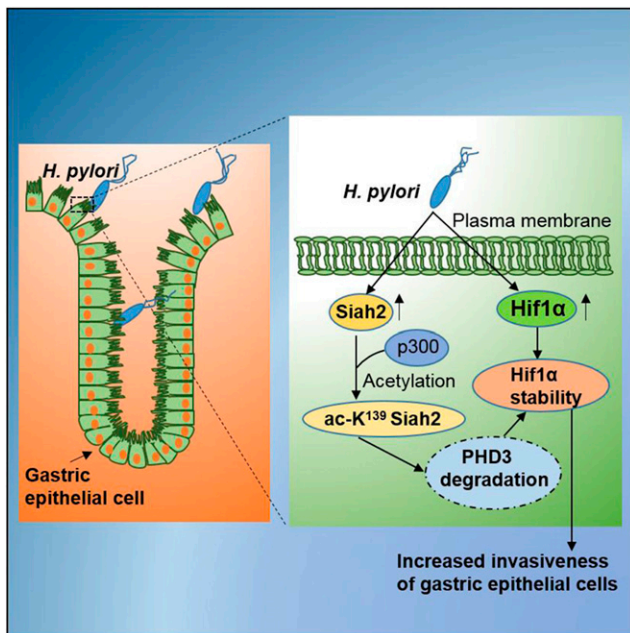


Figure 7. A schematic depicting that acetylation of Siah2 stabilizes Hif1 α expression through PHD3 degradation in *H. pylori*-infected GCCs. Siah2 expression is induced in *H. pylori*-infected GCCs. p300 HAT-mediated acetylation of Siah2 at K¹³⁹ position increases Siah2 protein stability, resulting in enhanced degradation of PHD3 and accumulation of Hif1 α . Accumulation of Hif1 α increases invasiveness of *H. pylori*-infected gastric epithelial cells.

Furthermore, we show that acetylation at the K¹³⁹ residue in the substrate binding domain does not affect Siah2 interaction with PHD3. Decreased PHD3 availability due to increased stability of ac-Siah2 promotes proteasomal degradation of PHD3 and Hif1 α protein accumulation in *H. pylori*-infected GCCs. This work affirms the importance of Siah2 in regulation of tumorigenesis and validates another finding (54) that shows that *H. pylori*-mediated Hif1 α protein stabilization is a *cag* PAI-independent event. This finding shows that all *H. pylori* strains might regulate Siah2 acetylation to establish infection and warrants further investigation.

SUMOylation has been reported to regulate Siah2 stability (45–47). Phosphorylation has also been reported to increase the transcriptional activation of Siah2 (48) and regulates its interaction with HIPK2, a Ser/Thr kinase (25). Ours is the first report on Siah2 acetylation and its functional impact. This report further describes the importance of acetylation in enhancing the stability of Siah2 in *H. pylori*-infected GCCs. Because acetylation of Siah2 is highly induced in *H. pylori*-infected human gastric or *H. felis*-infected murine tissue samples but not in uninfected GCCs, we believe that deacetylation approaches would be effective to target ac-Siah2-positive cancers. Since this study demonstrates that the HAT/KAT inhibitor CTK7A reduces Siah2 acetylation, we believe that deacetylation of Siah2 would be a successful therapeutic checkpoint to treat gastric cancer. FJ

ACKNOWLEDGMENTS

This work was supported by the Indian Department of Biotechnology (BT/PR15092/GBD/27/311/2011), and by the Indian Science and Engineering Research Board (SB/SO/BB-0015/2014) (to A.B.). S.B.K., P.D., A.D.R., I.P., and D.C. are supported by fellowships from Indian Department of Atomic Energy (DAE). The authors declare no conflicts of interest.

AUTHOR CONTRIBUTIONS

S.B.K. performed the experiments and analyzed the results; P.D. generated the histology data; L.D. and S.R. prepared the stable cells; A.D.R., I.P., and D.C. assisted in manuscript preparation and managing the figures; N.R. and S.P.S. helped with gastric cancer biopsy collection and analysis; and A.B. conceived the work, designed experiments, analyzed the data, supervised the work, and wrote the paper.

REFERENCES

- Zhao, C., Lu, X., Bu, X., Zhang, N., and Wang, W. (2010) Involvement of tumor necrosis factor- α in the upregulation of CXCR4 expression in gastric cancer induced by *Helicobacter pylori*. *BMC Cancer* **10**, 419
- Noto, J. M., Chopra, A., Loh, J. T., Romero-Gallo, J., Piazuelo, M. B., Watson, M., Leary, S., Beckett, A. C., Wilson, K. T., and Cover, T. L. (2017) Pan-genomic analyses identify key *Helicobacter pylori* pathogenic loci modified by carcinogenic host microenvironments. *Gut*. **Sep 18**, pii: gutjnl-2017-313863
- Hatakeyama, M. (2014) *Helicobacter pylori* CagA and gastric cancer: a paradigm for hit-and-run carcinogenesis. *Cell Host Microbe* **15**, 306–316
- Guillemin, K., Salama, N. R., Tompkins, L. S., and Falkow, S. (2002) Cag pathogenicity island-specific responses of gastric epithelial cells to *Helicobacter pylori* infection. *Proc. Natl. Acad. Sci. USA* **99**, 15136–15141
- Tsugawa, H., Suzuki, H., Saya, H., Hatakeyama, M., Hirayama, T., Hirata, K., Nagano, O., Matsuzaki, J., and Hibi, T. (2012) Reactive oxygen species-induced autophagic degradation of *Helicobacter pylori* CagA is specifically suppressed in cancer stem-like cells. *Cell Host Microbe* **12**, 764–777
- Gobert, A. P., and Wilson, K. T. (2017) Human and *Helicobacter pylori* interactions determine the outcome of gastric diseases. In *Molecular Pathogenesis and Signal Transduction by Helicobacter pylori*, pp. 27–52, Springer, New York
- Park, J.-H., Kim, T.-Y., Jong, H.-S., Kim, T. Y., Chun, Y.-S., Park, J.-W., Lee, C.-T., Jung, H. C., Kim, N. K., and Bang, Y.-J. (2003) Gastric epithelial reactive oxygen species prevent normoxic degradation of hypoxia-inducible factor-1 α in gastric cancer cells. *Clin. Cancer Res.* **9**, 433–440
- Bhattacharyya, A., Chattopadhyay, R., Hall, E. H., Mebrahtu, S. T., Ernst, P. B., and Crowe, S. E. (2010) Mechanism of hypoxia-inducible factor 1 α -mediated Mcl1 regulation in *Helicobacter pylori*-infected human gastric epithelium. *Am. J. Physiol. Gastrointest. Liver Physiol.* **299**, G1177–G1186
- Jung, J.-H., Im, S., Jung, E. S., and Kang, C. S. (2013) Clinicopathological implications of the expression of hypoxia-related proteins in gastric cancer. *Int. J. Med. Sci.* **10**, 1217–1223
- Thomas, S., Harding, M. A., Smith, S. C., Overvest, J. B., Nitz, M. D., Frierson, H. F., Tomlins, S. A., Kristiansen, G., and Theodorescu, D. (2012) CD24 is an effector of HIF-1-driven primary tumor growth and metastasis. *Cancer Res.* **72**, 5600–5612
- Zhao, Q., Li, Y., Tan, B. B., Fan, L. Q., Yang, P. G., and Tian, Y. (2015) HIF-1 α induces multidrug resistance in gastric cancer cells by inducing MiR-27a. *PLoS One* **10**, e0132746
- Zhao, Q., Tan, B.-B., Li, Y., Fan, L.-Q., Yang, P.-G., and Tian, Y. (2016) Enhancement of drug sensitivity by knockdown of HIF-1 α in gastric carcinoma cells. *Oncol. Res.* **23**, 129–136

13. Zhu, C. L., Huang, Q., Liu, C. H., Lin, X. S., and Xie, F. (2013) Prognostic value of HIF-1 α expression in patients with gastric cancer. *Mol. Biol. Rep.* **40**, 6055–6062
14. Teeling, E. C., Springer, M. S., Madsen, O., Bates, P., O'Brien, S. J., and Murphy, W. J. (2005) A molecular phylogeny for bats illuminates biogeography and the fossil record. *Science* **307**, 580–584
15. Das, L., Kokate, S. B., Dixit, P., Rath, S., Rout, N., Singh, S. P., Crowe, S. E., and Bhattacharyya, A. (2017) Membrane-bound β -catenin degradation is enhanced by ETS2-mediated Siah1 induction in *Helicobacter pylori*-infected gastric cancer cells. *Oncogenesis* **6**, e327
16. Wong, C. S., and Möller, A. (2013) Siah: a promising anti-cancer target. *Cancer Res.* **73**, 2400–2406
17. Knauer, S. K., Mahendrarajah, N., Roos, W. P., and Krämer, O. H. (2015) The inducible E3 ubiquitin ligases SIAH1 and SIAH2 perform critical roles in breast and prostate cancers. *Cytokine Growth Factor Rev.* **26**, 405–413
18. Das, L., Kokate, S. B., Rath, S., Rout, N., Singh, S. P., Crowe, S. E., Mukhopadhyay, A. K., and Bhattacharyya, A. (2016) ETS2 and Twist1 promote invasiveness of *Helicobacter pylori*-infected gastric cancer cells by inducing Siah2. *Biochem. J.* **473**, 1629–1640
19. Sarkar, T. R., Sharan, S., Wang, J., Pawar, S. A., Cantwell, C. A., Johnson, P. F., Morrison, D. K., Wang, J.-M., and Sterneck, E. (2012) Identification of a Src tyrosine kinase/SIAH2 E3 ubiquitin ligase pathway that regulates C/EBP δ expression and contributes to transformation of breast tumor cells. *Mol. Cell. Biol.* **32**, 320–332
20. Müller, S., Chen, Y., Ginter, T., Schäfer, C., Buchwald, M., Schmitz, L. M., Klitzsch, J., Schütz, A., Haitel, A., Schmid, K., Moriggl, R., Kenner, L., Friedrich, K., Haan, C., Petersen, I., Heinzel, T., and Krämer, O. H. (2014) SIAH2 antagonizes TYK2-STAT3 signaling in lung carcinoma cells. *Oncotarget* **5**, 3184–3196
21. Griffiths, E. A., Pritchard, S. A., Valentine, H. R., Whitcho, N., Bishop, P. W., Ebert, M. P., Price, P. M., Welch, I. M., and West, C. M. (2007) Hypoxia-inducible factor-1 α expression in the gastric carcinogenesis sequence and its prognostic role in gastric and gastroesophageal adenocarcinomas. *Br. J. Cancer* **96**, 95–103
22. Nakayama, K., Frew, I. J., Hagensen, M., Skals, M., Habelhah, H., Bhoumik, A., Kadoya, T., Erdjument-Bromage, H., Tempst, P., Frappell, P. B., Bowtell, D. D., and Ronai, Z. (2004) Siah2 regulates stability of prolyl-hydroxylases, controls HIF1 α abundance, and modulates physiological responses to hypoxia. *Cell* **117**, 941–952
23. Nihira, N. T., Ogura, K., Shimizu, K., North, B. J., Zhang, J., Gao, D., Inuzuka, H., and Wei, W. (2017) Acetylation-dependent regulation of MDM2 E3 ligase activity dictates its oncogenic function. *Sci. Signal.* **10**, pii: eaai8026
24. Hatakeyama, S. (2011) TRIM proteins and cancer. *Nat. Rev. Cancer* **11**, 792–804
25. Calzado, M. A., de la Vega, L., Möller, A., Bowtell, D. D., and Schmitz, M. L. (2009) An inducible autoregulatory loop between HIPK2 and Siah2 at the apex of the hypoxic response. *Nat. Cell Biol.* **11**, 85–91
26. Bhattacharyya, A., Chattopadhyay, R., Burnette, B. R., Cross, J. V., Mitra, S., Ernst, P. B., Bhakat, K. K., and Crowe, S. E. (2009) Acetylation of apurinic/aprimidinic endonuclease-1 regulates *Helicobacter pylori*-mediated gastric epithelial cell apoptosis. *Gastroenterology* **136**, 2258–2269
27. Rath, S., Das, L., Kokate, S. B., Ghosh, N., Dixit, P., Rout, N., Singh, S. P., Chattopadhyay, S., Ashktorab, H., Smoot, D. T., Swamy, M. M., Kundu, T. K., Crowe, S. E., and Bhattacharyya, A. (2017) Inhibition of histone/lysine acetyltransferase activity kills CoCl₂-treated and hypoxia-exposed gastric cancer cells and reduces their invasiveness. *Int. J. Biochem. Cell Biol.* **82**, 28–40
28. Wade, M., Li, Y.-C., and Wahl, G. M. (2013) MDM2, MDMX and p53 in oncogenesis and cancer therapy. *Nat. Rev. Cancer* **13**, 83–96
29. Roy, R., Chun, J., and Powell, S. N. (2011) BRCA1 and BRCA2: different roles in a common pathway of genome protection. *Nat. Rev. Cancer* **12**, 68–78
30. Liu, S., Fei, W., Shi, Q., Li, Q., Kuang, Y., Wang, C., He, C., and Hu, X. (2017) CHAC2, downregulated in gastric and colorectal cancers, acted as a tumor suppressor inducing apoptosis and autophagy through unfolded protein response. *Cell Death Dis.* **8**, e3009
31. Chaugule, V. K., and Walden, H. (2016) Specificity and disease in the ubiquitin system. *Biochem. Soc. Trans.* **44**, 212–227
32. Liang, Y., Hu, J., Li, J., Liu, Y., Yu, J., Zhuang, X., Mu, L., Kong, X., Hong, D., Yang, Q., and Hu, G. (2015) Epigenetic activation of TWIST1 by MTDH promotes cancer stem-like cell traits in breast cancer. *Cancer Res.* **75**, 3672–3680
33. Qian, J., Luo, Y., Gu, X., Zhan, W., and Wang, X. (2013) Twist1 promotes gastric cancer cell proliferation through up-regulation of FoxM1. *PLoS One* **8**, e77625
34. Deng, W., Wang, C., Zhang, Y., Xu, Y., Zhang, S., Liu, Z., and Xue, Y. (2016) GPS-PAIL: prediction of lysine acetyltransferase-specific modification sites from protein sequences. *Sci. Rep.* **6**, 39787
35. Fang, S., Jensen, J. P., Ludwig, R. L., Voudsen, K. H., and Weissman, A. M. (2000) Mdm2 is a RING finger-dependent ubiquitin protein ligase for itself and p53. *J. Biol. Chem.* **275**, 8945–8951
36. Li, M., Luo, J., Brooks, C. L., and Gu, W. (2002) Acetylation of p53 inhibits its ubiquitination by Mdm2. *J. Biol. Chem.* **277**, 50607–50611
37. Ito, A., Kawaguchi, Y., Lai, C. H., Kovacs, J. J., Higashimoto, Y., Appella, E., and Yao, T. P. (2002) MDM2-HDAC1-mediated deacetylation of p53 is required for its degradation. *EMBO J.* **21**, 6236–6245
38. Du, Z., Song, J., Wang, Y., Zhao, Y., Guda, K., Yang, S., Kao, H.-Y., Xu, Y., Willis, J., Markowitz, S. D., Sedwick, D., Ewing, R. M., and Wang, Z. (2010) DNMT1 stability is regulated by proteins coordinating deubiquitination and acetylation-driven ubiquitination. *Sci. Signal.* **3**, ra80
39. Aprelikova, O., Chandramouli, G. V., Wood, M., Vasselli, J. R., Riss, J., Maranchie, J. K., Linehan, W. M., and Barrett, J. C. (2004) Regulation of HIF prolyl hydroxylases by hypoxia-inducible factors. *J. Cell. Biochem.* **92**, 491–501
40. Appelhoff, R. J., Tian, Y.-M., Raval, R. R., Turley, H., Harris, A. L., Pugh, C. W., Ratcliffe, P. J., and Gleadle, J. M. (2004) Differential function of the prolyl hydroxylases PHD1, PHD2, and PHD3 in the regulation of hypoxia-inducible factor. *J. Biol. Chem.* **279**, 38458–38465
41. Minamishima, Y. A., Moslehi, J., Padera, R. F., Bronson, R. T., Liao, R., and Kaelin, W. G., Jr. (2009) A feedback loop involving the Phd3 prolyl hydroxylase tunes the mammalian hypoxic response in vivo. *Mol. Cell. Biol.* **29**, 5729–5741
42. Baba, K., Morimoto, H., and Imaoka, S. (2013) Seven in absentia homolog 2 (Siah2) protein is a regulator of NF-E2-related factor 2 (Nrf2). *J. Biol. Chem.* **288**, 18393–18405
43. Rath, S., Das, L., Kokate, S. B., Pratheek, B. M., Chattopadhyay, S., Goswami, C., Chattopadhyay, R., Crowe, S. E., and Bhattacharyya, A. (2015) Regulation of Noxa-mediated apoptosis in *Helicobacter pylori*-infected gastric epithelial cells. *FASEB J.* **29**, 796–806
44. Rohwer, N., Lobitz, S., Daskalow, K., Jöns, T., Vieth, M., Schlag, P. M., Kemmer, W., Wiedenmann, B., Cramer, T., and Höcker, M. (2009) HIF-1 α determines the metastatic potential of gastric cancer cells. *Br. J. Cancer* **100**, 772–781
45. Cheng, J., Kang, X., Zhang, S., and Yeh, E. T. (2007) SUMO-specific protease 1 is essential for stabilization of HIF1 α during hypoxia. *Cell* **131**, 584–595
46. Carbia-Nagashima, A., Gerez, J., Perez-Castro, C., Paez-Pereda, M., Silberstein, S., Stalla, G. K., Holsboer, F., and Arzt, E. (2007) RSUME, a small RWD-containing protein, enhances SUMO conjugation and stabilizes HIF-1 α during hypoxia. *Cell* **131**, 309–323
47. Bae, S.-H., Jeong, J.-W., Park, J. A., Kim, S.-H., Bae, M.-K., Choi, S.-J., and Kim, K.-W. (2004) Sumoylation increases HIF-1 α stability and its transcriptional activity. *Biochem. Biophys. Res. Commun.* **324**, 394–400
48. Richard, D. E., Berra, E., Gothié, E., Roux, D., and Pouyssegur, J. (1999) p42/p44 mitogen-activated protein kinases phosphorylate hypoxia-inducible factor 1 α (HIF-1 α) and enhance the transcriptional activity of HIF-1. *J. Biol. Chem.* **274**, 32631–32637
49. García-Limones, C., Lara-Chica, M., Jiménez-Jiménez, C., Pérez, M., Moreno, P., Muñoz, E., and Calzado, M. A. (2016) CHK2 stability is regulated by the E3 ubiquitin ligase SIAH2. *Oncogene* **35**, 4289–4301
50. Werth, N., Beerlage, C., Rosenberger, C., Yazdi, A. S., Edelmann, M., Amr, A., Bernhardt, W., von Eiff, C., Becker, K., Schäfer, A., Peschel, A., and Kempf, V. A. (2010) Activation of hypoxia inducible factor 1 is a general phenomenon in infections with human pathogens. *PLoS One* **5**, e11576
51. Hartmann, H., Eltzschig, H. K., Wurz, H., Hantke, K., Rakin, A., Yazdi, A. S., Matteoli, G., Bohn, E., Autenrieth, I. B., and Karhausen, J. (2008) Hypoxia-independent activation of HIF-1 by enterobacteriaceae and their siderophores. *Gastroenterology* **134**, 756–767
52. Jantsch, J., Chakravorty, D., Turza, N., Prechtel, A. T., Buchholz, B., Gerlach, R. G., Volke, M., Gläser, J., Warnecke, C., Wiesener, M. S., Eckardt, K. U., Steinkasserer, A., Hensel, M., and Willam, C. (2008) Hypoxia and hypoxia-inducible factor-1 α modulate lipopolysaccharide-induced dendritic cell activation and function. *J. Immunol.* **180**, 4697–4705
53. Schaffer, K., and Taylor, C. T. (2015) The impact of hypoxia on bacterial infection. *FEBS J.* **282**, 2260–2266
54. Matak, P., Heinis, M., Mathieu, J. R., Corriden, R., Cuvelier, S., Delga, S., Mounier, R., Rouquette, A., Raymond, J., Lamarque, D., Emile,

- J. F., Nizet, V., Touati, E., and Peyssonnaud, C. (2015) Myeloid HIF-1 is protective in Helicobacter pylori-mediated gastritis. *J. Immunol.* **194**, 3259–3266
55. Anand, R. J., Gribar, S. C., Li, J., Kohler, J. W., Branca, M. F., Dubowski, T., Sodhi, C. P., and Hackam, D. J. (2007) Hypoxia causes an increase in phagocytosis by macrophages in a HIF-1 α -dependent manner. *J. Leukoc. Biol.* **82**, 1257–1265
 56. Kelly, C. J., Zheng, L., Campbell, E. L., Saeedi, B., Scholz, C. C., Bayless, A. J., Wilson, K. E., Glover, L. E., Kominsky, D. J., Magnuson, A., Weir, T. L., Ehrentraut, S. F., Pickel, C., Kuhn, K. A., Lanis, J. M., Nguyen, V., Taylor, C. T., and Colgan, S. P. (2015) Crosstalk between microbiota-derived short-chain fatty acids and intestinal epithelial HIF augments tissue barrier function. *Cell Host Microbe* **17**, 662–671
 57. Rius, J., Guma, M., Schachtrup, C., Akassoglou, K., Zinkernagel, A. S., Nizet, V., Johnson, R. S., Haddad, G. G., and Karin, M. (2008) NF-kappaB links innate immunity to the hypoxic response through transcriptional regulation of HIF-1 α . *Nature* **453**, 807–811
 58. Jaakkola, P., Mole, D. R., Tian, Y.-M., Wilson, M. I., Gielbert, J., Gaskell, S. J., von Kriegsheim, A., Hebestreit, H. F., Mukherji, M., Schofield, C. J., Maxwell, P. H., Pugh, C. W., and Ratcliffe, P. J. (2001) Targeting of HIF- α to the von Hippel-Lindau ubiquitylation complex by O₂-regulated prolyl hydroxylation. *Science* **292**, 468–472
 59. Kuschel, A., Simon, P., and Tug, S. (2012) Functional regulation of HIF-1 α under normoxia: is there more than post-translational regulation? *J. Cell. Physiol.* **227**, 514–524
 60. Nolan, K. A., Brennan, E. P., Scholz, C. C., Cullen, C., Ryan, A., Taylor, C. T., and Godson, C. (2015) Paricalcitol protects against TGF- β 1-induced fibrotic responses in hypoxia and stabilises HIF- α in renal epithelia. *Exp. Cell Res.* **330**, 371–381
 61. Kaelin, W. G., Jr., and Ratcliffe, P. J. (2008) Oxygen sensing by metazoans: the central role of the HIF hydroxylase pathway. *Mol. Cell* **30**, 393–402
 62. Mazzon, M., Peters, N. E., Loenarz, C., Krysztofinska, E. M., Ember, S. W., Ferguson, B. J., and Smith, G. L. (2013) A mechanism for induction of a hypoxic response by vaccinia virus. *Proc. Natl. Acad. Sci. USA* **110**, 12444–12449
 63. Fong, G.-H., and Takeda, K. (2008) Role and regulation of prolyl hydroxylase domain proteins. *Cell Death Differ.* **15**, 635–641
 64. Anavi, S., Hahn-Obercyger, M., Madar, Z., and Tirosh, O. (2014) Mechanism for HIF-1 activation by cholesterol under normoxia: a redox signaling pathway for liver damage. *Free Radic. Biol. Med.* **71**, 61–69
 65. Niecknig, H., Tug, S., Reyes, B. D., Kirsch, M., Fandrey, J., and Berchner-Pfannschmidt, U. (2012) Role of reactive oxygen species in the regulation of HIF-1 by prolyl hydroxylase 2 under mild hypoxia. *Free Radic. Res.* **46**, 705–717
 66. Nakayama, K., Qi, J., and Ronai, Z. (2009) The ubiquitin ligase Siah2 and the hypoxia response. *Mol. Cancer Res.* **7**, 443–451
 67. Qi, J., Nakayama, K., Gaitonde, S., Goydos, J. S., Krajewski, S., Eroshkin, A., Bar-Sagi, D., Bowtell, D., and Ronai, Z. (2008) The ubiquitin ligase Siah2 regulates tumorigenesis and metastasis by HIF-dependent and -independent pathways. *Proc. Natl. Acad. Sci. USA* **105**, 16713–16718

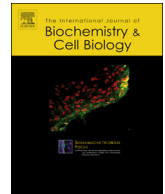
Received for publication November 16, 2017.

Accepted for publication April 16, 2018.



Contents lists available at ScienceDirect

International Journal of Biochemistry and Cell Biology

journal homepage: www.elsevier.com/locate/biocel

Testin and filamin-C downregulation by acetylated Siah2 increases invasiveness of *Helicobacter pylori*-infected gastric cancer cells

Shrikant Babanrao Kokate^a, Pragyesh Dixit^a, Indrajit Poirah^a, Arjama Dhar Roy^a, Debashish Chakraborty^a, Niranjana Rout^b, Shivaram Prasad Singh^c, Hassan Ashktorab^d, Duane T. Smoot^e, Asima Bhattacharyya^{a,*}

^a School of Biological Sciences, National Institute of Science Education and Research (NISER) Bhubaneswar, Homi Bhabha National Institute (HBNI), P.O. Bhubaneswar, Via Jatni, Dist. Khurda Jatni, 752050, Odisha, India

^b Department of Oncopathology, Acharya Harihar Regional Cancer Centre, Cuttack 753007, Odisha, India

^c Department of Gastroenterology, SCB Medical College, Cuttack 753007, Odisha, India

^d Department of Medicine, Howard University, Washington, DC 20060, USA

^e Department of Medicine, Meharry Medical Center, Nashville, TN 37208, USA

ARTICLE INFO

Keywords:

Actin filament
E3 ubiquitin ligase
Cancer invasiveness
Posttranslational modification
Proteasomal degradation

ABSTRACT

Helicobacter pylori is the strongest known risk-factor for gastric cancer. However, its role in gastric cancer metastasis remains unclear. Previously we have reported that *H. pylori* promotes gastric cancer invasiveness by stabilizing the E3 ubiquitin ligase Siah2 which is mediated by Siah2 acetylation at Lys 139 (K¹³⁹) residue. Here we identify that cell adhesion-related proteins testin (TES) and filamin-C (FLN-C) interact with Siah2 and get proteasomally degraded. The efficiency of TES and FLN-C degradation is significantly potentiated by K¹³⁹-acetylated Siah2 (ac-K¹³⁹ Siah2) in infected gastric cancer cells (GCCs). ac-Siah2-mediated downregulation of TES and FLN-C disrupts filopodia structures but promotes lamellipodia formation and enhances invasiveness and migration of infected GCCs. Since *H. felis*-infected mice as well as human gastric cancer biopsy samples also show high level of ac-K¹³⁹ Siah2 and downregulated TES and FLN-C, we believe that acetylation of Siah2 is an important checkpoint that can be useful for therapeutic intervention.

1. Introduction

Gastric cancer is one of the most common cancers and frequent causes of cancer-related mortalities in the world. *Helicobacter pylori* has been classified by the International Agency for Research on Cancer (IARC) as a type I carcinogen responsible for causing gastric cancer (Buti et al., 2011). Strains possessing the cytotoxin-associated gene (*cag*) pathogenicity island (PAI), i.e. *cag* PAI(+) strains, are associated with more severity of the disease (Guillemin and Salama, 2002; Hatakeyama, 2014). *H. pylori* promotes motility of infected gastric epithelial cell (Das et al., 2016) but the mechanism is still not completely understood.

The actin cytoskeleton provides contractile forces that regulate cell motility. Gastric epithelial cells are actin rich (Wolosin et al., 1983). The family of actin-binding filamins (FLNs), FLN-A, B and C, stabilize actin networks and connect them to the cell membrane (Zhou et al., 2010). Silencing of *FLN-C* is associated with primary as well as metastatic gastric cancers (Qiao et al., 2015). Another actin-binding cytoskeletal protein linked with focal adhesion and tight junction is testin (TES) (Garvalov et al., 2003; Sala et al., 2017) and TES too shows tumor-suppressive effects in gastric cancer (Ma et al., 2010). Although *TES* and *FLN-C* are hypermethylated in gastric cancer (Drusco et al., 2005; Ma et al., 2010; Nakajima et al., 2010; Qiao et al., 2015), the

Abbreviations: ac-lys, acetylated lysine; ac-Siah2, acetylated Siah2; ac-K¹³⁹ Siah2, acetylated K¹³⁹ Siah2; ASB2, a suppressor of cytokine signalling box 2 gene; *cag*, cytotoxin-associated gene; CHIP, C-terminus of Hsc70 interacting protein; DAPI, 4',6-Diamidino-2-phenylindole dihydrochloride; CTK7A, sodium-4-(3,5-bis(4-hydroxy-3-methoxystyryl)-1H-pyrazol-1-yl) benzoate; EMT, epithelial to mesenchymal transition; GCCs, gastric cancer cells; *H. pylori*, *Helicobacter pylori*; FITC, fluorescein isothiocyanate; FLNs, filamins; HAT, histone acetyltransferase; Hif1 α , hypoxia-inducible factor 1 α ; IARC, international agency for research on cancer; IP, immunoprecipitation; LSM, laser scanning microscope; MDM2, mouse double minute 2; MOI, multiplicity of infection; PAGE, polyacrylamide gel electrophoresis; PAI, pathogenicity island; PAIL, prediction of acetylation on internal lysines; p.i, post infection; PHD3, prolyl-hydroxylase 3; ROS, reactive oxygen species; RUNX3, Runt-related transcription factor 3; SBD, substrate-binding domain; SDS, sodium dodecyl sulphate; Siah, seven in absentia homolog; siRNA, short interfering ribonucleic acid; TES, testin; WHO, world health organization; WB, western blotting; WT, wild-type

* Corresponding author.

E-mail address: asima@niser.ac.in (A. Bhattacharyya).

<https://doi.org/10.1016/j.biocel.2018.07.012>

Received 22 May 2018; Received in revised form 26 July 2018; Accepted 27 July 2018

Available online 29 July 2018

1357-2725/ © 2018 Elsevier Ltd. All rights reserved.

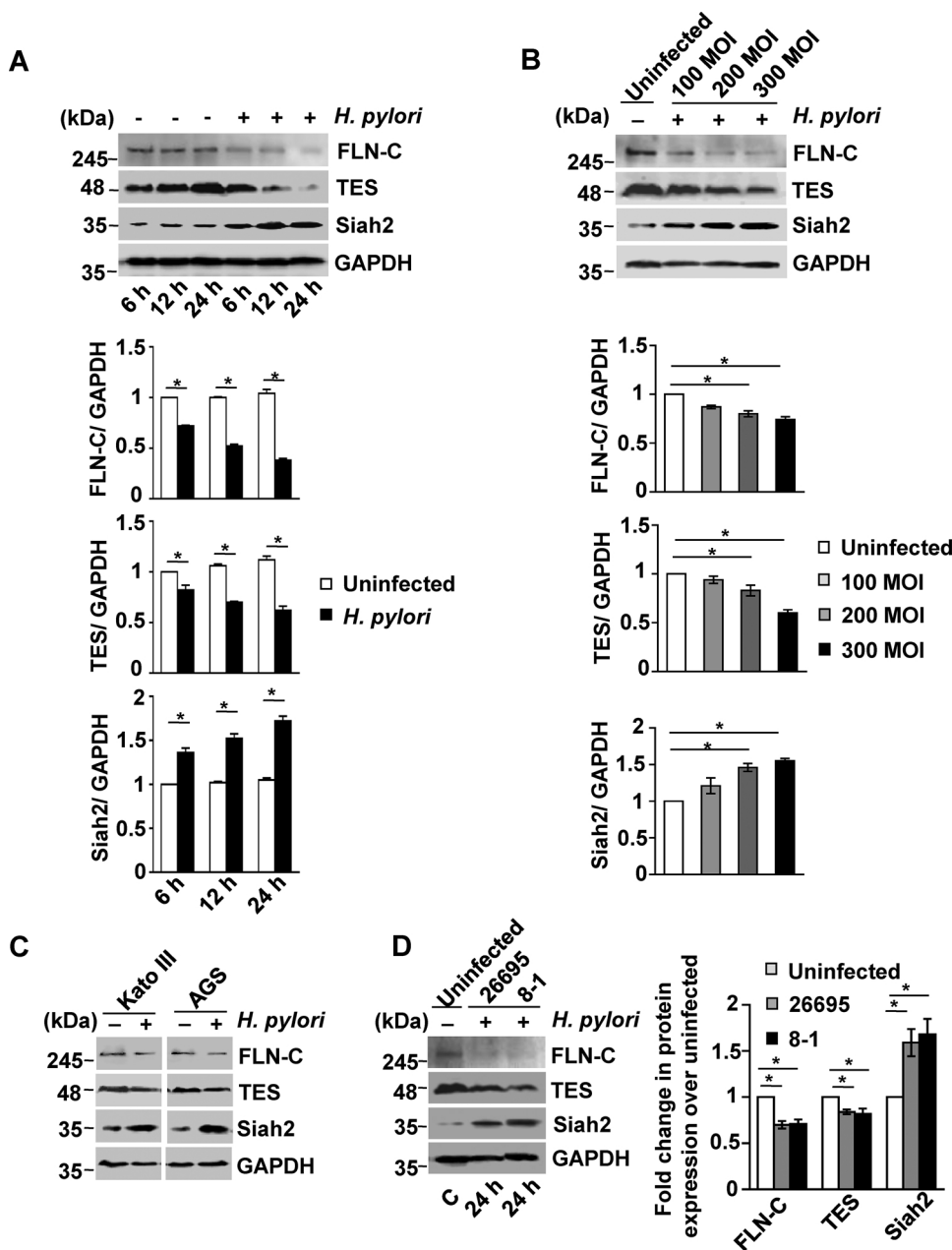


Fig. 1. *H. pylori*-infection results in the down-regulation of TES and FLN-C and increases Siah2 in GCCs. (A) A representative western blot of whole-cell lysates prepared from uninfected and infected (6, 12, and 24 h with a MOI of 200) MKN45 cells showed time-dependent induced increase in Siah2 expression and reduced expression of TES and FLN-C. Densitometric analysis of Siah2, TES, and FLN-C bands shown in (A) represented as normalized Siah2, TES, and FLN-C. Data were analyzed by Student's *t*-test ($n = 3$). Error bars, s.e.m., * $P < 0.05$. (B) A representative figure showing western blot of MKN45 cell lysates infected with MOI 100, 200, and 300 for 24 h. Densitometric analysis represented the expression of Siah2, TES, and FLN-C normalized to control. Data were analyzed by Student's *t* test ($n = 3$). Error bars, s.e.m., * $P < 0.05$. (C) Western blot showing status of Siah2, TES and FLN-C in the Kato III cells and AGS cells. (D) Immunoblotting performed using MKN45 whole-cell lysates infected with *H. pylori* strains 26695 and 8-1 showed that both the strains were equally competent in inducing Siah2 and reducing TES and FLN-C expressions. Bars represented fold change in protein expression over uninfected. Error bars, s.e.m., $n = 3$, * $P < 0.05$. All western blots used GAPDH as a loading control.

frequency and extent of hypermethylation increase in stage III/IV gastric cancer (Oue et al., 2006). Chronic inflammation induced by *H. pylori* also leads to hypermethylation of genes (Yoshida et al., 2013). Although proteasomal degradation of tumor suppressors is an important player in cancer progression, no group has studied proteasomal degradation of TES and FLN-C in *H. pylori*-infected GCCs.

Many tumor suppressor proteins are targeted for ubiquitination-dependent degradation in *H. pylori*-infected gastric epithelial cells (Coombs et al., 2011). Filamin-A (FLN-A) and FLN-B are proteasomally targeted by the E3 ubiquitin ligase ASB2 (Burande et al., 2009) while CHIP, a chaperone-dependent E3 ubiquitin ligase proteasomally degrades FLN-C (Arndt et al., 2010). However, E3 ubiquitin ligase-mediated TES degradation is not yet reported. Although, phosphorylation-mediated activation of E3 ligases is well-known (Chaugule and Walden, 2016), the effect of acetylation on E3 ligases is nearly unexplored. One study shows that the stability and function of mouse double minute 2 (MDM2), an E3 ubiquitin ligase, is critically regulated by p300-mediated acetylation of the protein (Nihira et al., 2017). We have previously shown that Siah2 induces invasiveness of gastric cancer cells

(GCCs) after *H. pylori* infection (Das et al., 2016). Another study from our group establishes that acetylation of Siah2 at K¹³⁹ residue confers invasiveness to *H. pylori*-infected GCCs by degrading prolyl-hydroxylase 3 (PHD3) and thereby stabilizing hypoxia-inducible factor 1 α (Hif1 α) (Kokate et al., 2018).

This study sought to know the effect of Siah2 on tumor-suppressors TES and FLN-C. By using gastric cancer cell lines, murine gastric cancer model and human gastric cancer biopsy samples we show that Siah2 degrades TES and FLN-C in *H. pylori*-infected gastric cancer cells (GCCs). In addition, this study identifies that acetylation at K¹³⁹ residue in the infected GCCs increases the efficiency of Siah2-mediated TES and FLN-C degradation. TES and FLN-C degradation leads to altered actin organization and increases invasiveness of GCCs.

2. Materials and methods

2.1. Cell and bacteria culture and reagents

Gastric cancer cell lines (GCCs) AGS, MKN45, KATO III and

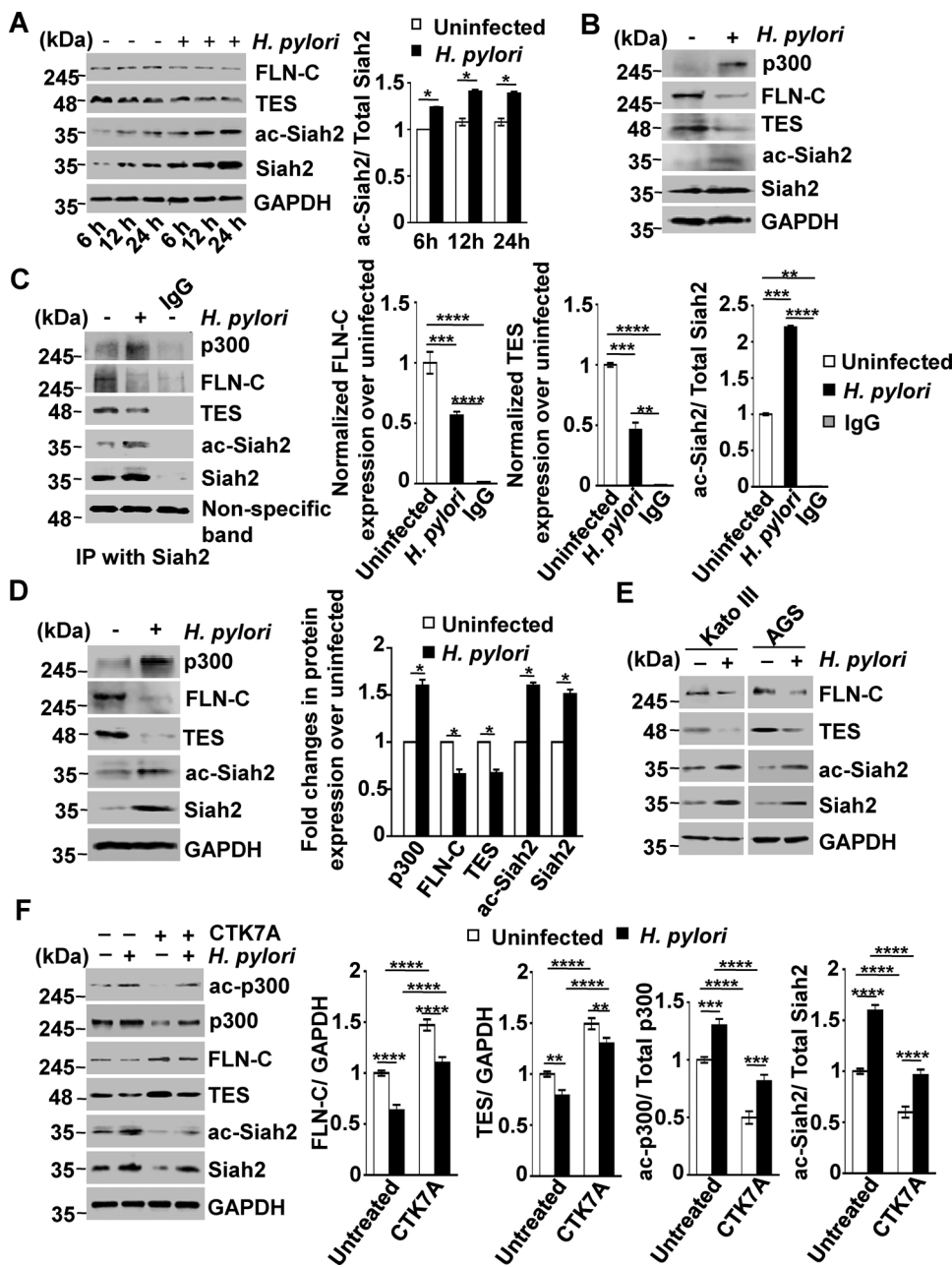


Fig. 2. p300 HAT activity acetylates Siah2 and downregulates TES and FLN-C expression in *H. pylori*-infected GCCs. (A) Western blot analysis of whole cell lysates prepared from control and 200 MOI *H. pylori*-infected MKN45 cells at various time points (6h, 12h, and 24h) was done to assess expression of FLN-C, TES, Siah2 and ac-Siah2. Densitometric analysis was represented as ac-Siah2: total Siah2 expression normalized to loading control. (B) A representative western blot result showing the expression of p300, FLN-C, TES, ac-Siah2 and Siah2 in the uninfected and infected MKN45 cells. (C) Immunoprecipitation experiment was performed to study interaction of Siah2 with p300, FLN-C and TES in the whole cell lysates prepared from uninfected and infected MKN45 cells. Proteins were immunoprecipitated by using Siah2 antibody. Bar graphs represented fold change in protein expression normalized to uninfected control. (D) Immunoblot analysis of whole cell lysates prepared from HFE145 cell, either infected with *H. pylori* (200 MOI) or uninfected, showed induced expression of p300, ac-Siah2, and Siah2 whereas, expression of FLN-C and TES was found to be decreased. Bars depicted fold change in p300, FLN-C, TES, ac-Siah2 and Siah2 proteins expression over uninfected. (E) A representative western blot showing the status of FLN-C, TES, ac-Siah2, and Siah2 proteins in uninfected and *H. pylori*-infected Kato III, MKN45 and AGS cells ($n = 3$). (F) A representative western blot result showing the effect of CTK7A on FLN-C, TES, ac-Siah2, Siah2 ($n = 3$). Representative graphs showed normalized protein expressions. GAPDH was the loading control in all western blot experiments. Error bars, s.e.m., $n = 3$, * $P < 0.05$; ** $P < 0.01$; *** $P < 0.003$; **** $P < 0.0001$.

immortalized GCC HFE145 were cultured and maintained as reported earlier (Rath et al., 2015). *H. pylori* strains 26695 *cag* PAI (+), 8-1 *cag* PAI (-) and *H. felis* strain 49179 (ATCC, Manassas, VA, USA) were cultured and maintained as described previously (Ding et al., 2004; Bhattacharyya et al., 2009). The proteasome inhibitor Z-Leu-Leu-Leu-al (MG132) (Sigma-Aldrich, Milwaukee, WI, USA) was used at 50 μ M concentration for 12 h before bacterial infection. When required, cells were treated with CTK7A (EMD Millipore Corp., Billerica, MA, USA), the inhibitor of HAT/KAT function, at 100 μ M concentration for 24 h.

2.2. Immunoblotting and immunoprecipitation

Whole cell extracts were prepared by standard protein isolation protocol, proteins were separated on SDS-PAGE gel followed by immunoblotting. The primary antibodies used were: Siah2, TES, FLN-C (all from Santa Cruz Biotechnology, Santa Cruz, CA, USA), acetylated lysine (Cell Signalling Technology, Danvers, MA, USA), p300 (Abcam, MD, USA), GAPDH (Abgenex, Bhubaneswar, OD, India). Secondary

antibodies were purchased from Cell Signalling Technology (CST). Bands were detected as reported earlier (Das et al., 2017).

Immunoprecipitation (IP) assays were performed using Siah2, FLN-C and TES antibodies. Equivalent normal goat IgG (Santa Cruz Biotechnology) was used to detect the specificity of immune interactions.

Customized human Siah2 antibody specific for ac-K¹³⁹ (anti-rabbit, polyclonal) was generated by Bioklone Biotech Pvt. Ltd, Chennai, India. This antibody was also suitable to detect ac-K¹⁴⁰ of mouse Siah2. The specificity of this antibody has been tested (Kokate et al., 2018).

2.3. Plasmids, site-directed mutagenesis, siRNAs, transient transfection and generation of stable cells

Empty vector (pcDNA3.1⁺) and *Siah2* WT constructs (Das et al., 2017) were used in this study. *Siah2* acetyl lysine mutant K139R was generated from the *Siah2* WT construct as reported earlier (Kokate et al., 2018). siRNA for *Siah2* (si*Siah2*) was purchased from Origene,

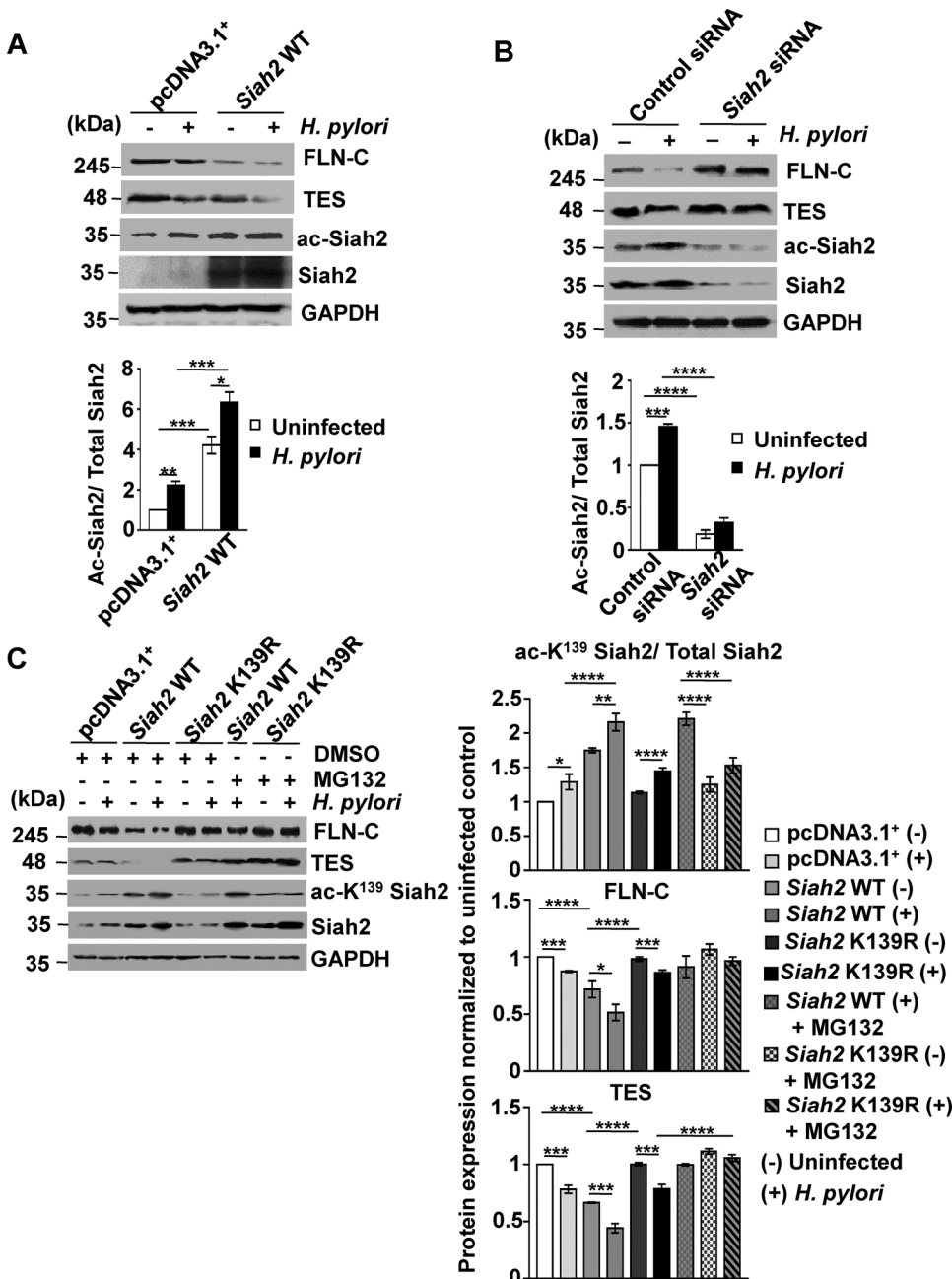


Fig. 3. *H. pylori*-mediated acetylation of Siah2 at K¹³⁹ enhances degradation of TES and FLN-C. (A) Western blotting performed using MKN45 cells transfected with empty vector and *Siah2* WT constructs showed a decreased expression of FLN-C and TES in *Siah2* WT-transfected expression of FLN-C and TES in *Siah2* WT-transfected *H. pylori*-infected cells. Bars represented ac-Siah2: total Siah2 expression normalized to loading control. (B) Immunoblot analysis of control siRNA and *Siah2* siRNA-transfected MKN45 cells demonstrated induced expression of FLN-C and TES in siRNA-transfected group as compared to control siRNA group. Densitometric analysis was represented as normalized ac-Siah2: total Siah2 expression. (C) Immunoblotting result showing the effect of MG132 treatment to rescue Siah2 K139R proteins from being degraded in *H. pylori* infected GGCs. Densitometric analysis was represented as TES or FLN-C or ac-K¹³⁹ Siah2: total Siah2. GAPDH was used as a loading control for all western blots. Error bars, s.e.m., $n = 3$, * $P < 0.05$; ** $P < 0.01$; *** $P < 0.003$; **** $P < 0.0001$.

Rockville, MD, USA, whereas siTES and siFLN-C were purchased from Santa Cruz Biotechnology.

For transient transfections, 1×10^6 MKN45 cells were seeded in 6-well plates. After 24 h, cells were transfected with 2.5 μ g of plasmid, 5 μ l of P3000 reagent and 7.5 μ l of Lipofectamine 3000 reagent (Invitrogen, Carlsbad, CA, USA). After 48 h of transfection, cells were infected with *H. pylori*. To knockdown the expression of *Siah2*, TES and FLN-C, 0.25×10^6 MKN45 and AGS cells were seeded in 6-well plates. After 18–24 h, cells were transfected with 10 nM siRNA using Lipofectamine 3000 reagent (Invitrogen). Stable over-expressing cells were generated following a standard protocol (Das et al., 2016).

2.4. Novel Siah2-binding partner analysis by mass spectrometry

MKN45 cells were transiently transfected with *Siah2* WT and *Siah2* ac-lys mutant construct *Siah2* K139R. Siah2 was immunoprecipitated from cell lysates prepared from uninfected and infected transfection

sets using anti-Siah2 antibody (Santa Cruz Biotechnology). The immunoprecipitated proteins were separated by SDS-PAGE and the gel was stained overnight in CBB-R250 staining solution (Bio-Rad Laboratories, Hercules, CA, USA). Bands were analyzed and protein identifications were performed using LC-MS/MS by University of Texas Medical Branch, Biomedical Resource Facility (UTMB-BRF), MS core unit, Galveston, Texas, USA. Only those proteins with minimum two peptides having ion score above 28 were selected for further studies.

2.5. Cell migration and invasion assay

Cell migration and invasion assay was performed using a fully adherent gastric cancer cell line AGS. Cells were transfected with control siRNA, siTES and siFLN-C and were infected for 24 h. Assays were done following a previously-reported protocol (Das et al., 2016).

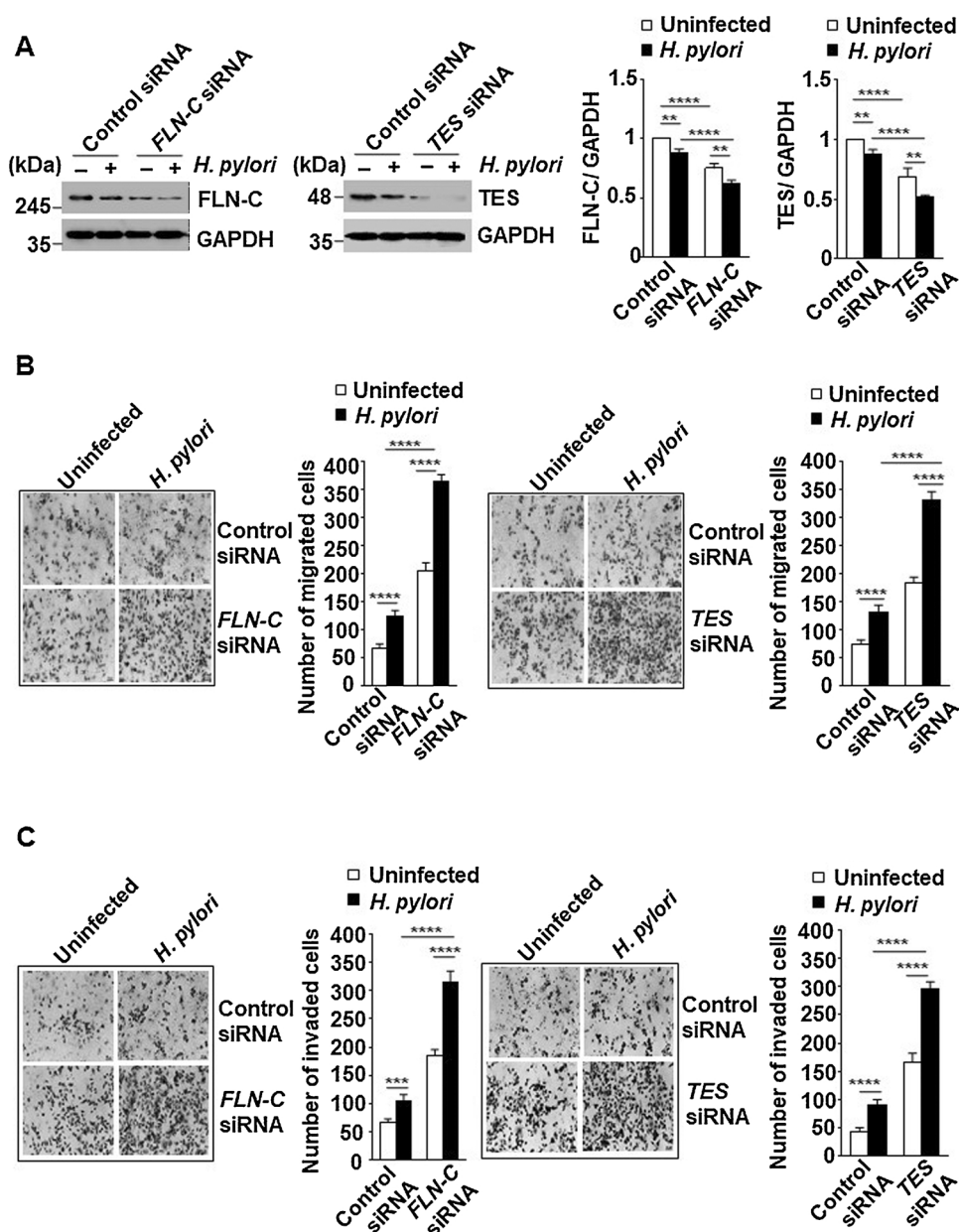


Fig. 4. TES and FLN-C degradation results in enhanced invasion and migration of *H. pylori*-infected GCCs. (A) Western blot data showing siRNA-mediated suppression of *FLN-C* and *TES* in AGS cells. Representative bar graphs showed significantly decreased *FLN-C* and *TES* expression in respective siRNA-transfected groups as compared to siControl group. (B) Cell migration assay performed with AGS cells showed induced migration of infected cells expressing si*FLN-C* and si*TES* as compared to their counterparts in siControl group; scales shown: 50 μ m. Bar graphs denoted the average number of migrated cells (mean \pm s.e.m., $n = 3$). Data were analyzed by two-way ANOVA with Tukey's post hoc test. Error bars, s.e.m. **** $P < 0.0001$. (C) Matrigel invasion assay with *FLN-C* and *TES*-suppressed AGS cells showing increased invasiveness in si*FLN-C* and si*TES*-transfected GCCs. Bar graphs denoted the average number of cells invaded through the Transwell matrigel (mean \pm s.e.m., $n = 3$). Data were analyzed by two-way ANOVA with Tukey's post hoc test. Error bars, s.e.m. *** $P < 0.003$; **** $P < 0.0001$. Scales shown: 50 μ m.

2.6. Wound-healing assay

The effect of knockdown of *TES* and *FLN-C* expression on the wound-healing property of GCCs was investigated using AGS cells as reported earlier (Rath et al., 2017).

2.7. Soft agar colony formation assay

Soft agar assay was performed to study the anchorage-independent growth of MKN45 cells transfected with control siRNA, si*TES* or si*FLN-C* and infected with *H. pylori* following a standard protocol (Rath et al., 2017).

2.8. Collection of human gastric biopsy samples

Metastatic gastric adenocarcinoma samples (stage III) were collected from the antral gastric mucosa from urease test-positive patients undergoing esophagogastroduodenoscopy following a National Institute of Science Education and Research (NISER) review board-approved protocol. Non-cancerous and uninfected gastric tissues were

used as control. Patients who have undergone *H. pylori* eradication therapy were excluded. Informed consent was obtained from each patient and anonymity was preserved.

2.9. *H. felis* infection and gastric tissue collection from mice

C57BL/6 mice (both male and female) aged between 4–5 wks were procured from the National Centre for Laboratory Animal Sciences (NCLAS) of the National Institute of Nutrition (NIN, Hyderabad, India). Mice were maintained as per the Committee for the Purpose of Control and Supervision of Experiments (CPCSEA) and Institutional Animal Ethics Committee (IAEC) guidelines for laboratory animals. 7–8 wks old mice were blindly divided into two groups-uninfected and infected. *H. felis* infection was given in accordance with standard protocol (Cai et al., 2005). After 12 months, tissues were necropsied.

2.10. Immunofluorescence and confocal microscopy

Empty vector (pcDNA3.1⁺), *Siah2* WT and K139R-expressing MKN45 stable cells were used for confocal microscopy. Cells were seeded on

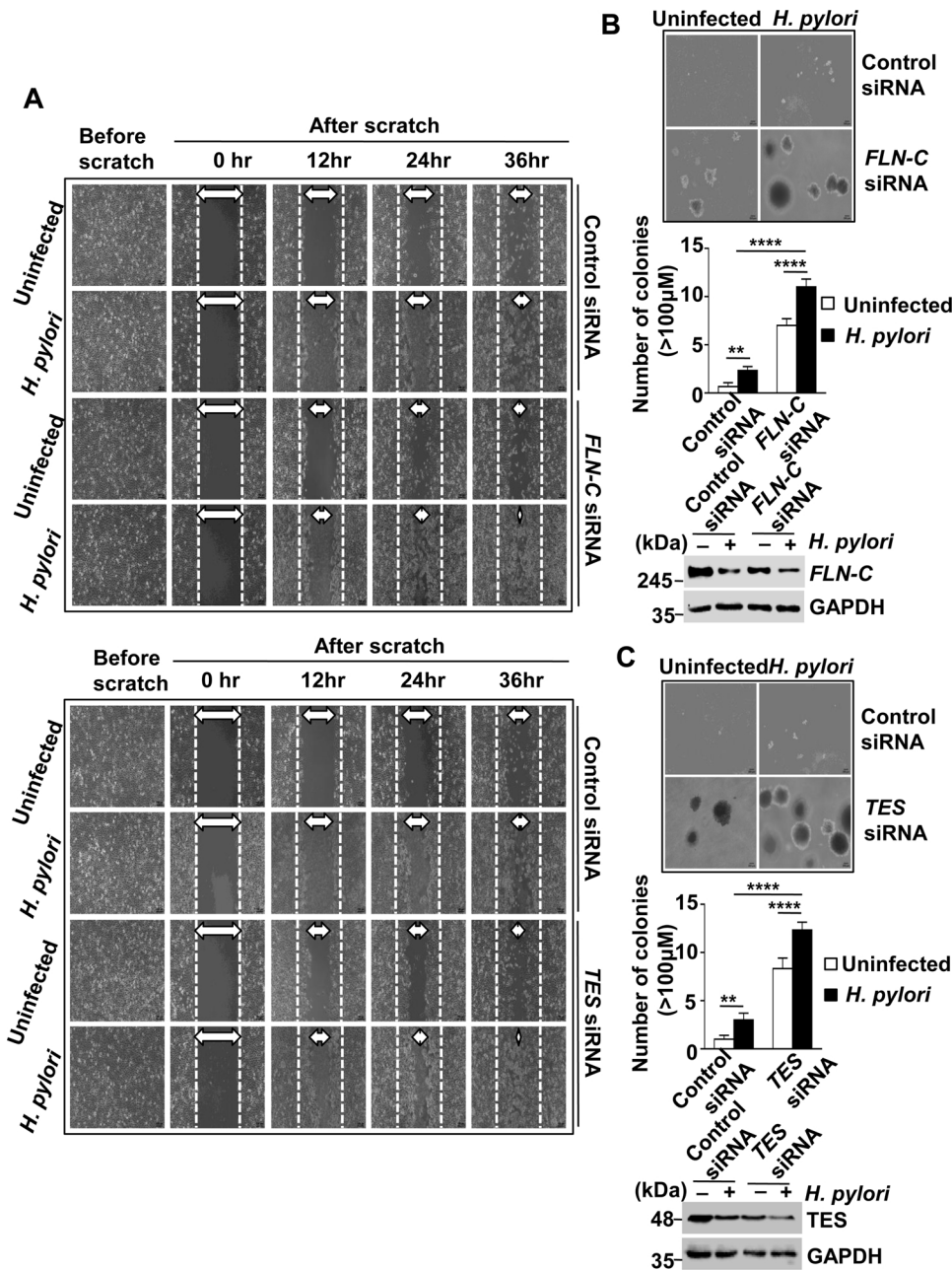


Fig. 5. TES and FLN-C downregulation results in enhanced invasion and migration of GCCs. (A) Wound healing assay performed with control siRNA, siFLN-C and siTES-transfected AGS cells showed increased migration ability of siFLN-C and siTES-transfected groups. Scales shown: 100 μm. (B) Soft agar colony formation assay was performed on MKN45 cells. siFLN-C-transfected cells showed a significant increase in colony forming ability post *H. pylori* infection as compared to cells expressing the control siRNA. Representative bar graphs showing average number of colonies formed. FLN-C level in siFLN-C-transfected MKN45 cells were assessed by western blotting (n = 3). (C) Soft agar assay performed with uninfected or infected MKN45 cells transfected with either siTES or siControl showed a substantial increase in colony forming ability of TES-silenced cells. TES level was detected in siControl and siTES-transfected MKN45 cells by western blotting (n = 3). GAPDH was used as a loading control. Data were analyzed by two-way ANOVA with Tukey's post hoc test. For all graphical representations, error bars, s.e.m, n = 3. ***P* < 0.01; *****P* < 0.0001. Scales shown in B and C: 200 μm.

coverslips in 24-well plates 24 h before *H. pylori*-infection for 12 h. Uninfected and *H. pylori*-infected cells were fixed with 4% paraformaldehyde (PFA) at 37 °C for 15 min followed by staining with Siah2, Siah2 ac-K¹³⁹, TES, FLN-C. Cells were stained with DAPI (4',6-Diamidino-2-phenylindolehydrochloride) and Phalloidin-FITC conjugate probe (Invitrogen) for 20 min. Imaging was done using a laser scanning confocal microscope (LSM) 800 (Carl Zeiss, Oberkochen, Germany).

Human gastric adenocarcinoma biopsy tissue sections and C57BL/6 mice antral gastric tissue sections were processed for immunostaining as reported previously (Das et al., 2016).

2.11. Statistical analysis

Except for the animal studies, experiments were performed in a non-randomized and non-blinded fashion. *In-vitro* experiments were performed at least three times with three technical repeats. Statistical significance of quantitative data was determined using Student's *t*-test and 2-way ANOVA with Tukey's post hoc test.

3. Results

3.1. *H. pylori* infection downregulates FLN-C and TES and increases expression of Siah2 in GCCs

TES and FLN-C downregulation has been associated with poor prognosis in cancer and is noticed in several invasive cancers including gastric cancer (Drusco et al., 2005; Qiao et al., 2015; Wang et al., 2017). We have shown earlier that the E3 ubiquitin ligase Siah2 is upregulated in *H. pylori*-infected gastric epithelial cells (Das et al., 2016). In an effort to identify novel binding partners of Siah2 in *H. pylori*-infected cells, MKN45 cells were either infected with *H. pylori* or left uninfected. Whole cell lysates were immunoprecipitated with Siah2 antibody, the immunocomplexes were run on SDS-PAGE and the gel was stained with CBB-R250. Analysis of bands by LC-MS/MS revealed that TES and FLN-C bind with Siah2 (Supplementary Fig. 1A). In order to experimentally decipher the interrelationship of Siah2 with FLN-C and TES protein level in *H. pylori*-infected cells, MKN45 cells were infected with

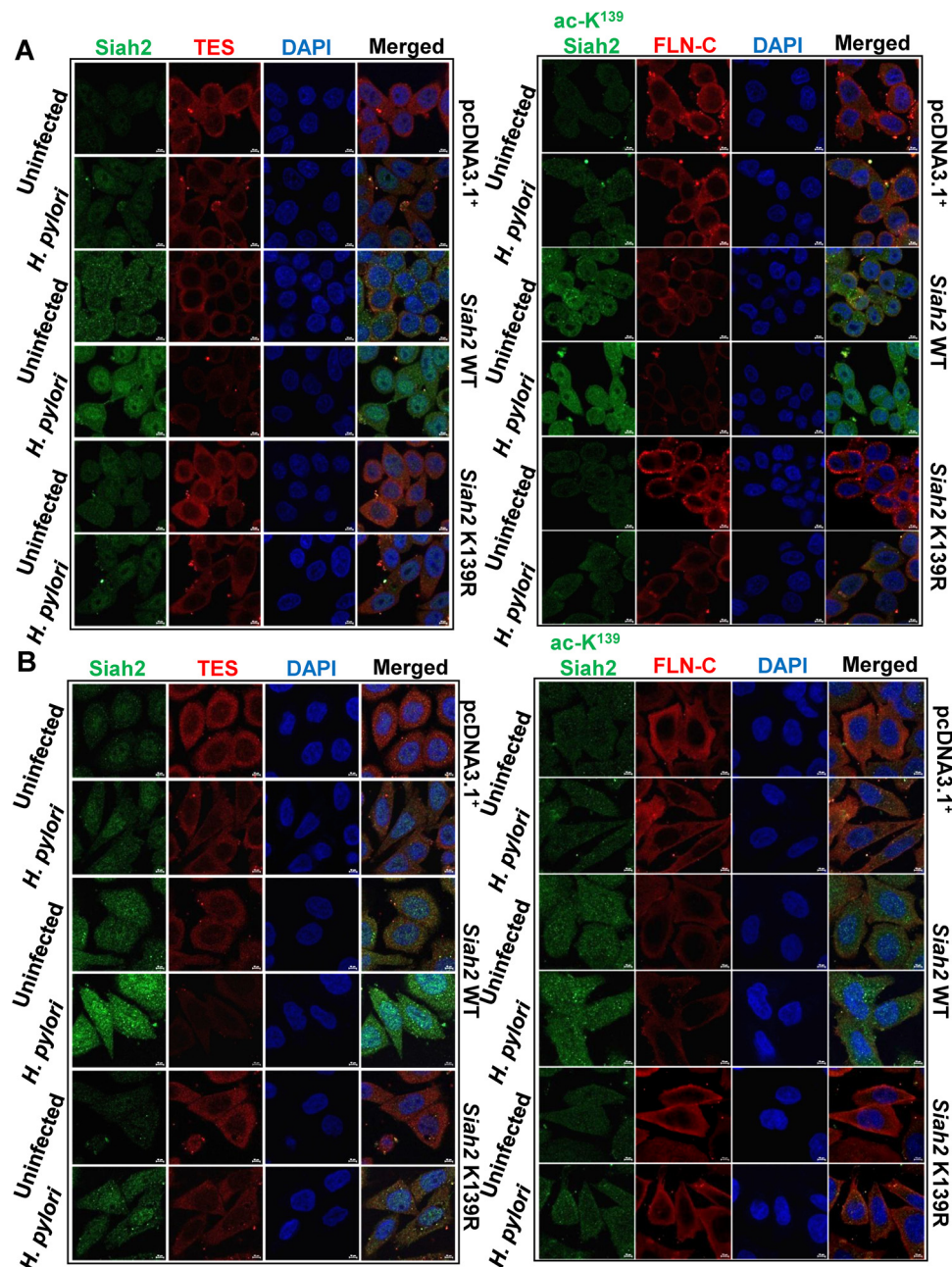


Fig. 6. TES and FLN-C are stabilized in K139R acetylation-null Siah2-expressed GCCs. (A) Confocal microscopy of MKN45 cells and (B) AGS cells stably expressing pcDNA3.1+, *Siah2* WT and *Siah2* K139R constructs showed marked downregulation of FLN-C and TES in *H. pylori*-infected *Siah2* WT-expressing cells as compared to their counterparts from the other two transfected groups. Original magnifications X630. Scale shown: 10 μ m.

cag PAI(+) *H. pylori* (strain 26695) at 200 multiplicity of infection (MOI) for various time periods. Whole cell lysates were prepared and western blot result revealed that *H. pylori* significantly induced Siah2 expression but downregulated TES-FLN-C proteins in a time-dependent manner with 24 h showing the maximal effect (Fig. 1A). For comparing the efficiency of MOI 100, 200 and 300 to regulate Siah2, TES and FLN-C proteins, whole cell lysates were prepared after infecting MKN45 cells with respective MOIs for 24 h and western blotted. Western blot results showed significantly increased Siah2 and significantly downregulated TES and FLN-C proteins in MOI 200 and MOI 300-infected cells (Fig. 1B). In all subsequent experiments, MOI 200 and 24 h infection with strain 26695 were used unless mentioned differently. MOI 200 also showed similar trends in Kato III and AGS cells (Fig. 1C). An equivalent decrease in TES and FLN-C proteins was noticed in MKN45 cells after being infected with the *cag* PAI(+) strain 26695 and the *cag*

PAI(-) strain 8-1, indicating that the phenomena observed were independent of the *cag* PAI status (Fig. 1D).

3.2. p300 causes acetylation of Siah2 and its HAT activity downregulates TES and FLN-C expression in *H. pylori*-infected GCCs

We have earlier reported that p300-mediated acetylation protects Siah2 from self-ubiquitination and degradation (Kokate et al., 2018). Here we identified by western blotting of whole cell lysates that the level of TES and FLN-C proteins was inversely correlated with ac-Siah2 in *H. pylori*-infected MKN45 cells (detected by using pan ac-lys antibody) (Fig. 2A). As the lys/histone acetyltransferase (KAT/HAT) activity of p300 regulates proteasomal degradation of target proteins (Kokate et al., 2018), we next examined the role of p300 in influencing the downregulation of TES and FLN-C in the infected cells. Our data

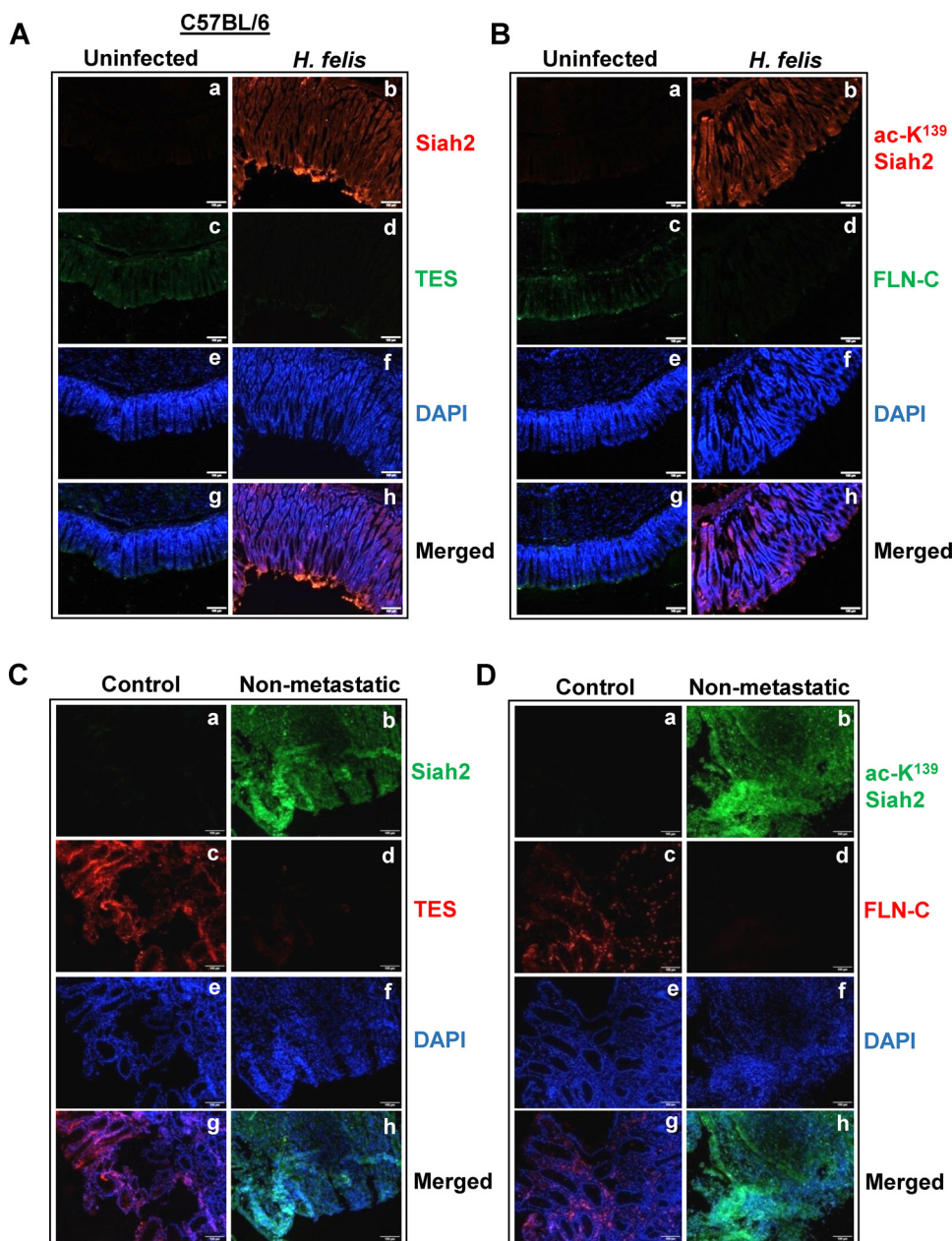


Fig. 7. Enhanced expression of ac-K¹³⁹ Siah2, Siah2 and downregulation of FLN-C and TES are noticed in mouse and human gastric epithelia after *Helicobacter* infection. (A) Fluorescence microscopy data of antral gastric tissues isolated from C57BL/6 mice showing Siah2 (a and b), TES (c and d), DAPI (e and f), merged (g and h) and (B) ac-K¹³⁹ Siah2 (a and b), FLN-C (c and d), DAPI (e and f) and merged (g and h) images. (C) Fluorescence microscopy of human non-cancer and non-metastatic biopsy samples (n = 10) showing Siah2 (a and b), TES (c and d), DAPI (e and f), merged (g and h) and (B) ac-K¹³⁹ Siah2 (a and b), FLN-C (c and d), DAPI (e and f) and merged (g and h) images. Original magnification 100 × . Scales shown 100 μm.

confirmed that a strikingly increased level of p300 at 24 h p.i. was accompanying TES and FLN-C downregulation (Fig. 2B). To determine whether Siah2 interacts with p300, TES and FLN-C, whole cell lysates were immunoprecipitated with Siah2 antibody, western blotted and probed with p300, ac-lys, Siah2, TES and FLN-C antibodies (Fig. 2C). TES and FLN-C were found to interact with Siah2. To further confirm FLN-C and TES interaction with Siah2, immunoprecipitation assay was performed with FLN-C and TES-specific antibodies to pull-down FLN-C and TES binding partners, respectively, from whole cell lysates of 6 h and 24 h, p.i (Supplementary Fig. 1B). Our data revealed that FLN-C and TES interacted with Siah2 at 6 h p.i. which further decreased at 24 h due to the degradation of FLN-C and TES. In order to find out the response of immortalized normal gastric epithelial cells HFE145 to *H. pylori* infection, these cells were infected with *H. pylori* 26695 strain at MOI 200 for 24 h. Like MKN45 cells, infected HFE145 cells also showed a similar response of significantly high p300, acetylated Siah2 (ac-Siah2) and Siah2 expression but significantly low TES and FLN-C (Fig. 2D). As expected, increased ac-Siah2 protein level was coupled with TES and FLN-C downregulation in infected Kato III and AGS cells

(Fig. 2E). CTK7 A, an inhibitor of p300 HAT/KAT activity, resulted in significant downregulation of Siah2 and ac-Siah2 proteins in MKN45 cells but TES and FLN-C level significantly increased in the CTK7 A-treated cells (Fig. 2F).

3.3. Siah2 acetylation at K¹³⁹ in *H. pylori*-infected GCCs enhances degradation of TES and FLN-C

To understand the effect of Siah2 on TES and FLN-C proteins, MKN45 cells were transfected with the empty vector and Siah2 WT construct. Following the infection with *H. pylori*, Siah2 WT-expressing cells showed significantly less TES and FLN-C proteins as compared to the empty vector-transfected cells (Fig. 3A and Supplementary Fig. 2A and B). To further evaluate the effect of Siah2 on TES and FLN-C, MKN45 cells were transfected with Siah2 siRNA. When compared with control vector-transfected cells, TES and FLN-C were not down-regulated in siSiah2 cells even after *H. pylori* infection, thus reaffirming the role of Siah2 in downregulating TES and FLN-C (Fig. 3B and Supplementary Fig. 2C and D). To find out whether acetylation at K¹³⁹

was protecting Siah2 from proteasomal degradation, K139R mutant-expressing MKN45 cells were treated with 50 μ M MG132 for 12 h prior to *H. pylori* infection. MG132 treatment increased K139R Siah2 level indicating that in the absence of acetylation at K¹³⁹, Siah2 was targeted for ubiquitination-mediated proteasomal degradation (Fig. 3C). MG132 also rescued FLN-C and TES from being degraded.

3.4. TES and FLN-C degradation results in enhanced invasion and migration of GCCs

The positive impact of Siah2 acetylation on migration and invasiveness of *H. pylori*-infected GCCs is already known (Kokate et al., 2018). We examined here the effect of TES and FLN-C silencing on the invasiveness of GCCs. These experiments were performed using AGS cells since MKN45 cells are semi-adherent in nature and thus, not suitable for the invasion and migration studies. To find out the effect of TES and FLN-C on the cell migration and invasion ability of AGS cells, these two genes were suppressed using siRNA. Western blot results showed significant suppression of TES and FLN-C following transfection with respective siRNAs (Fig. 4A). Migration ability was significantly upregulated in FLN-C and TES-suppressed cells (Fig. 4B). Significantly increased cell invasiveness was observed in Matrigel (Fig. 4C) and in wound healing assays (Fig. 5A and Supplementary Fig. 3, respectively) in FLN-C and TES-suppressed AGS cells as compared with control siRNA-transfected cells. The change in anchorage-independent clonogenicity of FLN-C and TES-suppressed MKN45 cells following *H. pylori* infection was also studied by soft-agar assay. Both FLN-C and TES suppression (Fig. 5B and C, respectively) resulted in significantly increased foci formation. Accompanying western blot results showed the status of FLN-C and TES suppression in the used cells.

3.5. TES and FLN-C are stabilized in K139R acetylation-null Siah2-expressed GCCs

To investigate the effect of Siah2 acetylation at K¹³⁹ residue on TES and FLN-C in *H. pylori*-infected cells, confocal microscopy was done using uninfected and *H. pylori*-infected MKN45 cells (Fig. 6A) or AGS cells (Fig. 6B) stably transfected with the empty vector, Siah2 WT and Siah2 K139R constructs. WT Siah2-transfected and infected cells showed marked downregulation of TES and FLN-C when compared with the other transfected groups.

To understand the effect of Siah2 acetylation on actin polymerization, AGS cells were transfected with the empty vector, WT Siah2 and K139R Siah2 constructs followed by infection with *H. pylori*. After staining cells with phalloidin-FITC to identify F-actin, we observed that filopodia length was markedly shortened in *H. pylori*-infected cells expressing the WT construct than the corresponding empty vector or K139R construct-expressing cells (Supplementary Fig. 4). Lamellipodia, the flat protrusive structures required for force generation during cell motility (Bear et al., 2002) were more uniformly seen on WT construct-expressing infected cells.

3.6. Enhanced ac-K¹³⁹ Siah2, Siah2 expression and downregulation of FLN-C and TES are noticed in mouse and human gastric epithelia after Helicobacter infection

C57BL/6 mice infected with *H. felis* show the classic sequence of events seen in humans infected with *H. pylori* and consistently show adenocarcinoma development (Correa and Houghton, 2007). After 12 months of infection (n = 16 for both control and infected groups) splenomegaly, marked hypertrophy of gastric mucosa, infiltration of mononuclear cells and development of adenocarcinoma were observed. Immunofluorescence microscopy showed high expression of Siah2, ac-K¹³⁹ Siah2 and downregulation of TES and FLN-C in the infected gastric tissue as compared with the uninfected samples (Fig. 7A and B). Similarly, non-metastatic gastric cancer biopsy samples (n = 10) also

showed very high expression of Siah2, ac-K¹³⁹ Siah2 but downregulation of TES and FLN-C when compared with the uninfected non-cancerous tissue (Fig. 7C and D).

These data collectively confirm that *H. pylori*-induced acetylation of Siah2 at K¹³⁹ residue increases its stability promoting the degradation of TES and FLN-C. TES and FLN-C degradation enhances invasiveness of *H. pylori*-infected GCCs by altering actin filament network.

4. Discussion

Proteasomal degradation of tumor suppressors contributes in the promotion of cancer (Jaenicke et al., 2016; Ni et al., 2016; Gao et al., 2017). The E3 ubiquitin ligase Siah2 is upregulated in various cancers (Qi et al., 2013) including gastric cancer (Das et al., 2016) and acetylated at K¹³⁹ residue (Kokate et al., 2018) in *H. pylori*-infected GCCs. p300-mediated acetylation at K¹³⁹ increases the stability of Siah2 leading to the degradation of adhesion-regulating proteins TES and FLN-C and increases the motility of *H. pylori*-infected gastric cancer cells. High correlation of Siah2 acetylation with TES and FLN-C degradation in *H. felis*-infected mouse model as well as in human gastric cancer biopsy samples presents ac-Siah2 as a promising new therapeutic target for patients with gastric cancer.

H. pylori has been identified by IARC/WHO as a definite (group I) carcinogen responsible for gastric cancer (Buti et al., 2011). It induces the expression of several proliferative and inflammatory genes and causes increased production of reactive oxygen species (ROS) (Gobert and Wilson, 2017). *H. pylori* infection from childhood leads to gastric cancer only in 1–2% cases and happens only after lifelong infection (Herrera and Parsonnet, 2009). The duration of infection plays a critical role in the disease progression. Although this study could not examine whether proteasomal degradation and hypermethylation are chronologically spaced or not, it establishes that ac-Siah2-mediated proteasomal degradation is significant in suppressing TES and FLN-C and enhancing invasiveness of GCCs. Another gastric tumor-suppressor RUNX3 is regulated by proteasome-mediated degradation (Tsang et al., 2010). Moreover, p53 (Wei et al., 2010) and p27 (Eguchi et al., 2003) tumor suppressors are also degraded by the proteasomal machinery in *H. pylori*-infected epithelia. Thus, our study promotes the notion that many cancerous events in gastric epithelial cancer cells are possibly regulated by the proteomics of proteasome-complexes.

Gastric cancer is highly metastatic. Disassembly of adhesion structures is essential for cancer cells to become invasive. Rearrangement of actin cytoskeleton by *H. pylori* is another essential component of its pathogenicity (Wessler et al., 2011). Actin and its interaction with binding proteins strongly influence not only cell shape and cell-cell interactions but also regulate crucial cell signalling events (Zhou et al., 2010; Zhao et al., 2016). Actin-interacting proteins TES and FLN-C show tumor-suppressive functions in gastric cancer (Drusco et al., 2005; Oue et al., 2006; Ma et al., 2010) and are involved in the downregulation of cell adhesion and motility (Coutts et al., 2003; Tanabe et al., 2017). Although it is known for a long time that *H. pylori* induces proteasomal degradation of tumor-suppressor proteins (Tsang et al., 2010; Buti et al., 2011; Coombs et al., 2011), to our knowledge, this is the first report deciphering the mechanism of proteasomal degradation of TES and FLN-C in *H. pylori*-infected GCCs. This study proved that downregulation of TES and FLN-C increases motility of *H. pylori*-infected cells. In addition, this study associated Siah2 acetylation with cell shape maintenance and F-actin assembly.

Filopodia are involved in cancer cell invasiveness and motility (Jacquemet et al., 2015). These special structures reinforce cell-cell attachments or cell-extracellular matrix attachments (Vasioukhin et al., 2000; Davis et al., 2015) and is considered as a marker of EMT. While long and protruding filopodia have continuous actin filaments, retracting filopodia have disrupted and disorganized actin fibres (Leijnse et al., 2015). Lamellipodia, are also actin-rich protrusive structures and are required for force generation and directional cell motility. These

sheet-like membrane protrusions can regulate cancer cell migration (Yamaguchi and Condeelis, 2007). It is known that FLN-A is involved in filopodia formation (Ohta et al., 1999; Chiang et al., 2017). Likewise, a TES-binding partner Mena can regulate the formation of actin filament and filopodia (Coutts et al., 2003). Our data show that TES and FLN-C are required for filopodia formation, but downregulation of these proteins promotes lamellipodia development. It is known that the distribution of capping proteins and actin-related proteins ARP2/3 varies between lamellipodia and filopodia, thus critically regulating cell motility (Davies, 2013). However, deciphering the exact nature of involvement of TES and FLN-C in regulating filopodia and lamellipodia structures would certainly need further investigation.

On the basis of our observations and explanations given above, we propose the following series of events in *H. pylori*-infected GCCs, *H. pylori* infection induces Siah2 stability by acetylating it at K¹³⁹ and causes degradation of TES and FLN-C. This results in the disruption of actin filopodia but promotes lamellipodia formation. At this stage, we believe that studying interaction of ac-Siah2 with TES, FLN-C and other yet unidentified cytoskeletal proteins would be beneficial in understanding gastric cancer cell invasiveness.

Conflict of interest

The authors declare that they have no conflict of interest.

Funding

This work was supported by two grants to A.B. (Sanction No. BT/PR15092/GBD/27/311/2011, Department of Biotechnology, Govt. of India) and (SB/SO/BB-0015/2014, Science and Engineering Research Board, Govt. of India). S.B.K., P.D., A.D.R., I.P. and D.C. are supported by fellowships from Department of Atomic Energy (DAE), Govt. of India.

Authors contributions

S.B.K performed experiments, analyzed the data and helped in manuscript preparation, P.D. generated histology data, I.P., A.D.R and D.C. performed some experiments, N.R. and S.P.S. helped with gastric cancer biopsy collection and analysis; H.A. and D.T.S. provided the HFE145 cell line, A.B. conceived the work, designed experiments, analyzed the data, supervised the work and wrote the paper.

Acknowledgements

We thank the Mass Spectrometry Core Lab, UTMB Biomolecular Resource Facility (UTMB BRF), Galveston TX, USA for mass spectrometry analysis. NISER core facilities are also acknowledged.

Appendix A. Supplementary data

Supplementary material related to this article can be found, in the online version, at doi:<https://doi.org/10.1016/j.biocel.2018.07.012>.

References

Arndt, V., Dick, N., et al., 2010. Chaperone-assisted selective autophagy is essential for muscle maintenance. *Curr. Biol.* 20 (2), 143–148.

Bear, J.E., Svitkina, T.M., et al., 2002. Antagonism between Ena/VASP proteins and actin filament capping regulates fibroblast motility. *Cell* 109 (4), 509–521.

Bhattacharyya, A., Chattopadhyay, R., et al., 2009. Acetylation of apurinic/aprimidinic endonuclease-1 regulates *Helicobacter pylori* mediated gastric epithelial cell apoptosis. *Gastroenterology* 136 (7), 2258–2269.

Burande, C.F., Heuzé, M.L., et al., 2009. A label-free quantitative proteomics strategy to identify E3 ubiquitin ligase substrates targeted to proteasome degradation. *Mol. Cell. Proteom.* 8 (7), 1719–1727.

Buti, L., Spooner, E., et al., 2011. *Helicobacter pylori* cytotoxin-associated gene A (CagA) subverts the apoptosis-stimulating protein of p53 (ASPP2) tumor suppressor pathway

of the host. *Proc. Natl. Acad. Sci.* 108 (22), 9238–9243.

Cai, X., Carlson, J., et al., 2005. *Helicobacter pylori* eradication restores normal architecture and inhibits gastric cancer progression in C57BL/6 mice. *Gastroenterology* 128 (7), 1937–1952.

Chaugule, V.K., Walden, H., 2016. Specificity and disease in the ubiquitin system. *Biochem. Soc. Trans.* 44 (1), 212–227.

Chiang, T.-S., Wu, H.-F., et al., 2017. ADP-ribosylation factor-like 4C binding to filamin-A modulates filopodium formation and cell migration. *Mol. Biol. Cell* 28 (22), 3013–3028.

Coombs, N., Sompallae, R., et al., 2011. *Helicobacter pylori* affects the cellular deubiquitinase USP7 and ubiquitin-regulated components TRAF6 and the tumour suppressor p53. *Int. J. Med. Microbiol.* 301 (3), 213–224.

Correa, P., Houghton, J., 2007. Carcinogenesis of *Helicobacter pylori*. *Gastroenterology* 133 (2), 659–672.

Coutts, A.S., MacKenzie, E., et al., 2003. TES is a novel focal adhesion protein with a role in cell spreading. *J. Cell. Sci.* 116 (5), 897–906.

Das, L., Kokate, S.B., et al., 2016. ETS2 and Twist1 promote invasiveness of *Helicobacter pylori*-infected gastric cancer cells by inducing Siah2. *Biochem. J.* 473 (11), 1629–1640.

Das, L., Kokate, S., et al., 2017. Membrane-bound β -catenin degradation is enhanced by ETS2-mediated Siah1 induction in *Helicobacter pylori*-infected gastric cancer cells. *Oncogenesis* 6 (5) e327.

Davies, J., 2013. *Mechanisms of Morphogenesis*. Academic Press.

Davis, J.R., Luchici, A., et al., 2015. Inter-cellular forces orchestrate contact inhibition of locomotion. *Cell* 161 (2), 361–373.

Ding, S.-Z., O'Hara, A.M., et al., 2004. *Helicobacter pylori* and H₂O₂ increase AP endonuclease-1/redox factor-1 expression in human gastric epithelial cells. *Gastroenterology* 127 (3), 845–858.

Drusco, A., Zanesi, N., et al., 2005. Knockout mice reveal a tumor suppressor function for Testin. *Proc. Natl. Acad. Sci. U. S. A.* 102 (31), 10947–10951.

Eguchi, H., Herschenhou, N., et al., 2003. *Helicobacter pylori* increases proteasome-mediated degradation of p27kip1 in gastric epithelial cells. *Cancer Res.* 63 (15), 4739–4746.

Gao, W., Li, W., et al., 2017. Inactivation of the PBRM1 tumor suppressor gene amplifies the HIF-response in VHL^{-/-} clear cell renal carcinoma. *Proc. Natl. Acad. Sci.* 114 (5), 1027–1032.

Garvalov, B.K., Higgins, T.E., et al., 2003. The conformational state of Tes regulates its zyxin-dependent recruitment to focal adhesions. *J. Cell Biol.* 161 (1), 33–39.

Gobert, A.P., Wilson, K.T., 2017. Human and *Helicobacter pylori* interactions determine the outcome of gastric diseases. *Molecular Pathogenesis and Signal Transduction by Helicobacter pylori*. Springer, pp. 27–52.

Guillemin, K., Salama, N.R., et al., 2002. Cag pathogenicity island-specific responses of gastric epithelial cells to *Helicobacter pylori* infection. *Proc. Natl. Acad. Sci.* 99 (23), 15136–15141.

Hatakeyama, M., 2014. *Helicobacter pylori* CagA and gastric cancer: a paradigm for hit-and-run carcinogenesis. *Cell Host Microbe* 15 (3), 306–316.

Herrera, V., Parsonnet, J., 2009. *Helicobacter pylori* and gastric adenocarcinoma. *Clin. Microbiol. Infect.* 15 (11), 971–976.

Jacquemet, G., Hamidi, H., et al., 2015. Filopodia in cell adhesion, 3D migration and cancer cell invasion. *Curr. Opin. Cell Biol.* 36, 23–31.

Jaenicke, L.A., von Eyss, B., et al., 2016. Ubiquitin-dependent turnover of MYC antagonizes MYC/PAF1C complex accumulation to drive transcriptional elongation. *Mol. Cell* 61 (1), 54–67.

Kokate, S.B., Dixit, P., et al., 2018. Acetylation-mediated Siah2 stabilization enhances PHD3 degradation in *Helicobacter pylori*-infected gastric epithelial cancer cells. *FASEB J* [fj.201701344RRR](https://doi.org/10.1096/faseb.201701344RRR).

Leijne, N., Oddershede, L.B., et al., 2015. An updated look at actin dynamics in filopodia. *Cytoskeleton* 72 (2), 71–79.

Ma, H., Weng, D., et al., 2010. Extensive analysis of D7S486 in primary gastric cancer supports TESTIN as a candidate tumor suppressor gene. *Mol. Cancer* 9 (1), 190.

Nakajima, T., Enomoto, S., et al., 2010. Persistence of a component of DNA methylation in gastric mucosae after *Helicobacter pylori* eradication. *J. Gastroenterol.* 45 (1), 37–44.

Ni, T., Li, X.-Y., et al., 2016. Snail1-dependent p53 repression regulates expansion and activity of tumour-initiating cells in breast cancer. *Nat. Cell Biol.* 18 (11), 1221.

Nihira, N.T., Ogura, K., et al., 2017. Acetylation-dependent regulation of MDM2 E3 ligase activity dictates its oncogenic function. *Sci. Signal.* 10 (466) eaai8026.

Ohta, Y., Suzuki, N., et al., 1999. The small GTPase RalA targets filamin to induce filopodia. *Proc. Natl. Acad. Sci.* 96 (5), 2122–2128.

Oue, N., Mitani, Y., et al., 2006. Accumulation of DNA methylation is associated with tumor stage in gastric cancer. *Cancer* 106 (6), 1250–1259.

Qi, J., Kim, H., et al., 2013. Regulators and effectors of Siah ubiquitin ligases. *Cell Biochem. Biophys.* 67 (1), 15–24.

Qiao, J., Cui, S.-J., et al., 2015. Filamin C, a dysregulated protein in cancer revealed by label-free quantitative proteomic analyses of human gastric cancer cells. *Oncotarget* 6 (2), 1171.

Rath, S., Das, L., et al., 2015. Regulation of Noxa-mediated apoptosis in *Helicobacter pylori*-infected gastric epithelial cells. *FASEB J.* 29 (3), 796–806.

Rath, S., Das, L., et al., 2017. Inhibition of histone/lysine acetyltransferase activity kills CoCl₂-treated and hypoxia-exposed gastric cancer cells and reduces their invasiveness. *Int. J. Biochem. Cell Biol.* 82, 28–40.

Sala, S., Catillon, M., et al., 2017. The PET and LIM1-2 domains of testin contribute to intramolecular and homodimeric interactions. *PLoS One* 12 (5) e0177879.

Tanabe, K., Shinsato, Y., et al., 2017. Filamin C promotes lymphatic invasion and lymphatic metastasis and increases cell motility by regulating Rho GTPase in esophageal squamous cell carcinoma. *Oncotarget* 8 (4), 6353–6363.

- Tsang, Y., Lamb, A., et al., 2010. *Helicobacter pylori* CagA targets gastric tumor suppressor RUNX3 for proteasome-mediated degradation. *Oncogene* 29 (41), 5643.
- Vasioukhin, V., Bauer, C., et al., 2000. Directed actin polymerization is the driving force for epithelial cell–cell adhesion. *Cell* 100 (2), 209–219.
- Wang, M., Wang, Q., et al., 2017. Testin is a tumor suppressor in non-small cell lung cancer. *Oncol. Rep.* 37 (2), 1027–1035.
- Wei, J., Nagy, T.A., et al., 2010. Regulation of p53 tumor suppressor by *Helicobacter pylori* in gastric epithelial cells. *Gastroenterology* 139 (4), 1333–1343 e1334.
- Wessler, S., Gimona, M., et al., 2011. Regulation of the actin cytoskeleton in *Helicobacter pylori*-induced migration and invasive growth of gastric epithelial cells. *Cell Commun. Signal.* 9 (1), 27.
- Wolosin, J.M., Okamoto, C., et al., 1983. Actin and associated proteins in gastric epithelial cells. *Biochim. Biophys. Acta (BBA)-Gen. Subj.* 761 (2), 171–182.
- Yamaguchi, H., Condeelis, J., 2007. Regulation of the actin cytoskeleton in cancer cell migration and invasion. *Biochim. Biophys. Acta (BBA)-Mol. Cell Res.* 1773 (5), 642–652.
- Yoshida, T., Kato, J., et al., 2013. Altered mucosal DNA methylation in parallel with highly active *Helicobacter pylori*-related gastritis. *Gastric Cancer* 16 (4), 488–497.
- Zhao, Y., Shapiro, S.S., et al., 2016. F-actin clustering and cell dysmotility induced by the pathological W148R missense mutation of filamin B at the actin-binding domain. *Am. J. Physiol.-Cell Physiol.* 310 (1), C89–C98.
- Zhou, A.-X., Hartwig, J.H., et al., 2010. Filamins in cell signaling, transcription and organ development. *Trends Cell Biol.* 20 (2), 113–123.